Understanding C/EBPβ LAP/LIP Transcriptional and Adipogenic Potential through Regulation by HDAC1 and GCN5

Houssein Salem Abdou

Thesis submitted to the
Faculty of Graduate and Postdoctoral Studies
In partial fulfillment of the requirements
For the Ph.D degree in Biochemistry

Department of Biochemistry, Microbiology and Immunology
Faculty of Medicine
University of Ottawa

I dedicate this thesis to my nephew Mohamed.

Abstract

The CCAAT/Enhancer Binding Protein Beta (C/EBPβ) is part of the leucine zipper family of transcription factors and is involved in a myriad of processes including cellular proliferation and differentiation. C/EBPβ is expressed as three isoforms (LAP*, LAP, LIP), translated from a single mRNA by a leaky ribosomal scanning mechanism. While LAP* and LAP have activating functions, LIP is recognized as being a repressor of transcription due to its lack of activation domains.

Numerous studies have shown that C/EBPβ acetylation state modulates its activity in a promoter-specific manner. For instance, the acetyltransferases GCN5/PCAF and the deacetylase complex mSin3A/HDAC1 regulate C/EBPβ activity on the C/EBPα promoter. GCN5/PCAF-mediated acetylation of C/EBPβ was shown to positively affect its transcriptional activity in a steroid-dependent mechanism via the glucocorticoid receptor (GR). GR relieves HDAC1 association from C/EBPβ by targeting the deacetylase for proteasomal degradation, hence favouring GCN5-mediated acetylation of C/EBPβ and allowing maximum activation capacity to be reached. In order to further elucidate C/EBPβ activation, I sought to characterize the interplay between GCN5 and HDAC1 in regulating C/EBPβ LAP/LIP activity during murine adipogenesis by identifying their binding domain in C/EBPβ.

I identified a minimal domain located within regulatory domain 1 (RD1) of C/EBPβ that is required for both GCN5 and HDAC1 binding. Furthermore, the loss of the identified domain in C/EBPβ appears to partially mimic the GR effect, thus giving C/EBPβ a higher basal transcriptional activity that accelerates NIH 3T3 and 3T3 L1 adipogenesis. Moreover, I also showed that the LIP isoform inhibitory mode of action is partially mediated through the mSin3A/HDAC1 repressor complex, which gives LIP an active repressor function. In addition to LIP inhibitory function, I also showed that a cysteine residue located in LAP* negatively regulates its transactivating function during murine adipogenesis.

Although RD1 of C/EBPβ has been suggested to act as a negative regulatory domain, I showed that only five residues are responsible for most of its inhibitory effect. Hence, in an attempt to further define sub-domains within RD1, I characterized a new positive regulatory

domain at its N-terminal region, which seems to be required for C/EBPβ activity in a promoter-specific manner.

In conclusion, this study not only supports previously hypothesized mechanisms by which C/EBPβ is regulated, but it also redefines the contribution of LAP*, LAP and LIP in regulating transcription. Most importantly, the results emphasize the countless possibilities by which C/EBPβ transactivation potential could be modulated during cellular differentiation.

Acknowledgements

Working in Dr Robert Haché's laboratory has thought me invaluable knowledge. Dr Haché has been my supervisor since I first started working in a research lab in 2004 as a summer student. He has been continuously supporting my projects and constantly challenging my scientific abilities with a sincere enthusiasm for science. For that, thank you.

I would also like to acknowledge members of my thesis advisory committee, Dr Steffany Bennett and Dr Stephen Lee, for their advice and encouragement on my research project. Also, thank you for allowing me to write and present my progress reports in French. Your willingness to discuss science in French during all the meetings that we had was very much appreciated and I hope that you enjoyed it as much as I did.

I was very lucky and grateful to be surrounded by wonderful lab members throughout my undergraduate and graduate studies, without whom research would have been unbearable. I would first like to acknowledge Dr Ella Atlas for her constant support and supervision and for reviewing my thesis on her own time. Thank you for all of your help. I also want to thank Dr Sebastien Soubeyrand for reviewing many of my progress reports in French and for insightful discussion about 'science' and many protocols that I used in this thesis. Also many thanks to Kyna Caminiti and Rahin Farzadfar for their friendship, support and for helping me improve my English throughout the years.

I would like to acknowledge the Heart and Stroke Foundation of Ontario and the Canadian Institutes of Health Research for funding my graduate studies over the past 5 years.

J'aimerai remercier ma belle-sœur Marie-France pour son encouragement et support constant durant toutes mes études universitaires; ma nièce Nadia et mes neveux Nouradin,

Mohamed et Amir qui, de part leur présence, m’ont toujours fait sourire et oublier les difficultés que j’ai rencontré depuis la dernière décennie. Finalement, j’aimerai remercier mes parents, Nadira et Salem, qui m’ont toujours encouragé, malgré la grande distance qui nous sépare.

Merci à tous!

Table of Contents

List of abbreviations

AD	activation domain
AMP	adenosine monophosphate
aP2	fatty acid binding protein (also FABP)
ATP	adenosine triphosphate
bZIP	basic leucine zipper
cAMP	cyclic AMP
C/EBP	CCAAT/enhancer-binding protein
ChIP	chromatin immunoprecipitation
CoIP	co-immunoprecipitation
CS	calf serum
DBD	DNA binding domain
dex	dexamethasone
DMEM	Dulbecco's modified Eagle's medium
DMSO	Dimethyl sulfoxide
DNA	deoxyribonucleic acid
EDTA	ethylenediamine tetra-acetic acid
FBS	fetal bovine serum
GR	glucocorticoid receptor
GRE	glucocorticoid receptor element
GSK3β	glycogen synthase kinase
HAT	histone acetyl transferase
HDAC	histone deacetylase
Hsp	heat shock protein
IP	immunoprecipitation
LAP*	liver-enriched activating protein 1
LAP	liver-enriched activating protein 2
LIP	liver-enriched inhibitory protein
MAPK	mitogene-activated protein kinase
MCE	mitotic clonal expansion
MI	MIX and insulin
MIX	3-isobutyl-1-methyl-xanthine
MID	MIX, insulin and dex
mRNA	messenger RNA
NP-40	nonidet P40
PBS	phosphate-buffered saline
PPAR	peroxisome proliferator-activated receptor
RD	regulatory domain
RLU	relative luciferase units
RU	relative units
RNA	ribonucleic acid
SEM	standard error of the mean
SD (or s.d.)	standard deviation
WT	wild-type

List of tables

List of figures

Results of Chapter 3.1

Results of Chapter 3.2

Discussion

Appendix 7: Additional experimental figures

CHAPTER 1 - INTRODUCTION

Obesity is currently one of the major health issues worldwide. Obesity is characterized by an excess of fat that is stored in the white adipose tissue (WAT) in response to excess of nutrient availability. Glucocorticoids seem to facilitate WAT development and favour central (or visceral) obesity, a condition that is strongly associated with insulin resistance, type 2 diabetes and heart diseases.

Studies performed over the past two decades have defined a transcriptional cascade responsible for the differentiation of preadipocytes. Such a process involves members of the basic leucine zipper (bZIP) family of transcription factors (CCAAT/enhancer binding proteins or C/EBPs) and members of the class I and II nuclear receptors (glucocorticoid receptor and peroxisome proliferator activated receptor gamma or PPARγ, respectively). Moreover, our laboratory has linked the pro-adipogenic effect of the glucocorticoid receptor (GR) to C/EBPβ transcriptional activity. Thus, my thesis work has focused on understanding the interplay between transcriptional regulatory complexes that are implicated in the activation of C/EBPα transcription by C/EBPβ in preadipocytes at the onset of differentiation. My objective has been to define the interaction of the co-regulatory factors PCAF/GCN5 and mSin3A/HDAC1 to C/EBPβ that is regulated by GR during murine adipogenesis.

1.1 General concepts in transcriptional regulation

1.1.1 Brief description of the chromatin fiber

Eukaryotic cells have evolved elegant ways to store and use the genetic information that is encoded within their DNA. The enormous size of this genomic material is confined

within the walls of a single organelle, where it can be read and maintained: the cell nucleus. Within the nucleus, DNA is packaged with histone proteins to form a highly condensed structure known as the chromatin fiber. The DNA molecule is packaged in a manner that 146 base pairs are wrapped around an octomer of core histones composed of two copies of each of the histones H2A, H2B, H3 and H4. Further, the octomer of histones is formed when two copies of H2A-H2B heterodimer independently associate with a heterotetramer composed of two histones H3 and H4 bound together (*1-3*).

The DNA-histones complex unit is called the nucleosome and represents the first of several levels of compaction. Nucleosomes have been proposed to form units of trinucleosomes arranged in a way that facilitates a triple helix structure that is seen under the microscope as a 30nm chromatin fiber (*2*). This rearrangement requires histone H1, which binds to the DNA sequence between adjacent nucleosomes (linker DNA) to bring them closer to each other and thus further condense them (*2*). Chromatin exhibits various levels of condensation at different loci, which allows the cell to have a meticulous control of gene expression by regulating the interactions between the DNA molecule and histones and non-histone proteins. Cell biology research is slowly providing a clearer picture of the processes by which such remarkable organization occurs into focus.

The chromatin fibers consist of two types of heterochromatin (constitutive and facultative) and euchromatin regions. The numbers, locations and lengths of these regions within the chromatin fiber vary between cell types, and such variations give rise to different phenotypes. While the constitutive heterochromatin is a highly compact regions mostly composed of repetitive satellite DNA (as in the centromeres and telomeres of chromosomes), the facultative heterochromatin harbour genetic materials that are silenced during development (*4*). Euchromatin is, however, a more loosely packed chromatin that is prone

for transcription. Gene expression within the euchromatin regions is regulated by coordinating the epigenomic state of the cell (the cytosine methylation state of DNA and histone N-terminal tail post-translational modification) and the recruitment of chromatin remodeling complexes and transcription factors. In short, the basic steps of gene transcription could be summarized as follows: 1) localization of gene locus by already expressed factors; 2) opening of promoter region by remodeling complexes; 3) binding of transcription factors to consensus sequences on promoters and recruitment of co-factors; 4) DNA-bound transcription factors and/or their co-factors will recruit the pre-initiation complex; 5) pre-initiation complex recruits RNA polymerase II to start transcription.

1.1.2 The histones code

Histone-core proteins are post-translationaly modified on their N and C-terminal ‘’tails’’ by a large number of enzymes. Example modifications include acetylation, sumoylation and ubiquitylation of lysines (*5-9*), poly-ADP ribosylation of arginines, aspartic/glutamic acids (mostly on H1) (*7*), phosphorylation of serine and threonines (*10-12*), methylation of lysines (mono,di,tri) and arginines (*13-15*) among others. Such covalent modifications modulate nucleosome positioning by affecting the DNA-histones interactions that will result in regulating transcription factors access to their regulatory elements. Generally speaking, deacetylated histones are associated with repressed genes (i.e. heterochromatin) (*6*) whereas acetylation and methylation of histones are associated with transcriptional activation of genes (*5, 16-18*). There are cases where specific combinations of lysine acetylation and methylation of tail histones could, however, repress gene expression.

Biochemical analysis has shown that histone acetylation weakens DNA-histone interactions because the acetyl group neutralizes the positive charge on basic lysines and thus reduces the electrostatic interactions holding them together (*19*). On the other hand, while

histone sumoylation generally represses transcription by recruiting HDACs and heterochromatin proteins to gene loci (*8, 20*), ubiquitylation has been shown to be associated both with transcriptional activation and repression depending on the promoter context (*21-23*). Phosphorylation of histones also weakens histones-DNA interactions because of charge repulsion from histone phosphate and DNA phosphate groups (*24-25*) and thus favours gene activation (*26-27*).

Due to the diversity of histone modifications and their downstream effect on gene expression, Strahl and Allis proposed a ‘’histone code’’ hypothesis in 2000. They proposed that a certain pattern of histone tail modifications on a locus will lead to a specific gene response on that locus (*28*). This hypothesis is now widely accepted as an extensive number of independent studies corroborated their observations using genome wide mapping of histone acetylation and methylation (*29-32*).

1.1.3 Chromatin remodeling machinery

The epigenome, transcriptome and proteome of a given cell dictate the loci to be transcribed to maintain a defined cellular state (*33-34*). Because of the obvious interconnection between the genome, transcriptome and proteome, any change that could occur in one will influence the others. Thus, given that some promoters are epigenetically more inclined or poised for transcription (caused by the cytosine methylation profile and histone modifications), chromatin remodeling complexes will destabilise DNA-histone interactions to allow recruitment of DNA-binding transcription factors to either activate or repress specific gene expression (*33*).

Since DNA-histones interactions are not covalent, certain fluidity could be expected in nucleosomes. In fact, sliding of histones along the DNA in the nucleosomes has been shown to occur *in vitro* (*35-36*) and to be sequence-dependent (*37-38*), although the detailed

mechanism is still controversial. Evidently, changes in histone-DNA juxtapositioning require energy that could either be thermal or chemical; the latter provided by chromatin remodeling complexes through the hydrolysis of ATP molecules.

Chromatin remodeling proteins that alter DNA-histone interactions are conserved through species. Different complexes have been identified, based partially by their substrate specificity, such as SWI/SNF, CHRAC, ISWI and NuRD (reviewed in *39*). For example, yeast chromatin remodeling complex SWI/SNF has been characterized to contain, in part, SWI1/ADR6, SWI2/SNF2, SWI3, SNF5, and SNF6 and also the ATP-hydrolysis function of SWI2 was not required to form such a complex (*40*). SWI/SNF complexes have been shown to have DNA-binding abilities in yeast, thus shedding more light into their mechanism of action (*41*). Interestingly, mutation of yeast histones (equivalent of H3/H4) residues, implicated in nucleosomes stabilization through interaction with DNA, partially replaces the need of SWI/SNF complex in gene activation, thus supporting the SWI/SNF remodeling function (*42*).

SWI/SNF has been shown to either be recruited by transcriptional activators to promoters (*43*) or recruit transcription factors to promoters, as shown by E-RC1 (EKLF coactivator-remodeling complex 1)-dependent activation of the human beta-globin gene by EKLF (erythroid kruppel-like factor) (*44*). Interestingly, the RNA polymerase II holoenzyme complex has also been shown to contain SWI/SNF proteins and this observation was proposed to facilitate the transcription elongation step by the polymerase (*45*).

1.1.4 The epigenetic era

Post-translational modifications of histones can be triggered indirectly in response to environmental clues that will alter the activity of modifying enzymes and thus alter the transcriptome and proteome of the cell. It was long thought that this was as far as external

stimuli could affect gene expression. It was not until the discovery of covalent modifications of DNA molecules that the scientific community started to realize the significant role and impact that our environment plays in re-programming the genome through generations. Cytosine methylation by DNA methyltransferases on CpG regions have been reported for some time now (*46-47*) and are generally associated with gene repression and enriched in heterochromatin (*16, 20*). The importance of DNA methylation is evident from an increasing amount of studies investigating genome wide mapping of cytosine-methylation in different disease conditions in an attempt to elucidate methylation patterns that could promote cellular dysfunction (*48-52*). For instance, methylation of over 200 CpG regions was observed in normal and cancerous pancreas, whose patterns affect numerous gene expression changes associated with pancreatic cancer (*48*). Moreover, genome wide DNA methylation profiling shows a cell-type specificity that is associated with the different levels of CpG-methylation sites (*52*).

1.1.5 Histone deacetylases (HDACs)

The RNA polymerase II core promoter elements (approximately -40 to +40 nucleotides, where +1 is defined to be the transcription start site) are now known to vary depending on the genes. For instance, most promoters lack a TATA box which is replaced by other core promoter elements sufficient to recruit the pre-initiation complex (*53-54*). The TATA binding protein (TBP) can be replaced by TBP-related factors (TRFs) to bind TATA-less promoters and these factors are usually associated with the transcription factor IID (TFIID) complex (*55*). The composition of TFIID varies depending on the promoter/cellular context but is usually composed of several (12 to 15) transcription associated factors (TAFs) in addition to either TBP or TRF (*55*), whose recruitment are regulated by transcriptional repressors and activators.

Initiation of mRNA synthesis by RNA polymerase II requires that the chromatin remodeling factors and the DNA-binding transcription factors reorganize promoters by altering the post-translational modifications of histones, displacing nucleosomes and thus promoting exposure of the core promoter elements that will further allow nucleation of the pre-initiation complex on the promoter. Several co-repressor complexes have been identified (e.g NCoR (nuclear receptor co-repressor), SMRT (silencing mediator of retinoid and thyroid hormone receptor), Sin3A/B and NuRD (nucleosome remodelling and histone deacetylation) (*56-58*)) and their protein composition varies depending on the cell type and the promoter.

NuRD and Sin3 complexes share common functions and proteins. NuRD possesses deacetylase activity mediated by class I HDACs containing complexes composed of RbAp46/48 (or Rbbp7/4), HDAC1/2 in addition to nucleosome remodelling function by Mi-2α/β, among others co-factors (*57, 59-60*). Like NuRD, mammalian Sin3A/B complexes also contain the core Rbbp4/7/HDAC1/2 deacetylases where Rbbp4/7 and Suds3 (or mSds3) mediate HDAC1/2 interaction with histones and Sin3 respectively (*58, 61-62*). Although having redundant functions, Sin3A/B protein composition varies and both complexes independently regulate different promoters and processes like cell proliferation, cell cycle progression, apoptosis and T-cell development (*63-70*).

Sin3 proteins act as adapter proteins linking DNA-bound transcription factors to the HDAC1/2 deacetylases. For example, p53-mediated inhibition of the Map4, stathmin and c-Myb is dependent on p53-mSin3A direct interaction whereas p53 does not directly interact with the HDACs (*71-72*). Moreover, mSin3A has been proposed to mediate the connection between HDAC1 and the TAL1 transcription factor (*73*) and between HDAC1/2 and C/EBPβ (*66*), further supporting the adapter role of this protein. Although only Sin3A

examples have been given due to extensive studies on Sin3A, the high homology between Sin3A/B suggests a similar role in their respective complexes.

It is important to note that although only HDAC1 and HDAC2 are discussed here, there are numerous other deacetylases which are classified into 3 different classes. HDAC1 and HDAC2 belong in the first class of these deacetylases, along with HDAC3 (found in SMRT/NCoR complexes) and HDAC8. Class I HDACs are inhibited by the drug trichostatin A, ubiquitously expressed in mammalian tissue and localized mainly in the nucleus (*56, 74-77*). Class 2 HDACs includes HDAC4/5/6/7/9/10 which are involved in diverse processes including myocyte development (*78-82*), glucose uptake (*83*) and microtubule-dependent cell motility (*84-86*). Class 2 HDACs are also trichostatin sensitive but, unlike class 1 HDACs, they are not exclusively found in the nucleus, with evidence of an active shuttling mechanism regulating their activity (*78-82, 87-88*). The last HDAC so far identified is HDAC11 and, due to lack of homology with the other 2 HDAC classes, a third class has been proposed to accommodate this particular enzyme (*89*). So far, HDAC11 has been shown to be involved in neuronal cell development and T-cell activation (*90-92*) and to be inhibited by the trichostatin A analog trapoxin (*89*).

1.1.6 PCAF/GCN5-histone acetyltransferases (HATs)

Contrasting co-repressors, transcriptional co-activators usually promote chromatin relaxation and recruitment of the pre-initiation complex to allow transcription to occur by generally altering the histone/DNA interactions and by promoting co-repressor exclusion from promoters. Acetyltransferases have been extensively studied and their role in promoting gene transcription by acetylating histones and non-histone proteins is now widely acknowledged. Different families of acetylases (classified by homology) have been identified including p300/CBP (p300/CREB-binding protein), the GNAT family (Gcn5-related N-

acetyltransferase including GCN5 and p300/CBP-associated factor or PCAF, among others), the MYST family (for its members MOZ, Ybf2/Sas2/3 and Tip60), TAF1 (for TATA-binding protein-associated factor 1), among others, as reviewed in (*93-94*).

GCN5 and PCAF bear 75% sequence homology and are ubiquitously expressed and both have an acetyltransferase domain and a bromo domain that mediates histone acetylation and interaction, respectively (*95-97*). GCN5 and PCAF have been shown to acetylate lysine residues on histone H3 and H4 N-terminal tails, although they differentially acetylate specific lysine substrates within histones (*98-99*). The specificity for their substrate depends on the composition of the complexes into which they associate, including the human STAGA (SPT3-TAF9-GCN5) complex and its yeast equivalent SAGA (SPT-ADA-GCN5), TFTC (TBP-free-TAF complex) and TRRAP (transactivation/ transformation domain associated protein), where GCN5 and PCAF can be interchanged (*93, 100-102*). These complexes share common proteins subunits and the presence of either GCN5 or PCAF influences their interacting partners.

In addition to histones, GCN5 and PCAF also acetylate non-histone proteins. For instance, PCAF-mediated acetylation of the tumour suppressor p53 has been shown to increase its DNA binding ability, thus activating it (*103*). Furthermore, MyoD transcriptional activity during myogenesis has also been shown to be activated by PCAF-mediated acetylation (*104-105*). It has been shown that the GCN5-mediated acetylation of C/EBPβ and nuclear receptor SF-1 (steroidogenic factor-1) promotes their transcriptional activity; conversely, it appears to have an inhibitory effect on the transcriptional activity of peroxisome proliferators gamma co-activator 1 (PGC-1) (*106-108*). Collectively, these

results show that GCN5/PCAF-mediated acetylation of non-histone proteins modulate their function and transcriptional activity, hence indirectly regulate gene expression.

By contrast to PCAF, GCN5 expression occurs during embryonic development whereas during adulthood, they are differentially expressed in the mouse organs (*109*). The significance of GCN5 has been demonstrated in studies showing that GCN5 knockout mice die during embryogenesis, thus suggesting an essential role for GCN5 during early development. PCAF deficiency however did not elicit any abnormalities (*109*). Although PCAF functions were thought to be dispensable in mice, it was recently proven otherwise. When behavioural studies were done in mice lacking PCAF, it was observed that these animals show an impaired short-term memory and response to stress due to high corticosterone levels, decreased number of CA1 cells in their hippocampus and altered learning capacities thus suggesting that PCAF function in the brain cannot be replaced by GCN5 (*110-111*).

1.2 Adipogenesis

1.2.1 Obesity

Obesity is currently a worldwide issue. The World Health Organisation (WHO) estimates that over one billion people are overweight or obese, with a body mass index (BMI) higher than 25 kg/m^2. Obesity is characterized by an excess of fat in the body due to the unbalance between caloric intake and energy expenditure. Numerous factors contribute to the caloric unbalance seen in obese patient, such as heredity, food habit, physical activity, environmental factors and stress. The consequences of obesity could impact an individual physically, psychologically and socially, thus making this condition a serious health hazard. Moreover, knowing that obesity increases the risk of a variety of diseases in addition to

affecting the psychosocial state of an individual, numerous studies have been conducted to discover the genetic factors associated with this condition.

Adipose tissue represents an important resource of energy for the organism. Since adipocytes are filled with lipids, their primary function has been long considered to be solely a depot of metabolic energy to be used in a negative energy balance situation. However, it is now known that adipose tissue is an endocrine gland that produces hormones such as TNF-α (tumour necrosis factor-α), PAI-1 (plasminogen activator inhibitor-1), leptin and glucocorticoids, among others (*112-115*). Thus, the adipose tissue can be considered as a major organ in maintaining the body's energy homeostasis and metabolic balance.

There are two main types of adipose tissues found within the body: white adipose tissue (WAT) and brown adipose tissue (BAT). WAT is the more predominant type of adipose tissue in the body and the adipocytes that constitute it present with a small number of very large lipid droplets that occupy most of their cytoplasm. BAT cells however consist of a high number of smaller droplets and contain higher mitochondrial content (reviewed in *116*). The most significant difference between WAT and BAT is that BAT cells express an uncoupling protein (UCP-1) in their internal mitochondrial membrane that allows them to dissipate the gradient of protons produced by lipid oxidation which causes the cells to produce heat instead of ATP.

We now know that preadipocytes originate from multipotent mesodermal stem cells. Characterization of adipocyte biology increased dramatically after murine 3T3 L1 and 3T3 F442A cell models from 3T3 swiss albino mouse embryos were isolated and extensively studied in culture (*117*). Subcutaneous injection of 3T3 F442A in *Balb C* mouse lead to a normal development of fat deposit, thus validating their *in vivo* adipogenic potential (*118*).

These findings have helped to create a cell culture differentiation protocol for murine preadipocytes that is now widely used to study adipogenesis.

Even if most of the current knowledge about preadipocyte differentiation arose from studies performed with the 3T3 L1 model, studies using primary preadipocytes that can be isolated from subcutaneous and visceral adipose tissue in mouse and human have corroborated most of the findings obtained from the immortalized 3T3 L1 cell line (*119*). Moreover, the transcriptional cascade that occurs prior to the maturation of preadipocytes (discussed on page 14) follows a similar trend between the 3T3 L1 model and human primary preadipocytes (*120*). Although studies using the human primary preadipocytes are more relevant when investigating adipogenesis, there are some key limitations. Not only do they take longer to differentiate (two weeks at least), they also cannot be cultured for a longer time to expand the limited initial material, thus creating more variability when using cells from different donors.

1.2.2 Murine adipogenesis

Adipocyte differentiation is initiated by treating preadipocytes or fibroblastic/stem cells with a defined cocktail of inducers two days after their confluency, causing growth arrest. Treatment with insulin, a synthetic glucocorticoid hormone dexamethasone (or dex) and a cAMP phosphodiesterase inhibitor 1-methyl 3- isobutyl xanthine (or MIX), will start the differentiation process very efficiently in culture (*121*). This treatment will then cause a series of 2-3 cell divisions, known as mitotic clonal expansion (or MCE), required for adipogenesis, as shown by numerous studies (*122-126*); however opposing results have also been published (*127*).

Although insulin treatment of preadipocytes is not required for a proper differentiation process, the hormone accelerates lipid accumulation (*128-129*). In addition to

increasing glucose import *via* the glucose transporter-4 (GLUT-4), insulin initiates the Ras signalling pathway by binding to the insulin-like growth factor-1 (IGF-1). This binding will result in the activation of mitogen-activating protein kinase (MAP kinase), whose role will be described in greater detail later. The importance of the Ras-signaling pathway is underlined by the fact that an active Ras-GTP can replace insulin during adipogenesis (*130-131*).

The increased concentration of cAMP levels caused by MIX during the initial phase of adipogenesis allows for expression of the cyclic AMP response element binding protein (CREB), followed by its activation by the protein kinase A (PKA)-dependent phosphorylation. CREB then acts to activate C/EBPβ expression by recruiting the co-activator complex p300/CREB binding protein (p300/CBP) to the CRE elements on its promoter (*132-135*).

The last inducer used in the differentiation process is dexamethasone. The precise mechanism of action of glucocorticoids during adipogenesis has been a mystery for some time now and remains to be fully elucidated despite significant progress in understanding GR's role in transcriptional regulation. Briefly, GR has been shown to induce C/EBPδ expression directly by binding to a GRE on its promoter, to repress the anti-adipogenic preadipocyte factor 1 and to activate C/EBPβ transcriptional activity during adipogenesis (*66, 106, 136-138*). The detailed molecular mechanism of C/EBPβ activation during adipocyte differentiation will be discussed in a later section.

1.2.3 NIH 3T3 adipocyte differentiation

The NIH 3T3 cell line is a pluripotent fibroblastic cell line originating from Swiss mouse embryos. They have the ability to differentiate into myoblast, chondrocyte and

adipocyte lineages in response to specific stimuli. Ectopic expression of C/EBPβ, C/EBPα or PPARγ drives adipogenesis in NIH 3T3 cells following treatment of the cells with the standard inducer cocktail (*106, 139-142*). Although over-expression of C/EBPδ induces 3T3 L1 differentiation only in the presence of inducers, the number of fully differentiated cells is lower than induction by C/EBPβ over-expression (*140*). This difference in C/EBPδ adipogenic potential is further evidenced in NIH 3T3 cells where its over expression results in much less differentiation than cells expressing C/EBPβ, thus highlighting C/EBPβ as a more prominent factor in adipogenesis in both fibroblastic and preadipocyte cell lines (*140*). Given these facts, it is important to note that some discrepancies still exist in the use of the NIH 3T3 system when investigating murine adipogenesis. For instance, the NIH 3T3 cells have been suggested to have a compromised glucose import function due to an absence of glucose transporter 4 (GLUT4) expression, which makes them insensitive to insulin (*139, 143*). Since it has been suggested that such a phenotype could be caused by a lack of C/EBPα expression (*139, 143*) and since our laboratory has previously showed that C/EBPα is in fact expressed in NIH 3T3 cells (*66, 106*), the reason why such conflicting results are observed will be discussed later on in relation to new findings presented in this thesis.

1.2.4 Transcriptional cascade during adipogenesis

It is now well established that C/EBPβ and C/EBPδ expression is detected within 2-4h after induction of differentiation, whereas C/EBPα and PPARγ are downstream of the former two proteins (*137, 140, 144*) (see figure 1 for a summary of the differentiation program). The function of C/EBPα and PPARγ are required for the completion of adipogenesis and also for maintaining their own expression at elevated levels (*145*). The relevance of C/EBPβ, C/EBPδ, C/EBPα and PPARγ in adipogenesis is evidenced in loss-of-

Figure 1: The murine adipogenesis model.

Two days post-confluent 3T3 L1 cells are induced to differentiate with MIX, insulin and dexamethasone (referred to as MID). The elevation of cyclic AMP levels will activate CREB, which will then bind and recruit the co-activator complex p300/CBP to the C/EBPβ promoter. In parallel, translocation of GR to the nucleus upon binding to its ligand (dex) will activate C/EBPδ expression. Additionally, the expression level of the inhibitory protein CHOP10 will start decreasing gradually, until its suppression at around 12-14h post-induction, time point after which C/EBPβ and C/EBPδ will start binding to the C/EBPα and PPARγ promoters and thus initiate their transcription. Concomitantly, both C/EBPβ and C/EBPδ will also initiate the mitotic clonal expansion process that will increase the cell number. Once C/EBPα and PPARγ proteins are expressed (48h post-induction), they will cross-regulate each others expression without further need of C/EBPβ and C/EBPδ activity, whose expression will interestingly be suppressed by day 4. Lastly, C/EBPα and PPARγ will initiate transcription of their target promoters and the ensuing proteins will then give rise to the mature adipocyte phenotype.

3T3 L1 preadipocytes differentiation program

Day -2 Cells at confluency

Day 0 Treatment with MIX, insulin and dexamethasone (MID)

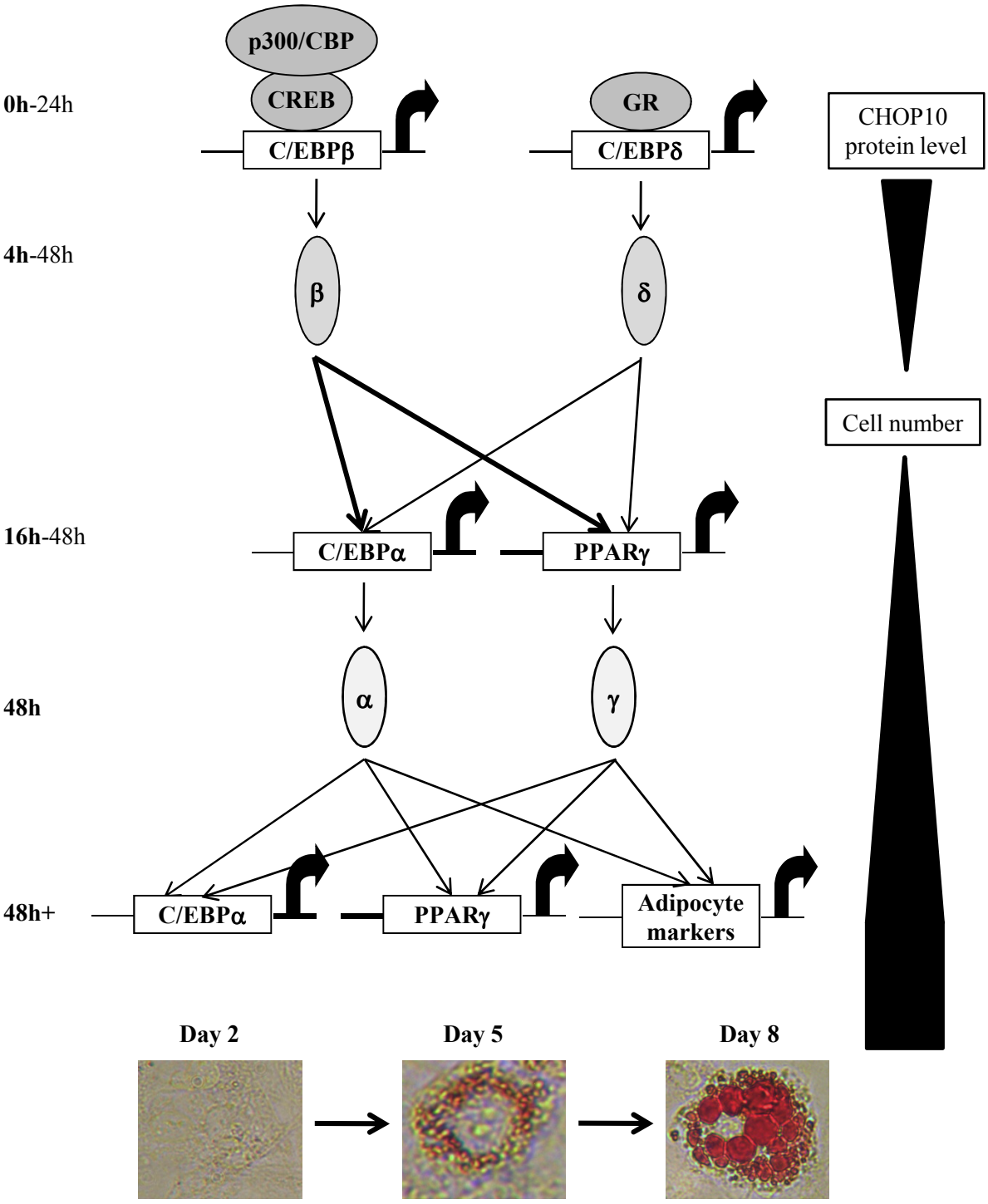

function studies using knockout mice models. C/EBPβ$^{-/-}$ and/or C/EBPδ$^{-/-}$ mice have impaired adipose tissue development as shown by smaller fat pads (*146*). More recently, C/EBPβ$^{-/-}$ mice were shown to be resistant to a high fat diet-induced obesity, exhibited increased beta-oxidation in their BAT, when compared to their wild type (WT) counterparts (*147*) and reduction of diabetes in Lepr mice (*148*). C/EBPα knockout mice exhibited severely impaired energy homeostasis and these animals died a few hours after birth (*149*). Adipocytes did not accumulate lipids as well as in WT mice, glycogen storage and neoglucogenesis in hepathocytes were severely decreased, and intriguingly, UCP-1 protein expression in BAT was also altered (*149*). Given that C/EBPβ$^{-/-}$δ$^{-/-}$ or C/EBPα$^{-/-}$ mice still showed WAT tissue, the results suggest that these factors could compensate for the absence of one another during WAT development. Since PPARγ knockout mice died during embryonic development due to a severe heart defect, chimeric mice were developed by injecting PPARγ$^{-/-}$ embryonic stem (ES) cells into blastocysts and the proportion of adipose tissue in PPARγ$^{-/-}$ chimeric mice were compared to those expressing PPARγ in the derived mice (*150-151*). The results show that PPARγ is indeed essential for adipogenesis and ES cells lacking PPARγ do not undergo differentiation (*151*).

When two days post-confluent 3T3 L1 cells are treated with the inducer cocktail, it triggers a relatively fast expression of C/EBPβ and C/EBPδ that reaches maximum levels at approximately 24h (*137, 152*). Although their protein levels can be detected 4 hours after induction, these two transcription factors are initially unable to regulate gene transcription. This is because the known C/EBP inhibitory protein, C/EBPζ/CHOP10, is expressed during the initial phase of preadipocyte differentiation (*153*) and inhibits C/EBPβ and C/EBPδ transcriptional capacities by suppressing their DNA-binding ability (*153-155*).

CHOP10 expression starts to decrease as soon as 4h post-treatment and continues to do so until it is not detected at around 16h, hence allowing C/EBPβ and C/EBPδ to be transcriptionally functional (*153*).

Even if one might expect C/EBPβ DNA-binding capacity to start with CHOP10 downregulation (i.e. 4h post-treatment), it does not occur until about 16h post-treatment (*153, 156*). This observation suggested that another mechanism regulates C/EBPβ DNA-binding ability. Indeed, it has been shown that C/EBPβ is phosphorylated at residue Thr^{188} by MAPK within 4h post-treatment, followed by GSK3β mediated phosphorylation of Thr^{179} and Ser^{184} (*156*). Interestingly, MAPK-mediated phosphorylation is a pre-requisite for GSK3β-mediated phosphorylation (*156-157*). These post-translational modifications are thought not only to expose the DNA-binding domain of C/EBPβ, but also to facilitate oxidation and disulfide bond formation between monomers to stabilise C/EBPβ binding to its target promoters (*156, 158-159*). Interestingly, numerous studies have shown the involvement of C/EBPβ DNA-binding capabilities in the MCE during adipogenesis (*124-125, 152, 160-166*) by binding to centromeric satellite DNA (*152*). Even though C/EBPδ has been shown to also bind centromeric satellite DNA, its involvement in MCE has not been studied as extensively as C/EBPβ (*152, 167*).

When C/EBPβ DNA-binding ability is acquired, its activity is further regulated by its acetylation state, to reach its maximum level at about 24h post-treatment (*66, 106*). The delayed activation of C/EBPβ is thought to prevent a premature C/EBPα expression to allow mitotic clonal expansion to occur since C/EBPα is a highly anti-mitotic factor (*168-170*). Activation of C/EBPβ (along with C/EBPδ) will initiate C/EBPα and PPARγ transcription, the two commitment factors in adipogenesis (*171-175*). Although it is still unclear whether

C/EBPα expression precedes PPARγ, there is some evidence suggesting this sequence of expression (*174, 176*). The PPARγ promoter has a KLF5 (kruppel-like factor 5) response element, in addition to its C/EBP element (*176*), thus possibly making its activation more complex than that of C/EBPα. This implies that the KLF5 transcription factor expression has to be upstream of PPARγ expression. Interestingly, C/EBPβ/δ have been shown to activate KLF5 expression thus adding another player in the initial transcriptional cascade (*176*). Together, these findings suggest that PPARγ expression requires either C/EBPβ/δ and KLF5 or C/EBPα (either alone or with KLF5, as no data is currently available supporting either regulation), hence making it more likely to be expressed after C/EBPα.

Once expressed in preadipocytes, C/EBPα and PPARγ are sufficient to finalize the adipogenic phenotype by expressing the adipocyte markers (such as aP2, adiponectin, adipsin, leptin, among others) (*177-181*), to maintain their own expression and to also cross-regulate each others' expression (*145, 182*) (figure 1). If either C/EBPα or PPARγ is over-expressed in preadipocytes, adipogenesis will efficiently occur without pre-treatment with MIX, insulin and dex, otherwise required to reach a similar level of differentiation (*183-184*). Although nearly all of the adipogenic genes require both C/EBPα and PPARγ transcriptional activity, the insulin-sensitivity phenotype is thought to be more dependent on C/EBPα expression (*145, 185*). Even if a recent genome wide ChIP-on-chip study confirmed the overlap in promoter-binding of C/EBPα and PPARγ to adipocyte-specific markers (*186*), PPARγ seems to have the primary role in fulfilling the final adipocyte phenotype (*151*).

1.3 Families of transcription factors involved in adipogenesis

1.3.1 CCAAT/Enhancer-Binding Proteins

More than two decades ago, the first member of the CCAAT/enhancer-binding protein (C/EBP) family of transcription factors has been cloned and its basic leucine zipper (bZIP) domain was characterized as being able to bind to the palindromic ATTGCGCAAT sequence in a ‘’scissor grip’’ way (*187-190*) **(**figure 2A**)**. Soon after C/EBP purification and characterization from rat livers, Spiegelman’s group linked for the first time the role of this C/EBP protein in regulating aP2 (or FABP, fatty acid binding protein) expression in adipocytes (*191*). This C/EBP protein is now known as C/EBPα.

C/EBPβ was independently identified by numerous laboratories. Its first characterization was in the activation of interleukin 6 in the acute phase response following bacterial LPS treatment of cells and was consequently named nuclear factor for interleukin 6 (NF-IL6) (*192-193*). Additionally, Cortise’s and Lee’s group showed C/EBPβ involvement in IL-6 signal transduction (naming it IL-6DBP) and in alpha 1-acid glycoprotein expression (naming it AGP/EBP) (*194*), respectively. Moreover, Schibler’s group characterized it as being a liver-enriched transcriptional activator protein (or LAP) that regulates albumin expression and that could dimerize with C/EBPα (*195*).

Soon after C/EBPβ, C/EBPγ was identified in B-cells and was shown to bind to CCAAT elements in the variable heavy chain locus during B-cell development and to heterodimerize with C/EBPα (*196*). Johnson’s group then identified two new C/EBP members, C/EBPε (which they named CRP-1) and C/EBPδ (or CRP3), along with the known C/EBPβ (here referred to as CRP2) (*197*). After identifying C/EBPα, McKnight’s group identified C/EBPβ and C/EBPδ together and showed that they can heterodimerize and activate the albumin gene promoter, as previously showed by Schibler’s group (*137*). More importantly, McKnight’s study was the first one to identify the transcriptional cascade that

Figure 2: The CCAAT/Enhancer-Binding Protein family of transcription factors.

Schematic representation of C/EBPα/β/γ/δ/ε and ζ showing their activation domains (AD), regulatory domains (RD), basic DNA-binding domain (B) and the leucine zipper dimerization domain (zip). The figure also shows the different translation product for C/EBPα (42 and 30 KDa proteins), C/EBPβ (34, 30 and 15 KDa proteins) and C/EBPε (32, 30, 27 and 14 KDa proteins). Note that C/EBPζ (or CHOP) has a compromised DNA-binding domain, which makes it a dominant-negative dimerization partner. The lower panel shows the crystal structure of what two bZIP domains (blue and red) bound to DNA (green) look like. Notice the ''scissor grip'' way by which the two bZIP domains bind to their target DNA.

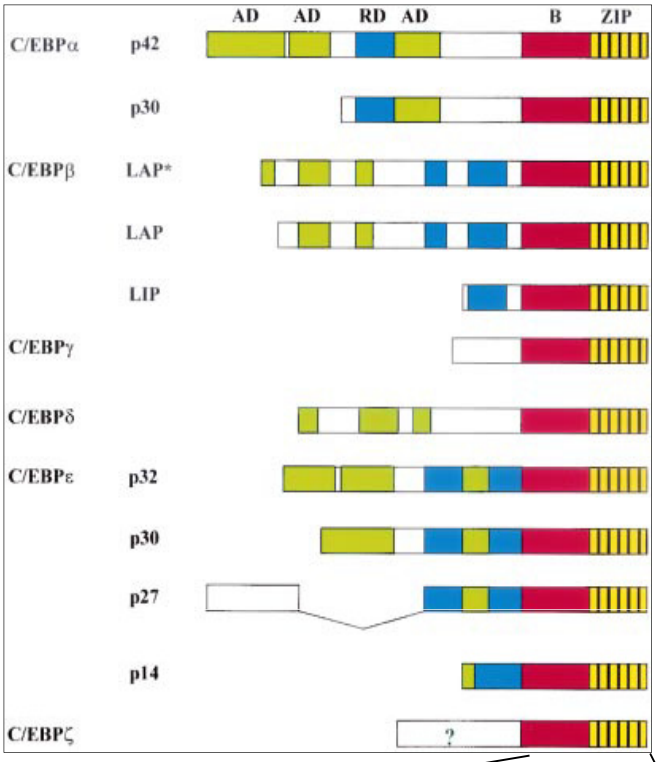

Ramji et al. (2002)

occurs in murine adipogenesis involving C/EBPα, C/EBPβ and C/EBPδ (*137*).

The last C/EBP member identified was C/EBPζ (also known as CHOP-10 or gadd153) (*198*). Due to its distinct structure, its homology to the other members was not immediately noticed (see figure 2B). CHOP-10 has been shown to bind and inhibit C/EBPα and C/EBPβ activity by Ron *et al.* (1992). It has a disrupted DNA-binding domain that prevents its binding to the CCAAT DNA sequence and thus acts as a dominant-negative factor for all the other C/EBPs (*155*). Together, these studies have shown that the C/EBPα, C/EBPβ, C/EBPγ and C/EBPδ genes are a family of intronless genes that have a bZIP domain that is highly conserved, except for CHOP-10 which lacks a functional basic domain. By contrast to the other members, CHOP-10 and C/EBPγ are ubiquitously expressed (*196, 198*).

The C/EBPs bZIP domain is composed of a heptad repeat of leucine residues that form alpha-helices exposing the leucine hydrophobicity in a way that allows them to interact with the monomere leucine region and then allows the dimer to form a scissor-like structure (*190*). C/EBPs can heterodimerize with other bZIP proteins like ATFs, CREB, FOS and JUN (reviewed in *199*). C/EBPβ binds to Fos and Jun *in vitro* independently of DNA and this interaction represses its activation potential, most likely due to a weaker interaction with the C/EBPβ cognate promoter elements (*200*). However, C/EBPβ has been shown to heterodimerize with another family of bZIP proteins without losing its activity, as shown by its dimerization with ATF4 that allows them to promote osteoblast maturation by activating the osteocalcin promoter (*201*).

Knowing that these transcription factors could form homo- and/or heterodimers, one could expect that each dimer will behave differently thus causing a differential gene

expression profile. In fact, EMSA analysis using the same oligonucleotide showed that C/EBPβ binds DNA with a higher affinity when compared to C/EBPα or C/EBPδ, based on their dissociation constant (*137*). When Luciferase-based transcription assays were done in mammalian cells, each homo- or heterodimer exhibited different transactivation potential on the PPARγ, albumin, IR1, IR2 or aP2 promoters (*137, 145, 171*). Since there are no crystal structures of any of the full length C/EBPs, it is challenging to understand how these proteins position themselves on DNA molecules in their homo/heterodimers form; although structural and biochemical studies are slowly unveiling this mystery.

1.3.2 Peroxysome proliferator activated receptors

The peroxysome proliferator activated receptors (PPARs) belong to the second class of nuclear receptors, along with the thyroid, vitamin D and retinoic acid receptors that function as transcriptional regulators that are activated upon binding to their ligands. They bind to their cognate DNA sequence as obligate heterodimers with the retinoic X receptor (*202-205*). There are currently three known members of the PPAR subfamily (α, β/δ and γ) identified in vertebrates and they are all involved in tissue development, energy metabolism and inflammation (reviewed in *206*). Although it is established that unsaturated fatty acids are PPARs' ligands (*206*), endogenous ones have yet to be identified.

PPARγ transcription produces two mRNAs (1 and 2) via usage of two different promoter elements that give rise to two protein isoforms (PPARγ1 and 2), where the first one has an extra N-terminal domain composed of 30 residues in human (28 in rodent) (*207-209*). Although PPARγ1 expression is more ubiquitous than that of PPARγ2, the latter is expressed at the highest level in adipose tissue, thus making it the primary PPAR transcription factor involved in energy metabolism (*205, 210*).

1.3.3 Glucocorticoid receptor

Cushing syndrome is a human condition characterized by an elevated level of cortisol due to a pituitary or an adrenal gland tumour causing elevated protein catabolism, immune system suppression and ultimately visceral fat accumulation (*211*). Moreover, when patients with inflammatory diseases are treated with glucocorticoids, they also show similar symptoms as those observed in individuals with Cushing syndrome (*211-213*). It has been long known that the effect of the steroid hormone cortisol is mediated through the glucocorticoid receptor (GR). The function of this protein is almost omnipotent in an individual due to its ubiquitous expression, therefore underlining its physiological importance (*211*).

GR is part of the class I nuclear receptor family which includes the mineralocorticoid, progesterone and androgen receptors. GR is a transcription factor that regulates diverse processes like cell growth, differentiation, inflammation and thus various physiological responses (*214-218*). The importance of GR is evident in studies carried out with mice where the GR gene was disrupted. These mice died a few hours after birth mainly due to lung atelectasis (*219*). These mice exhibited several phenotypes including impaired neoglucogenesis and elevated corticosterone and adrenocorticotropic hormone (ACTH) levels, which the authors speculate may be the result of altered pro-opiomelanocortin (POMC) expression (*219*). GR has been extensively studied and this summary will be to emphasize the mechanism of action of GR in transcriptional regulation of preadipocyte differentiation.

Prior to binding to its ligand, GR is found in a cytosolic complex partly composed of heat shock proteins (HSP) 90/70/50/20, which keeps GR in an inactive state, while maximizing its ligand-binding potential (*211*). Physiologically, GR is activated upon binding

to its glucocorticoid ligands secreted by the adrenal cortex during time of stress (*220*). The GR-ligand complex translocates to the nucleus where it positively/negatively regulates gene transcription by either binding to glucocorticoid response element (GRE)-containing promoters as a homodimer and/or by modulating the transcriptional activity of other DNA-bound transcription factors (*221-223*).

The GR consist of four main domains that includes an N-terminal regulatory domain, followed by a DNA-binding, a highly flexible hinge domain and a ligand binding domain at its C-terminal end (*224-225*). The presence of the activation domains AF-1 and AF-2 in GR's N-terminal and C-terminal domains, respectively, differentially modulate its activity and the latter domain requires the receptor to be bound to its ligand for it to be functional (*226*). Although full length GR (GRα) possesses all of its domains, it is also translated in an isoform (GRβ) which lacks a portion of its steroid binding domain that functions as a dominant negative isoform in the GRα/GRβ dimer (*224, 227*). As previously mentioned, GR regulates gene expression by directly binding to GREs on promoters, preferentially as a homodimer as opposed to a monomer (*228*). In many instances, GR activating function depends on recruitment of p160 co-activators family member and the SWI/SNF chromatin remodelling complexes to gene promoters (*229-232*).

GR can positively and negatively regulate gene expression via its ability to bind GRE on promoters. For instance, GR can activate the AGP (alpha1-acid glycoprotein) gene along with C/EBPβ and transcriptional intermediary factor 1β (TIF1β) (*233*). GR DNA-binding ability has also been shown to inhibit the osteocalcin expression by competing with the TBP to bind the immediate promoter region since the GRE was overlapping with the TATA box (*234*). Interestingly, GR activity could also be modulated by binding to variant GRE

sequences that decrease its affinity to DNA (*235*). Moreover, the inhibitory role of GR can be initiated via recruitment of co-repressor complexes, as shown by the SMRT co-repressor complex recruitment on the glutathione S-transferase (GST) A2 gene (*236*). These observations underline the important concept of gradual gene expression regulation that could be caused by the number of transcription factors that bind to different elements on a promoter and by their affinity for their respective DNA sequence.

Although the previous examples illustrate the GRE-dependent mechanisms by which GR regulates gene expression, a DNA-independent mechanism also exists. For instance GR inhibited activator protein 1 (AP-1) activity via protein-protein interaction (*237*) and inhibited vasopressin expression from a promoter construct that did not contain GREs (*238*). Moreover, a GR construct lacking its DNA binding domain has been shown to regulate C/EBPα transcription during murine adipogenesis (*66*). Finally, the fact that mice lacking GR DNA-binding domain are still viable confirms the important function of the DNA-independent modes of action of GR (*239-240*).

1.3.4 C/EBPα regulation in preadipocytes

The significance of C/EBPα in white adipose tissue is well established as to its role in mediating not only the insulin-sensitivity phenotype in mature cells but also in co-regulating and maintaining, along with PPARγ, the final differentiation markers' expression, including themselves (*186*). Although C/EBPα is required for white adipose tissue, it is dispensable for brown adipose tissue development (*241*). Regulation of C/EBPα expression has been studied thoroughly, but the precise mechanism of its activation remains to be elucidated. We know that C/EBPα expression is repressed in preadipocytes and that the repressed state is thought to be caused by the presence of two CUP (C/EBPα undifferentiated protein) elements in the

proximal 5' promoter and in the 5' untranslated region of C/EBPα gene; and by the binding of the Sp1 DNA-binding protein on its promoter element, immediately upstream to the C/EBP element (*242-243*). Therefore, in preadipocytes, the C/EBPα promoter is in a repressed state characterized by the presence of DNA-binding factors that restrain C/EBPβ access to its sequence-specific site and thus keeping C/EBPα expression minimal until MCE occurs. Nonetheless, this promoter is in an accessible state in preadipocytes (as opposed to the fibroblastic NIH 3T3 cell line), as shown by its histone H4 acetylation state, therefore suggesting that it is poised for transcriptional activation (*66*). Moreover, this acetylation is thought to be mediated by the Sp1-dependent recruitment of p300/CBP acetylase complex to the C/EBPα promoter. Sp1 and p300 association within the same regulatory complex has been shown to regulate numerous gene promoters, including p16(INK4a) (*244*), involucrin (*245*), keratin 16 (*246*), cytochrome P450scc (*247*), among others, therefore further supporting the previous hypothesis.

The treatment of preadipocytes with the differentiation cocktail MIX and insulin displaces Sp1 from the C/EBP element on the C/EBPα promoter and allows binding of C/EBPβ since Sp1 and C/EBPβ elements overlap (thus making Sp1 an inhibitor of C/EBPα expression in adipocytes) (*242*). It is suggested that Sp1 displacement is caused by MIX and that it occurs in two ways: by an increase in proteasomal degradation and by a decreased DNA-binding ability due to increase in its phosphorylation state (*242, 248*). Insulin may also contribute to Sp1 inactivation since the ERK/MAPK pathway has been linked to Sp1 transcriptional regulation on the versican promoter (*249*).

Once bound to the C/EBPα promoter, C/EBPβ recruits an acetylase complex (p300/GCN5) and a deacetylase complex (mSin3A/HDAC1), as shown by chromatin

immunoprecipitation analysis at 24h post-treatment (*66, 106*). Furthermore, HDAC1 recruitment to the promoter decreases histone H4 acetylation, counteracts the p300/GCN5 co-activator effect and prevents recruitment of the pre-initiation complex (*66*). However, upon the addition of glucocorticoid to the MIX and insulin duo, GR translocates to the nucleus where it helps increase C/EBPα expression. Chromatin immunoprecipitation assays in these conditions showed that, 24h following treatment, mSin3A/HDAC1 occupancy decreases from the C/EBPα promoter, thus allowing the co-activator complex p300/GCN5 to acetylate local histone H4 and C/EBPβ, consequently recruiting RNA polymerase II holoenzyme complex to initiate transcription (*66, 106*). Although the precise role of GR in this activation is not fully understood, evidence from our laboratory and others suggest that this receptor will not only promote the 26S proteasomal-mediated degradation of HDAC1 but it will also decrease HDAC1 activity by promoting p300-mediated acetylation of HDAC1 (*66, 250*). Interestingly, GR is not detected at the promoter after treatment with either MI or MID; although its immunoprecipitation with HDAC1 after glucocorticoid treatment suggests that GR is directly involved in regulating HDAC1 activity possibly by promoting its proteasomal degradation (*66*).

1.4 C/EBPβ transcriptional potential

1.4.1 C/EBPβ transcriptional regulation

C/EBPβ is involved in a myriad of processes as it is highly expressed in many organs including, but not limited to, the liver, intestine, lung, adipose tissue, kidney and spleen (*137, 192, 195, 251*). C/EBPβ has been shown to activate cytokine and chemokine expression in the acute phase response after inflammation (*193, 252*), differentiation of macrophages

(*253*), tumour cell proliferation (*254-255*), breast cancer progression (*255-258*), prostate cancer (*259-260*), apoptosis (*261-264*), liver proliferation and function (*265-269*) and adipocyte differentiation (*137*), amongst others.

Although C/EBPβ is translated from one messenger RNA, three protein isoforms are produced from the first three in-frame methionines due to a leaky ribosomal scanning mechanism (*270-271*). These isoforms are called liver-enriched activating protein 1, 2 and liver-enriched inhibitory protein, referred to as LAP*, LAP and LIP, respectively. C/EBPβ transcriptional activity has been thoroughly studied and its transcriptional activation domains mapped and are located roughly between amino acids 22 to 93, as shown by sequence homology analysis with C/EBPα, C/EBPδ, C/EBPε and by deletion analysis using transcription assays (*158, 272-273*). LAP* and LAP are considered to be transcription activators since they both have the activation and bZIP domains, while LIP has only the bZIP domain, and is considered to function as a passive transcriptional repressor (schema in figure 3A) (*158, 270*). Importantly, LIP has been shown to inhibit LAP activity at substoichiometric levels since the majority of LIP forms LAP/LIP heterodimers, making it a potent passive inhibitor of C/EBP proteins (*270*). Although LIP and CHOP are C/EBP inhibitory proteins, it is important to keep in mind that they differ in their modes of action.

Other than being regulated by heterodimerization with various isoforms, C/EBPβ has been proposed to have two additional intrinsic transcriptional regulatory domains, RD1 and RD2, located between amino acids 138-169 and 183-211, respectively. RD1 has been shown to have general negative regulatory activity whereas RD2 was shown to affect C/EBPβ DNA-binding ability in a fibroblastic cell line only (*158*). The authors proposed that these two domains act independently to regulate C/EBPβ transcriptional activity. It was speculated

Figure 3: C/EBPβ-dependent regulation of C/EBPα transcription in preadipocytes: hypothesized model.

(A) Schematic representation of the C/EBPβ LAP* showing the N-terminal activation domains (AD) and the bZIP domain composed of the DNA binding (DBD) and the leucine zipper dimerization (zip). Some of C/EBPβ's post-translational modifications include methylation at arginine 3, GCN5/PCAF dependent acetylation (Ac) at lysines 98, 101, 102, sumoylation (SUMO) at lysine 133, phosphorylation (Ph) at threonine 179, 188, and serine 184 (located in RD2). The regulatory domain 1 (amino acids 136-166) and 2 (amino acids 183-211) are identified as RD1 and RD2, respectively. The activating LAP and inhibitory LIP isoforms are also represented. **(B)** In 3T3 L1 preadipocytes not induced to differentiate, C/EBPα expression is not upregulated and histone 4 is acetylated due to the presence of the HATs p300 and GCN5. When 3T3 L1 cells are induced to differentiate with MIX and insulin alone (MI) C/EBPβ binds and recruits an HDAC1-containing complex that leads to histone 4 deacetylation and low transcriptional activity is observed. Addition of dexamethasone to the differentiation cocktail (MID) results in GCN5-mediated acetylation of C/EBPβ, exclusion of HDAC1 from the C/EBPβ-interacting complex, increased acetylation of histone 4 and subsequent recruitment of RNA Pol II to the promoter. **(C)** By contrast to the 3T3 L1 preadipocytes, the NIH 3T3 fibroblasts do not show histone H4 acetylation on the C/EBPα promoter. Only ectopic expression of C/EBPβ will result in recruitment of the mSin3A/HDAC1 and GCN5/p300 containing complexes on the promoter. Like in 3T3 L1 preadipocytes, addition of dexamethasone will also result in potentiation of transcription.

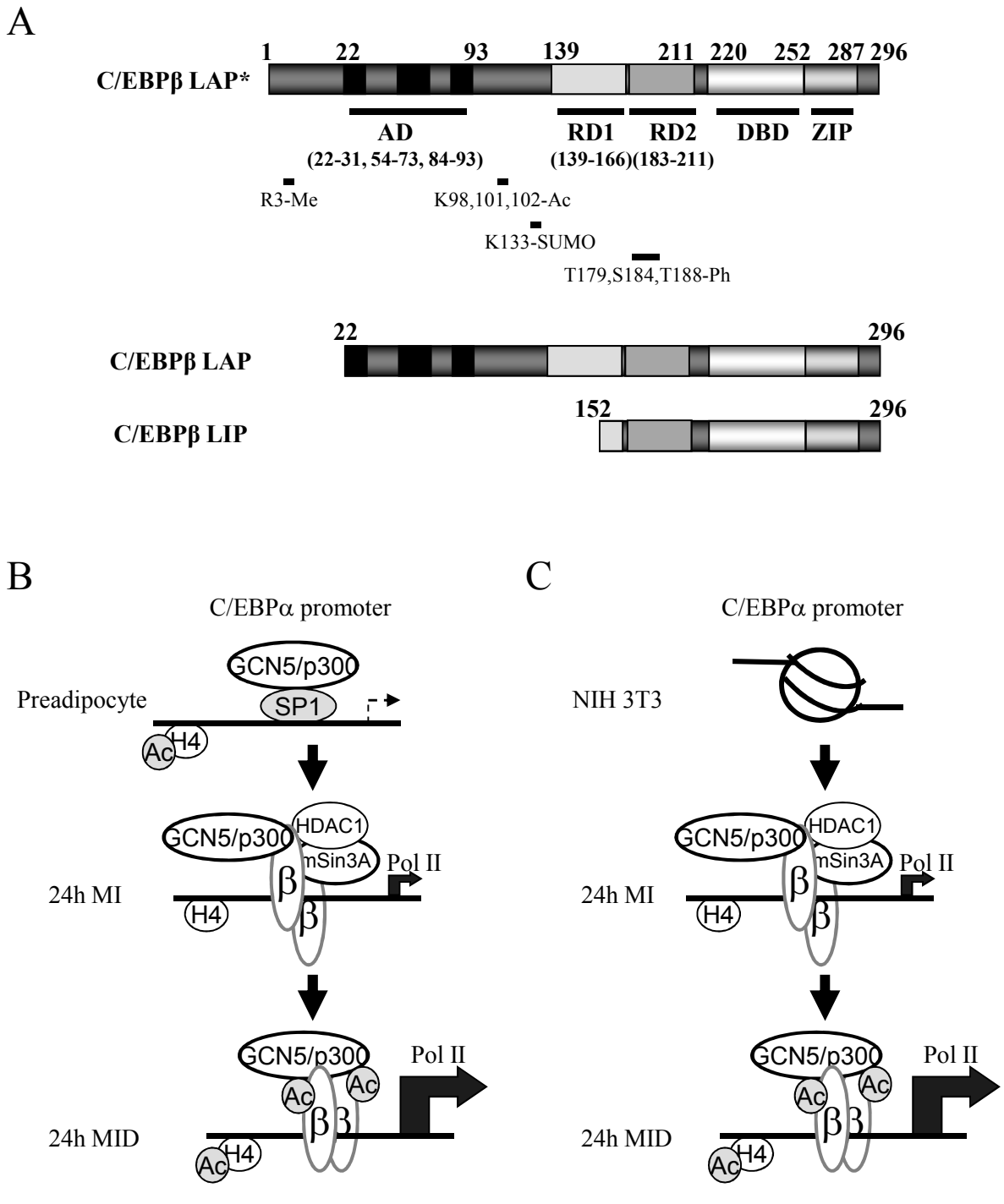
A
1
22
93
139
211
220
252
287
296
C/EBPβ LAP*
AD
(22-31, 54-73, 84-93)
RD1
(139-166)
RD2
(183-211)
DBD
ZIP
R3-Me
K98,101,102-Ac
K133-SUMO
T179,S184,T188-Ph
22
296
C/EBPβ LAP
152
296
C/EBPβ LIP
B
C/EBPα promoter
Preadipocyte
GCN5/p300
SP1
Ac
H4
GCN5/p300
HDAC1
mSin3A
Pol II
24h MI
H4
β
β
GCN5/p300
Pol II
Ac
Ac
24h MID
Ac
H4
β
β
C
C/EBPα promoter
NIH 3T3
GCN5/p300
HDAC1
mSin3A
Pol II
24h MI
H4
β
β
GCN5/p300
Pol II
Ac
Ac
24h MID
Ac
H4
β
β

that RD1 inhibits transcription by interfering with the activation domains via steric interactions whereas RD2 blocks the DNA-binding ability by interacting with the bZIP domain (*158*).

In addition to its intrinsic regulatory properties, C/EBPβ activity is also modulated by post-translational modifications. For instance, phosphorylation at threonine 188 has been shown to be required for growth hormone (GH)-induced c-fos expression (*274*) and for the induction of C/EBPα and adiponectin expression during adipogenesis (*157*). Additionally, phosphorylation at threonine 188 by MAPK followed by phosphorylation at serine 184 and threonine 179 by GSK3β has been shown to activate C/EBPβ DNA-binding ability (*156*).

Other than phosphorylation, acetylation of lysines 39, 98, 101 and 102 by p300/PCAF/GCN5 has also been shown to be required for C/EBPβ activity on the C/EBPα, PPARγ, leptin and GLUT4 promoters (*65, 106, 275*). Additionally, mSin3A/HDAC1 activity has been shown to negatively regulate C/EBPβ activity by deacetylation on the aforementioned promoters (*66, 275*).

C/EBPβ has also been shown to be methylated at arginine 3 (present on LAP* but not LAP) via an interaction with the methyl transferase PRMT4/CARM1 (*276*). This modification impairs the interaction of C/EBPβ with the SWI/SNF complex and MAPK-mediated phosphorylation and thus decreases its activity (*276*). Since C/EBPβ undergoes numerous modifications that affect its interaction with partners and consequently its activity, the researchers proposed that C/EBPβ modifications exemplify a ‘‘*transcription factor code of modifications that tunes transregulatory functions*’’, in analogy to the histone code (*276*).

Although a small fraction of the literature is used to describe the C/EBP family in this text, the complex role and regulation of these few genes and their products reflect on how a

small number of genes can have such a profound impact at the cellular level. When the human genome was sequenced, the scientific community was expecting to discover thousands of new genes to explain the complexity of the cell and the human body. Surprisingly, less than 27000 protein-coding transcripts were identified and their sequences span only 1.1% of the genome whereas the introns by themselves cover 24% of genomic DNA (*277*). Seemingly a small number of transcripts, we now know that the determining phenotypes of an organism arise from the combinatorial effect of transcripts splicing, level of expression, localization and post-translational modification of proteins.

1.4.2 Differential roles of LAP*, LAP and LIP during murine adipogenesis

Although it is widely accepted that the differential expression of C/EBPβ isoforms is tightly regulated in different cellular contexts, little is known about LAP* and LAP contribution to the activation of C/EBPα and adipocyte differentiation. We know that LIP inhibits adipogenesis when expressed in 3T3 L1 and NIH 3T3 cells (*140*). LIP decreases C/EBPβ and C/EBPδ activity by forming heterodimers that lack one of the activation domains located at the N-terminal domain of either LAP*, LAP or C/EBPδ dimers (*158, 270*), thus making LIP mode of action a passive repression mechanism.

While both LAP* and LAP isoforms have the same activation domains, LAP* does not seem to activate transcription as efficiently as LAP. Numerous studies suggest that C/EBPβ may be susceptible to sumoylation (*278-281*) where LAP* sumoylation is inhibitory to its activity (*278, 281*). Interestingly, the first 21 amino acids (in murine C/EBPβ) are not sumoylated. The conserved SUMO consensus ([I/V/L]KXEP) site is located upstream of the RD1 and lysine residue 133 has been shown to be sumoylated within the consensus LKAE in LAP* (*280-281*).

A second reason why LAP* activity may be reduced is that its N-terminal domain contains a cysteine (Cys11) that has been suggested to form an intramolecular disulfide bond with Cys33 that acts as an inhibitor of transcription by diminishing LAP* DNA-binding ability *in vitro* (*282*). Moreover, oxidation of cysteines present in the C-terminal domain of LAP* (upstream and downstream of the bZIP domain) have been shown to also decrease LAP*/LAP DNA-binding ability and thus its transcriptional activity (*283*). Together, these findings support an important role of the nuclear redox state in modulating C/EBPβ transcriptional activity.

1.5 Rationale and objectives

C/EBPβ transcriptional activity has been shown to be regulated by numerous post-translational modifications mediated by its interacting partners. Current evidence suggests that the increasing diversity of these modifications differentially regulates C/EBPβ activity depending on the cellular environment in which it is expressed. Although numerous regulatory domains (i.e RD1 and RD2 as negative regulatory domains) have been proposed to regulate the basal transactivation potential of C/EBPβ, their hypothesized modes of action were speculative because the conclusions were based on results obtained from the analysis of relatively large deletions of C/EBPβ LAP and from transcription assays only. To circumvent this problem, I sought to delineate smaller domains and to define their contributions in regulating C/EBPβ transcriptional activity with respect to the known mSin3A/HDAC1 and PCAF/GCN5 co-regulatory complexes involved in modulating its activity. Moreover, since C/EBPβ is one of the main factors regulating adipogenesis, I also assessed the contribution of the identified domains in potentiating preadipocyte differentiation.

I hypothesized that GR regulates the dynamic interaction of GCN5 and mSin3A/HDAC1 with C/EBPβ to modulate C/EBPβ adipogenic potential through its ability to induce C/EBPα transcription at the onset of differentiation. To elucidate the mechanism of action of C/EBPβ during murine adipogenesis, the result section was divided in two main sections:

1. To characterize GCN5 and mSin3A/HDAC1 interplay in regulating C/EBPβ LAP/LIP activity during murine adipogenesis by identifying their binding domain in C/EBPβ;
2. To elucidate the contribution of newly identified C/EBPβ regulatory domains in potentiating NIH 3T3 and 3T3 L1 adipogenesis.

To test my hypotheses, standard assays in transcriptional regulation were used. To examine the transcriptional activity of C/EBPβ, Luciferase-based transcription assays were used, where the proximal promoter of C/EBPα or PPARγ were cloned upstream of the Luciferase cDNA. This method allows us to measure the rate at which a transcription factor would activate a known promoter and also helps us predict quickly if a factor regulates a potential promoter bearing the DNA regulatory element of interest. The sensitivity and simplicity of this method allows us to quickly test hypotheses before performing more complex but physiologically relevant experiments. Since it is now widely known that distal regulatory elements of genes modulate their expression as much as the proximal ones, their absence in the Luciferase-based assays represent an important limitation as it excludes the contribution of distal co-regulators. Moreover, since epigenetic modifications account for a major fraction of gene regulation, the absence of a well chromatinized DNA on the

Luciferase plasmids adds a great limitation as to how epigenetic modifications could affect the transcriptional activation of the factor studied.

To support results from the Luciferase-based transcription assays, endogenous mRNA levels of the target genes are also measured to confirm that the transcription factor studied behaves similarly in a more physiological system. This method however does not measure the transcription rate of one factor as multiple transcription factors collaborate to modulate the level of gene expression *in vivo*.

Further, chromatin immunoprecipitation assays are used to show that the transcription factor of interest can be recruited to a known promoter. This method however does not differentiate direct or indirect binding to promoters. Such a limitation could be resolved by using the *in vitro* electromobility shift assay (EMSA), which assesses direct binding of a factor to a DNA template.

In summary, my results established that the interaction of mSin3A/HDAC1 with C/EBPβ occurs through all of its three isoforms (LAP*, LAP and LIP) and thus identified a new HDAC1-dependent mechanism by which LIP inhibitory function occurs on the C/EBPα promoter during murine adipogenesis. Moreover, I showed that GCN5-dependent activation of C/EBPβ seems to be dispensable in conditions where HDAC1 is unable to associate with C/EBPβ, hence making HDAC1 a dominant inhibitor of C/EPBβ activity when investigated on the C/EBPα promoter and preadipocyte differentiation. I also showed that GR-dependent activation of C/EBPβ LAP* requires expression of the LIP isoform and that some of LAP* inhibitory function is mediated through the redox-state of cysteine 11. Finally, I defined region 141-149 of C/EBPβ as being required for a suitable activation of C/EBPα transcription, but not of PPARγ, by LAP*/LAP, when investigated in murine adipogenesis.

CHAPTER 2 - MATERIALS AND METHODS

2.1 Plasmid constructs and preparations

Cloning was performed using standard techniques. The list of primers used to generate all constructs and plasmids used in the subsequent experiments are listed in Appendix 1**.** Briefly, C/EBPβ mutants 108C, N107, N140, N168, N184 and N217 were constructed by a PCR strategy to amplify the region of interest using pMSV-C/EBPβ as template (kindly provided to our lab by Dr S.K. McKnight). Forward primers had an EcoRI restriction site upstream of the first ATG and reverse primers had a BamHI restriction downstream of the stop codon. The PCR was performed using Vent DNA polymerase (New England BioLabs) as per the manufacturer instructions, with 5% DMSO to reduce non-specific amplifications. After performing the PCR reaction, the amplified fragments were separated on a 1% agarose gel and the fragment of interest was purified from the gel using a commercially available gel purification kit (Qiagen). After purification, the sample was digested with BamHI and EcoRI (New England BioLabs), followed by heat-inactivation of the enzymes and then used in a ligation reaction with T4 Ligase (New England BioLabs). Inserts were ligated with the pGEX-2T vector (GE healthcare), which was also pre-digested with the appropriate enzymes. The ligated plasmids were then transformed into competent *Escherichia coli* (E. coli) DH5α.

C/EBPβ was subcloned from pMSV-C/EBPβ to the mammalian pcDNA3.1(-) vector (Invitrogen) between the BamHI and EcoRI restriction site located in the multiple cloning sites. To do so, full length C/EBPβ was PCR amplified using a forward primer with a BamHI restriction site upstream of the first ATG and a reverse primer with an EcoRI restriction

downstream of the stop codon. C/EBPβ_{LIP} and C/EBP$\beta_{LIP\ 6C}$ were PCR amplified and cloned in pcDNA3.1(-) in the same manner (refer to appendix 1 for primers).

For the internal deletion mutants, an inverse PCR strategy was used to amplify the region of interest. The primers used in all internal deletions were first phosphorylated with the T4 polynucleotide kinase (New England BioLabs) prior to the PCR reaction. Briefly, C/EBP$\beta_{\Delta 141\text{-}168,\ \Delta 141\text{-}149,\ \Delta 141\text{-}156,\ \Delta 151\text{-}156,\ \Delta 153\text{-}156}$ were PCR amplified using the Pfu polymerase (Stratagene) following the manufacturer instructions, with 5% DMSO to reduce non-specific amplifications, using either pGEX2T-C/EBPβ, pMSV-C/EBPβ or pcDNA3.1(-)-C/EBPβ as templates. The samples were resolved on a 1% agarose gel, after which the fragment of interest was purified from the gel, digested with DpnI to remove any parental plasmids, ligated and transformed into competent E. coli DH5α by electroporation using the electromax instrument (BioRad).

All pLXSN (Clonetech) constructs were subcloned from pcDNA3.1(-) constructs. Briefly, the pcDNA3.1 constructs were digested with EcoRI and BamHI to isolate the appropriate inserts, after which they were ligated into the pLXSN plasmids and transformed into E. coli DH5α. In all cases, clones were sequenced to ensure the absence of any PCR-generated mutations and the plasmids were amplified using the Maxi-prep kit from Qiagen. Note: All constructs are listed in appendix 2.

2.2 Cell culture and transient transfection

2.2.1 Cos7 and Phoenix Ampho cells

Cos7 (ATCC CRL-1651) and Phoenix Ampho (Orbigen RVC-10001) cells were maintained in Dulbecco's Modified Eagle's Medium (DMEM, 4.5 g/L) supplemented with

penicillin, streptomycin, 10% fetal bovine serum (FBS) and grown in an incubator at 37^{o}C and 5% carbon dioxide (CO_2). Cos7 cells were maintained with 25 µg/ml of plasmocin to eliminate mycoplasma contamination (Invivogen).

2.2.2 NIH 3T3 and 3T3 L1

NIH 3T3 cells (ATCC CRL-1658) were maintained in DMEM supplemented with penicillin, streptomycin, 10% calf serum (CS) and grown in an incubator at 37^{o}C and 10% CO_2. 3T3 L1 cells (ATCC CL-173) were maintained as per the NIH 3T3 cells, however a low glucose DMEM was used instead (1.5 g glucose per litre).

For the dual luciferase assay, NIH 3T3 cells were maintained and grown as previously described. However, when the cells were ready to be split, they were re-suspended and seeded into 6 well dishes (7-8X10^4 cells per well) in a phenol red-free DMEM supplemented with sodium pyruvate, penicillin, streptomycin and 10% charcoal stripped FBS.

All DMEM media, sodium pyruvate, antibiotics and serums are from GIBCO, Invitrogen and used as recommended by the manufacturer. In all cases, the media is changed every two days to ensure proper growth.

2.2.3 Transient Transfection

Cos7, NIH 3T3 and Phoenix cells were transfected using the FuGENE HD reagent (Roche) as recommended by the manufacturer. The quantity of DNA transfected is specified in each experimental section that follows and the FuGENE:DNA ratio used was 3µl:1µg respectively. Briefly, the FuGENE HD reagent was first mixed with either DMEM (with no supplements) or OptiMEM (GIBCO) at a ratio of 3µl FuGENE HD per 100µl media (for each 1µg of DNA) and left at room temperature for 5-10 minutes. The FuGENE/media was then added to the DNA sample, mixed and incubated at room temperature for 15-30 minutes.

The FuGENE:media:DNA mixture was then added to the cells, which had been seeded the day before to reach about 80% confluency on the day of the transfection. The media was replaced the next day and at two days post-transfection, the cells were ready to be analysed.

2.3 Retroviral infection of murine cells

2.3.1 Transfection of the Phoenix Ampho packaging cells

In order to generate replication incompetent retroviruses, Phoenix cells were transfected with 2µg of pLXSN construct using the FuGENE HD reagent after being seeded onto 10 cm plates (70-80% confluency). The following day, the media was changed and replaced with 6 mL of fresh media. Two days post-transfection, the supernatant containing the viruses was removed and filtered through a 0.45µm filter using a 5mL sterile syringe. The virus stock was either used directly for infection or was stored at -80^{o}C in a 15mL falcon tube.

2.3.2 Infection of 3T3 L1 and NIH 3T3

Prior to infection, 3T3 L1 and NIH 3T3 cells were seeded at approximately 70% confluency onto 10 cm plates. The next day, the media was replaced with 5mL of fresh media and 5 mL of the viral supernatant was added to the cells in addition to 4µg/mL of polybrene (Millipore). The following day, the media was changed and the cells were grown for an additional day before being split to avoid confluency. Thereafter, cells were maintained with the geneticin antibiotic (G418, 400µg/mL) for 10 days, which was sufficient to select for cells expressing the constructs

2.4 Differentiation of NIH 3T3 and 3T3 L1 cells

2.4.1 Differentiation protocol

Two days post-confluent 3T3 L1 and NIH 3T3 cells were treated with either 1-methyl 3-isobutyl xanthine (MIX, 500µM), insulin (100 nM) or MIX, insulin and dexamethasone (dex, 250 nM) for 48h, designated as MI or MID respectively. Cells were subsequently incubated in their respective media supplemented with 100nM insulin until they were harvested, as specified in each experimental section. Differentiation of LIP-expressing 3T3 L1 cells was done with increased inducer's concentration (1mM MIX, 200nM insulin and 1µM dex) to promote a higher differentiation level.

The differentiation experiments were performed in 6 well dishes for western analysis, RNA extraction for real time RT-PCR and Oil Red O staining. Ten centimetres plates were used for all co-immunoprecipitation (CoIP) and chromatin immunoprecipitation (ChIP) experiments.

The calf serum used for the 3T3 L1 and NIH 3T3 cells was previously screened from different lots before being used in any experiments. Regular differentiation experiments were done using the 3T3 L1 cells and the lot that displayed a low adipogenic potential without the hormone was kept and used throughout all other experiments to ensure a consistent glucocorticoid response.

2.4.2 Oil Red O staining

3T3 L1 cells were differentiated for 8 days and NIH 3T3 cells for 6 days before being stained. Briefly, each well of cells was gently washed twice with 1mL of PBS (phosphate buffer) before being fixed for 30-60 minutes in 1mL of 4% formaldehyde (10% formalin). Following the fixation period, the wells were rinsed twice with PBS before adding 500µl of Oil Red O stain (Sigma-Aldrich) dissolved in propylene glycol (3.5g/500mL) for either 2h or

overnight. Cells were then extensively washed with water to remove as much Oil Red O excess as possible to decrease background colouration and were stored at 4°C in water.

After the staining process, cells were visualised with a phase contrast light microscope at 2X magnification in order to have a visual representation of the lipid accumulation in the cells, by detecting the red lipid-Oil Red O complex. The pictures taken typically represent most of the well, whereas the extremities were usually avoided. The cells around these areas tended to lift more than the center area, and most likely occurred during media replacement. The photomicrographs shown are a representation of 3 to 4 different experiments.

2.5 Mammalian cell extracts and Western analysis

2.5.1 Whole cell extracts

For all Western analyses, whole cell extracts from 3T3 L1 and NIH 3T3 cells were prepared as follows. Cells were washed twice with 1mL of cold PBS, scraped, collected into a 1.5mL eppendorf tube and centrifuged for 4 minutes at 4000g at 4°C. The cell pellet from each well was re-suspended in 100µl of a lysis buffer (50mM Tris-HCl pH 7.4, 150mM NaCl, 5mM EDTA, 0.5% nonidet P-40 and freshly added 1mM DTT and 1X complete protease inhibitor cocktail from Roche), incubated on ice for 10 minutes to swell and then sonicated for 10 seconds, at power level 10% with a Branson Sonifier 450 sonicator. The extract was then centrifuged at a minimum of 10,000g for 5 minutes at 4°C to pellet cellular debris and the supernatant was transferred to a new tube. A Bradford assay was used to quantify the protein content of the sample and 30-50µg of total protein was used for the subsequent electrophoresis.

2.5.2 SDS-PAGE and Western transfer

SDS-PAGE (Sodium Dedecyl Sulfate-Polyacrylamide Gel Electrophoresis) gels were prepared using standard protocols with the mini-PROTEAN kit (BioRad). Either 10%, 12% or 15% acrylamide SDS-PAGE were made. Proteins samples were denatured using the Laemmli loading buffer (62.5mM Tris pH6.8, 10% Glycerol, 2% sodium dodecyl sulphate (SDS), 0.05% bromophenol blue, 355mM 2-mercaptoethanol), boiled at 95^{o}C for 5 minutes, centrifuged at 10,000g for 1 minute, loaded in the appropriate acrylamide gel and then migrated until desired resolution was obtained. Transfer of the gels was performed according to standard transfer protocols using a PVDF membrane (BioRad).

2.5.3 Western blot analysis

After the transfer of proteins, the PVDF membranes were blocked for either 1h at room temperature or overnight at 4^{o}C in 5% (m/v) skim milk solubilized in 30mL PBS-T (PBS with 0.1% (v/v) of Tween-20 detergent). Incubation with the primary antibody (see appendix 3 for details) was performed in 5% skim milk in PBS-T for 2h at room temperature or overnight at 4^{o}C on a nutator, after which the membranes were washed 3 times with approximately 50mL PBS-T for 10 minutes each. The membranes were then incubated with a horseradish peroxidise (HRP)-conjugated secondary antibody for 1h at room temperature.. The dilution used was 1:10,000 for anti-rabbit (GE Healthcare), 1:10,000 for anti-goat (Santa Cruz Biotechnology) and 1:50,000 for anti-mouse (GE Healthcare) in 5% skim milk PBS-T. Following the secondary antibody incubation, the membranes were again washed with approximately 50mL PBS-T 3 times for 10 minutes each. The ECL developing reagent mix (enhanced chemiluminescence, Perkin Elmer) was then added to the membranes, which were then exposed on an autoradiography film (Kodak BioMax). Following exposure, the

membranes were stripped using the re-blot plus solution (Millipore) for 20 minutes at room temperature and the whole procedure was repeated with another antibody.

2.5.4 Indirect immunofluorescence

Prior to seeding cells in 6 well dishes, sterilized coverslips were added to each well. Coverslips were sterilized by ethanol dip and passed through a flame. The cells were then added to the dishes and spread carefully to ensure an even distribution of cells on the surface of the coverslip. The following day, the cells were transfected with 500ng of the pcDNA-C/EBPβ constructs using the FuGENE HD reagent. Two days post-transfection, the cells were washed twice with 1X PBS and then fixed with 4% formaldehyde for 30 minutes in a dark fridge. Cells were then permeabilized with 2mL of 0.5% Triton X-100 in PBS for 30 minutes at room temperature. The permeabilization buffer was then replaced with 0.5mL of blocking solution (5% bovine serum albumin (BSA)) in PBS for 1h rocking at room temperature. The blocking buffer was replaced with 0.5mL of a primary antibody against C/EBPβ (C-19) (Santa Cruz Biotechnology) re-suspended in PBS-T (dilution 1:400) for 2h at room temperature. The wells were then washed 3 times with PBS for 2 minutes each time. Five hundred microlitres of the Alexa 488-conjugated (donkey anti-rabbit, 1:400 dilution in PBS) (Molecular Probes) secondary antibody was then added to the cells for 45 minutes on a rocking platform at room temperature with an aluminum cover. The coverslips were washed again 3 times with PBS for 2 minutes each time, dried and placed face down on top on a drop of Vectashield mounting medium with DAPI (Vector Laboratories) on slides. Nail-polish was used to seal the edge of the coverslip to the slide, which were then wrapped in aluminum foil and stored at -20^{o}C. A fluorescence microscope was used to visualise the green fluorescence (Zeiss-Axiovert, 200M microscope) with 63X objective lens and pictures were

taken using the multi channel acquisition function so that overlap between DAPI and C/EBPβ could be seen.

2.5.5 Immunoprecipitation

Cos7 cells grown to 80% confluency were transiently transfected with 2 μg of the expression plasmid for either Flag-HDAC1 or Flag-GCN5 and 2ug of the pcDNA-C/EBPβ constructs using the FuGENE HD reagent using a 3:1 ratio for 16h. The media was changed the next day and cells were allowed to grow for an additional 16-24h. Cells were then lysed using a lysis buffer (150mM NaCl, 1mM EDTA pH 8.0, 50mM Tris-HCl pH 7.0, 0.5% NP-40 and freshly added 1mM DTT and 1X protease inhibitor cocktails) for 25 minutes at 4^{o}C on a rotating wheel. Whole cell extract was obtained by spinning the lysed cells at 4^{o}C for 10 minutes at 10,000g.

HDAC1 immunoprecipitation was performed with 500μg of total protein (1μg protein per 1μl buffer) in the lysis buffer with 0.15% NP-40 for 2h at 4^{o}C using 30μl of the M2 FLAG resin (Sigma). Following 3X1mL washes with the same buffer (0.15% NP-40), proteins were resolved on a 10% SDS-PAGE and transferred to a PVDF membrane. Blots were probed with antibodies against C/EBPβ (C-19) (Santa Cruz Biotechnology) and FLAG (FLAG M2 monoclonal, Sigma). GCN5 immunoprecipitation was performed similarly. However, following the protein extraction in the lysis buffer containing 150mM NaCl, the sodium chloride and NP-40 content was reduced to 100mM and 0.10%, respectively, during the binding with the M2 FLAG resin and during the washes.

For the endogenous HDAC1 immunoprecipitation in NIH 3T3 and 3T3 L1 cells stably expressing the C/EBPβ constructs, 2μg of the HDAC1 C-19 antibody (Santa Cruz Biotechnology) was used for 2h 4^{o}C on a rotating wheel. For the negative control, 2μg of a

non-specific antibody was used (Gal4 DBD N-19, Santa Cruz Biotechnology). Following the incubation, 40µl of protein-G sepharose slurry (Sigma Aldrich) was added to the samples and incubated for 1h at 4^{o}C on a rotating wheel. The precipitates were then washed 3X1mL with the lysis buffer and the proteins resolved on a 10% SDS-PAGE and transferred to a PVDF membrane. The same HDAC1 antibody (1:400 dilution) used in the immunoprecipitation reaction was used to probe the membrane.

2.5.6 Chromatin immunoprecipitation

NIH 3T3 and 3T3 L1 cells stably expressing the various C/EBPβ constructs were grown and treated with MIX (500µM) and insulin (100 nM) at 2 days post-confluency for 24h. Cells were then washed twice in serum free media, collected via scraping, transferred to a 15mL falcon tube in 5mL serum free media and fixed with 1% formaldehyde for 10 minutes at room temperature, on a rotating wheel. Tubes were then centrifuged using a table top centrifuge for 4 minutes at 2000g, at 4^{o}C and the cells were then washed twice with 1mL of cold PBS. Pelleted cells were washed with two sets of 10 minutes washes at 4^{o}C with 1mL cold buffer I (0.25% Triton X-100, 10mM EDTA, 0.5mM EGTA, 10mM HEPES pH 6.5) and then once with 1mL cold buffer II (200mM NaCl, 1mM EDTA, 0.5mM EGTA, 10mM HEPES pH 6.5). The cell pellet was then re-suspended in 100µL sonication buffer (1% SDS, 10mM EDTA, 50mM Tris pH 8.0, freshly added 1mM DTT and 1X complete protease inhibitor cocktail), sonicated twice for 10 seconds at power level 10% with the Branson Sonifier 450 sonicator and then centrifuged at 4^{o}C for 10 minutes at 10,000g. Ten microlitres of the supernatant was used as input control by adding to it 290µL of extraction buffer (1% SDS, 0.1M $NaHCO_3$), incubated overnight at 65^{o}C to reverse the cross-linking reaction and then stored at -20^{o}C until the immunoprecipitates were ready. Eighty microlitres of the

supernatant were used for the immunoprecipitation. Briefly, the sample was diluted 20X in dilution buffer (1% Triton X-100, 150mM NaCl, 2mM EDTA, 50mM Tris pH 8.0, freshly added 1mM DTT and 1X complete protease inhibitor cocktail). The diluted sample was pre-cleared with 60µl of protein-G sepharose slurry (Sigma Aldrich) and 2µg of sheared salmon sperm DNA (Invitrogen) for 2h at 4^{o}C on a rotating wheel. The sample was then centrifuged for 2 minutes at 2,000g at 4^{o}C and the supernatant was transferred to a new tube where it was incubated with 5µg of HDAC1 C-19 antibody (Santa Cruz Biotechnology) overnight at 4^{o}C on a rotating wheel. The following day, the precipitation reaction was accomplished by adding 60µL of the protein-G sepharose slurry (Sigma Aldrich) to the sample with 2µg of sheared salmon sperm DNA and incubated for 1h at 4^{o}C on a rotating wheel. The precipitates were then washed sequentially with 1mL of TSE I (0.1% SDS, 1% Triton X-100, 2 mM EDTA, 20mM Tris pH 8.0, 150mM NaCl), TSE II (0.1% SDS, 1% Triton X-100, 2 mM EDTA, 20mM Tris pH 8.0, 500mM NaCl), buffer III (0.25M LiCl, 1% NP-40, 1% sodium deoxycholate, 1mM EDTA, 10mM Tris pH 8.0) and twice in TE. All washes were performed at 4^{o}C on a rotating wheel. For the extraction, the precipitates were extracted 3 times in 100µL of 1% SDS, 0.1M $NaHCO_3$ at room temperatures for 10 minutes each time. To reverse the cross-linking reaction, the eluates were incubated overnight at 65^{o}C. The DNA fragments from the immunoprecipitates and from the input were purified using the QIAquick PCR purification kit (Qiagen). A PCR reaction using Taq DNA polymerase (Invitrogen) was then performed with primers against the murine C/EBPα promoter -334/-118 (sequence in appendix 4). Sonicated genomic DNA from NIH 3T3 cells was always used as a positive control for PCR while H_2O was used as a negative control to ensure a specific amplification of immunoprecipitated DNA. Each ChIP experiment was independently repeated 3 times.

2.5.7 ^{3}H-thymidine incorporation assay

To evaluate DNA synthesis in 3T3 L1 undergoing differentiation without or with the inducer cocktails, the cells were plated in 12 well dishes (each condition in triplicate) and pulsed with 2uCi ^{3}H-thymidine (Amersham) for 6h before harvesting. Following exposure to the thymidine, the cells were washed with ice-cold PBS and then incubated with ice-cold 5% TCA twice for 15 minutes at room temperature. Following an additional wash with PBS, the cellular extracts were scraped with 0.250mL of 0.5N NaOH/0.5% SDS and transferred to scintillation vials. Once all time points were collected, DPM values of incorporated ^{3}H-thymidine were measured in a scintillation counter (Beckman Coulter LS6500).

2.6 Dual Luciferase assay

2.6.1 C/EBPα-Luciferase assay

Approximately 7X10^{4} NIH 3T3 cells were seeded in each well of a 6 well dish and maintained in standard phenol red-free media supplemented with charcoal stripped FBS, as in the cell culture protocol section. The next day, 200 ng of the C/EBPα-promoter (-350 to +6 of murine gene) Firefly Luciferase reporter plasmid, 100 ng of pTL-GR construct (full length rat glucocorticoid receptor), 25 ng of the CMV-driven Renilla-Luciferase reporter plasmid as an internal control (Promega) and 50 ng of the different pcDNA-C/EBPβ constructs were transfected in each well. For transcription assays with the LIP isoforms, the same protocol was applied with the addition of 50 ng of either LIP_{wt} or LIP_{6C}. Total transfected DNA was brought to 1 ug with the addition of empty pcDNA plasmid and the FuGENE HD reagent was used (3:1 ratio). Sixteen hours after transfection, media was changed and the cells were treated with either ethanol (vehicle) or 1μM dexamethasone.

Approximately 16-24h later, cells were washed twice with 1mL PBS, lysed directly in their well using 300µl of the 1X passive lysis buffer provided in the dual luciferase reporter assay kit (Promega) and incubated for 20-30 minutes at room temperature before acquiring Luciferase readings for each sample. Twenty microlitres of each well was added to a 96 well plate and the Luciferase activity of each sample was read using a luminometer (LUMIstar, BMG Labtech), as per the manufacturer instructions. Each experiment was performed 3 times (each condition in duplicate or triplicate where indicated) and corrected for transfection efficiency by using the cotransfected renilla expression plasmid. Values were expressed in relative luciferase units since they were normalized independently.

2.6.2 PPARγ-Luciferase assay

The same procedure as the C/EBPα protocol was used with few modifications. Briefly, the NIH 3T3 cells were transfected with 400ng of the PPARγ-promoter (-609 to +52 of the murine gene) Firefly Luciferase reporter plasmid, 100 ng of pTL-GR construct, 25 ng of the CMV-driven Renilla-Luciferase reporter plasmid and 200 ng of the different pcDNA-C/BPβ constructs or 400ng of the pMSV-C/EBPα, pMSV-C/EBPβ, pMSV-C/EBPδ (from Dr McKnight). Total transfected DNA was brought to 1 ug with the pcDNA3.1(-) plasmid and the FuGENE HD reagent was used with a 3:1 ratio.

2.7 Real time reverse-transcriptase PCR reaction

2.7.1 RNA extraction and reverse transcriptase reaction

On the day of extraction, cells were washed twice with 1mL PBS and then RNA was extracted using the RNeasy Mini Kit (Qiagen), as per the manufacturer's instructions. Total RNA was quantified and 5 to 10µg of RNA was used for the reverse transcriptase reaction,

as follows for every sample. Two and a half microlitres of 10X DnaseI buffer and 0.5µL DnaseI enzyme were added to the RNA sample, for a total volume of 25µL, and incubated at 37°C for 10 minutes. Two and a half microlitres of 50mM EDTA (pH 7.5) was added to the sample and incubated for 10 minutes at 65°C to inactivate DnaseI. After being quick chilled on ice, 22µL of the sample was added to a new tube with 2µL of Oligo (dT) universal primer (Invitrogen) and 2µL of 10mM dNTPs followed by an incubation of 5 minutes at 70°C to ensure annealing of the primers to the cDNA. The sample was again quick chilled on ice, centrifuged and 8µL of 5X First-Strand Buffer, 4µL 0.1M DTT and 0.2µL Rnasin were added. The reaction mixture was incubated for 2 minutes at 42°C, after which 1µL of Superscript II DNA polymerase (Invitrogen) was added and incubated as follows: 50 minutes at 42°C, 15 minutes at 70°C and finally cooled down to 4°C. Samples were stored at -20°C until subsequent quantification.

2.7.2 Quantitative PCR reaction

To quantify C/EBPα and PPARγ (β-actin as an internal control), 12.5µL of a 2X SYBR green Master Mix (Applied Biosystems) was used with 2-4µL of cDNA (a blank reaction with no DNA was also used), 0.75µL of each primer (10µM) in a total volume brought to 25µL using ddH_2O. An addition of 1µL DMSO was added to the C/EBPα reactions to reduce non-specific amplification. Standards containing 1pg, 0.1pg, 0.01pg, 0.001pg, 0.0001pg of the appropriate DNA fragment were also run. Each sample was run in duplicate, excluding the blank reaction, on a 96 well plate (Applied Biosystems) that was properly sealed with its appropriate plastic cover (Applied Biosystems). The 7500 Real Time PCR System LightCycler (Applied Biosystems) was used and the results were quantified using the 7500 System SDS Software. All primers used are listed in appendix 4.

2.8 Acetylation and GST pulldown assays

2.8.1 Acetylation assay

GST fusion proteins bound to GST-Sepharose beads were expressed in *Escherichia coli* BL21 following GE Healthcare protocols. To ensure proper expression, proteins were resolved by 10% SDS-PAGE, stained with the Coomassie Blue Brilliant (0.1%, Sigma) and quantified relative to BSA protein standards of known concentration that were run on the same gel.

For the acetylation reactions, 2µg of GST fusion proteins (bound to GST-Sepharose beads) were incubated with either 500ng of recombinant PCAF (Upstate Biotechnology) or 1µg of recombinant His-GCN5 (bacterially expressed and purified using the TALON® His-Tag Purification Resins (Clontech)) in HAT buffer (50mM Tris pH 8.0, 0.1mM EDTA, 1mM DTT, 10% glycerol, 5µM TSA) with 0.2µCi of 14C-labeled acetyl-CoA at 30^{o}C for 1h. The mix was then resolved on a 10% SDS-PAGE and stained with Coomassie Blue (0.1%, Sigma). After drying the gel, each GST-fusion protein band was excised from the gel, put into a scintillation tube containing 3mL of scintillation liquid and the radioactivity was read with a scintillation counter (Beckman).

2.8.2 GST pulldown assay

In vitro translated (TNT coupled reticulocyte lysate system, Promega) and ^{35}S-labeled GCN5 and mSIN3A proteins were produced following the manufacturer's instruction. To verify proper translation, 1µL (out of 50µL) of translated proteins were migrated on a 10% SDS-PAGE, dried and the radioactive signal was visualised by PhosphoImager analysis (Typhoon Molecular Dynamics). GST fusion proteins were produced as mentioned before.

Once expression of both *in vitro* translated and bacterially expressed proteins were confirmed, 5µL of the *in vitro* translated proteins were incubated with 1-2µg of GST fusion

proteins (bound to GST-Sepharose beads) for 2h at 4^{o}C in 0.6X lysis buffer (25mM Herpes pH 9.9, 100mM KCl, 2mM EDTA, 20% glycerol and freshly added 2mM DTT and 1mM PMSF) containing 0.15% NP40. After 3X1mL washes using the same binding buffer, proteins were resolved by 10% SDS-PAGE, stained with Coomassie Blue (0.1%, Sigma) and dried. Binding was visualised by PhosphoImager analysis (Typhoon Molecular Dynamics). The levels of either mSin3A or GCN5 that were pulled-down with the GST- C/EBPβ fusion peptides were quantified using the ImageQuant software by taking into accounts the amount of the GST-C/EBPβ peptides used in the binding assay.

2.9 Statistical analysis

All P-values were calculated with the Microsoft Excel software using the one-tailed, paired Student's t-tests. A P-value smaller than 0.05 was considered significant.

CHAPTER 3 - RESULTS

3.1 Characterizing the interplay of GCN5 and mSin3A/HDAC1 in regulating C/EBPβ LAP/LIP activity during murine adipogenesis

Previous studies from the Haché laboratory and other groups have revealed the involvement of HDAC1-mediated deacetylation and p300/PCAF/GCN5-mediated acetylation of C/EBPβ in regulating gene expression, as mentioned previously (*65-66, 106, 275, 284-288*). However, the mechanism by which C/EBPβ is activated and the interplay between the acetylases and deacetylases on C/EBPβ-targeted promoters is still poorly defined.

To start investigating C/EBPβ transcriptional regulation by GR, HDAC1 and GCN5, I hypothesized that: 1) mutation in either the HDAC1 or the GCN5 binding domain in C/EBPβ will differentially the activation of C/EBPβ and 2) GR will regulate the activity of C/EBPβ LAP/LIP isoforms by affecting their interacting partners. My first objective was set to characterize C/EBPβ interaction with mSin3A after being acetylated by either PCAF or GCN5 *in vitro* and then to map the GCN5 and mSin3A binding domain in C/EBPβ. Following the delineation of the binding domains, my second objective was to characterize the transcriptional activity of C/EBPβ mutants lacking either GCN5 or mSin3A/HDAC1 binding domains in various assays. Luciferase-based assays of the C/EBPα promoter were used, in addition to the murine preadipocyte differentiation system to confirm the physiological importance of GCN5 and mSin3A in modulating C/EBPβ adipogenic potential.

My final objective was to define GR involvement in regulating the transcriptional activity of C/EBPβ isoforms (LAP*, LAP and LIP) during preadipocyte differentiation.

3.1.1 Identifying mSin3A and GCN5 binding domains in C/EBPβ

3.1.1.1 PCAF/GCN5-mediated acetylation of C/EBPβ reduces its *in vitro* binding to mSin3A

GR-dependent acetylation of C/EBPβ at lysine residues 98, 101 and 102 by PCAF/GCN5 has been shown to promote C/EBPβ activity, and this activation coincides with mSin3A/HDAC1 displacement from C/EBPβ upon treatment of cells with glucocorticoids (*106*). Therefore, I hypothesized that PCAF/GCN5-mediated acetylation of C/EBPβ at lysines 98-102 might interfere with the association between C/EBPβ and mSin3A. I sought to test this hypothesis by performing binding assays between *in vitro* acetylated (by either recombinant PCAF or GCN5) bacterially expressed GST-C/EBPβ fusion proteins and *in vitro* translated, ^{35}S-labelled, mSin3A.

The WT or the acetylation-compromised MT (mutant, where Lys 98,101,102 were substituted by Arg) GST-C/EBPβ proteins were first bacterially expressed, purified and *in vitro* acetylated with either recombinant GCN5 (bacterially expressed and His-tag purified) or recombinant PCAF (commercially available). The specificity of the acetylation reactions were assessed by counting the incorporated ^{14}C-acetate levels of GST alone, GST-C/EBPβ_{wt} and GST-C/EBP$\beta_{K98,101,102R}$ (referred to as βmt). GCN5 and PCAF-mediated acetylation of GST-C/EBPβ_{wt} were 5 and 10 fold higher than background levels (GST alone) respectively (figure 4A). Moreover, the ^{14}C-acetate incorporation count of GST-C/EBP$\beta_{K98-102R}$

Figure 4: GCN5/PCAF-mediated acetylation of C/EBPβ decreases mSin3A binding *in vitro*.

(A) GST-C/EBPβ (referred to as β) and GST-C/EBP$\beta_{K98,101,102R}$ (βmt) were bacterially expressed, purified with glutathione sepharose beads and subjected to an *in vitro* acetylation assay with either bacterially expressed recombinant GCN5 (left panel) or commercially available recombinant PCAF (right panel) with ^{14}C-Acetyl-CoA as an acetate donor. Following washes of the GST-fusion peptides bound to the sepharose beads, the incorporated ^{14}C-acetate was determined by liquid scintillation count. The results are presented relative to WT GST-C/EBPβ, which was set to 100% acetylation level (N=3, + s.d.). **(B,C)** Following confirmation of the acetylation reactions, a separate sample of each of the acetylated GST-fusion peptides were also used in an *in vitro* binding assay with *in vitro* translated and ^{35}S-labelled mSin3A. Briefly, following acetylation by either GCN5 **(B)** or PCAF **(C)**, the acetylated proteins were incubated with mSin3A, followed by extensive washes and then resolved by SDS-PAGE. The left panels show the radioblot of ^{35}S-labelled mSin3A that was pulled down with GST-C/EBPβ fusion peptides. The Coomassie stain of the GST-fusion peptides is also shown as a loading control underneath the radioblot. The right panels show the quantification of the binding (N=3, + s.d.).

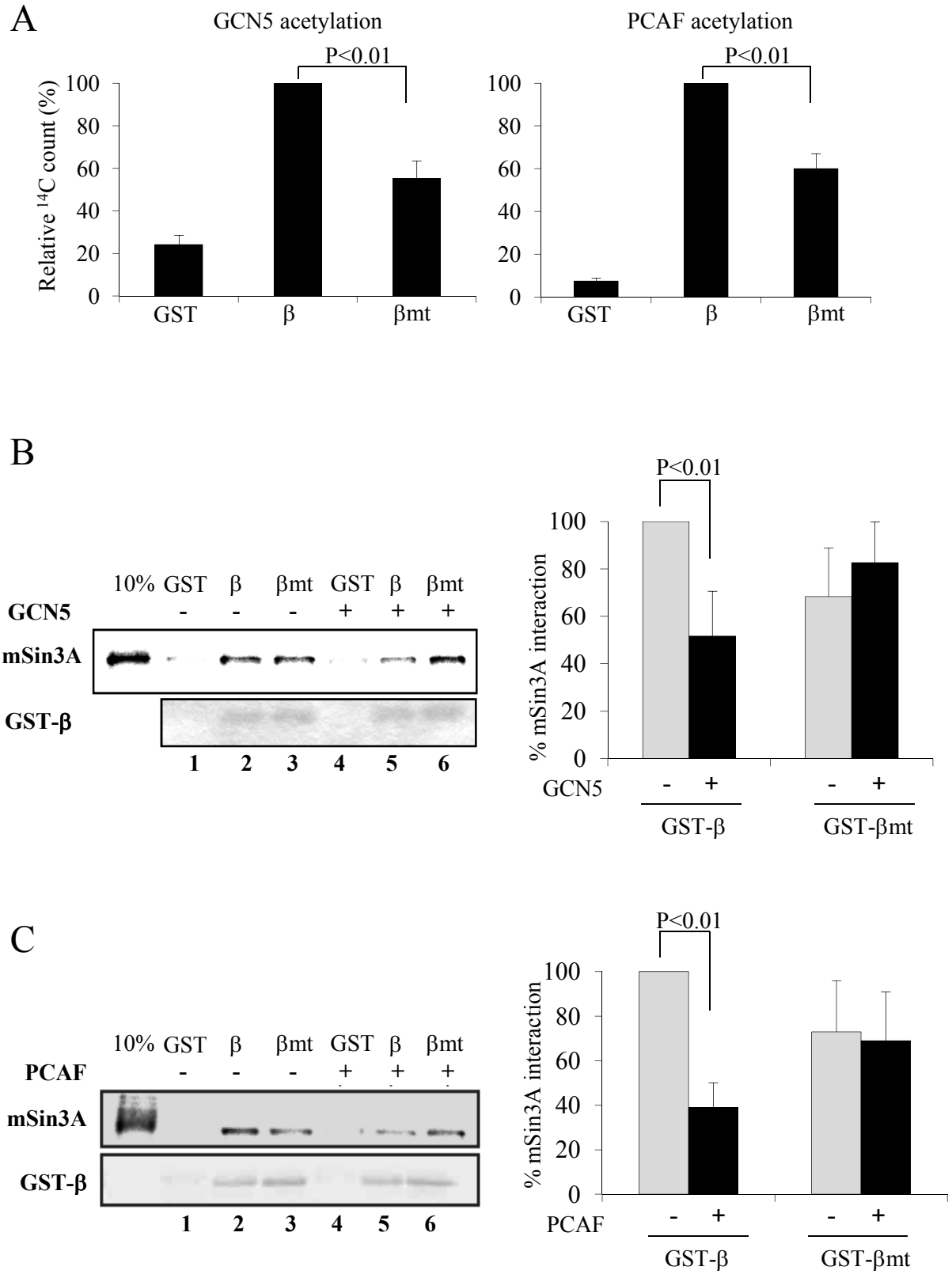
A
GCN5 acetylation
PCAF acetylation
P<0.01
P<0.01
Relative 14C count (%)
100
80
60
40
20
0
GST
β
βmt
B
10% GST β βmt GST β βmt
GCN5 - - - + + +
mSin3A
GST-β
1 2 3 4 5 6
P<0.01
% mSin3A interaction
GCN5 - + - +
GST-β
GST-βmt
C
10% GST β βmt GST β βmt
PCAF - - - + + +
mSin3A
GST-β
1 2 3 4 5 6
P<0.01
% mSin3A interaction
PCAF - + - +
GST-β
GST-βmt

was reduced by 40% when compared to WT GST-C/EBPβ, when either GCN5 or PCAF were used as acetylases (figure 4A). The reduced acetylation observed with GST-C/EBP$\beta_{K98,101,102R}$ was not due to a compromised interaction with GCN5 or PCAF (*106*), thus confirming that lysines 98,101,102 are among the residues that are in fact acetylated by GCN5 or PCAF. That the acetylation of GST-C/EBP$\beta_{K98\text{-}102R}$ was not abolished suggests that PCAF and GCN5 could acetylate other residues. Indeed, murine C/EBPβ bears 21 lysines, of which 4 (lysines 39, 117, 215, 216) were also shown to be acetylated by PCAF (*275*).

Following the confirmation of the *in vitro* acetylation reactions of the GST-fusion peptides, I performed an *in vitro* binding assay using the acetylated WT or MT GST-C/EBPβ proteins with *in vitro* translated and ^{35}S-labelled mSin3A. The results indicate that the interaction of mSin3A with C/EBPβ is decreased by 50% when the latter is acetylated by either GCN5 (figure 4B, left panel, lanes 2 and 5 of the radioblot and quantification in the right panel) or PCAF (figure 4C, left panel, lanes 2 and 5 of the radioblot and quantification in the right panel). When the interaction between C/EBP$\beta_{K98,101,102R}$ and mSin3A was tested, no change was observed following either GCN5 or PCAF-mediated acetylation (figure 4B and 4C, lanes 3 and 6 of the radioblots). Together, these results suggest that PCAF/GCN5-mediated acetylation of C/EBPβ at lysines 98, 101, 102 interferes with mSin3A binding (published in 106).

3.1.1.2 Amino acids 153-156 in C/EBPβ are required for GCN5 association

GCN5 has been shown to actively regulate C/EBPβ activity by acetylating lysines 98, 101 and 102, thus increasing C/EBPβ transcriptional activity in a GR-dependent manner (*106*). Moreover, this acetylation reaction has been shown to favour mSin3A dissociation from C/EBPβ (*106*). To further characterize the interplay between GCN5 and

mSin3A/HDAC1 in regulating C/EBPβ activity, the GCN5 binding domain was determined. To do so, N and C-terminal deletions of C/EBPβ, including either both the activation domains and the cluster of lysines 98-102 (C/EBPβ_{N107}, C/EBPβ_{N140} and C/EBPβ_{N168},) or both the DNA binding and dimerization domain (C/EBPβ_{108C}) were constructed (see appendix 5 for schemas of the constructs).

Bacterially expressed GST-C/EBPβ fusion proteins were tested for *in vitro* binding to ^{35}S-labelled *in vitro* translated GCN5. Although this approach is not the preferred one as it does not reflect physiological systems, it is a good way to test for direct binding between two factors. Small scale bacterial expression of proteins allows us to get a high quantity of start up material (microgram range), whereas *in vitro* translated reactions using mammalian systems generates much lower amount of proteins (few nanograms). The latter system is however closer to *in vivo* conditions as the rabbit reticulocytes lysate used contain most determinants required for proper folding and for some post-translational modifications. Therefore, combining the two systems allows us to create an artificial system that is optimal to test for direct interactions of proteins of interests. In our case, the mammalian *in vitro* translation system was used for the bigger proteins (GCN5 in this case) to mimic as much as we can proper *in vivo* folding. However, results from such assay always need to be confirmed *in vivo* by co-immunoprecipitation assays.

The results in figure 5A (radioblot upper-left panel and quantification of the binding in the right panel) show that GCN5 interaction with a C/EBPβ protein lacking the N-terminal 107 amino acids (β_{108C}) is only slightly decreased. However, when the first 107 or 140 amino acids of C/EBPβ (β_{N107} and β_{N140} respectively) were tested for interaction with GCN5, both peptides showed an 80% decrease in binding with GCN5. Since the previous results

suggested that a domain located downstream of amino acid 140 might be responsible for mediating GCN5 interaction, I generated additional constructs with smaller C-terminal deletions to further delineate GCN5 binding domain in C/EBPβ. When I deleted the C-terminal domains of C/EBPβ encompassing either amino acids 169-296 (referred to as β_{N168}), 185-296 or 218-296 (β_{N184} or β_{N217} respectively, data not shown) and performed the binding assays, all three C/EBPβ peptides showed similar binding capacity to GCN5 compared to WT C/EBPβ (figure 5A). Hence, the results suggested that the binding was likely to require amino acids 141-168.

To confirm the potential location of the binding domain in a C/EBPβ construct that closely mimics its WT counterpart by having most of its functional domains, a C/EBPβ construct with an internal deletion was generated by removing amino acids 141-168 (referred to as C/EBP$\beta_{\Delta 141\text{-}168}$). Yet again, C/EBP$\beta_{\Delta 141\text{-}168}$ showed an 80% decreased association with GCN5 (figure 5B), thus suggesting that amino acids 141-168 are in fact required for binding with GCN5.

Using online bioinformatic tools that allow predictions of protein secondary structures using different algorithms (i.e. HNN, PHD, DPM) was unsuccessful in predicting a definite structural nature of the domain covering amino acids 141-168 in C/EBPβ. However, residues located within region 141-156 had a 20% probability of forming α-helical structures. I thus sought to generate two C/EBPβ constructs with smaller deletions that lacked either amino acids 141-149 or 151-156 to define more specific residues involved in GCN5 binding and to also limit structural changes that might occur due to the deletions. When C/EBP$\beta_{\Delta 141\text{-}149}$ and C/EBP$\beta_{\Delta 151\text{-}156}$ were tested for their ability to bind GCN5 *in vitro*, they showed a 60% and 80% decrease in binding with GCN5, respectively (figure 5B).

Figure 5: Amino acids 151-156 of C/EBPβ are required for GCN5 binding *in vitro* and *in vivo*.

(A) N-terminal and C-terminal deletions of GST-C/EBPβ were constructed, bacterially expressed and subjected to an *in vitro* binding assay with *in vitro* translated and ^{35}S-labelled GCN5. The left panel shows the radioblot of ^{35}S-labelled GCN5 that was pulled down with GST-C/EBPβ fusion peptides. The Coomassie stain of the GST-fusion peptides is also shown as a loading control. The right panel shows the quantified binding (N=3, + s.d.). **(B)** Internal deletions of C/EBPβ lacking amino acids 151-156, 141-149 and 141-168 (C/EBP$\beta_{\Delta 151\text{-}156}$, C/EBP$\beta_{\Delta 141\text{-}149}$ and C/EBP$\beta_{\Delta 141\text{-}168}$ respectively) were tested for GCN5 binding, as in (A) (N=3, +s.d.). **(C)** Cos7 cells were co-transfected with expression plasmids for flag-GCN5 and either pcDNA-C/EBPβ_{wt} or C/EBP$\beta_{\Delta 153\text{-}156}$. Whole cell lysates were immunoprecipitated with a FLAG affinity resin. Only the LAP isoform is shown because of a non-specific band that overlaps with LAP* (N=3, + s.d.). **(D)** GST-C/EBPβ constructs were bacterially expressed and subjected to an *in vitro* acetylation assay with PCAF using ^{14}C-Acetyl-CoA as an acetate donor. After the acetylation reaction, the proteins were loaded on a SDS-PAGE gel, which was Coomassie stained and the bands corresponding to GST-C/EBPβ were cut from the gel (inset as loading control) and the radioactivity was determined with a scintillation counter (N=3, +s.d).

A

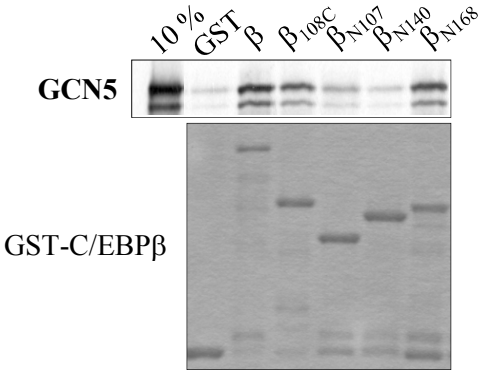
10 %
GST
β
β108C
βN107
βN140
βN168
GCN5
GST-C/EBPβ

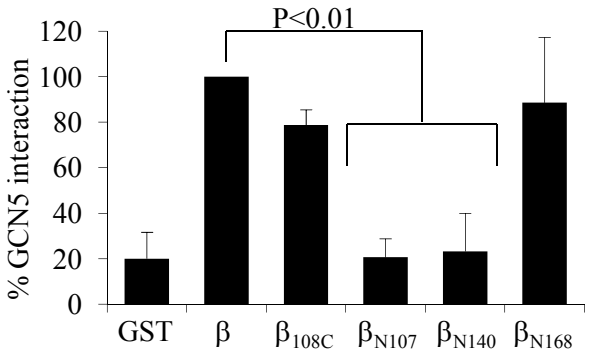
P<0.01
% GCN5 interaction
120
100
80
60
40
20
0
GST
β
β108C
βN107
βN140
βN168

B

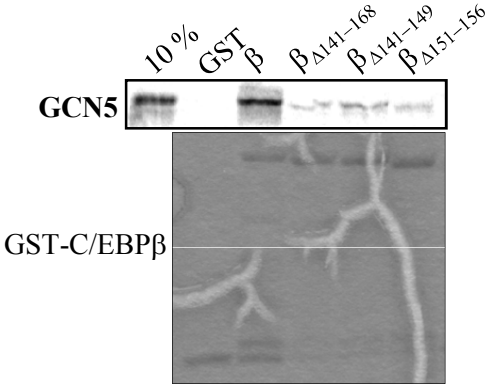
10 %
GST
β
βΔ141–168
βΔ141–149
βΔ151–156
GCN5
GST-C/EBPβ

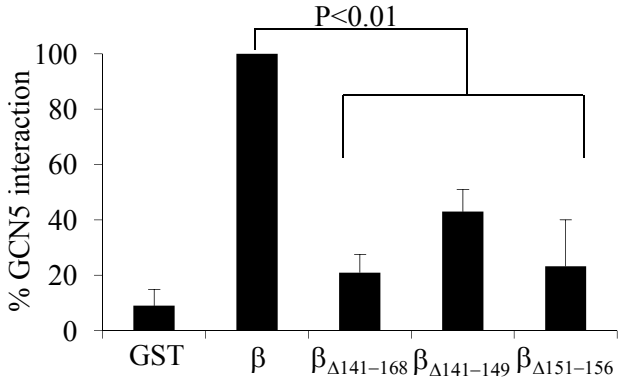
P<0.01
% GCN5 interaction
100
80
60
40
20
0
GST
β
βΔ141–168
βΔ141–149
βΔ151–156

C

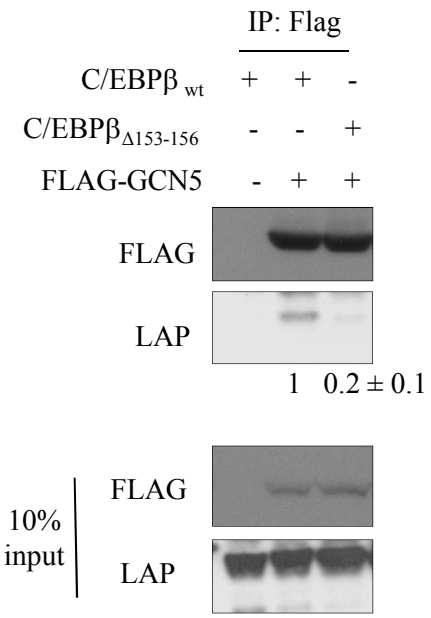
IP: Flag
C/EBPβ wt + + -
C/EBPβΔ153-156 - - +
FLAG-GCN5 - + +
FLAG
LAP
1 0.2 ± 0.1
10% input
FLAG
LAP

D

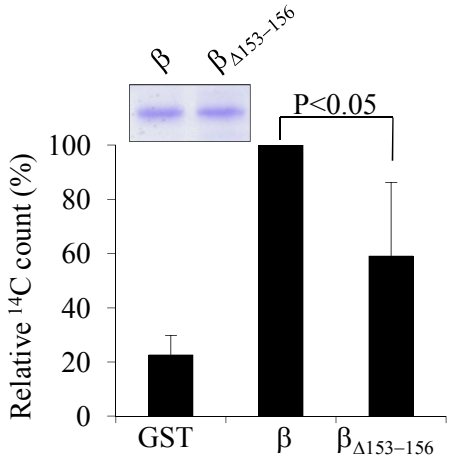
β
βΔ153–156
P<0.05
Relative 14C count (%)
100
80
60
40
20
0
GST
β
βΔ153–156

Consequently, I hypothesized that the minimal domain encompassing amino acids 141-156 in C/EBPβ was required for binding with GCN5, in an *in vitro* setting, where both domains 141-149 and 151-156 were required for such an interaction to occur.

Since the previous results were obtained with purified and bacterially expressed GST-C/EBPβ, one can argue that this system does not mimic the physiological environment of the factor due to a large amount of protein used in the assay and to a lack of post-translational modifications that usually occurs in mammalian cells to ensure proper folding. To circumvent this limitation, a co-immunoprecipitation (CoIP) assay was done in Cos7 cells by transiently co-transfecting constructs expressing FLAG-GCN5 and the different C/EBPβ constructs. Although this system is still artificial, it is better than the *in vitro* GST-pulldown assay as it closely mimics a physiological environment. Moreover, since C/EBP$\beta_{\Delta 151\text{-}156}$ does not encode the C/EBPβ LIP isoform, as it lacks the initiator methionine 152, I prepared another deletion mutant (C/EBP$\beta_{\Delta 153\text{-}156}$), which retains expression of LIP.

When FLAG-GCN5 and either C/EBPβ_{wt}, C/EBP$\beta_{\Delta 153\text{-}156}$ or C/EBP$\beta_{\Delta 141\text{-}149}$ were transiently co-expressed in Cos7 cells, almost no C/EBP$\beta_{\Delta 153\text{-}156}$ immunoprecipitated with FLAG-GCN5, when compared to C/EBPβ_{wt} (figure 5C). C/EBP$\beta_{\Delta 141\text{-}149}$ interaction was however not affected (data is shown in the second result section, figure 25). Only the LAP isoform of C/EBPβ is shown on the Western blot due to a band that overlaps with LAP*. Moreover, when GCN5's ability to acetylate C/EBP$\beta_{\Delta 153\text{-}156}$ was assessed *in vitro*, there was a 40% decrease in ^{14}C-acetate incorporation in C/EBP$\beta_{\Delta 153\text{-}156}$ when compared to WT C/EBPβ (figure 5D). We can thus suggest with confidence that amino acids 153-156 in C/EBPβ are required for GCN5 interaction both *in vitro* and *in vivo.*

3.1.1.3 Amino acids 153-156 in C/EBPβ are also required for mSin3A binding

Since the interaction of mSin3A (and consequently HDAC1) is compromised by C/EBPβ acetylation at lysines 98, 101 and 102, one might expect that the mSin3A binding domain could be located in close proximity to these residues. To validate this hypothesis and to further delineate the extent to which GR-mediated titration of mSin3A/HDAC1 from C/EBPβ affects C/EBPβ activity, I sought to map the mSin3A binding domain in C/EBPβ. To do so, the same N and C-terminal deletions of C/EBPβ that were used for GCN5 binding (see appendix 5 for schemas) were used in an *in vitro* binding assay with ^{35}S-labelled mSin3A.

Similar to GCN5, C/EBPβ$_{108C}$ was able to efficiently associate with mSin3A whereas C/EBPβ$_{N107}$ and C/EBPβ$_{N140}$ were not (figure 6A). As opposed to GCN5, however, C/EBPβ$_{N168}$, C/EBPβ$_{N184}$ and C/EBPβ$_{N217}$ were all unable to efficiently bind to mSin3A, with a 60-80% decrease in their binding when compared to C/EBPβ$_{wt}$ (figure 6A). These observations suggested that either (1) the bZIP domain is important for the interaction between the two factors and its deletion prevents proper binding or (2) that the mSin3A binding domain is located downstream of amino acids 217. To test whether the bZIP domain was in fact required, I tried the same internal deletion mutants used for binding with GCN5.

Fortuitously, the GST-pulldown assays showed that both C/EBPβ$_{\Delta 141\text{-}168}$ and C/EBPβ$_{\Delta 151\text{-}156}$ interact less efficiently with mSin3A when compared to C/EBPβ$_{wt}$ (figure 6B), as it was previously shown for GCN5 (figure 5). Thus, four conclusions could be drawn from these experiments: 1) the absence of lysines 98, 101 and 102 (whose acetylation impaired mSin3A binding) did not significantly affect mSin3A interaction with C/EBPβ; 2) mSin3A binding depended strongly on amino acids 151-156 in C/EBPβ; 3) the bZIP domain

Figure 6: Amino acids 151-156 and the bZIP domain of C/EBPβ are required for mSin3A binding *in vitro*.

(A) N-terminal and C-terminal deletions of GST-C/EBPβ were constructed, bacterially expressed and subjected to an *in vitro* binding assay with *in vitro* translated and ^{35}S-labelled mSin3A. The upper panel shows the radioblot of ^{35}S-labelled mSin3A that was pulled down with GST-C/EBPβ fusion peptides. The Coomassie stain of the GST-fusion peptides is also shown as a loading control. The lower panel shows the quantified binding (N=3, + s.d.). **(B)** Internal deletions of C/EBPβ lacking amino acids 151-156 and 141-168 (C/EBPβ$_{\Delta 151\text{-}156}$ and C/EBPβ$_{\Delta 141\text{-}168}$ respectively) were tested for mSin3A binding, as in A (N=3, +s.d.).

A

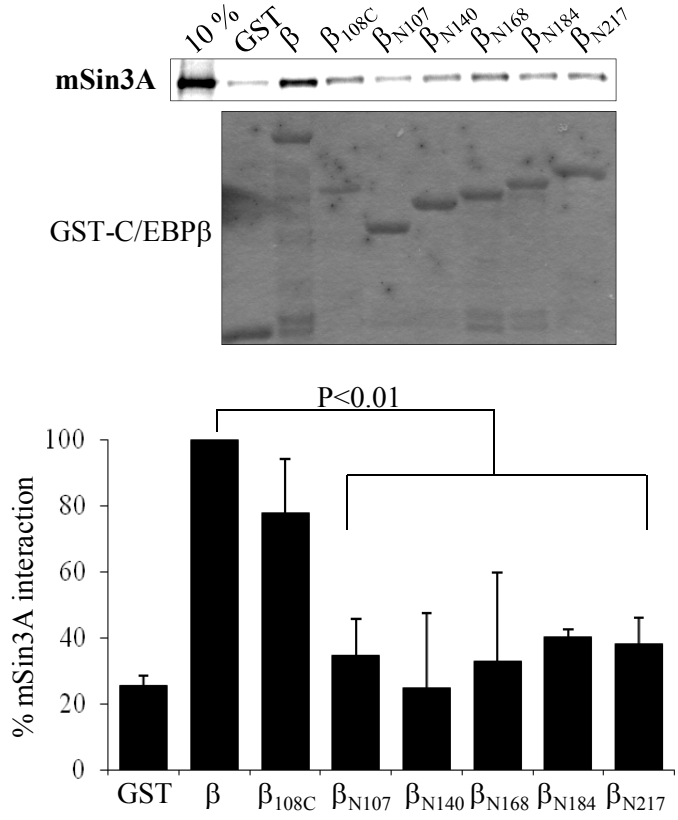
10 %
GST
β
β108C
βN107
βN140
βN168
βN184
βN217
mSin3A
GST-C/EBPβ
P<0.01
% mSin3A interaction
100
80
60
40
20
0
GST
β
β108C
βN107
βN140
βN168
βN184
βN217

B

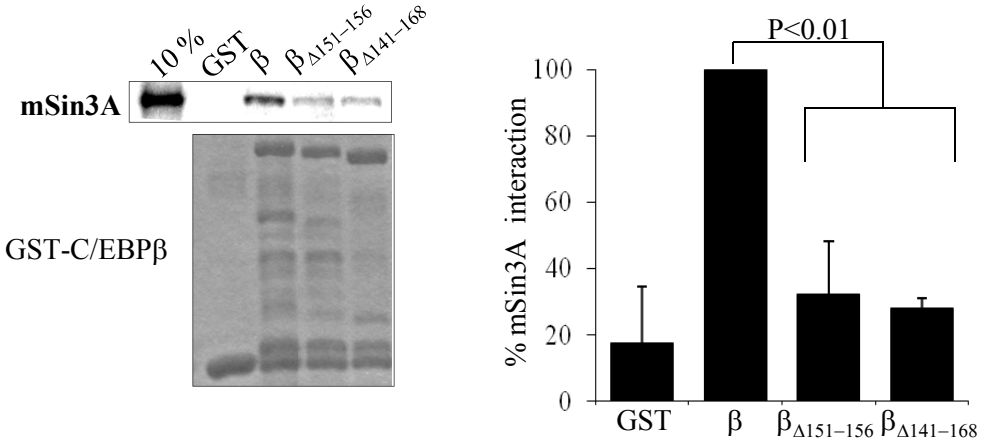
10 %
GST
β
βΔ151–156
βΔ141–168
mSin3A
GST-C/EBPβ
P<0.01
% mSin3A interaction
100
80
60
40
20
0
GST
β
βΔ151–156
βΔ141–168

appears to be required for optimal interaction between C/EBPβ and mSin3A *in vitro* and 4) the required site for GCN5 and mSin3A binding with C/EBPβ appears to overlap closely in that binding of both factors depends on amino acids 151-156. Further, since C/EBPδ was also shown to require its bZIP domain to mediate a proper interaction with mSin3A (*289*), it supports our third conclusion.

In co-immunoprecipitation experiments, C/EBP$\beta_{\Delta 153\text{-}156}$ precipitated 70% less with HDAC1, when compared to WT C/EBPβ, thus confirming the *in vitro* binding assay (figure 7A). These results further support the suggestion that GCN5 and mSin3A might have overlapping requirements in C/EBPβ, hence placing them in potential competition for interaction with C/EBPβ.

Although a decreased interaction in a transient transfection experiment is sufficient to validate the *in vitro* binding assays, such a method has an important limitation: it causes a very high expression of the proteins in the cells in a relatively short period of time (figure 7B). To assess C/EBPβ and HDAC1 interaction in a physiologically more relevant condition, both C/EBPβ constructs were stably expressed in NIH 3T3 cells using a retroviral transduction strategy. When endogenous HDAC1 was immunoprecipitated, C/EBP$\beta_{\Delta 153\text{-}156}$ was still unable to properly associate with HDAC1 (figure 7C), therefore confirming that amino acids 153-156 of C/EBPβ are required for an optimal interaction with mSin3A/HDAC1 *in vivo*.

Figure 7: C/EBPβ$_{\Delta 153\text{-}156}$ interacts less efficiently with HDAC1 compared to WT C/EBPβ

(A) Cos7 cells were co-transfected with expression plasmids for flag-HDAC1 and either pcDNA-C/EBPβ$_{wt}$ or C/EBPβ$_{\Delta 153\text{-}156}$. Whole cell lysates were immunoprecipitated with a FLAG affinity resin. Data represent results observed in three independent experiments. **(B)** Western blot showing the C/EBPβ expression levels in NIH 3T3 transiently transfected with the pcDNA3.1-C/EBPβ vector or stably expressing C/EBPβ by retroviral transduction. **(C)** NIH 3T3 cells stably expressing C/EBPβ and C/EBPβ$_{\Delta 153\text{-}156}$ were subjected to an immunoprecipitation assay with an HDAC1 antibody (and Gal4 DBD as a non specific control). Data represent results observed in two independent experiments.

A

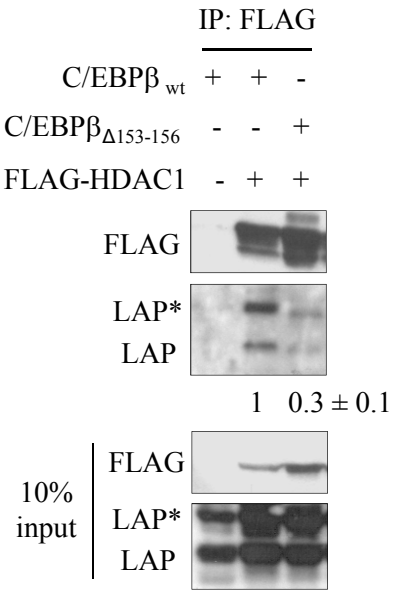
IP: FLAG
C/EBPβ wt + + -
C/EBPβΔ153-156 - - +
FLAG-HDAC1 - + +
FLAG
LAP*
LAP
1 0.3 ± 0.1
10% input
FLAG
LAP*
LAP

B

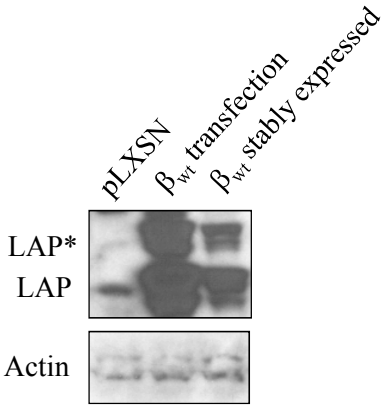
pLXSN
βwt transfection
βwt stably expressed
LAP*
LAP
Actin

C

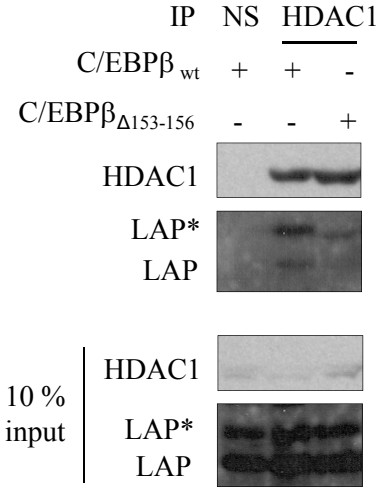
IP NS HDAC1
C/EBPβ wt + + -
C/EBPβΔ153-156 - - +
HDAC1
LAP*
LAP
10 % input
HDAC1
LAP*
LAP

3.1.2 Characterization of C/EBPβ$_{\Delta 153\text{-}156}$ transcriptional activity and adipogenic potential

3.1.2.1 C/EBPβ$_{\Delta 153\text{-}156}$ transcriptional activity is enhanced on the C/EBPα promoter but not on the PPARγ promoter

As the Δ153-156 deletion in C/EBPβ compromised both GCN5 and mSin3A interaction, it would be expected to impact on the transcriptional regulatory potential of C/EBPβ, although the specific effect was difficult to predict. Nonetheless, the increase of C/EBPβ activity would be expected to be proportional to the loss of HDAC1 activity and to the acetylase activity of GCN5 on the C/EBPβ targeted promoters.

To test C/EBPβ$_{\Delta 153\text{-}156}$ transcriptional activity, a Luciferase reporter assay was performed in NIH 3T3 cells by transient transfection experiments where the transcription of the reporter was driven by the C/EBPα promoter (-355/+7) (figure 8A,B). C/EBPβ$_{\Delta 153\text{-}156}$ proved to be a more potent activator of transcription with an almost two fold increase in the baseline state when compared to WT C/EBPβ. Moreover, treatment of the NIH 3T3 cells with the synthetic glucocorticoid hormone dexamethasone (dex) resulted in a three fold increase of transcription by WT C/EBPβ as predicted, since it is known that GR promotes C/EBPβ activity by targeting HDAC1 for proteasomal degradation and hence favouring acetylation of C/EBPβ and the C/EBPα promoter environment (*66, 106*). When C/EBPβ$_{\Delta 153\text{-}156}$ activity was tested in the presence of dex, it also displayed an increase in transcription from the C/EBPα promoter (approximately 2.5 fold) when compared to its basal state, although the overall level of transcription was still higher than that of WT C/EBPβ (figure 7D). To verify whether the increase in transcription observed with C/EBPβ$_{\Delta 153\text{-}156}$ was not

Figure 8: C/EBPβ$_{\Delta 153\text{-}156}$ has a higher transcriptional activity than C/EBPβ$_{wt}$

(A) Schematic presentation of C/EBPβ$_{wt}$ or C/EBPβ$_{\Delta 153\text{-}156}$ showing the different isoforms expressed. **(B)** C/EBPβ activity is measured by the Luciferase reporter assay from the -350/+7 C/EBPα promoter. C/EBPβ$_{wt}$ or C/EBPβ$_{\Delta 153\text{-}156}$ were transfected in NIH 3T3 cells along with the C/EBPα-luciferase reporter and the glucocorticoid receptor constructs. Cells were treated with either vehicle (□) or 1μM dex (■) the following day for 16h. Luciferase activity was corrected for transfection efficiency by using a co-transfected Renilla expression plasmid (N=4 duplicates, + s.e.m.). **(C)** Western analysis showing the expression level of endogenous C/EBPβ, exogenous C/EBPβ$_{wt}$ or C/EBPβ$_{\Delta 153\text{-}156}$ in NIH 3T3 cells treated with either vehicle or dex. Data represent results observed in three independent experiments.

A

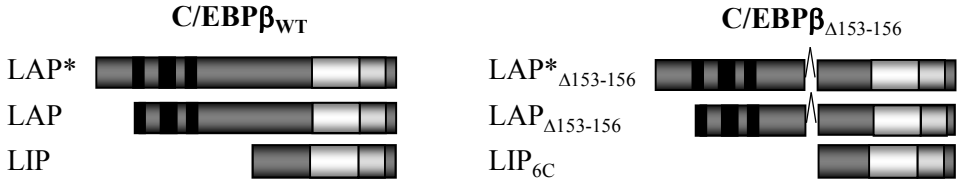
C/EBPβWT
C/EBPβΔ153-156
LAP*
LAP
LIP
LAP*Δ153-156
LAPΔ153-156
LIP6C

B

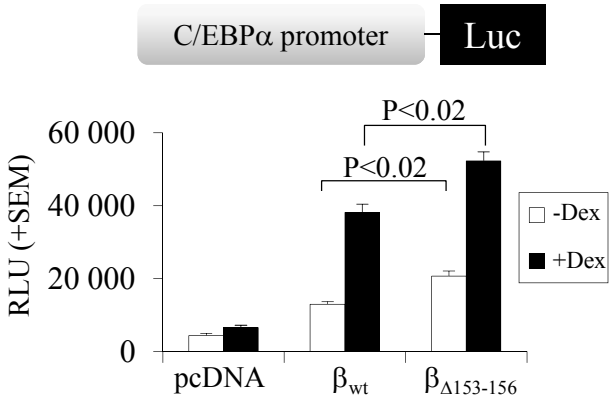
C/EBPα promoter
Luc
P<0.02
P<0.02
60 000
40 000
20 000
0
RLU (+SEM)
-Dex
+Dex
pcDNA
βwt
βΔ153-156

C

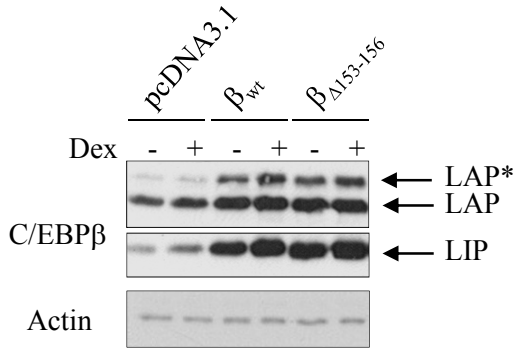
pcDNA3.1
βwt
βΔ153-156
Dex
- + - + - +
LAP*
LAP
C/EBPβ
LIP
Actin

due to increase in its protein expression, a Western blot analysis was performed and confirmed similar expression levels of the constructs (figure 8C).

Since C/EBP$\beta_{\Delta 153\text{-}156}$ still required dex to reach higher transcriptional activity, we can suggest that GR-induced activation was still able to increase its activity by means that could be HDAC1-independent. As GR-dependent activation of C/EBPβ involves exclusion of HDAC1, the initial absence of the co-repressor complex from C/EBP$\beta_{\Delta 153\text{-}156}$ could also allow it to recruit co-activators faster than the WT counterpart independently of GR.

Moreover, since stable expression of C/EBPβ has been shown to activate C/EBPα and PPARγ2 expression in the NIH 3T3 fibroblastic cell line when promoting adipogenesis (*66, 106, 139-140*), I sought to evaluate if the increased potential of C/EBP$\beta_{\Delta 153\text{-}156}$ to activate C/EBPα transcription would also be reproduced on the endogenous C/EBPα promoter. To test this, I performed a quantitative RT-PCR (qRT-PCR) analysis of C/EBPα mRNA levels in extracts of NIH 3T3 cells stably expressing the C/EBPβ constructs and induced to differentiate either with MIX and insulin (MI) or MIX, insulin and dex (MID). To focus on the initial activation of C/EBPα that is C/EBPβ-dependent, the qRT-PCR reaction was performed on RNA prepared 24h after inducing the cells to differentiate.

Consistent with the transient transfection results, C/EBPα mRNA levels were increased significantly by two fold in the absence of dex in cells stably expressing C/EBP$\beta_{\Delta 153\text{-}156}$ (figure 9A, left panel, MI condition). However, addition of glucocorticoid did not further increase C/EBP$\beta_{\Delta 153\text{-}156}$ transcriptional activity, when compared to WT C/EBPβ (figure 9A, left panel, MID condition), by contrast to the results obtained in the transient transcription assay (figure 8B). The same trend continued 48h post-induction (figure 9A, right panel). Notably, these results show that C/EBP$\beta_{\Delta 153\text{-}156}$ activity in the absence of dex

Figure 9: C/EBP$\beta_{\Delta 153\text{-}156}$ transcribes endogenous C/EBPα more efficiently when compared to C/EBPβ_{wt}.

NIH 3T3 cells stably expressing either C/EBPβ_{wt} or C/EBP$\beta_{\Delta 153\text{-}156}$ were subjected to a quantitative RT-PCR reaction 24h and 48h after induction of differentiation without (MI) or with (MID) dex. The C/EBPα **(A)** and PPARγ2 **(B)** mRNA levels were normalized to actin (N=3, + s.d.). Quantification of C/EBPα and PPARγ2 are relative to the MI pLXSN control condition where the values are defined as 1 relative unit (RU). **(C)** The NIH 3T3 cells were also harvested at day 1, 2 and 3 for western analysis of PPARγ2 protein expression. Data represent results observed in three independent experiments. **(D)** The glucose transporter 4 (GLUT4) mRNA levels were also assessed 48h after induction of differentiation (N=3, + s.d.).

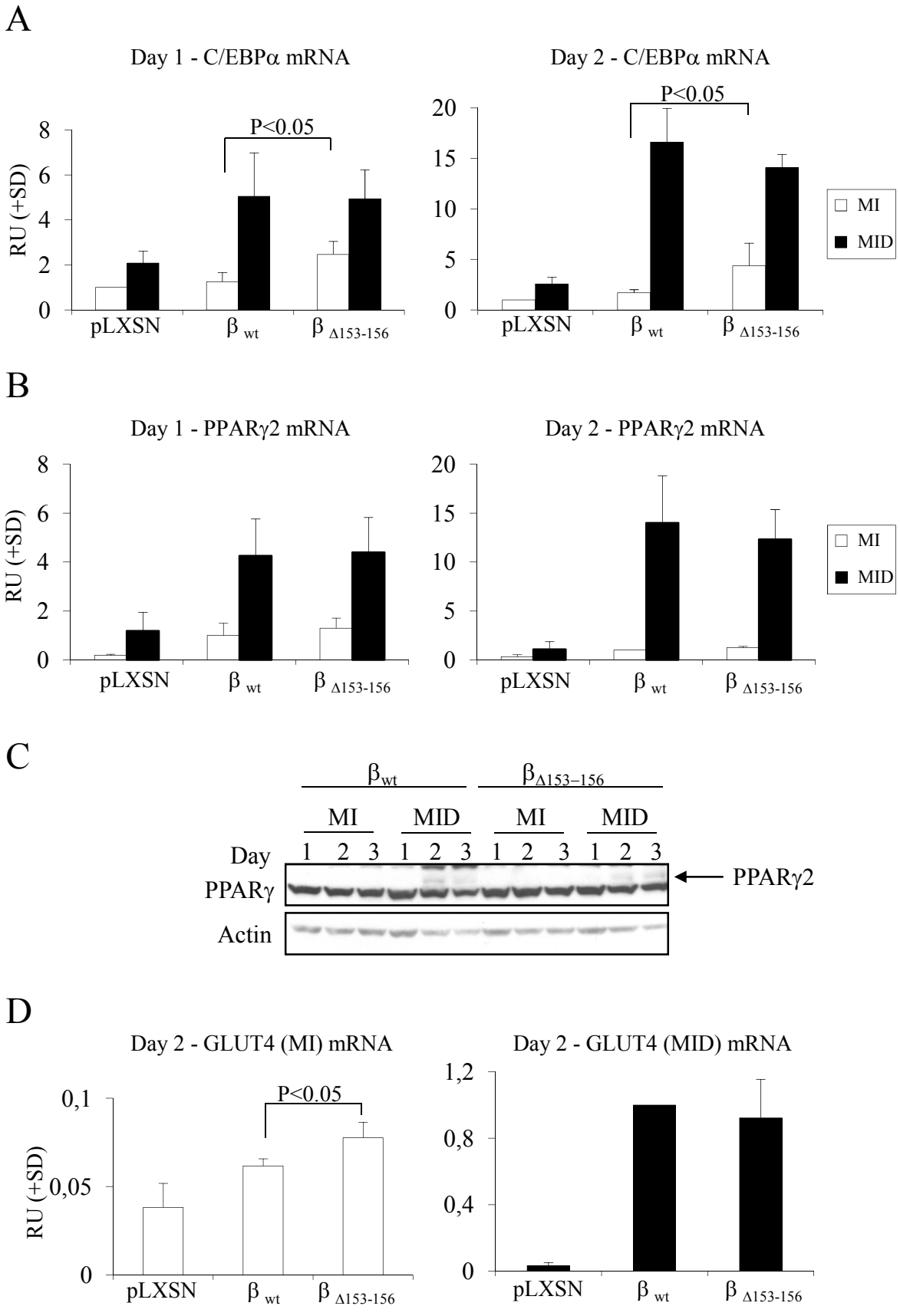
A
Day 1 - C/EBPα mRNA
Day 2 - C/EBPα mRNA
P<0.05
P<0.05
RU (+SD)
8
6
4
2
0
20
15
10
5
0
pLXSN
β wt
β Δ153-156
MI
MID
B
Day 1 - PPARγ2 mRNA
Day 2 - PPARγ2 mRNA
C
βwt
βΔ153–156
MI
MID
MI
MID
Day
1 2 3 1 2 3 1 2 3 1 2 3
PPARγ
PPARγ2
Actin
D
Day 2 - GLUT4 (MI) mRNA
Day 2 - GLUT4 (MID) mRNA
P<0.05
0,1
0,05
0
1,2
0,8
0,4

was not restored to the same level as C/EBPβ_{wt} in the presence of dex, indicating that (1) the effect of GR on C/EBPβ activation is probably not limited to the titration of the mSin3A/HDAC1 co-repressor complex and (2) that GR is essential for C/EBPβ to reach its maximal activity.

C/EBPβ has been shown to bind and activate the PPARγ promoter in transcription assays and upon differentiation of the 3T3 L1 preadipocytes (*65, 174*). Since previous results from Dr Haché's laboratory suggested HDAC1-mediated repression of C/EBPβ was important for C/EBPα but not PPARγ expression (*66*), I sought to determine whether Δ153-156 of C/EBPβ would affect PPARγ2 expression. A quantitative RT-PCR analysis of RNA extracted from NIH 3T3 cells (as in figure 9A) showed that both C/EBPβ_{wt} and C/EBP$\beta_{\Delta 153-156}$ activated PPARγ2 transcription equally (figure 9B, left and right panels). Additionally, PPARγ2 protein levels were also shown to be similar in the cells expressing either WT or MT C/EBPβ (figure 9C). Thus, the results suggest that the effect of mSin3A/HDAC1 on C/EBPβ could be promoter-specific.

The glucose transporter 4 (GLUT4) is one of the adipogenic markers whose expression has been shown to be induced by the collective action of C/EBPβ (or C/EBPα) and PPARγ2 together (*145*). When the mRNA levels of GLUT4 was assessed 48h post-induction of differentiation (figure 9D), its expression was slightly, but significantly, increased in cells expressing C/EBP$\beta_{\Delta 153-156}$, in the absence of dex. Since the expression of PPARγ2 was not detected in the absence of dex in cells expressing WT or Δ153-156 C/EBPβ (figure 9C, MI condition), the higher basal GLUT4 mRNA level could be due to the increased transcriptional activity of C/EBP$\beta_{\Delta 153-156}$.

3.1.2.2 C/EBP$\beta_{\Delta 153\text{-}156}$ is more efficient at inducing the differentiation of the NIH 3T3 cells into mature adipocytes by recruiting less HDAC1 to its target promoters

Since ectopic expression of C/EBPβ in the NIH 3T3 fibroblastic cell line promotes adipogenesis upon treatment of the cells with glucocorticoids (*139-140*), this system provides the opportunity for evaluating the effect of the Δ153-156 of C/EBPβ in the induction of adipocyte differentiation. Using a retroviral transduction strategy, C/EBPβ_{wt} and C/EBP$\beta_{\Delta 153\text{-}156}$ were stably expressed in NIH 3T3 cells at near physiological levels and they both showed similar expression (figure 10A).

Following induction of differentiation, cells expressing C/EBP$\beta_{\Delta 153\text{-}156}$ consistently differentiated to a greater extent into mature adipocytes when compared to cells expressing C/EBPβ_{wt}, in the absence of dex, as shown by western analysis of the adipocyte marker adipsin and by Oil red O staining of the lipids, 4 and 6 days post-treatment, respectively (figure 10B, C). Hence, the results confirm that C/EBP$\beta_{\Delta 153\text{-}156}$ has indeed a higher adipogenic potential than WT C/EBPβ.

As previously shown in our laboratory, treatment of 3T3 L1 (and NIH 3T3) cells with dex results in GR-mediated titration of HDAC1 from the C/EBPα promoter, thus potentiating C/EBPα transcription during adipogenesis (*66, 106*). Knowing that C/EBP$\beta_{\Delta 153\text{-}156}$ interacts less efficiently with HDAC1 when compared to C/EBPβ_{wt}, HDAC1 occupancy would be predicted to be decreased on C/EBP$\beta_{\Delta 153\text{-}156}$-targeted promoters. To verify this hypothesis, a chromatin-immunoprecipitation (ChIP) assay was performed 24h after induction of differentiation of NIH 3T3 cells stably expressing C/EBP$\beta_{\Delta 153\text{-}156}$ (figure 10D).

In cells expressing WT C/EBPβ, HDAC1 was effectively recruited on the C/EBPα promoter as previously demonstrated (66,106). However, the recruitment of HDAC1 was

Figure 10: C/EBPβ$_{\Delta 153\text{-}156}$, differentiates the NIH 3T3 fibroblastic cell line more efficiently when compared to C/EBPβ$_{wt}$ in the absence of dex.

NIH 3T3 cells that were retrovirally transduced to express either C/EBPβ$_{wt}$ or C/EBPβ$_{\Delta 153\text{-}156}$ were harvested at either day 0 **(A)** or day 4 **(B)** post-induction of differentiation without (MI) or with (MID) dex and subjected to a western analysis with the C/EBPβ **(A)** or adipsin **(B)** antibodies. **(C)** The cells were also stained with Oil red O 6 days after induction of differentiation to qualitatively assess lipid accumulation. **(D)** A chromatin immunoprecipitation analysis was also performed in NIH 3T3 cells expressing C/EBPβ. Briefly, the cells were treated with MI for 24h, harvested, cross-linked and the nuclear extract was immunoprecipitated using an HDAC1 antibody. Following several washes, the precipitated DNA was isolated and subjected to a PCR reaction that amplifies region -460/-244 of the C/EBPα promoter. The figure represents results observed in three independent experiments.

A

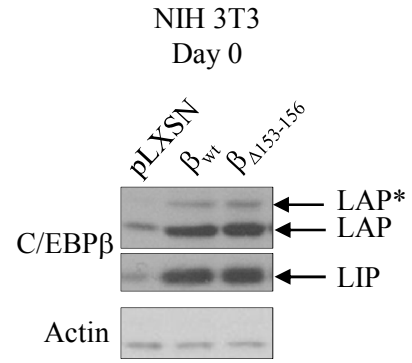
NIH 3T3
Day 0
pLXSN
βwt
βΔ153-156
C/EBPβ
LAP*
LAP
LIP
Actin

B

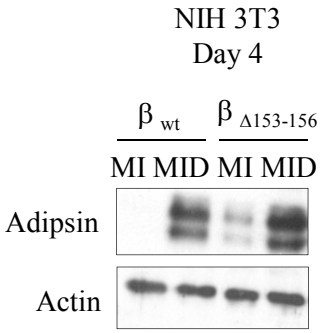
NIH 3T3
Day 4
β wt
β Δ153-156
MI MID MI MID
Adipsin
Actin

C

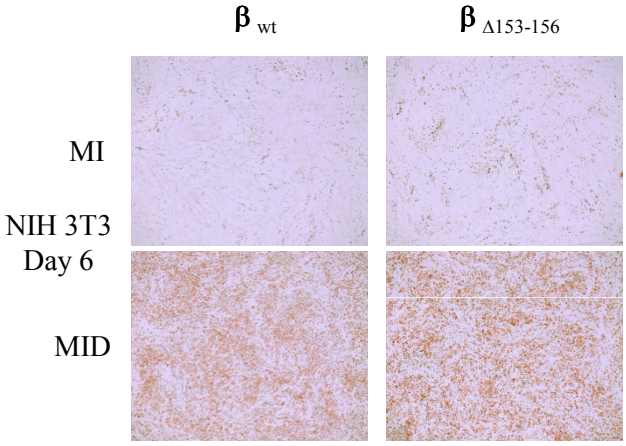
β wt
β Δ153-156
MI
NIH 3T3
Day 6
MID

D

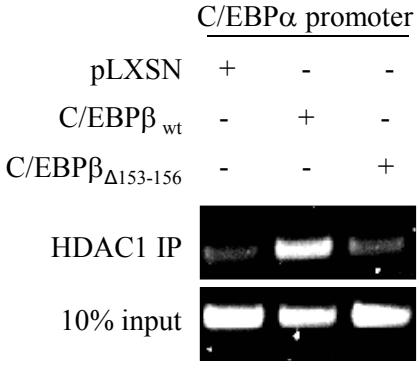
C/EBPα promoter
pLXSN + - -
C/EBPβ wt - + -
C/EBPβΔ153-156 - - +
HDAC1 IP
10% input

highly compromised from the C/EBPα promoter in cells expressing C/EBP$\beta_{\Delta 153\text{-}156}$ (figure 10D). Taken together, these results validate the hypothesized molecular mechanism by which the co-repressor complex mSin3A/HDAC1 represses C/EBPα transcription during murine adipogenesis through its recruitment by C/EBPβ in the absence of glucocorticoids (figure 3).

3.1.2.3 C/EBP$\beta_{\Delta 153\text{-}156}$ adipogenic potential is also increased in 3T3 L1 cells

While NIH 3T3 cells are a good model for testing C/EBPβ activity, they are pluripotent fibroblasts, rather than preadipocytes. On the other hand, 3T3 L1 cells are preadipocytes in which ectopic expression of C/EBPβ is sufficient to induce adipogenesis without the need of the differentiation inducers (*140, 173, 183*). To verify the adipogenic potential of C/EBP$\beta_{\Delta 153\text{-}156}$ in a cell line committed to the adipocyte lineage, the transcription factor was stably expressed in the 3T3 L1 cell line and its adipogenic potential was tested.

Similarly to the NIH 3T3 cells, 3T3 L1 cells expressing C/EBP$\beta_{\Delta 153\text{-}156}$ differentiated more efficiently into mature adipocytes in the absence of any treatment (i.e. without MIX, insulin and/or dex) (figure 11). The early expression of C/EBPα by C/EBP$\beta_{\Delta 153\text{-}156}$ was able to induce more effectively the expression of the adipocyte markers PPARγ and adipsin (figure 11A). Furthermore, lipid accumulation was also increased in cells expressing C/EBP$\beta_{\Delta 153\text{-}156}$, as shown by the Oil Red O stain (figure 11B). The reason why PPARγ expression was more effectively increased in 3T3 L1 cells expressing C/EBP$\beta_{\Delta 153\text{-}156}$ and not in the NIH 3T3 cells will be discussed in the discussion (pages 144-145). Together, the results suggest that the increased activity of C/EBP$\beta_{\Delta 153\text{-}156}$ could be responsible for the increased adipogenesis observed.

3.1.2.4 C/EBP$\beta_{K98\text{-}102R}$ transcriptional activity and adipogenic potential are increased upon deletion of amino acids 153-156

Figure 11: C/EBP$\beta_{\Delta 153\text{-}156}$ differentiates more efficiently the 3T3 L1 preadipocyte cell line when compared to C/EBPβ_{wt} in the absence of the inducer cocktail.

(A) 3T3 L1 cells were retrovirally transduced to express either empty pLXSN plasmid, C/EBPβ_{wt} or C/EBP$\beta_{\Delta 153\text{-}156}$, grown for 10 days after confluency with no differentiation inducers and harvested for immunoblot analysis to assess the expression profile of some of the adipogenic markers. Note that only the smaller isoform (30KDa) of C/EBPα is shown because of a non-specific overlapping band with the 42KDa isoform. **(B)** The cells were also stained with Oil red O to assess lipid accumulation. The figure represents results observed in three independent experiments.

A

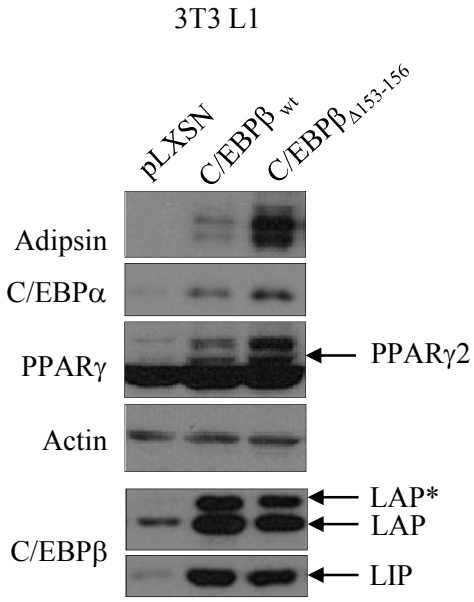
3T3 L1
pLXSN
C/EBPβ wt
C/EBPβΔ153-156
Adipsin
C/EBPα
PPARγ
PPARγ2
Actin
C/EBPβ
LAP*
LAP
LIP

B

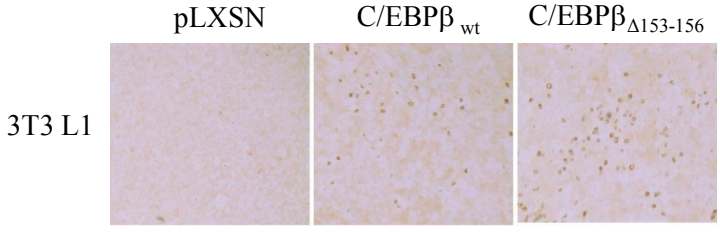
pLXSN
C/EBPβ wt
C/EBPβΔ153-156
3T3 L1

In a previous study in the Haché laboratory where Lys 98,101,102 of C/EBPβ were mutated to compromise GCN5-mediated acetylation, C/EBP$\beta_{K98,101,102R}$ showed a reduced transcriptional activity on the C/EBPα promoter and a compromised adipogenic potential (*106*). The resultant phenotype was correlated with the persistent interaction of C/EBP$\beta_{K98-102R}$ with HDAC1 and with the occupancy of HDAC1 on the C/EBPα promoter even upon dex treatment. Thus abrogation of HDAC1 binding via Δ153-156 might be expected to restore C/EBP$\beta_{K98-102R}$ transcriptional activity and adipogenic potential.

C/EBP$\beta_{K98-102R}$ transcriptional activity was first confirmed to be compromised when compared to C/EBPβ_{wt} in a reporter assay where transcription is driven by the C/EBPα promoter (figure 12A). Moreover, when amino acids 153-156 were deleted from C/EBP$\beta_{K98-102R}$ (giving rise to C/EBP$\beta_{K98-102R,\Delta153-156}$), the new mutant exhibited a transcriptional potential that was higher than C/EBP$\beta_{K98-102R}$ in the absence and presence of glucocorticoids (figure 12A and the protein expression levels in 12B). The activity of C/EBP$\beta_{K98-102R,\Delta153-156}$ reached that of WT C/EBPβ levels but not C/EBP$\beta_{\Delta153-156}$, therefore suggesting that the acetylation of lysines 98,101 and 102 might be required for maximal activity.

Most notably, when C/EBP$\beta_{K98-102R,\Delta153-156}$ adipogenic potential was assessed in 3T3 L1 cells, it induced adipogenesis more efficiently than WT C/EBPβ (figure 12C,D) and to a level similar to that of C/EBP$\beta_{\Delta153-156}$ (see quantification of the protein levels in figure 12E). These results thus suggest that acetylation of C/EBPβ at lysines 98,101,102 by GCN5 is of secondary importance when HDAC1 is unable to bind to (and thus repress) C/EBPβ. The inconsistency between the transcription assay and the differentiation assay is further discussed on pages 125-128.

Figure 12: C/EBPβ$_{K98\text{-}102R,\Delta153\text{-}156}$ is a more potent inducer of preadipocyte differentiation than C/EBPβ$_{wt}$.

(A) C/EBPβ activity is measured by the Luciferase reporter assay from the C/EBPα promoter (-350/+7), as previously mentionned. The pMSV-C/EBPβ constructs (200ng) were co-transfected in NIH 3T3 cells along with the C/EBPα-Luciferase reporter and the glucocorticoid receptor constructs. Cells were treated with either vehicle or 1μM dex the following day for 16h. Luciferase activity was corrected for transfection efficiency by using a co-transfected Renilla expression plasmid (N=3 duplicates, + s.e.m.). **(B)** Western analysis showing the expression level of endogenous C/EBPβ, exogenous C/EBPβ$_{wt}$, C/EBPβ$_{K98\text{-}102R}$ or C/EBPβ$_{K98\text{-}102R,\Delta153\text{-}156}$ in NIH 3T3 cells. **(C)** 3T3 L1 cells were retrovirally transduced to express either empty pLXSN plasmid, C/EBPβ$_{wt}$ or C/EBPβ$_{K98\text{-}102R,\Delta153\text{-}156}$, grown for 10 days after confluency with no differentiation inducers and harvested for immunoblot analysis to assess the expression profile of some of the adipogenic markers. **(D)** The cells were also stained with Oil red O to assess lipid accumulation. The figure represents results observed in two independent experiments. **(E)** Relative expression of the adipsin, C/EBPα and PPARγ2 protein levels from cells expressing either C/EBPβ$_{wt}$, C/EBPβ$_{\Delta153\text{-}156}$ or C/EBPβ$_{K98\text{-}102R,\Delta153\text{-}156}$ (N=2, ± s.d., where * is $p < 0.02$).

A

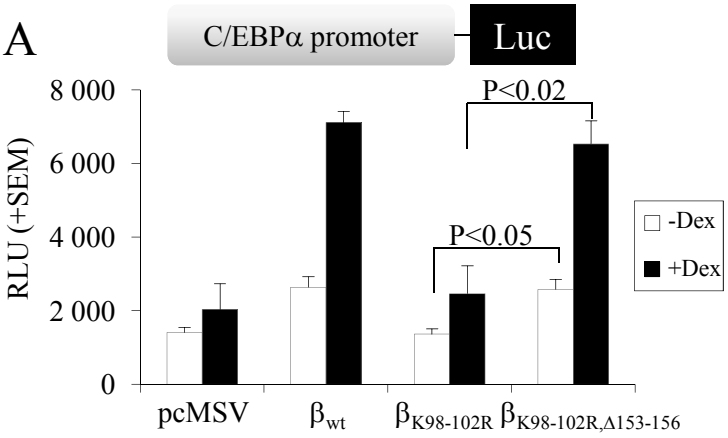

B

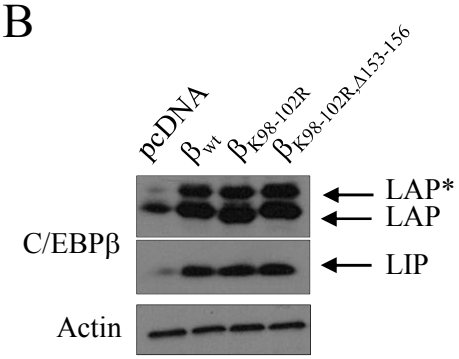

C

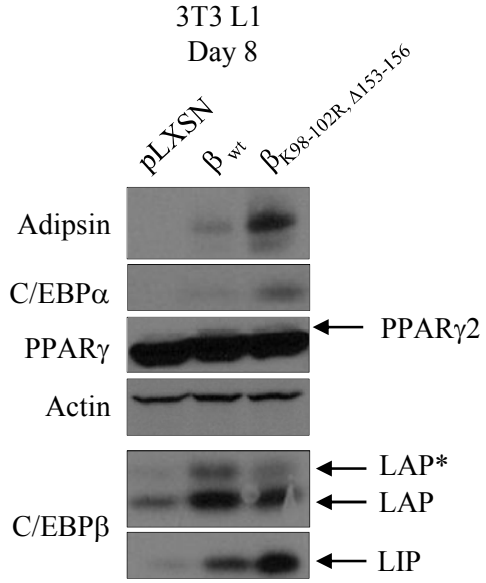

D

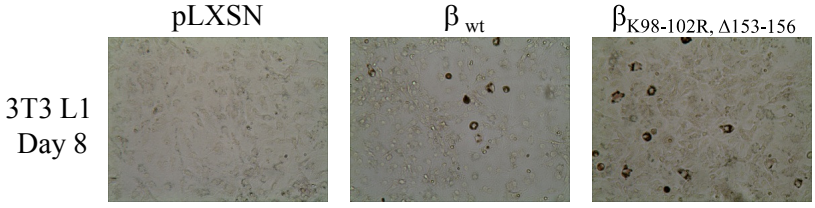

E

	C/EBPβ$_{wt}$	**C/EBPβ$_{Δ153-156}$**	**C/EBPβ$_{K98-102R,Δ153-156}$**
Adipsin	1	6 ± 0.5*	5 ± 0.8*
C/EBPα	1	3 ± 0.2*	3 ± 0.6*
PPARγ2	1	2 ± 0.2*	1 ± 0.2

3.1.3 Characterizing C/EBPβ LIP repressive effect during adipogenesis

3.1.3.1 LIP inhibitory function is partially due to its association with mSin3A/HDAC1

As shown previously in figure 7, amino acids 153-156 of C/EBPβ were required for mSin3A/HDAC1 binding. Interestingly, these amino acids are not only located in a regulatory domain (RD1), but they also represent the N-terminal region of the C/EBPβ LIP isoform, which is defined as C/EBPβ_{152C} (figure 13A). This observation implies that the mSin3A/HDAC1 co-repressor complex could bind to the N-terminal domain of LIP and that LIP might function as an active transcriptional repressor.

CoIP experiment performed in 3T3 L1 cells stably expressing LIP at near physiological levels clearly validated its association with HDAC1 (figure 13B). Moreover, when a LIP mutant lacking the first four amino acids following its first methionine (LIP_{6C}) was used instead of WT LIP, its co-immunoprecipitation with HDAC1 was reduced by approximately 50%, further supporting the importance of amino acids 153-156 for binding to the co-repressor complex. That the interaction between LIP_{6C} and HDAC1 was not completely abolished is most likely due to the heterodimerization between endogenous C/EBPβ isoforms (i.e. LAP*, LAP and LIP) with exogenous LIP_{6C}.

Since LIP_{6C} association with HDAC1 appeared compromised, I sought to test if its inhibitory function would also be affected. Prior to the transcription assay, the protein level of the LIP isoforms were assessed by western blot analysis (figure 13C). Using the C/EBPα-promoter driven Luciferase assay, as previously described in figure 8B, the results showed that increasing expression of LIP proportionally decreased C/EBPβ basal activity,

Figure 13: The LIP_{6C} isoform is a less potent inhibitor of C/EBPβ activity when compared to LIP_{wt}.

(A) Schematic representation of C/EBPβ LAP* indicating the first methionine residue in the LIP isoform, located within the RD1. **(B)** 3T3 L1 cells stably expressing either LIP or LIP_{6C} were subjected to a co-immunoprecipitation assay with endogenous HDAC1. Whole cell lysates were immunoprecipitated with an HDAC1 or a non-specific antibody (Gal4 DBD) followed by incubation with protein-G sepharose beads for antibody precipitation. Data represents results observed in three independent experiments (Student's t-test *P* value was less than 0.05). **(C)** Western analysis showing the expression level of either exogenous C/EBPβ alone (50 ng) or co-transfected with 100 ng of either LIP or LIP_{6C} two days post-transfection in NIH 3T3 cells that were either untreated or treated with dex. **(D)** C/EBPβ activity is measured by the Luciferase reporter assay from the C/EBPα promoter (-350/+7). $C/EBP\beta_{wt}$ with increasing DNA quantity of pcDNA-LIP or pcDNA-LIP_{6C} were co-transfected in NIH 3T3 cells along with the C/EBPα-Luciferase reporter and the glucocorticoid receptor constructs. Cells were treated with either vehicle (left panel) or 1μM dex (right panel) the following day for 16h. Luciferase activity was corrected for transfection efficiency by using a co-transfected Renilla expression plasmid. The two conditions are shown in two separate graphs to easily evidence the phenotype observed in the condition with no steroids. (N=3 duplicates, + s.e.m.).

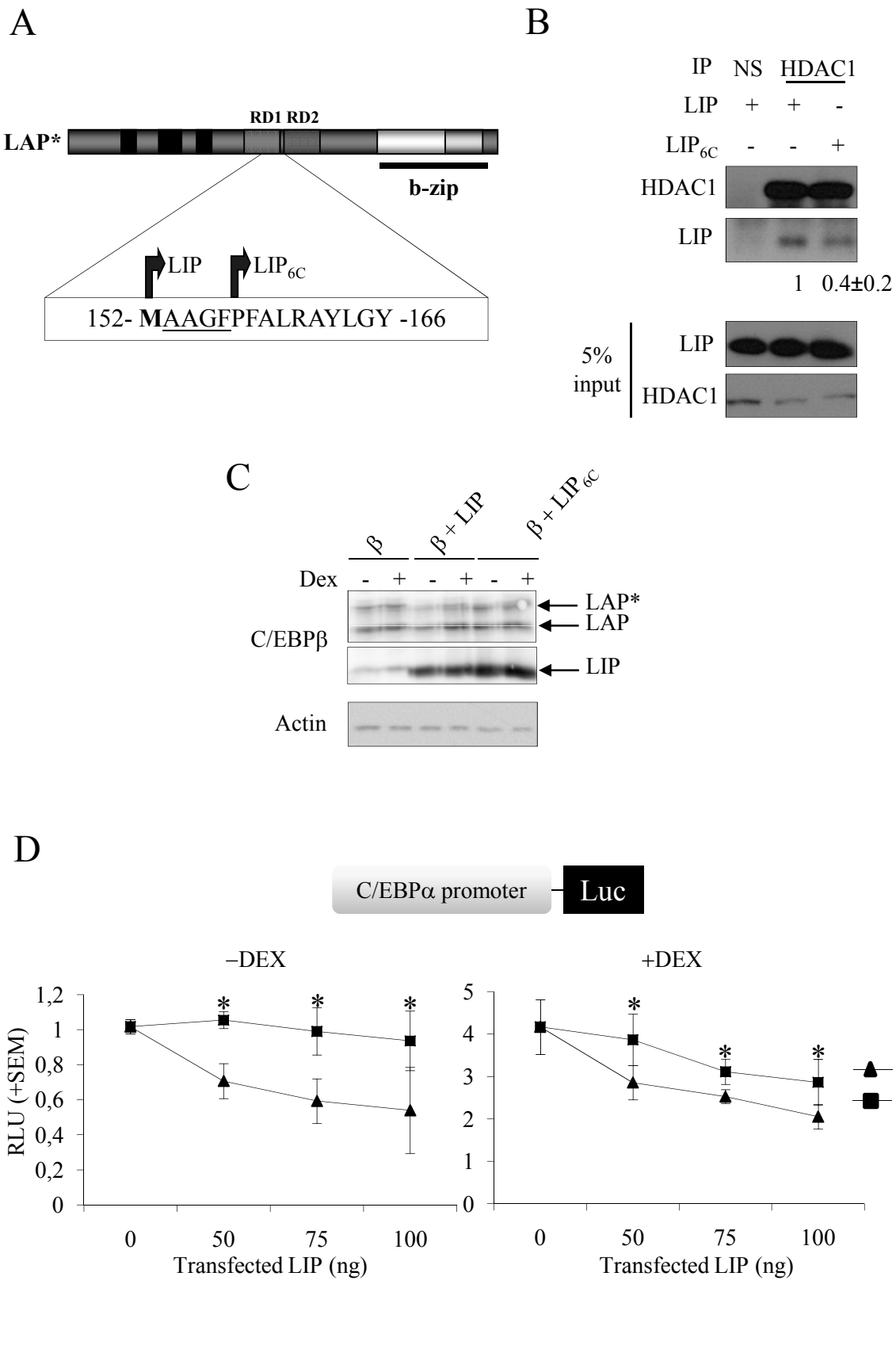
A
RD1 RD2
LAP*
b-zip
LIP
LIP6C
152- MAAGFPFALRAYLGY -166
B
IP NS HDAC1
LIP + + -
LIP6C - - +
HDAC1
LIP
1 0.4±0.2
5% input
LIP
HDAC1
C
β
β + LIP
β + LIP 6C
Dex - + - + - +
LAP*
LAP
C/EBPβ
LIP
Actin
D
C/EBPα promoter
Luc
–DEX
+DEX
RLU (+SEM)
1,2
1
0,8
0,6
0,4
0,2
0
5
4
3
2
1
0
0 50 75 100
Transfected LIP (ng)
LIP
LIP6C

approaching two fold inhibition at 100ng of transfected plasmid (figure 13D, left panel). LIP_{6C} failed to significantly affect C/EBPβ activity. Although the same trend in LIP-mediated inhibition of C/EBPβ was observed in the presence of glucocorticoids, LIP_{6C} was in this condition able to slightly (approximately 25%) decrease C/EBPβ activity, only at higher expression levels (figure 13D, right panel). One should notice that the overall activity of C/EBPβ in the presence of dex was still higher than in its absence (compare right panel to left panel of figure 13D, where C/EBPβ activity in the absence of dex is defined as 1 RLU).

3.1.3.2 Deletion of the first 4 amino acids in LIP alleviates its inhibitory function in preadipocyte differentiation

Since ectopic expression of LIP in 3T3 L1 cells completely abolishes adipogenesis (*140*), I sought to test the extent to which LIP_{6C} retains this inhibitory function. After stably expressing LIP or LIP_{6C}, 3T3 L1 cells were differentiated with MID and adipogenesis was monitored 8 days post-treatment. As shown in figure 14A,B, 3T3 L1 cells infected with the pLXSN control plasmid differentiated efficiently, showing high levels of adipsin, C/EBPα, PPARγ2 and high lipid accumulation, as seen by Oil red O staining. Expression of LIP however strongly reduced adipsin, C/EBPα and PPARγ2 expression. While 3T3 L1 cells expressing LIP_{6C} differentiated poorly when compared to control cells, they still showed an intermediate level of adipogenesis, as shown by Western analysis of C/EBPα, PPARγ2, adipsin and Oil Red O staining of the lipids.

When expressed from a retroviral vector, LIP and LIP_{6C} expression persists throughout differentiation (figure 14A). However, endogenous LIP expression ceases within 3 days of the induction of differentiation (figure 14C), as C/EBPβ expression is replaced by C/EBPα (*137, 140*). To exclude the possibility of an artifactual effect of the sustained

Figure 14: LIP_{6C} inhibits less efficiently C/EBPα, PPARγ2 and adipsin protein expression during preadipocyte differentiation.

3T3 L1 cells were retrovirally transduced to express either pLXSN vector, LIP or LIP_{6C}, grown for 8 days following MID treatment. Cells were either harvested for western analysis using the adipsin, C/EBPα or PPARγ2 and actin antibodies **(A)** or stained with Oil red O **(B)**. In the PLXSN mock condition, only 25% of the protein lysate was loaded to avoid a saturated signal. Data represent results observed in three independent experiments. **(C)** Time-course western analysis of endogenous C/EBPβ levels in 3T3 L1 cells following their treatment with either MI (-) or MID (+) at two days post-confluency. Data represent results observed in three independent experiments. **(D)** Western blot analysis showing the expression level of either endogenous (pcDNA mock plasmid) or exogenous LIP in 3T3 L1 cells three days following transfection with 100ng of the DNA constructs. **(E)** The transfected 3T3 L1 cells were also harvested two days post-treatment (or 5 days following transfection with the LIP constructs) to evidence decrease in exogenous LIP expression, as shown by similar expression levels in all three lanes. **(F)** One day before confluency, 3T3 L1 cells were transiently transfected with increasing DNA quantity of the pcDNA-LIP or pcDNA-LIP_{6C} constructs. Three days later, the cells were induced to differentiate with MID for 8 days and harvested for immunoblot analysis of the adipogenic markers. Data represent results observed in two independent experiments.

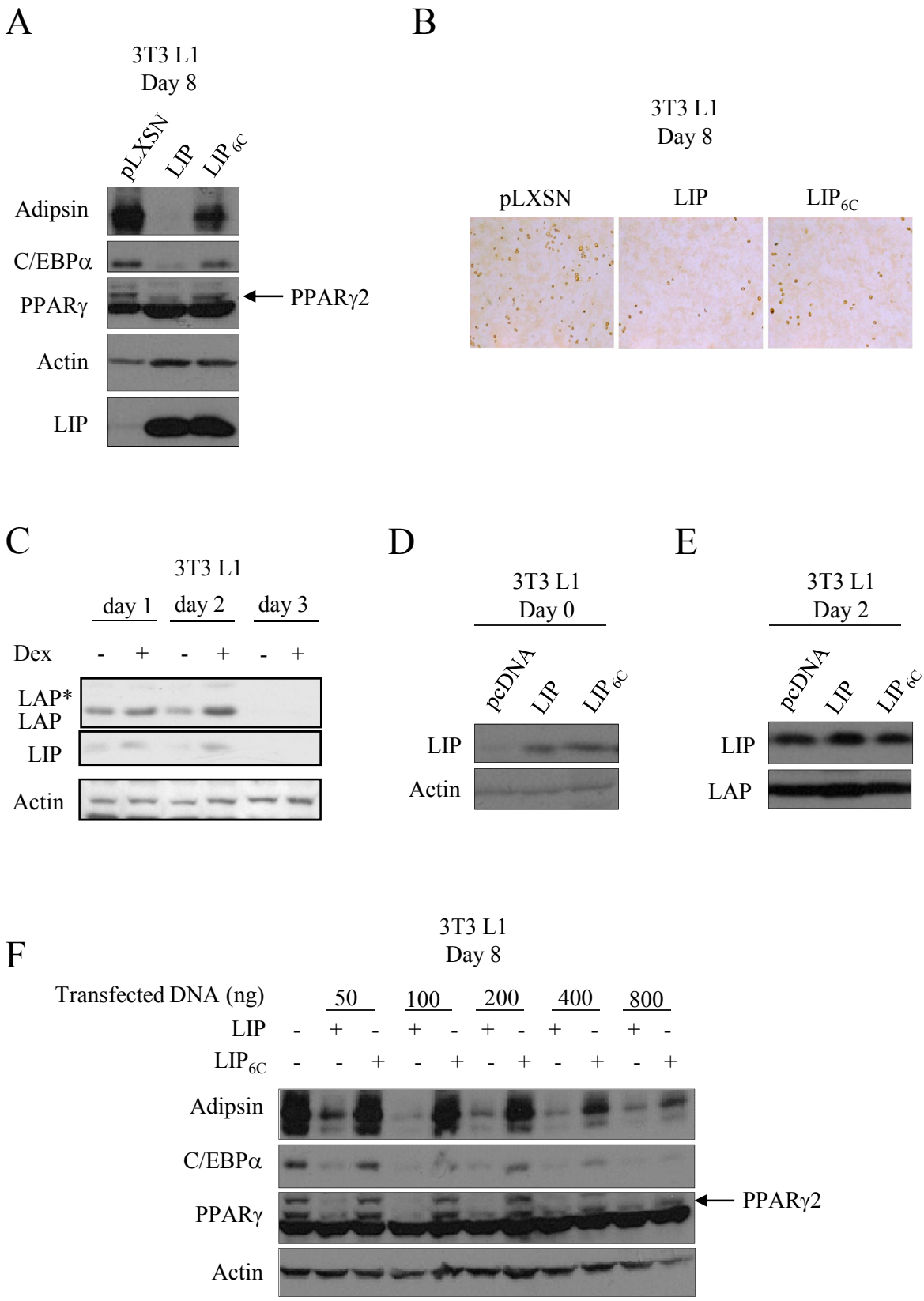
A
3T3 L1
Day 8
pLXSN
LIP
LIP6C
Adipsin
C/EBPα
PPARγ
PPARγ2
Actin
LIP
B
3T3 L1
Day 8
pLXSN
LIP
LIP6C
C
3T3 L1
day 1
day 2
day 3
Dex
- + - + - +
LAP*
LAP
LIP
Actin
D
3T3 L1
Day 0
pcDNA
LIP
LIP6C
LIP
Actin
E
3T3 L1
Day 2
pcDNA
LIP
LIP6C
LIP
LAP
F
3T3 L1
Day 8
Transfected DNA (ng)
50
100
200
400
800
LIP
LIP6C
Adipsin
C/EBPα
PPARγ
PPARγ2
Actin

expression of LIP in the differentiation of preadipocytes, I repeated the 3T3 L1 differentiation experiments with cells in which LIP and LIP_{6C} were expressed by transient transfection prior to the initiation of differentiation. In this case, the levels of exogenous LIP were elevated over endogenous LIP at day 0 (figure 14D), but had declined by day 2 so that an increase in LIP expression over the endogenous factor was no longer evident (figure 14E). Under these conditions, LIP still effectively inhibited preadipocyte differentiation at the early stages of differentiation (when C/EBPβ is expressed prior to C/EBPα and PPARγ) as reflected by a reduction in adipsin, C/EBPα and PPARγ2 at day 8 of differentiation, with the strongest inhibition at higher expression levels (figure 14F). Again, LIP_{6C} was only partially effective in repressing differentiation compared to LIP, even at elevated expression levels.

To briefly summarize the results in this section, I showed that the mSin3A/HDAC1 complex depends on a domain encompassing amino acids 153-156 of C/EBPβ for its interaction with C/EBPβ. Further, I have identified amino acids 153-156 as conferring active transcriptional repression on LIP that plays an important role in the dampening of adipogenesis.

3.1.4 Characterizing HDAC1 involvement on 3T3 L1 MCE through LAP/LIP

3.1.4.1 C/EBPβ_{wt} expressing cells show a slightly increased DNA replication rate than cells expressing C/EBP$\beta_{\Delta 153\text{-}156}$ during MCE

An extensive body of evidence shows C/EBPβ involvement in the mitotic clonal expansion (MCE) process that is required for adipogenesis (*162-163, 290-291*). However, it is not known how precisely C/EBPβ promotes MCE, although its DNA-binding ability has been shown to be required in this process (*162*). Additionally, HDAC1 has been shown to

promote proliferation in liver cells through C/EBPβ (*285*), hence suggesting that C/EBPβ activity could be involved in potentiating cellular proliferation that occurs during MCE.

Since we altered C/EBP$\beta_{\Delta 153\text{-}156}$ activity by compromising its interaction with HDAC1, I sought to assess if the absence of HDAC1 would actually decrease MCE during 3T3 L1 differentiation by first evaluating the expression levels of some of the key cell cycle regulators. We know that upon treatment of 3T3 L1 cells with the differentiation cocktail, upregulation of cyclin A and cyclin B1 occurs as early as 16h post-induction whereas p27/kip1, whose expression blocks the G_1-S checkpoint by inhibitory interactions with cyclin A, decreases gradually to reach its lowest level at about 16h post-treatment (*123, 162, 291*). The concomitant increase of cyclin A and decrease of p27/kip1 are thus markers for MCE in 3T3 L1 cells.

Curiously, untreated cells expressing either C/EBPβ_{wt} or C/EBP$\beta_{\Delta 153\text{-}156}$ that were harvested 3 days post-confluency (where 2 days post-confluency is when the cells are usually treated with the inducers) did not express any detectable cyclin A and had relatively higher levels of p27/kip1 (figure 15A, lane 1-3), thus suggesting that the cells cannot enter the S phase to initiate DNA replication. In fact, an ^{3}H-thymidine incorporation assay also confirmed that MCE was not initiated in these conditions (figure 15B, left panel), when compared to the MI condition (figure 15B, right panel), which has been shown to be sufficient to induce mitosis (*120*). These results thus confirm that the increased adipogenesis observed in 3T3 L1 cells expressing C/EBP$\beta_{\Delta 153\text{-}156}$ in the absence of inducers was not due to its ability to increase cell number, but mainly to its higher transactivation potential on adipogenic promoters.

Figure 15: Ectopic expression of WT C/EBPβ affects the expression of some of the cell cycle regulators during 3T3 L1 differentiation

(A) 3T3 L1 cells were retrovirally transduced to express either empty pLXSN plasmid, C/EBPβ_{wt} or C/EBP$\beta_{\Delta 153\text{-}156}$, grown for three days post-confluency (where two days post-confluency is defined as being day 0) either with no treatment (–) or with MI during the third day. The cells were then harvested for immunoblot analysis of the cell cycle regulators cyclin B1, cyclin A and p27/kip1. Data represent results observed in three independent experiments. **(B)** DNA synthesis was also evaluated in 3T3 L1 cells by ^{3}H-thymidine incorporation assay at 6h, 24h and 48h following treatment of 3T3 L1 with either MI or untreated, as specified. Each condition was performed in triplicate (N=2, ±SEM) **(C)** 3T3 L1 cells stably expressing either the pLXSN vector, LIP or LIP_{6C} were harvested either prior to treatment (day 0), 4h or 24h following treatment with MID and subjected to western blot analysis as in **(A)**. Data represent results observed in three independent experiments. **(D)** DNA synthesis was evaluated as in **(B)**, but in 3T3 L1 cells stably expressing pLXSN, LIP or LIP_{6C}. Each condition was performed in triplicate (N=2, ±SEM)

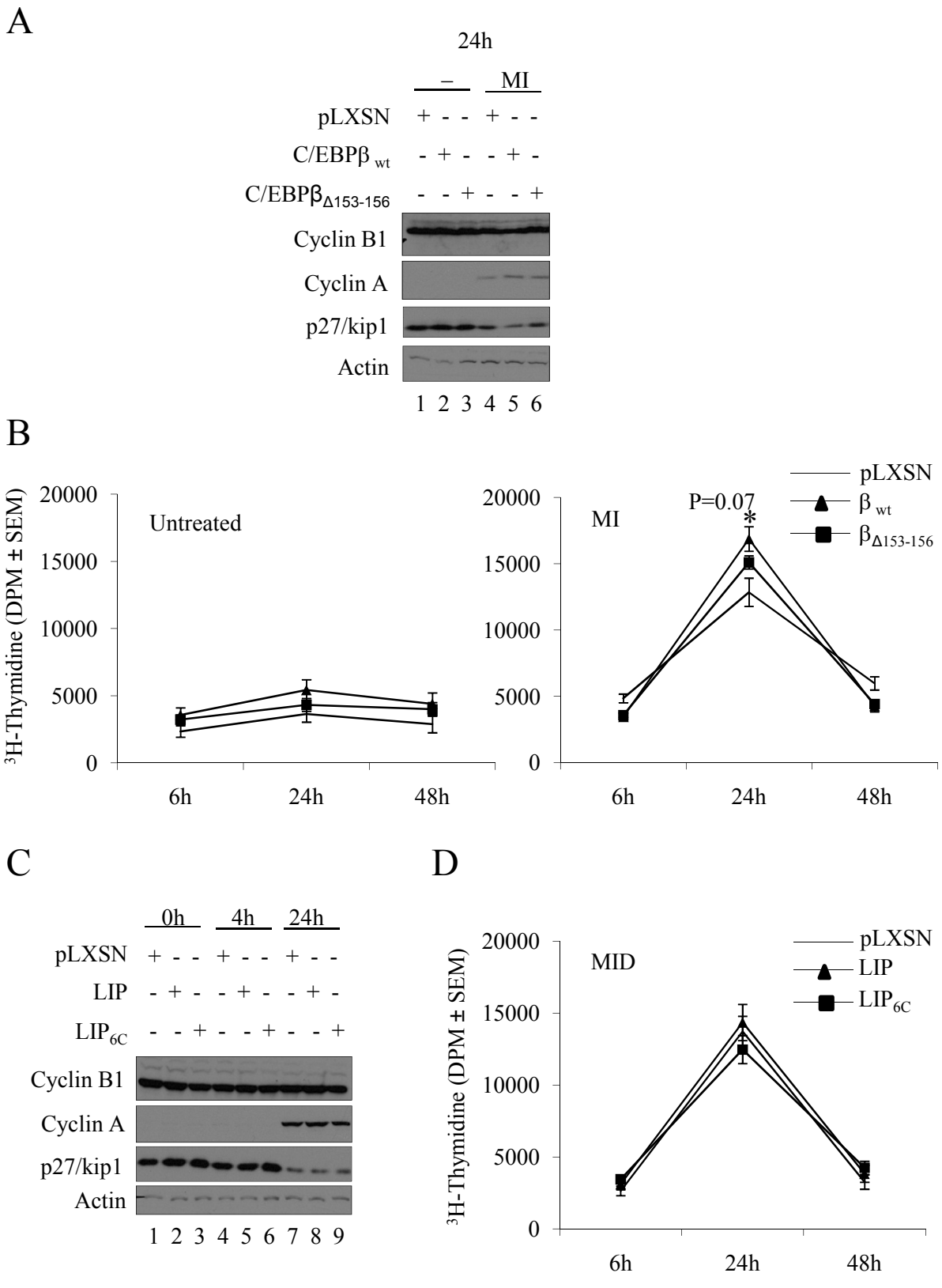
A
24h
–
MI
pLXSN + - - + - -
C/EBPβ wt - + - - + -
C/EBPβΔ153-156 - - + - - +
Cyclin B1
Cyclin A
p27/kip1
Actin
1 2 3 4 5 6
B
3H-Thymidine (DPM ± SEM)
20000
15000
10000
5000
0
Untreated
MI
P=0.07
*
pLXSN
β wt
βΔ153-156
6h
24h
48h
C
0h
4h
24h
pLXSN + - - + - - + - -
LIP - + - - + - - + -
LIP6C - - + - - + - - +
Cyclin B1
Cyclin A
p27/kip1
Actin
1 2 3 4 5 6 7 8 9
D
3H-Thymidine (DPM ± SEM)
MID
pLXSN
LIP
LIP6C

When the cells were treated with MI, an increased expression of cyclin A and decreased p27/kip1 expression was observed (figure 15A, lane 4-6), thus favouring mitosis (figure 15B, right panel). Curiously, p27/kip1 expression was constantly observed to be the lowest in cells expressing C/EBPβ_{wt} than C/EBP$\beta_{\Delta 153\text{-}156}$, in the MI condition (figure 15A, compare lane 5 and lane 6).

Furthermore, cells expressing C/EBPβ_{wt} also showed a slightly higher DNA replication level than mock infected and C/EBP$\beta_{\Delta 153\text{-}156}$ expressing cells, as shown by a thymidine incorporation assay (~17000 VS 15000 DPM respectively, figure 15B, right panel). Collectively, these results suggest that treatment of 3T3 L1 cells with MI is required for the cells to initiate mitosis during adipogenesis and that HDAC1 association with C/EBPβ might play an important role in promoting MCE. However, the over-expression of C/EBPβ by itself was not sufficient to replace the effect of the cocktail treatment in inducing cell division when MCE was evaluated 3 days following confluency. Although these results suggest that in conditions where C/EBPβ is over-expressed, MCE is not vital for adipogenesis to occur, this process amplifies the adipogenic program as a MI treatment of 3T3 L1 cells stably expressing C/EBPβ results in more differentiation when compared to a condition without the inducers (data not shown).

3.1.4.2 Over-expression of LIP_{wt} and LIP_{6C} did not alter MCE during 3T3 L1 adipogenesis in the presence of the full adipogenic inducers

As previously mentioned, HDAC1 seems to be involved in regulating C/EBPβ-dependent cellular proliferation (*285*). More importantly, LIP has also been shown to regulate cellular proliferation (*292-293*), thus making it a good candidate to promote MCE. In light of these findings, I sought to confirm whether LIP over-expression might affect MCE

during adipogenesis. Analysis of some of the key cell cycle regulators suggests that there is no major difference in cellular proliferation in cells over-expressing either LIP or LIP_{6C} when compared to pLXSN infected cells, as seen by a similar increase in cyclin A expression and similar decrease in p27/kip1 levels (figure 15C, lane 7-9). Again, ^{3}H-thymidine incorporation assay did not show any significant differences ($p > 0.25$) when evaluated during the first 48h of differentiation in the presence of the differentiation inducers. These results thus suggest that over-expression of LIP did not affect MCE and that the increased differentiation in cells expressing LIP_{6C} is not due to increased MCE.

3.1.5 Defining the inhibitory contribution of LIP and mSin3A/HDAC1 in repressing C/EBPβ adipogenic potential

3.1.5.1 C/EBPβ_{M152A} and C/EBP$\beta_{\Delta 151\text{-}156}$ have similar transcriptional activity

Given that LIP and mSin3A/HDAC1 are both involved in inhibiting C/EBPβ LAP activity by decreasing the number of activation domains (passive repression by decreasing co-activator loading on LAP*/LAP) and by deacetylating LAP*/LAP and the promoter environment (active repression), respectively, I sought to determine whether their inhibitory effects were additive. If they are additive, then a C/EBPβ protein that lacks both mSin3A binding domain and can not express LIP would be much more transcriptionally active than one that lacks either mSin3A binding domain or can not express LIP. To address this question, two additional mutants were constructed: C/EBPβ_{M152A} (compromised for LIP expression) and C/EBP$\beta_{\Delta 151\text{-}156}$ (compromised for both LIP expression and mSin3A binding). Transient transfection experiments performed in Cos7 cells confirmed that

Figure 16: C/EBPβ$_{M152A}$ and C/EBPβ$_{Δ151-156}$ both have a higher transcriptional activity than C/EBPβ$_{wt}$

(A) Cos 7 cells were co-transfected with expression plasmids for flag-HDAC1 and either C/EBPβ$_{wt}$, C/EBPβ$_{M152A}$ or C/EBPβ$_{Δ151-156}$. Whole cell lysates were immunoprecipitated with a FLAG affinity resin. Data represent results observed in three independent experiments. Only the LAP isoform is shown because of a non-specific band that overlaps with LAP*. **(B)** Summary of the different C/EBPβ constructs with respect to LAP*/LAP and LIP expression and to HDAC1 binding. **(C)** Schema of the different constructs used. **(D)** Upper panel: C/EBPβ activity was measured by the Luciferase reporter assay from the -350/+7 C/EBPα promoter. C/EBPβ$_{wt}$, C/EBPβ$_{Δ153-156}$, C/EBPβ$_{M152A}$ and C/EBPβ$_{Δ151-156}$ were transfected in NIH 3T3 cells along with the C/EBPα-Luciferase reporter and the glucocorticoid receptor constructs. Cells were treated with either vehicle (□) or 1μM dex (■) the following day for 16h. Luciferase activity was corrected for transfection efficiency by using a co-transfected Renilla expression plasmid (N=4 duplicates, + s.e.m.). Right panel: Western analysis showing the expression level of the transfected C/EBPβ constructs in NIH 3T3 cells.

A

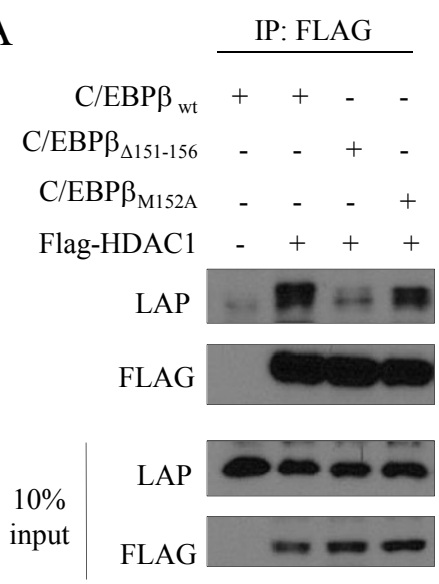

B

	LAP*/LAP	LIP	HDAC1 binding
β_{wt}	+	+	+
$\beta_{\Delta153-156}$	+	+	-
β_{M152A}	+	-	+
$\beta_{\Delta151-156}$	+	-	-

C

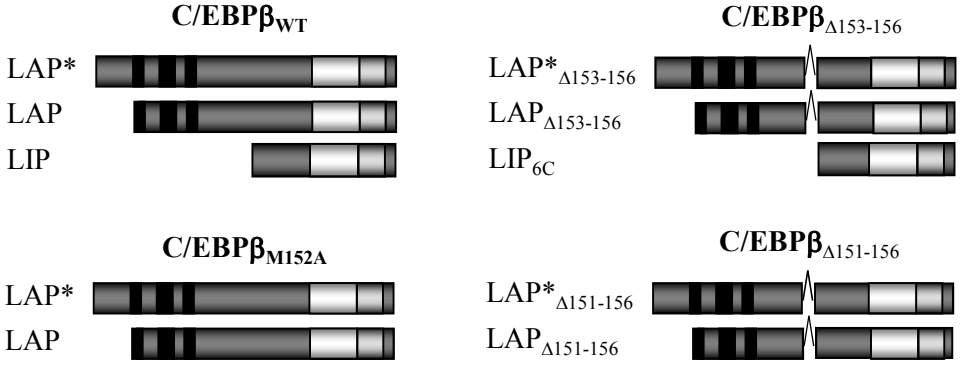

D

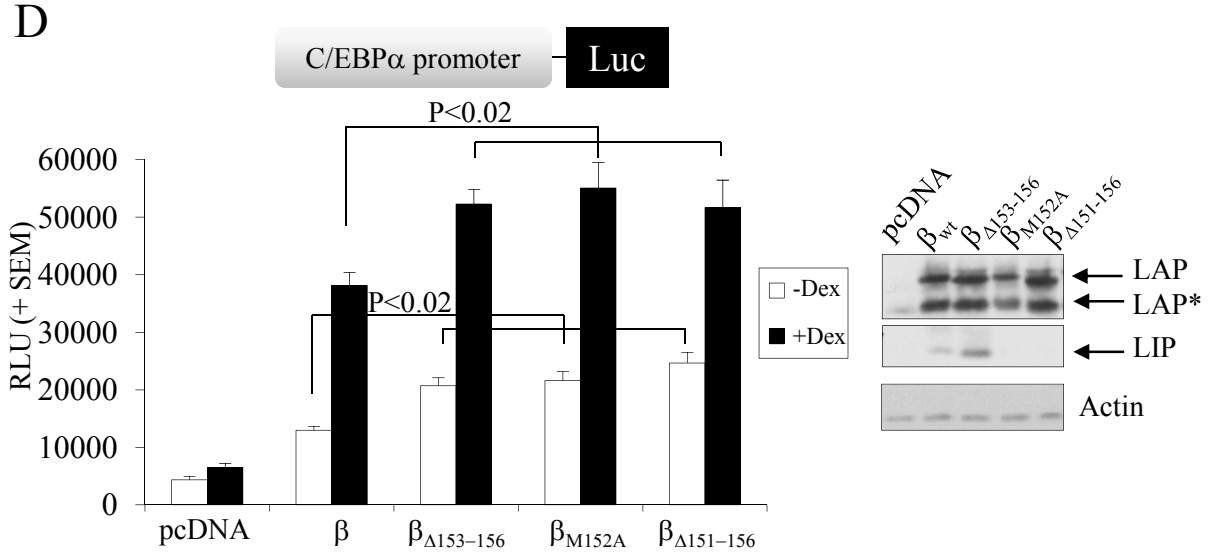

C/EBPβ$_{M152A}$, but not C/EBPβ$_{\Delta 151\text{-}156}$, co-immunoprecipitated with HDAC1 (figure 16A and summary in 16B).

To compare their transcriptional activity, a C/EBPα-promoter driven Luciferase assay was performed and C/EBPβ$_{wt}$, C/EBPβ$_{\Delta 153\text{-}156}$, C/EBPβ$_{M152A}$ and C/EBPβ$_{\Delta 151\text{-}156}$ (schema in figure 16C) activity were tested either in the absence or presence of dex. As illustrated in figure 16D, all three mutated proteins behaved similarly in the absence and presence of dex: they were all more transcriptionally active than C/EBPβ$_{wt}$. Western blot analysis (figure 16D, right panel) shows that this effect was not attributable to discrepancies between the expression levels of each protein. Hence, LIP and mSin3A/HDAC1 inhibitory effects were not additive in this assay.

3.1.5.2 HDAC1 presence is decreased from the C/EBPα promoter in NIH 3T3 cells expressing C/EBPβ$_{\Delta 151\text{-}156}$ but not C/EBPβ$_{M152A}$

Since LAP and LIP can independently associate with HDAC1, I sought to determine whether HDAC1 recruitment to the C/EBPα promoter depends exclusively on LIP expressed from the WT C/EBPβ transcript. To clarify this question, I performed a ChIP experiment by immunoprecipitating HDAC1 24h after MI treatment of the NIH 3T3 cells stably expressing either WT C/EBPβ or C/EBPβ$_{M152A}$, which lacks the initiator methionine encoding LIP. As illustrated in figure 17A, HDAC1 was confirmed to be recruited on the C/EBPα promoter by LAP*/LAP without further requirement for LIP expression, in cells expressing C/EBPβ$_{M152A}$. Furthermore, when the minimal domain encompassing amino acids 153-156 required for HDAC1 binding in C/EBPβ was removed from C/EBPβ$_{M152A}$, giving rise to C/EBPβ$_{\Delta 151\text{-}156}$, HDAC1 recruitment was eliminated from the C/EBPα promoter (figure 17B).

Figure 17: C/EBPβ$_{M152A}$ but not C/EBPβ$_{Δ151-156}$ recruits HDAC1 to the C/EBPα promoter.

C/EBPβ expressing NIH 3T3 cells were treated with MI for 24h to assess HDAC1 recruitment on the C/EBPα promoter by either **(A)** C/EBPβ$_{M152A}$ or **(B)** C/EBPβ$_{Δ151-156}$. The cells were then harvested, cross-linked and the nuclear extract was immunoprecipitated using an HDAC1 antibody. Following several washes, the precipitated DNA was isolated and subjected to a PCR reaction that amplifies region -460/-244 of the C/EBPα promoter (N=2 for each C/EBPβ construct).

A

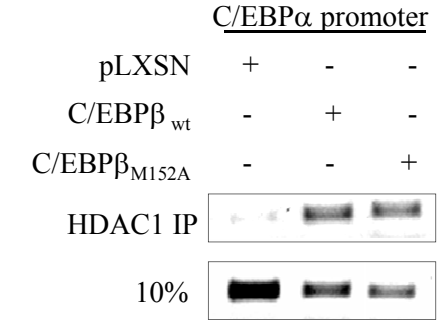
C/EBPα promoter
pLXSN + - -
C/EBPβ wt - + -
C/EBPβM152A - - +
HDAC1 IP
10%

B

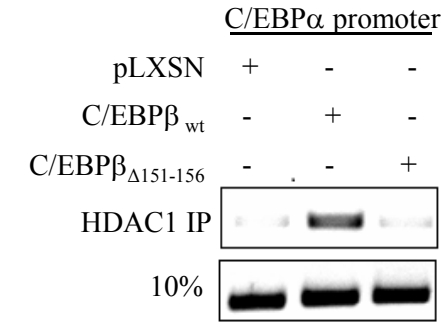
C/EBPα promoter
pLXSN + - -
C/EBPβ wt - + -
C/EBPβΔ151-156 - - +
HDAC1 IP
10%

These results thus confirm that LAP*/LAP are sufficient to recruit HDAC1 to the C/EBPα promoter independently of LIP. Moreover the elevated activity of C/EBPβ_{M152A} could be due to a higher number of activation domains present on the promoter (from LAP-LAP homodimers), rather than decreased co-repressor association due to absence of LIP since LAP can still bind to HDAC1. We could therefore speculate that the activating effect of C/EBPβ activation domains could be dominant over the repressive effect of mSin3A/HDAC1, thus explaining why C/EBP$\beta_{\Delta 151\text{-}156}$ (no LIP and no mSin3A/HDAC1 interaction) activity was not higher than that of C/EBPβ_{M152A} on the synthetic C/EBPα promoter (figure 16B,C).

3.1.5.3 C/EBP$\beta_{\Delta 151\text{-}156}$ has the highest dex-dependent adipogenic potential when compared to C/EBPβ_{wt}, C/EBP$\beta_{\Delta 153\text{-}156}$ or C/EBPβ_{M152A}

Given that the transcription assay did not show any additive effect when comparing C/EBPβ_{M152A} and C/EBP$\beta_{\Delta 151\text{-}156}$ under the conditions employed, I sought to confirm these observations in a more physiologically relevant system. To do so, I stably expressed the mutant constructs in NIH 3T3 cells and monitored their adipogenic potential. Figure 18 shows that NIH 3T3 cells expressing C/EBPβ_{M152A} or C/EBP$\beta_{\Delta 151\text{-}156}$ differentiated much more efficiently into mature adipocytes than C/EBPβ_{wt} and C/EBP$\beta_{\Delta 153\text{-}156}$, as shown by the Western analysis of the adipogenic marker adipsin (figure 18A) and the Oil Red O staining of lipids (figure 18B). Interestingly, cells expressing C/EBP$\beta_{\Delta 151\text{-}156}$ consistently showed the highest adipsin levels in conditions where dex was added to the differentiation media, thus suggesting that the effect of both the absence of LIP and HDAC1 were additive when it comes to adipsin induction in a dex-dependent manner.

Figure 18: C/EBPβ$_{M152A}$ and C/EBPβ$_{Δ151-156}$ both have a higher adipogenic potential than either C/EBPβ$_{Δ153-156}$ or C/EBPβ$_{wt}$.

(A) NIH 3T3 cells that were retrovirally transduced to express the C/EBPβ constructs were harvested 4 days post-induction without (MI) or with (MID) 250nM dex and subjected to a western analysis with the adipsin and actin antibodies. Quantification of the adipsin level was obtained from three independent experiments ($p<0.05$). **(B)** The cells were also stained with Oil red O 6 days after induction of differentiation to qualitatively assess lipid accumulation. Data represents results observed in two independent experiments.

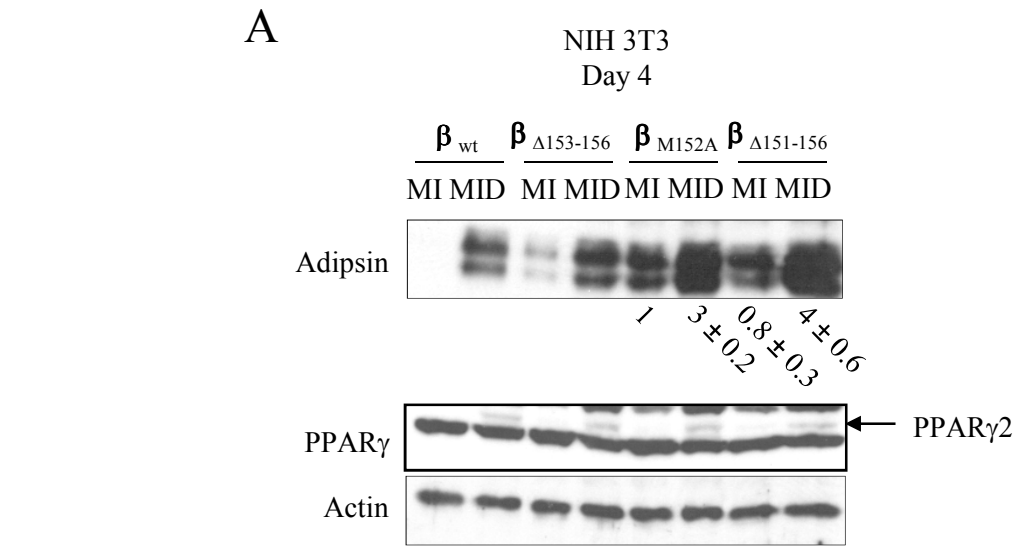
A
NIH 3T3
Day 4
β wt
β Δ153-156
β M152A
β Δ151-156
MI MID MI MID MI MID MI MID
Adipsin
1
3±0.2
0.8±0.3
4±0.6
PPARγ
PPARγ2
Actin

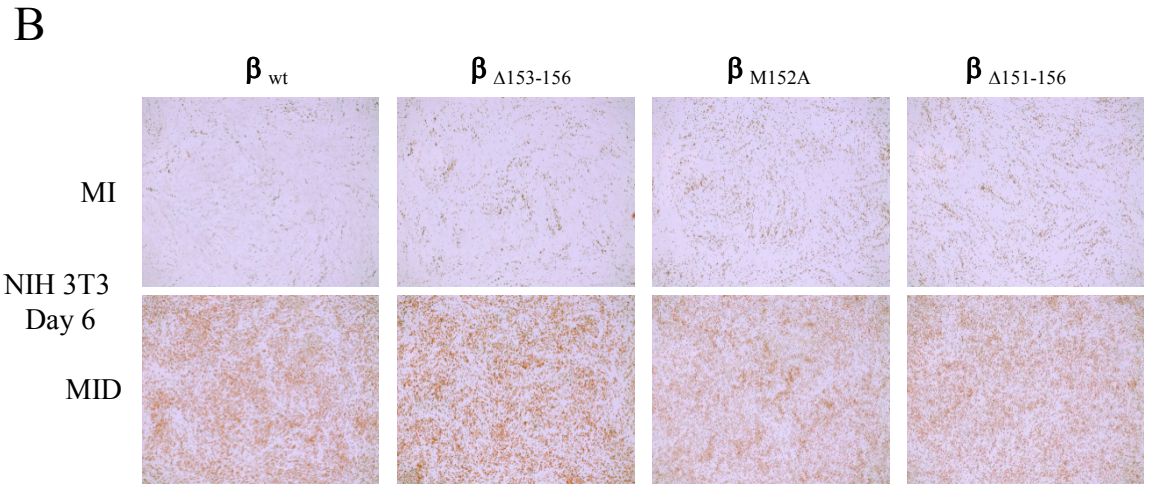
B
β wt
β Δ153-156
β M152A
β Δ151-156
MI
NIH 3T3
Day 6
MID

3.1.5.4 C/EBPβ$_{M152A}$ and C/EBPβ$_{\Delta 151\text{-}156}$ activate C/EBPα and PPARγ2 mRNA expression more efficiently than C/EBPβ$_{wt}$

The best time to test for C/EBPβ activity is at the beginning of the differentiation process when the protein levels of C/EBPα and/or PPARγ are undetectable by Western analysis. Knowing that these two transcription factors cross-regulate the expression of one another, having one of them expressed might interfere with the conclusions reached when C/EBPβ activity is involved. To avoid incorrect interpretation of the results, C/EBPβ activity was measured on the first 2 days post-treatment by quantifying C/EBPα and PPARγ2 mRNA levels by a quantitative RT-PCR reaction.

As illustrated in figure 19A (left panel), C/EBPβ$_{M152A}$ and C/EBPβ$_{\Delta 151\text{-}156}$ both induced C/EBPα expression to the same extent when its level was measured 24h post-treatment. Moreover, C/EBPα expression induced by C/EBPβ$_{wt}$ in the presence of steroids was similar to C/EBPα levels induced by C/EBPβ$_{M152A}$ and C/EBPβ$_{\Delta 151\text{-}156}$ in the absence of glucocorticoids. Interestingly, addition of dex in cells expressing either C/EBPβ$_{M152A}$ or C/EBPβ$_{\Delta 151\text{-}156}$ further increased C/EBPα expression levels two fold, as we can see with ratio of MID/MI.

When C/EBPα mRNA expression was assessed 48h post-induction (figure 19A, right panel), the trends of its expression was similar to the 24h time period, although the overall levels of C/EBPα mRNA expression was higher in all C/EBPβ-expressing cells when compared to the pLXSN-infected cells. Moreover, the dex-dependent induction of C/EBPα in cells expressing C/EBPβ$_{wt}$, C/EBPβ$_{M152A}$ and C/EBPβ$_{\Delta 151\text{-}156}$ were all higher (approximately 7, 3 and 3 fold increase in the ratio of MID/MI, respectively), probably due

Figure 19: C/EBPβ$_{M152A}$ and C/EBPβ$_{Δ151-156}$ transcribe more efficiently endogenous C/EBPα and PPARγ2 when compared to C/EBPβ$_{wt}$.

NIH 3T3 cells stably expressing either C/EBPβ$_{wt}$, C/EBPβ$_{M152A}$ or C/EBPβ$_{Δ151-156}$ were subjected to a real time RT-PCR reaction 24h (left panels) and 48h (right panels) after induction of differentiation without (MI) or with (MID) dex. **(A)** C/EBPα and **(B)** PPARγ2 mRNA levels were normalized to actin (N=3, + s.d.). **(C)** The glucose transporter 4 (GLUT4) mRNA levels were also assessed 48h after induction of differentiation (N=3, + s.d.).

A

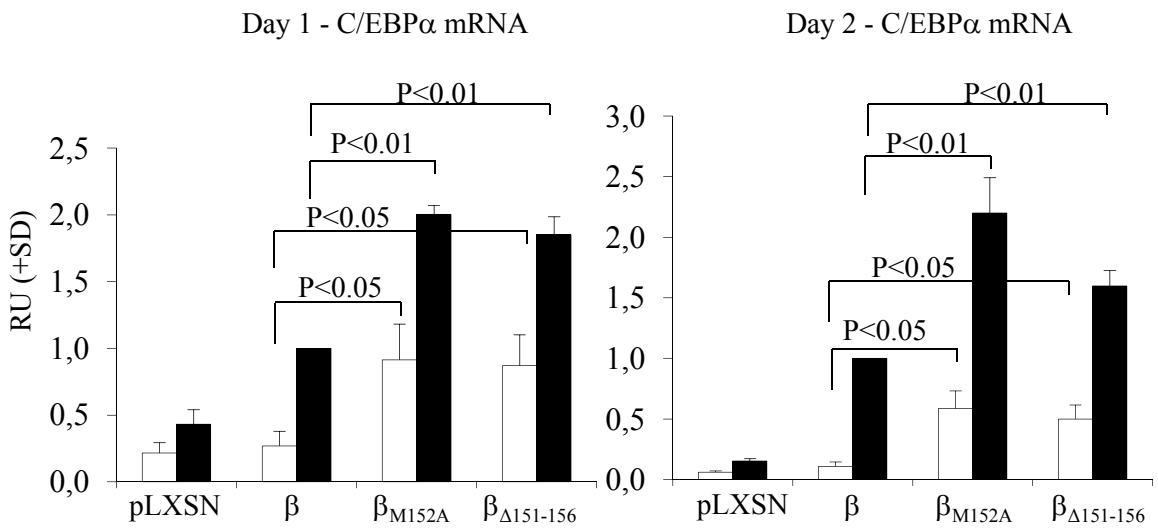
Day 1 - C/EBPα mRNA
Day 2 - C/EBPα mRNA
RU (+SD)
P<0.01
P<0.05
pLXSN
β
βM152A
βΔ151-156

B

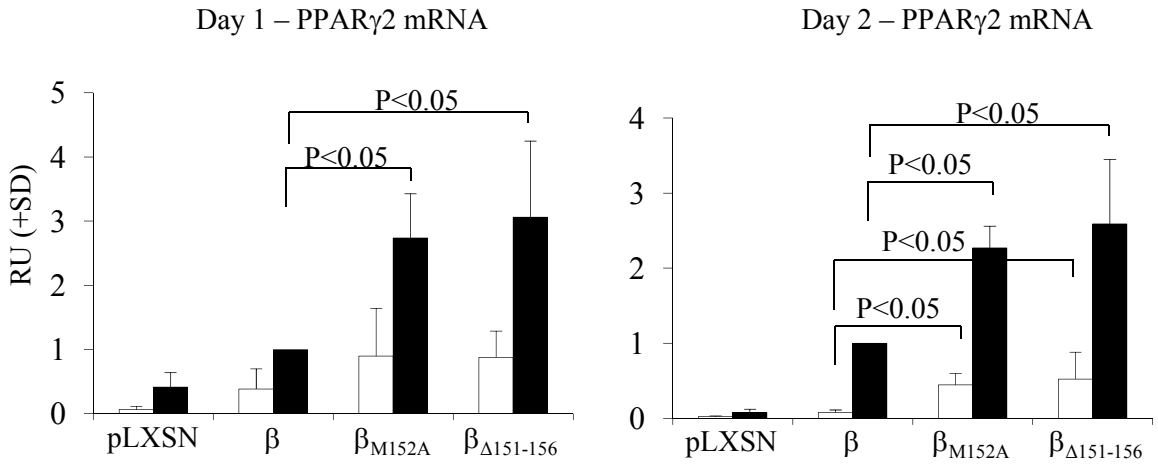
Day 1 – PPARγ2 mRNA
Day 2 – PPARγ2 mRNA
RU (+SD)
P<0.05
pLXSN
β
βM152A
βΔ151-156

C

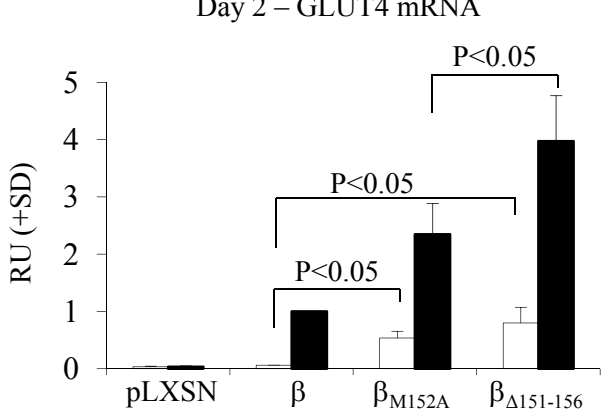
Day 2 – GLUT4 mRNA
RU (+SD)
P<0.05
pLXSN
β
βM152A
βΔ151-156

to PPARγ2 activity, which has been shown to be detected by Western analysis at 48h post-treatment (figure 9C).

Furthermore, knowing that PPARγ expression cannot be induced by C/EBPδ alone in NIH 3T3 cells (*175*), we can infer that the induction of PPARγ observed in our case is mostly C/EBPβ-dependent. When PPARγ2 mRNA expression was quantified, C/EBPβ_{M152A} and C/EBP$\beta_{\Delta 151\text{-}156}$ dependent activation were not significantly different from that of C/EBPβ_{wt} in conditions where dex was omitted from the differentiation cocktail. Hence, this observation suggests that, unlike C/EBPα activation, PPARγ activation seems to be unaffected by the absence of LIP or mSin3A/HDAC1 earlier in the differentiation process (figure 19B, left panel), corroborating the results presented in figure 9. However, when cells were treated with dex, PPARγ expression in cells expressing C/EBPβ_{M152A} or C/EBP$\beta_{\Delta 151\text{-}156}$ increased substantially, suggesting that their transcriptional activity on the PPARγ promoter is more efficient in the presence of dex. Moreover, the dex-dependent fold induction of both mutants was similar to that of WT C/EBPβ as this 24h time point.

Interestingly, when the PPARγ2 levels were measured 48h post-induction of differentiation, both C/EBPβ_{M152A} and C/EBP$\beta_{\Delta 151\text{-}156}$ seemed to activate PPARγ transcription independently of dex and to an even greater extent with the hormone, when compared to C/EBPβ_{wt} (figure 19B, right panel). Once more, there was no significant difference between C/EBPβ_{M152A} and C/EBP$\beta_{\Delta 151\text{-}156}$ transcriptional activity. Given that a longer time point proved to be more beneficial for C/EBPβ_{M152A} and C/EBP$\beta_{\Delta 151\text{-}156}$ to activate the PPARγ promoter in a dex-independent manner, the presence of additional co-factors might have favoured their transcriptional potential under such conditions. Similar reasoning might explain the increased dex-dependent fold induction at this 48h time point.

3.1.5.5 C/EBP$\beta_{\Delta 151\text{-}156}$ is a more potent activator of GLUT4 expression than C/EBPβ_{wt} or C/EBPβ_{M152A}

As shown in figure 17A, C/EBP$\beta_{\Delta 151\text{-}156}$ seems to induce a higher adipsin level during NIH 3T3 differentiation. One might argue that this induction could not necessarily be due to C/EBP$\beta_{\Delta 151\text{-}156}$ activity since the adipsin level was measured in a later time point during the induction of differentiation. However, when the adipsin level was assessed at an earlier time point (i.e. two days post-induction), the same trend was also observed (data not shown), thus suggesting that C/EBPβ_{M152A} and C/EBP$\beta_{\Delta 151\text{-}156}$ might behave differently depending on their promoter environment. To further support this hypothesis, I sought to test C/EBPβ_{M152A} and C/EBP$\beta_{\Delta 151\text{-}156}$ transcriptional activity on a different downstream target. To do so, I measured GLUT4 mRNA levels by qRT-PCR reaction 48h post-induction of differentiation, as previously performed in figure 9. Although both C/EBPβ_{M152A} and C/EBP$\beta_{\Delta 151\text{-}156}$ induced GLUT4 mRNA more effectively than C/EBPβ_{wt}, C/EBP$\beta_{\Delta 151\text{-}156}$ showed the highest transcriptional activity in the presence of dex (figure 19C), paralleling the adipsin expression profile (figure 18A). To conclude, the results presented strongly suggest that LIP and mSin3A/HDAC1-dependent regulation of C/EBPβ activity varies depending on the promoter context.

3.1.6 Investigating C/EBPβ LAP* adipogenic potential

3.1.6.1 HA-tagged LAP* is transcriptionally inactive on the C/EBPα promoter

During the optimization procedure of the previously mentioned CoIP experiments, an interesting result was observed. During this process, an HA tag was cloned upstream of the first initiation codon of C/EBPβ (thus upstream of LAP*) for use in subsequent CoIP assays.

Additionally, the adipogenic potential of HA-C/EBPβ_{wt} and HA-C/EBP$\beta_{\Delta 151\text{-}156}$ were compared. After the standard retroviral transduction protocol, the constructs were stably expressed in NIH 3T3 cells before inducing differentiation with the cocktail of MIX, insulin and dex. Curiously, no differentiation phenotype was observed (i.e. no lipid accumulation and no detectable adipsin expression). To troubleshoot these results, a transcription assay on the C/EBPα promoter was performed using the WT C/EBPβ construct in addition to the HA-C/EBPβ. Surprisingly, the results clearly showed that the activity of HA-C/EBPβ was highly compromised when compared to C/EBPβ_{wt} (figure 20A). Curiously, the ratio of HA-LAP*/LAP was also higher than the ratio observed with WT C/EBPβ (inset), giving rise to much more LAP* isoform when compared to LAP.

A paper by Uematsu and colleagues (294) presented results involving the activity of C/EBPβ LAP* and LAP isoforms. When comparing WT, C/EBPβ knock-out and C/EBPβ_{M22A} knock-in mice (only expressing LAP* and LIP isoforms), the study showed that C/EBPβ knock-out macrophages and macrophages expressing LAP*/LIP were similarly unable to express their target genes, thus suggesting an inhibitory role for LAP* in transcriptional regulation (*294*). Interestingly, LAP* has been shown to be preferentially sumoylated over LAP and this modification was shown to inhibit its activity on the cyclin D1 promoter (*281*). These findings thus suggested that LAP* has an inhibitory function on the promoters tested.

To confirm that LAP* was inhibitory in our system (i.e. C/EBPα-promoter activation) and that this effect was not caused by the HA tag cloned at its N-terminal domain, I constructed another clone where the HA tag was cloned upstream of the second initiation codon, thus encoding LAP but not LAP* (HA-C/EBPβ_{22C}, figure 20B, inset). When a

Figure 20: LAP* is transcriptionally inactive on the C/EBPα promoter.

(A,B) C/EBPβ activity was measured by the Luciferase reporter assay from the -350/+7 C/EBPα promoter, as previously described (N=3 duplicates, + s.e.m.). HA-C/EBPβ was produced by cloning the HA tag sequence upstream of the LAP* initiator codon, while in HA-C/EBPβ_{22C} the tag was cloned upstream of the LAP initiator codon (encoding methionine 22).

A

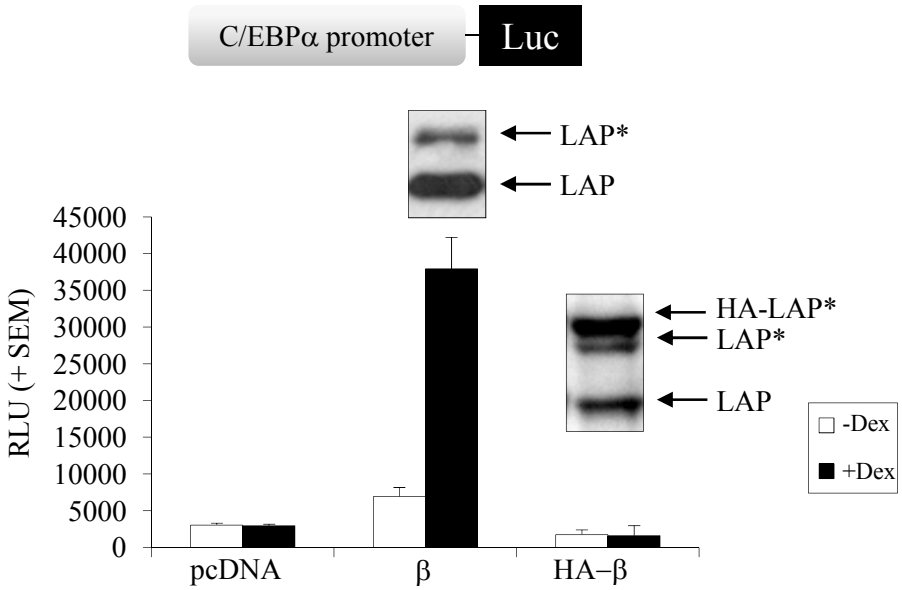
C/EBPα promoter
Luc
LAP*
LAP
HA-LAP*
LAP*
LAP
RLU (+ SEM)
45000
40000
35000
30000
25000
20000
15000
10000
5000
0
pcDNA
β
HA–β
-Dex
+Dex

B

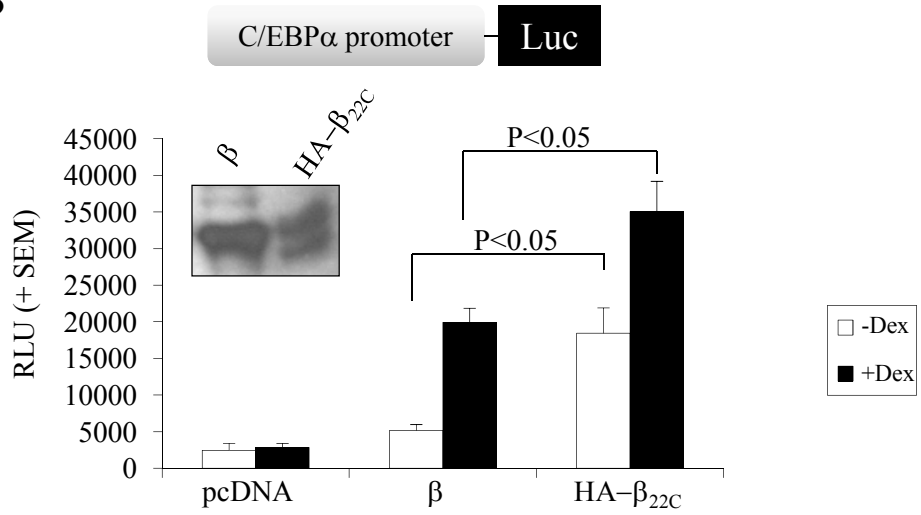
C/EBPα promoter
Luc
β
HA–β22C
P<0.05
P<0.05
RLU (+ SEM)
45000
40000
35000
30000
25000
20000
15000
10000
5000
0
pcDNA
β
HA–β22C
-Dex
+Dex

transcription assay was performed, the results clearly showed that HA-C/EBPβ_{22C} activity was higher than that of C/EBPβ_{wt}, both in the absence and presence of dex (figure 20B), thus supporting the activating property of LAP. I hence concluded that amino acids 1-21 in C/EBPβ were in fact negatively regulating its transcriptional activity on the C/EBPα promoter.

3.1.6.2 GR-dependent activation of LAP* requires expression of LIP

When LAP* activity was assessed on the C/EBPα promoter, the construct used also expressed the LIP inhibitory isoform, whose translation initiation starts at amino acid 152. Therefore, the inhibitory phenotype observed in the aforementioned situation (figure 20A) could be due to the collective effect of LAP* and/or LIP. To further define the contribution of LAP* in inhibiting LAP activity, I sought to compare the inhibitory effect induced by either LAP* alone or by LAP* and LIP (see schema of the constructs used in figure 21A). The transcriptional activity of a C/EBPβ mutant protein expressing only the LAP* isoform (C/EBP$\beta_{M22,152A}$) was similar to that of WT C/EBPβ in conditions where glucocorticoids were not used (figure 21B, -dex). However, LAP* did not show any dex-induced potentiation on the C/EBPα promoter (+dex), thus suggesting that this construct was insensitive to the glucocorticoid in this system.

When LIP was co-expressed with LAP* in C/EBPβ_{M22A}, a reduced activity was observed in the absence of dex (figure 21B), which was predictable knowing that LIP lacks its activation domain and can also function as an active repressor of LAP*/LAP. Interestingly, treatment with the steroid restored the dex-induced potentiation to a level that approached that of WT C/EBPβ (3 fold increase of +dex/-dex ratio), although C/EBPβ_{M22A} overall activity was reduced to about 60% of WT C/EBPβ, with and without dex.

Figure 21: LIP expression is required for a GR-dependent activation of C/EBPβ LAP* activity on the C/EBPα promoter.

(A) Schematic representation of each of the C/EBPβ constructs used in **(B)** showing the different isoforms encoded by C/EBPβ$_{wt}$, C/EBPβ$_{M22A,152A}$ and C/EBPβ$_{M22A}$. The 'x' refers to a mutation from a methionine to an alanine residue. **(B)** C/EBPβ activity was measured by the Luciferase reporter assay from the -350/+7 C/EBPα promoter as described previously (N=3 duplicates, + s.e.m.). **(C)** Sequence comparison of the N-terminal domain of C/EBPβ accross different species highlighting some of their conserved and functional residues.

A

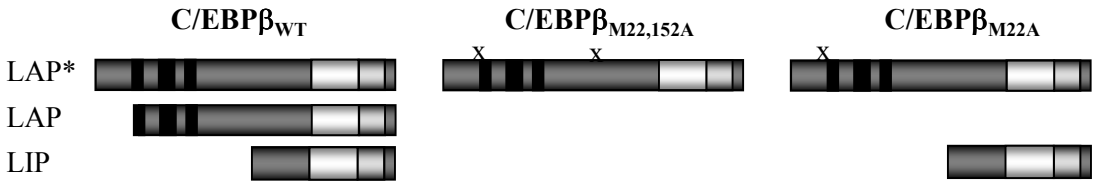

B

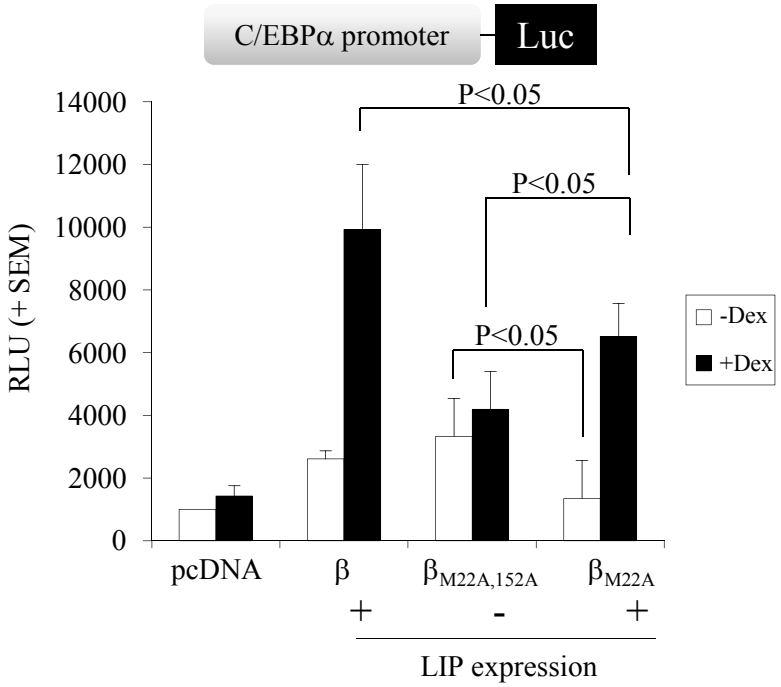

C

1	MHRLLAWDAACLP--PPPAAFRPM	22	**Mouse**
1	MQRLVAWDPACLPLPPPPPAFKSM	24	Human
1	MQRLVAWDPACLPLPPPPPAFKSM	24	Chimpanzee
1	MHRLLAWDAACLP--PPPAAFRPM	22	Rat
1	MQRLVAWDAACLPIQPP--AFKSM	22	Chicken

Given that 1) LAP*, LAP and LIP all associate with HDAC1 (figure 7,13); 2) when C/EBPβ$_{wt}$ (expressing LAP*, LAP and LIP) or C/EBPβ$_{M22A}$ (expressing LAP* and LIP) are expressed, the dex-mediated potentiation of C/EBPβ$_{wt}$ is at least 3 fold; and 3) suppression of LIP co-expression with LAP* (as in C/EBPβ$_{M22A,152A}$) abolishes the dex-dependent potentiation of LAP*, it is possible that GR's ability to potentiate LAP* homodimer is compromised because of the absence of LIP.

3.1.6.3 Cysteine 11 in C/EBPβ is partially responsible for the inability of LAP* to activate transcription

C/EBPβ's N-terminal domain is highly conserved throughout species (figure 21C). The murine protein contains two arginine residues (position 3 and 20) susceptible to post-translational modifications and one cysteine (position 11) that could potentially form a disulfide bridge. Interestingly, R3 dimethylation has been shown to repress LAP* activity on a subset of its target promoters by decreasing its interaction with a SWI/SNF chromatin remodelling complex (*276*). No reports, however, have investigated C11 or R20 involvement in regulating LAP* transcriptional activity during murine adipogenesis.

Since C/EBPβ's redox state has been shown to affect its dimerization and DNA-binding ability (*159, 282*), I hypothesized that the presence of C11 in LAP* could form a disulfide bond that could be required for its activating potential. To test this hypothesis, I mutated C11 to alanine in C/EBPβ$_{M22,152A}$ (LAP*$_{C11A}$) and assessed its transcriptional and adipogenic potential (figure 22).

To confirm that LAP*$_{C11A}$ protein expression was similar to that of WT LAP*, I performed a Western analysis. Figure 22A shows that LAP* and LAP*$_{C11A}$ both have similar LAP* to endogenous LAP/LIP ratio, where the LAP* isoform was clearly over-expressed

Figure 22: C/EBPβ$_{C11A,M22,152A}$ is a more potent inducer of preadipocyte differentiation than C/EBPβ$_{M22,152A}$.

(A) Western analysis showing the expression level of endogenous C/EBPβ, exogenous C/EBPβ$_{wt}$, C/EBPβ$_{M22,152A}$ (LAP*) or C/EBPβ$_{C11A,M22,152A}$ (LAP*$_{C11A}$) in NIH 3T3 cells. **(B)** C/EBPβ activity is measured by the Luciferase reporter assay from the C/EBPα promoter (-350/+7), as previously mentioned. The C/EBPβ constructs were co-transfected in NIH 3T3 cells along with the C/EBPα-Luciferase reporter and the glucocorticoid receptor constructs. Cells were treated with either vehicle or 1μM dex the following day for 16h. Luciferase activity was corrected for transfection efficiency by using a co-transfected Renilla expression plasmid (N=3 duplicates, + s.e.m.). **(C)** 3T3 L1 cells were retrovirally transduced to express either empty pLXSN plasmid, C/EBPβ$_{wt}$, C/EBPβ$_{M22,152A}$ (LAP*), C/EBPβ$_{C11A,M22,152A}$ (LAP*$_{C11A}$) or C/EBPβ$_{22C,M152A}$ (LAP), grown for 10 days after confluency with no differentiation inducers and harvested for immunoblot analysis to assess the expression profile of some of the adipogenic markers. **(D)** The cells were also stained with Oil red O to assess lipid accumulation. The figure represents results observed in two independent experiments.

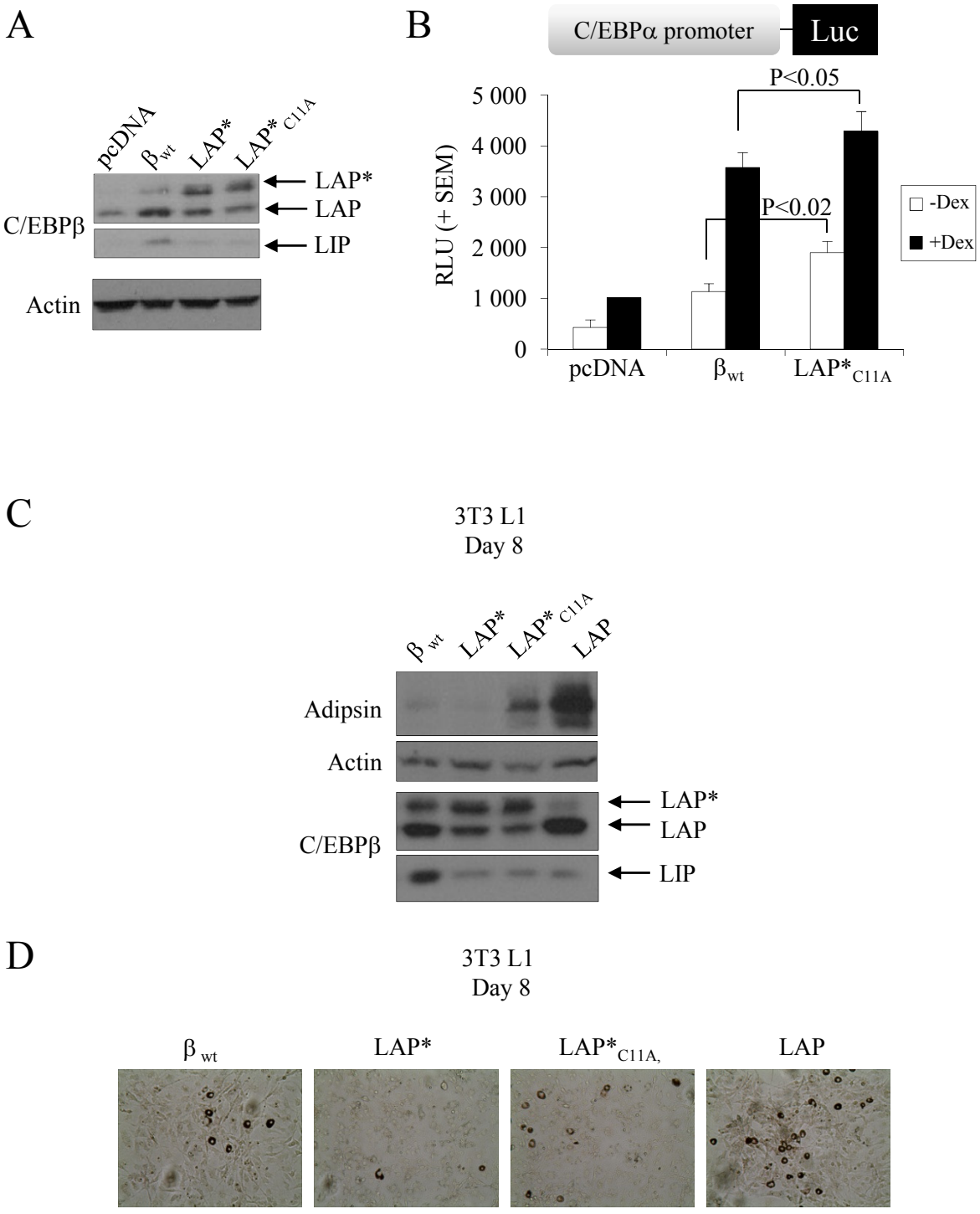
A
pcDNA
βwt
LAP*
LAP* C11A
C/EBPβ
LAP*
LAP
LIP
Actin
B
C/EBPα promoter
Luc
P<0.05
P<0.02
RLU (+ SEM)
5 000
4 000
3 000
2 000
1 000
0
-Dex
+Dex
pcDNA
βwt
LAP* C11A
C
3T3 L1
Day 8
βwt
LAP*
LAP* C11A
LAP
Adipsin
Actin
C/EBPβ
LAP*
LAP
LIP
D
3T3 L1
Day 8
βwt
LAP*
LAP* C11A,
LAP

when compared to the pcDNA-transfected cell extracts. WT C/EBPβ has the highest LAP to LAP* ratio. When the transient transfection experiment was repeated with the reporter construct driven by the C/EBPα promoter, LAP*$_{C11A}$ showed an almost two fold increase in its transcriptional potential when compared to C/EBPβ$_{wt}$ in the absence of glucocorticoids (figure 22B). Since C/EBPβ$_{wt}$ and LAP* (C/EBPβ$_{M22,152A}$) showed similar activation potential (figure 21B), we can thus infer that LAP*$_{C11A}$ also has a better transactivation potential than LAP*. Moreover, LAP*$_{C11A}$ glucocorticoid response was also increased more than two fold.

LAP*$_{C11A}$ induced more efficiently 3T3 L1 differentiation when compared to WT LAP* or C/EBPβ$_{wt}$, as shown by the adipsin expression profile and by the Oil red O staining of lipids (figure 22C,D). For comparison purposes, C/EBPβ$_{22C,M152A}$ (encoding only the LAP isoform) showed the highest adipogenic potential, as predicted (figure 22 C,D).

All together, these results not only support the importance of LIP in conveying the activating effect of GR on C/EBPβ LAP* activity, but they also show for the first time a repressive role for cysteine 11 on C/EBPα transactivation and adipogenesis. Moreover, C11 is suggested to be involved at inducing LAP* activating potential in a glucocorticoid-dependent manner based on the transcription assays on the C/EBPα promoter.

3. 2 Elucidating the contribution of C/EBPβ regulatory domains in potentiating NIH 3T3 and 3T3 L1 adipogenesis

One of the first deletion mutants that I generated lacked most of the RD1 domain (C/EBP$\beta_{\Delta 141\text{-}168}$) and I showed that this mutant interaction with mSin3A and GCN5 was compromised in an *in vitro* assay (figure 4B) and in a CoIP experiment (data not shown). Since the LIP translational methionine is located at amino acid 152 and mSin3A/HDAC1 binding domain is potentially located between amino acids 153-156 on C/EBPβ, the increased transcriptional activity observed when RD1 was deleted was not unforeseen. Moreover, since the C-terminal domain of RD1 (amino acids downstream of methionine 152) was shown to be inhibitory and since region 141-149 (see figure 23A for schema) was initially thought to be a functional domain due its possible α-helical structure as suggested by a bioinformatic analysis, I hypothesized that the RD1 region of C/EBPβ might contain at least two sub-domains that might independently regulate its activity. To test my hypothesis, I set out three objectives. My first objective was to generate a C/EBPβ mutant lacking part of the N-terminal domain of RD1 (Δ141-149), to test its transcriptional activity and its interaction with mSin3A/HDAC1 and GCN5. My second objective was to define the effect of this deletion in regulating C/EBPβ activity during murine adipogenesis.

3.2.1 C/EBP$\beta_{\Delta 141\text{-}149}$ is transcriptionally inactive on the C/EBPα promoter

To evaluate C/EBP$\beta_{\Delta 141\text{-}149}$ transcriptional activity, I performed a Luciferase-based transcription assay driven by the C/EBPα promoter, by transiently transfecting NIH 3T3 cells. C/EBP$\beta_{\Delta 141\text{-}149}$ did not show any transcriptional potential, as its activity was similar

Figure 23: C/EBPβ$_{\Delta 141\text{-}149}$ transcriptional activity is compromised on the C/EBPα promoter.

(A) Amino acid sequence of one of the hypothesized C/EBPβ regulatory domain highlighting the LIP initiator methionine and a potentially independent N-terminus domain within RD1, located upstream of the negative regulatory domain identified in chapter 3.1. **(B)** C/EBPβ activity was measured by the Luciferase reporter assay from the -350/+7 C/EBPα promoter. C/EBPβ$_{wt}$ or C/EBPβ$_{\Delta 141\text{-}149}$ were transfected in NIH 3T3 cells along with the C/EBPα-luciferase reporter and the glucocorticoid receptor constructs. Cells were treated with either vehicle (□) or 1μM dex (■) the following day for 16h. Luciferase activity was corrected for transfection efficiency by using a co-transfected Renilla expression plasmid (N=4 duplicates, + s.e.m.). **(C)** Western analysis showing the expression level of transfected C/EBPβ$_{wt}$ or C/EBPβ$_{\Delta 141\text{-}149}$ in NIH 3T3 cells. **(D)** The C/EBPβ constructs were transiently transfected in NIH 3T3 cells and an indirect immunofluorescence was performed using the C/EBPβ antibody. A fluorescence microscope was used to visualise the green fluorescein with 63X objective lens and pictures were taken using the multi channel acquisition function so that overlap between DAPI and C/EBPβ could be seen.

A

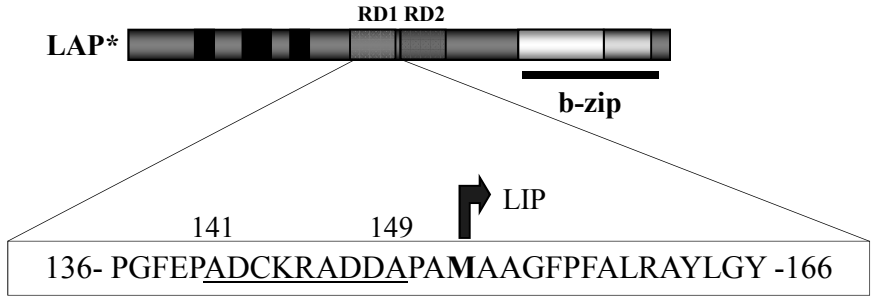
RD1 RD2
LAP*
b-zip
LIP
141
149
136- PGFEPADCKRADDAPAMAAGFPFALRAYLGY -166

B

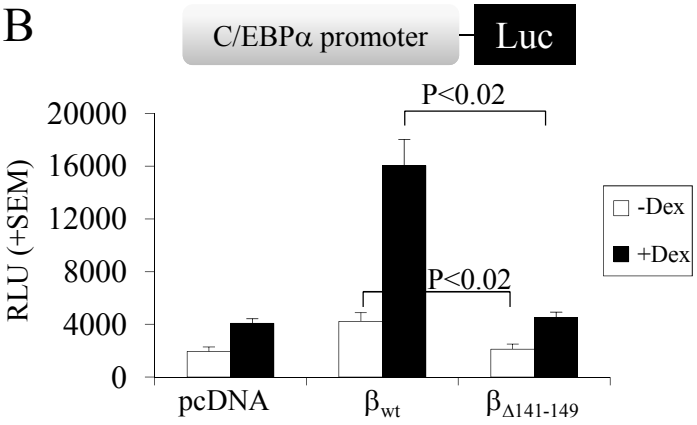
C/EBPα promoter
Luc
P<0.02
P<0.02
20000
16000
12000
8000
4000
0
RLU (+SEM)
-Dex
+Dex
pcDNA
βwt
βΔ141-149

C

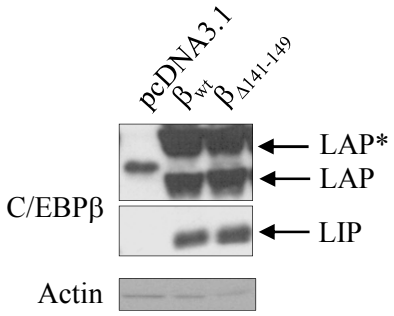
pcDNA3.1
βwt
βΔ141-149
LAP*
LAP
C/EBPβ
LIP
Actin

D

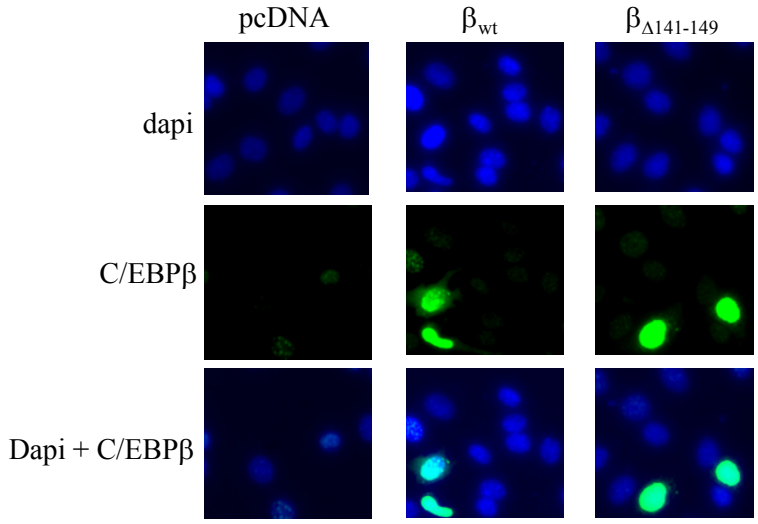
pcDNA
βwt
βΔ141-149
dapi
C/EBPβ
Dapi + C/EBPβ

to that of the background level where empty pcDNA vector was transfected (figure 23B). Western analysis confirmed that this mutant was properly expressed and that its LAP:LIP ratio was not affected (figure 23C). Further, to confirm that C/EBP$\beta_{\Delta 141\text{-}149}$ retained its nuclear import capacity, an indirect immunofluorescense experiment was performed in NIH 3T3 cells by transient transfection of the C/EBPβ constructs. As seen in figure 23D, C/EBP$\beta_{\Delta 141\text{-}149}$ was localized in the nucleus to the same extent as WT C/EBPβ.

Since localization to the nucleus does not preclude that a transcription factor can not bind to DNA, I next sought to confirm that C/EBP$\beta_{\Delta 141\text{-}149}$ can still activate another promoter containing CCAAT elements. A PPARγ-promoter Luciferase construct that has been previously shown to be activated by C/EBPβ was used (*65*). C/EBPδ was included as a positive control since it was shown to effectively activate transcription from this PPARγ-Luciferase construct (*171-172*). Not only was C/EBP$\beta_{\Delta 141\text{-}149}$ able to transactivate the PPARγ promoter to levels similar to WT C/EBPβ, but it also showed a glucocorticoid response that was equivalent to levels observed on the C/EBPα promoter (figure 24). Thus, C/EBP$\beta_{\Delta 141\text{-}149}$ was not transcriptionally compromised per se, but specifically inactive for transcription at the C/EBPα promoter. These results suggest for either a differential recruitment of co-factors to these two promoters or for a conformational change in the protein that might affect C/EBP$\beta_{\Delta 141\text{-}149}$ activity in a promoter specific manner.

3.2.2 C/EBP$\beta_{\Delta 141\text{-}149}$ interacts with mSin3A/HDAC1 and GCN5

Since we know that the co-repressor complex mSin3A/HDAC1 and the co-activator GCN5 both interacted directly with C/EBPβ, I hypothesized that Δ141-149 in C/EBPβ might

Figure 24: C/EBP$\beta_{\Delta 141\text{-}149}$ transcriptional activity is comparable to WT C/EBPβ on the PPARγ2 promoter.

C/EBPβ activity was measured by the Luciferase reporter assay from the -609/+52 PPARγ promoter. C/EBPδ (as a positive control), C/EBPβ_{wt} or C/EBP$\beta_{\Delta 141\text{-}149}$ were transfected in NIH 3T3 cells along with the PPARγ-luciferase reporter and the glucocorticoid receptor constructs. Cells were treated with either vehicle (□) or 1μM dex (■) the following day for 16h. Luciferase activity was corrected for transfection efficiency by using a co-transfected Renilla expression plasmid (N=4 duplicates, + s.e.m.).

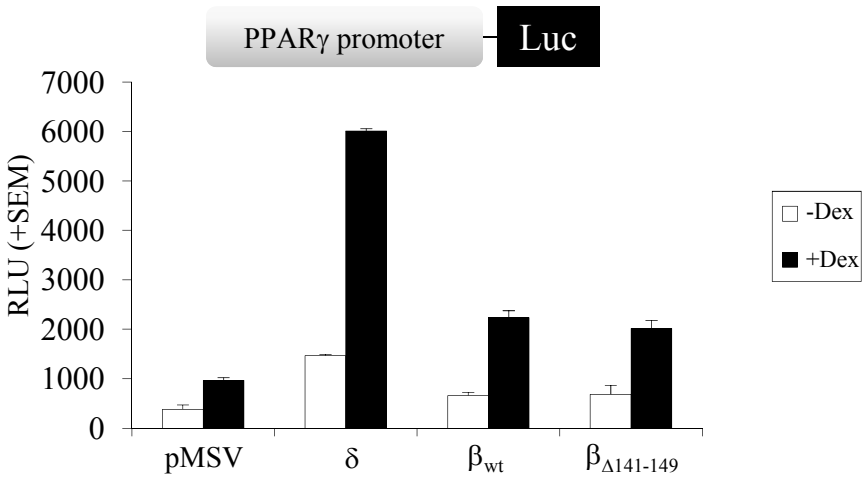
PPARγ promoter
Luc
7000
6000
5000
4000
3000
2000
1000
0
RLU (+SEM)
-Dex
+Dex
pMSV
δ
βwt
βΔ141-149

affect binding with the co-factors in a way that favours HDAC1 interaction, thus explaining the minimal activity observed on the C/EBPα promoter since HDAC1 effect is specific for C/EBPα but not PPARγ transcription (chapter 3.1). When the interaction of C/EBP$\beta_{\Delta 141\text{-}149}$ with HDAC1 and GCN5 was tested in a transient transfection experiment of Cos7 cells by CoIP, it was observed that C/EBP$\beta_{\Delta 141\text{-}149}$ co-precipitated with both exogenously expressed HDAC1 and GCN5 (figure 25A and B respectively), as opposed to C/EBP$\beta_{\Delta 153\text{-}156}$ which was included as an additional negative control.

C/EBPβ activity has been shown to be regulated by its acetylation status, where acetylation of lysines 98-102 and/or lysine 39 was shown to be required for C/EBPβ to reach higher transactivation levels (*65, 106, 275*). To further confirm that C/EBP$\beta_{\Delta 141\text{-}149}$ activity was not due to a decrease in GCN5/PCAF-mediated acetylation, I performed an *in vitro* acetylation assay using GST-fusion C/EBPβ constructs that were bacterially expressed as substrate for a commercially available PCAF. Both WT C/EBPβ and C/EBP$\beta_{\Delta 141\text{-}149}$ showed a similar level of ^{14}C-acetate incorporation following incubation with PCAF (figure 25C), thus suggesting that a decrease of its acetylation status was probably not responsible for the phenotype observed on the C/EBPα promoter.

To explore how C/EBP$\beta_{\Delta 141\text{-}149}$ affected the recruitment of HDAC1 and GCN5 to the C/EBPα promoter, I performed ChIP experiments on NIH 3T3 cells stably expressing either the mock pLXSN plasmid, WT C/EBPβ or C/EBP$\beta_{\Delta 141\text{-}149}$ 24h following treatment of the cells with MI only (figure 26). Both HDAC1 and GCN5 were recruited to the C/EBPα promoter when the NIH 3T3 cells expressed WT C/EBPβ, but not the pLXSN mock plasmid, as shown previously (chapter 3.1 and *66, 106*). The fact no HDAC1 or GCN5 are observed in the pLXSN condition confirms that the C/EBPα promoter in this fibroblastic cell line is

Figure 25: C/EBPβ$_{\Delta 141\text{-}149}$ interaction with mSin3A/HDAC1 or GCN5 is not compromised *in vivo*.

Cos7 cells were co-transfected with expression plasmids for flag-HDAC1 **(A)** or GCN5 **(B)** and either C/EBPβ$_{wt}$, C/EBPβ$_{\Delta 153\text{-}156}$ (as a negative control) or C/EBPβ$_{\Delta 141\text{-}149}$. Whole cell lysates were immunoprecipitated with a FLAG affinity resin. Data represent results observed in three independent experiments. **(C)** GST-C/EBPβ constructs were bacterially expressed and subjected to an *in vitro* acetylation assay with PCAF using ^{14}C-Acetyl-CoA as an acetate donor. After the acetylation reaction, the proteins were loaded on an SDS-PAGE gel, which was Coomassie stained and the bands corresponding to GST-C/EBPβ were cut from the gel (inset as loading control) and the radioactivity was counted with a scintillation counter (N=3, +s.d.).

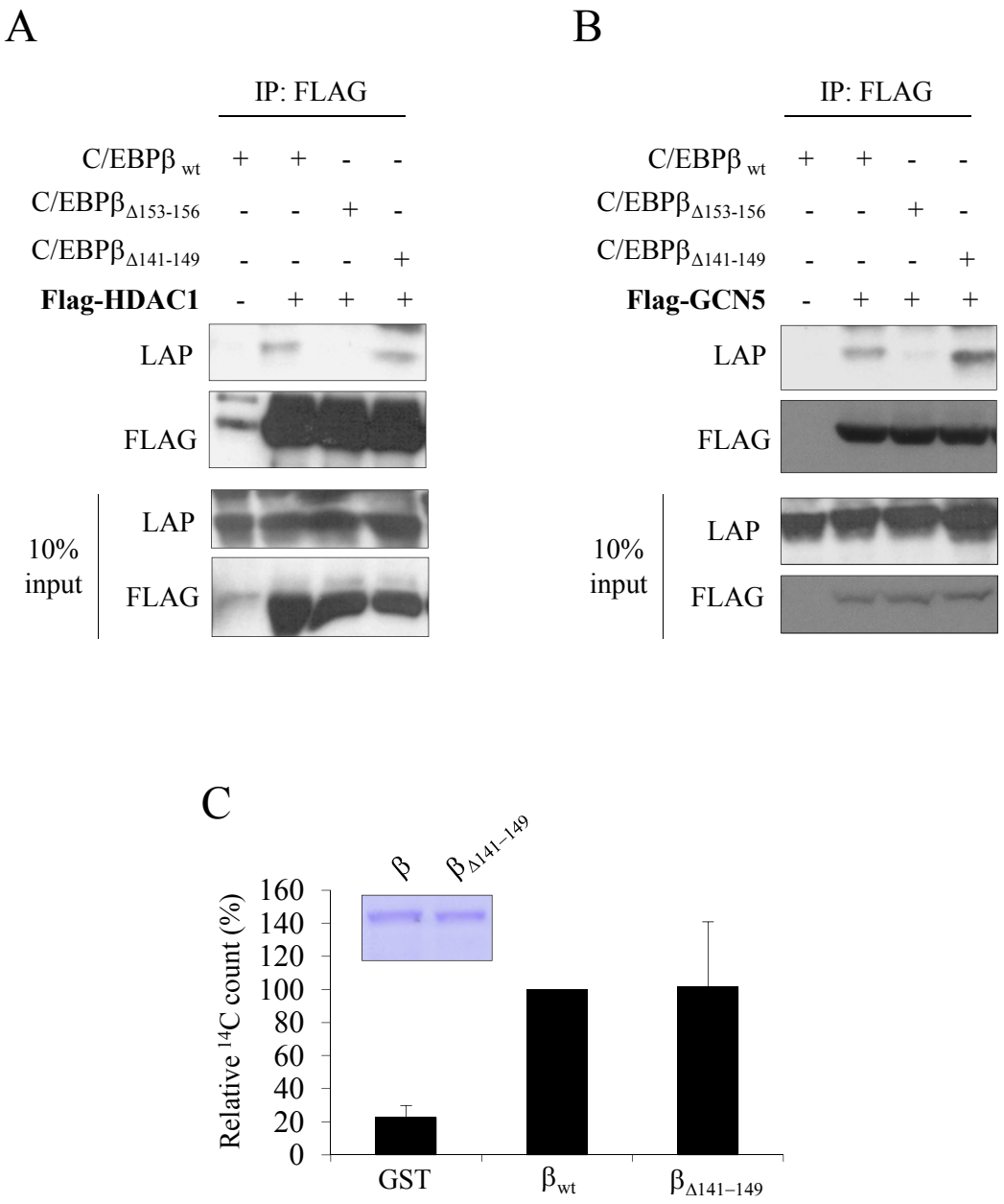
A
IP: FLAG
C/EBPβ wt + + - -
C/EBPβΔ153-156 - - + -
C/EBPβΔ141-149 - - - +
Flag-HDAC1 - + + +
LAP
FLAG
10% input
LAP
FLAG
B
IP: FLAG
C/EBPβ wt + + - -
C/EBPβΔ153-156 - - + -
C/EBPβΔ141-149 - - - +
Flag-GCN5 - + + +
LAP
FLAG
10% input
LAP
FLAG
C
β
βΔ141–149
Relative 14C count (%)
160
140
120
100
80
60
40
20
0
GST
βwt
βΔ141–149

Figure 26: C/EBPβ$_{\Delta 141\text{-}149}$ recruits HDAC1 and GCN5 to the C/EBPα promoter.

C/EBPβ expressing NIH 3T3 cells were treated with MI for 24h to assess HDAC1 and GCN5 recruitment on the C/EBPα promoter by C/EBPβ$_{\Delta 141\text{-}149}$. The cells were then harvested, cross-linked and the nuclear extract was immunoprecipitated using an HDAC1 or a GCN5 antibody. Following several washes, the precipitated DNA was isolated and subjected to a PCR reaction that amplifies region -460/-244 of the C/EBPα promoter (N=3 for each).

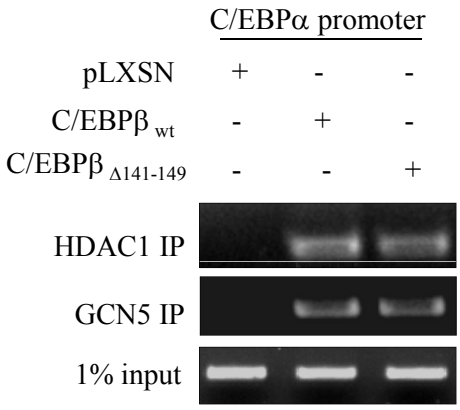
C/EBPα promoter
pLXSN + - -
C/EBPβ wt - + -
C/EBPβ Δ141-149 - - +
HDAC1 IP
GCN5 IP
1% input

not accessible by GCN5 or HDAC1 unless C/EBPβ is over-expressed (*66, 106*). When C/EBP$\beta_{\Delta 141\text{-}149}$ was expressed in the NIH 3T3 cells, it also effectively recruited both factors to a level that was similar to WT C/EBPβ (figure 26), thus corroborating the CoIP experiments.

3.2.3 The ability of C/EBP$\beta_{\Delta 141\text{-}149}$ to induce NIH 3T3 differentiation to adipocytes is compromised

Although C/EBPα expression is required for a fully functional adipocyte, PPARγ expression alone is sufficient to give rise to mature adipocytes. These adipocytes retain the ability to express their specific markers and accumulate lipids; however they are deficient in their insulin sensitivity (*145, 151, 185*). Thus I hypothesized that if C/EBP$\beta_{\Delta 141\text{-}149}$ can activate PPARγ but not C/EBPα, adipogenesis could still occur and PPARγ would still be able to activate C/EBPα.

To test its adipogenic potential, C/EBP$\beta_{\Delta 141\text{-}149}$ was stably expressed in NIH 3T3 cells using the retroviral transduction system (figure 27A). The stably-infected cells were then differentiated using the standard protocol and analysed. Western analysis confirmed the expression of the adipsin marker in cells expressing C/EBPβ_{wt} or C/EBP$\beta_{\Delta 141\text{-}149}$, although the adipsin level was approximately 40% lower in cells expressing the deletion mutant (figure 27B). Oil red O staining of the cells did not show a notable difference (figure 27C).

Given that C/EBP$\beta_{\Delta 141\text{-}149}$ was not capable of activating a Luciferase reporter gene under the control of the C/EBPα promoter, I sought to investigate if its transcriptional activity would still be abolished on the endogenous C/EBPα gene. As this gene is present in the natural chromatin environment of the cells, this scenario represents a more

Figure 27: C/EBPβ$_{\Delta 141\text{-}149}$ has a lower adipogenic potential than C/EBPβ$_{wt}$.

NIH 3T3 cells that were retrovirally transduced to express the C/EBPβ constructs were harvested prior to the differentiation process **(A)** and 4 days post-induction without (MI) or with (MID) 250nM dex **(B)** and subjected to western analysis (N=3, +s.d. $p < 0.05$). **(C)** The cells were also stained with Oil red O 6 days after induction of differentiation to qualitatively assess lipid accumulation. Data represents results observed in three independent experiments.

A

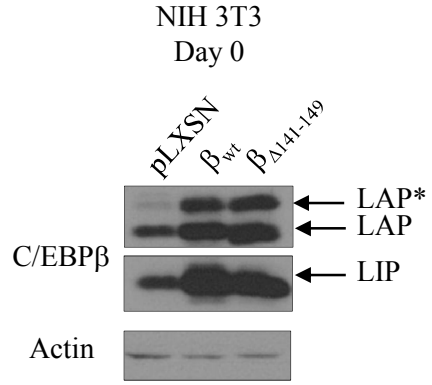
NIH 3T3
Day 0
pLXSN
βwt
βΔ141-149
LAP*
LAP
C/EBPβ
LIP
Actin

B

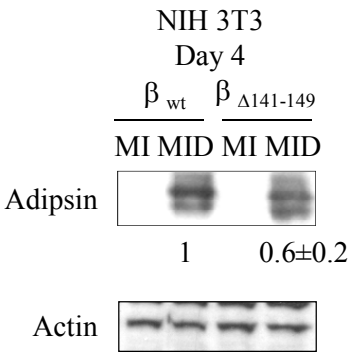
NIH 3T3
Day 4
β wt
β Δ141-149
MI MID MI MID
Adipsin
1
0.6±0.2
Actin

C

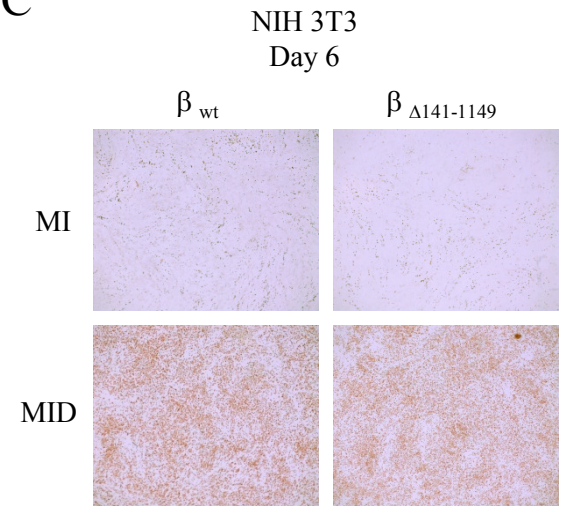
NIH 3T3
Day 6
β wt
β Δ141-1149
MI
MID

physiologically relevant experiment. To do so, I measured C/EBPα mRNA expression 24h after initiation of differentiation of the NIH 3T3 cells (equivalent treatment with dex in the reporter assay). The analysis showed that cells expressing C/EBP$\beta_{\Delta 141\text{-}149}$ had a C/EBPα mRNA level similar to that observed in the pLXSN infected cells and significantly lower than that observed in cells expressing C/EBPβ_{wt} (figure 28A, left panel), confirming that C/EBP$\beta_{\Delta 141\text{-}149}$ activity was compromised on the C/EBPα promoter even though HDAC1 and GCN5 recruitment was unaffected. Additionally, PPARγ expression was not affected by the C/EBPβ deletion, as its mRNA level was similar in cells expressing C/EBPβ_{wt} or C/EBP$\beta_{\Delta 141\text{-}149}$, both in the absence or presence of steroids (figure 28B, left panel) thus supporting the transcription assay results in figure 24.

By 48h post-treatment, C/EBPα mRNA levels in cells expressing C/EBP$\beta_{\Delta 141\text{-}149}$ largely caught up to that of C/EBPβ_{wt} expressing cells (figure 28A, right panel) likely due to activation by PPARγ, as its expression was induced normally by C/EBP$\beta_{\Delta 141\text{-}149}$ (figure 28B). Finally, when GLUT4 (whose activation requires both C/EBPβ and PPARγ) mRNA levels were measured, it also showed a reduced level in cells expressing C/EBP$\beta_{\Delta 141\text{-}149}$ (figure 28C), thus confirming the inability of C/EBP$\beta_{\Delta 141\text{-}149}$ in selectively activating some promoters.

3.2.4 C/EBP$\beta_{\Delta 141\text{-}149}$ inability to activate the C/EBPα promoter seems to be partially dependent on HDAC1 activity

Since the interaction of C/EBP$\beta_{\Delta 141\text{-}149}$ with mSin3A/HDAC1 was not compromised and its recruitment to the C/EBPα promoter was unaffected, I sought to test whether HDAC1 activity might be responsible for the C/EBP$\beta_{\Delta 141\text{-}149}$ transcriptional phenotype. To test this

Figure 28: C/EBP$\beta_{\Delta 141\text{-}149}$ transcribes endogenous PPARγ2 but not C/EBPα.

NIH 3T3 cells stably expressing either C/EBPβ_{wt} or C/EBP$\beta_{\Delta 141\text{-}149}$ were subjected to a real time RT-PCR reaction 24h and 48h after a standard induction of differentiation without (□) or with (■) dex. The C/EBPα **(A)** and PPARγ2 **(B)** mRNA levels were normalized to actin (N=3, + s.d.). Quantification of C/EBPα and PPARγ2 values are relative to the MID β_{wt} condition, which is defined as 1 RU. **(C)** The glucose transporter 4 (GLUT4) mRNA levels were also assessed 48h after induction of differentiation without (□) or with (■) dex (N=3, + s.d.).

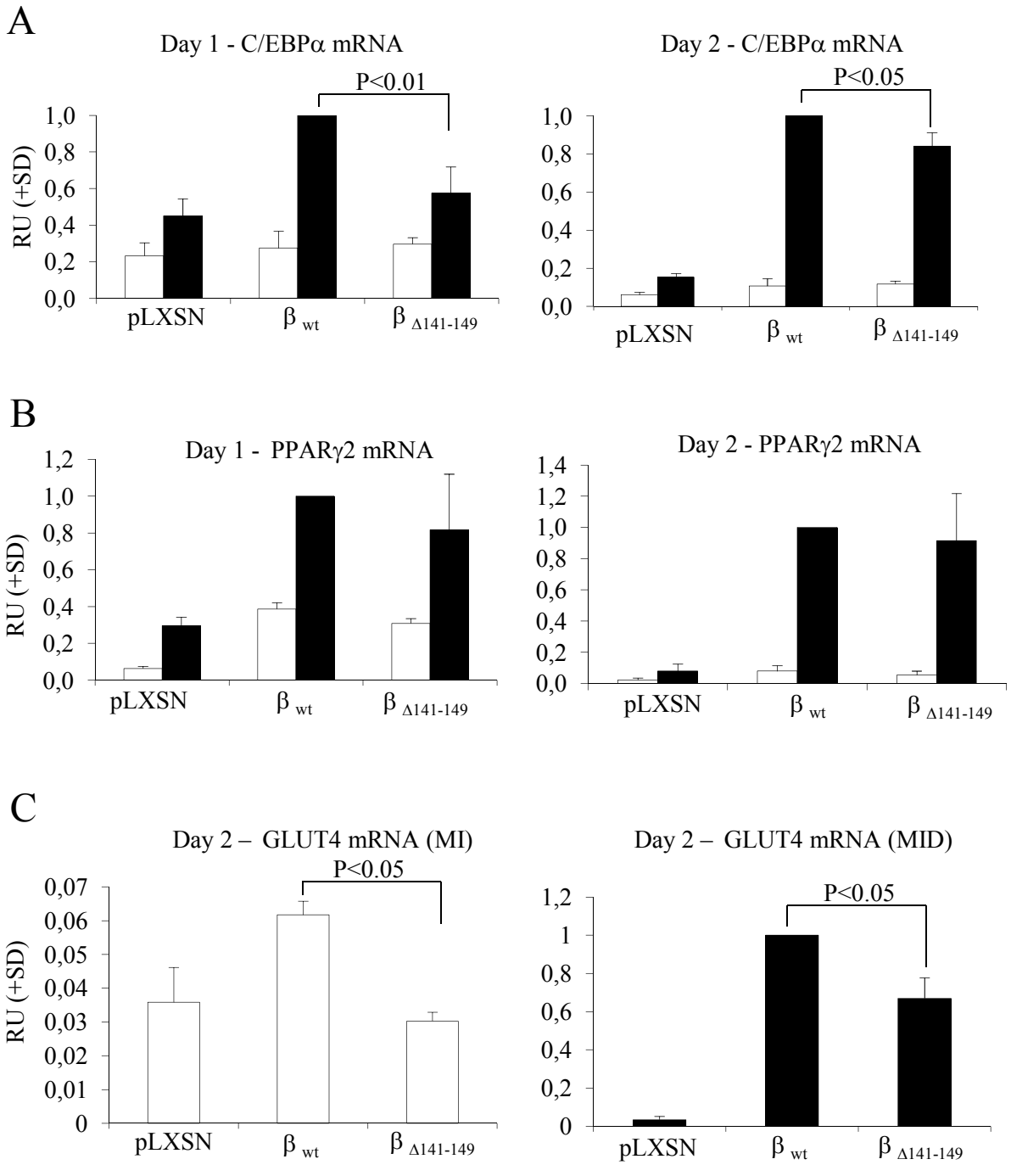
A
Day 1 - C/EBPα mRNA
P<0.01
RU (+SD)
1,0
0,8
0,6
0,4
0,2
0,0
pLXSN
β wt
β Δ141-149
Day 2 - C/EBPα mRNA
P<0.05
B
Day 1 - PPARγ2 mRNA
1,2
Day 2 - PPARγ2 mRNA
1,4
C
Day 2 – GLUT4 mRNA (MI)
0,07
0,06
0,05
0,04
0,03
0,02
0,01
0
Day 2 – GLUT4 mRNA (MID)

hypothesis, an inactive HDAC1, whose charge relay system responsible for deacetylating its substrate was disrupted by mutating aspartic acid 181 to alanine, was used (Kuzmochka *et al.* unpublished results and (*295*)). When inactive $HDAC1_{D181A}$ was co-transfected with WT C/EBPβ, it significantly increased its activity in the presence of glucocorticoids exclusively (figure 29A). Interestingly, when $C/EBP\beta_{\Delta 141\text{-}149}$ was co-expressed with HDAC1 instead of WT C/EBPβ, its activity was significantly increased in the absence and presence of glucocorticoids when compared to pcDNA control condition. This finding suggests that HDAC1 activity accounts for a fraction of the inhibition observed in $C/EBP\beta_{\Delta 141\text{-}149}$ since $C/EBP\beta_{\Delta 141\text{-}149}$ did not reach the transcriptional activity of WT C/EBPβ in the presence of inactive $HDAC1_{D181A}$ (figure 29A).

When amino acids 150-156 were also deleted in addition to Δ141-149 to reduce mSin3A/HDAC1 binding, $C/EBP\beta_{\Delta 141\text{-}156}$ showed a further increase in transcription in the absence and presence of glucocorticoids, when compared to WT or Δ141-149 C/EBPβ (figure 29B). These results suggest that reduction of mSin3A/HDAC1 binding from LAP*/LAP overcomes the inhibition caused by the absence of amino acids 141-149 in the presence of glucocorticoids and they establish a link between the Δ141-149 phenotype and a requirement for HDAC1. The fact that $C/EBP\beta_{\Delta 141\text{-}156}$ activity did not reach the transcriptional level observed in $C/EBP\beta_{\Delta 151\text{-}156}$ in the presence of glucocorticoids implies that some of the activating properties of amino acids 141-149 are still required to display a maximal dex-dependent activity (figure 29B).

Figure 29: C/EBPβ$_{\Delta 141\text{-}149}$ transcriptional activity is increased on the C/EBPα promoter when co-expressed with an inactive HDAC1.

(A,B) C/EBPβ activity was measured by the Luciferase reporter assay from the -350/+7 C/EBPα promoter as described previously. Catalytically inactive HDAC1$_{D181A}$ was co-transfected where indicated (N=3 duplicates, + s.e.m.). The protein expression level of the different C/EBPβ constructs is also shown in the lower panel of **B**. **(C)** Amino acid sequence of the N-terminal domain of RD1 in C/EBPβ highlighting conserved residues among different species.

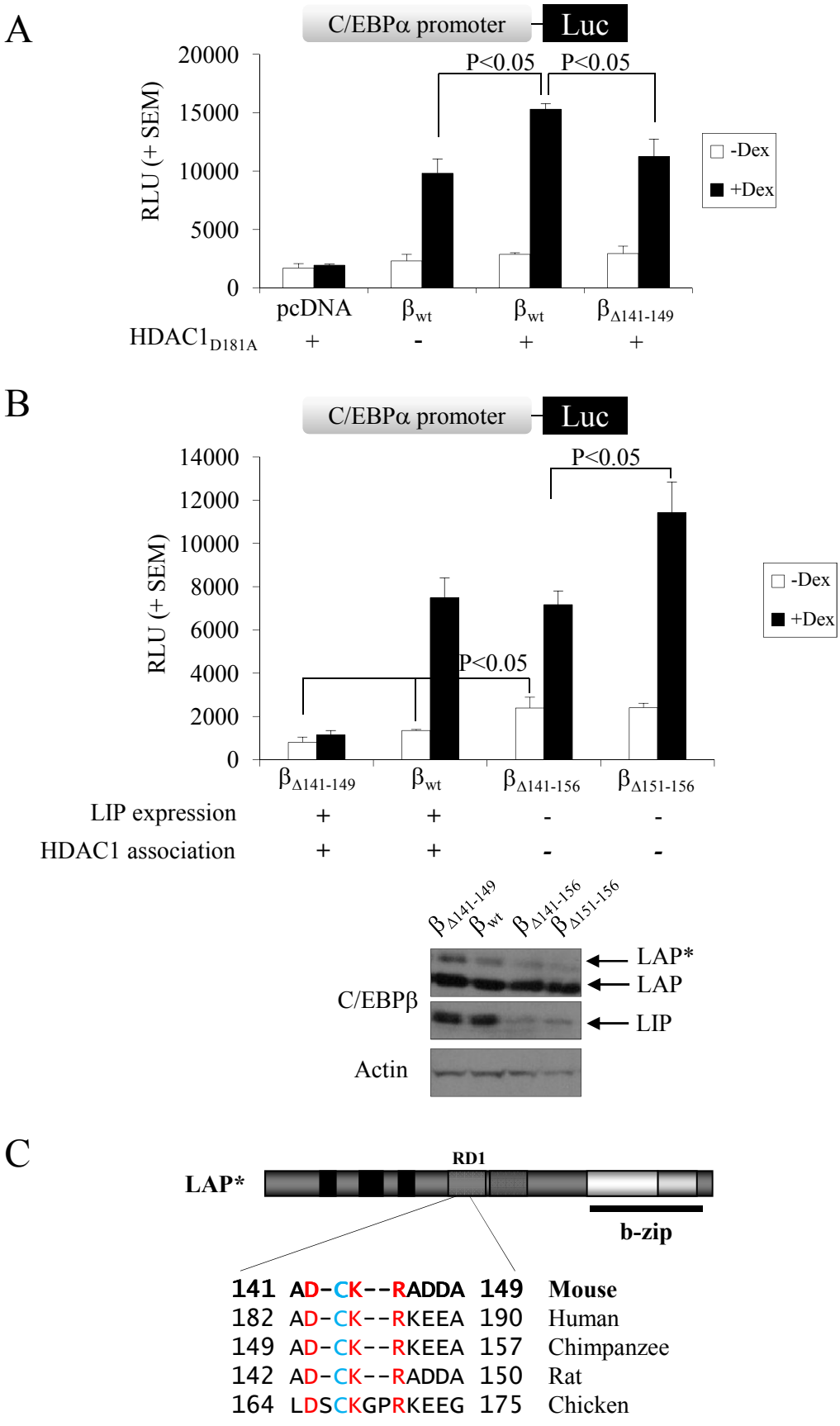
A
C/EBPα promoter
Luc
RLU (+ SEM)
20000
15000
10000
5000
0
P<0.05
P<0.05
-Dex
+Dex
pcDNA
βwt
βwt
βΔ141-149
HDAC1D181A
+
-
+
+
B
C/EBPα promoter
Luc
RLU (+ SEM)
14000
12000
10000
8000
6000
4000
2000
0
P<0.05
P<0.05
-Dex
+Dex
βΔ141-149
βwt
βΔ141-156
βΔ151-156
LIP expression
HDAC1 association
+
+
-
-
+
+
-
-
βΔ141-149
βwt
βΔ141-156
βΔ151-156
C/EBPβ
LAP*
LAP
LIP
Actin
C
LAP*
RD1
b-zip
141 AD-CK--RADDA 149 Mouse
182 AD-CK--RKEEA 190 Human
149 AD-CK--RKEEA 157 Chimpanzee
142 AD-CK--RADDA 150 Rat
164 LDSCKGPRKEEG 175 Chicken

3.2.5 Cysteine 143 within RD1 is partially required for C/EBPβ-dependent activation of C/EBPα

Comparison of the amino acid sequence of the N-terminus domain of RD1 shows several residues that are highly conserved (figure 29C). The charged residues could participate in increasing solubility of this domain since they have been proposed to be exposed to the environmental solvent (*296*), thus favouring a thermodynamically stable structure. The presence of a cysteine residue also suggests disulfide bond formation that might help to stabilize LAP/LAP dimer formation, as previously suggested (*159*). Although cysteine 143 (C143) was previously proposed to be an important residue in regulating C/EBPβ activity, its precise role *in vivo* was not evaluated (*282-283*). C143 has been suggested to form an intermolecular disulfide bond in LAP/LAP homodimer (*283*) or an intramolecular bond with C123 within the LAP* monomer. Notably, C143 was proposed to be in a constitutive reduced state in LAP (*282*).

In an attempt to verify that the phenotype observed by C/EBP$\beta_{\Delta 141\text{-}149}$ was not caused by the deletion of C143, I generated a mutant C/EBPβ where cysteine 143 was substituted by an alanine residue and then tested C/EBPβ_{C143A} for transcriptional and adipogenic potential. When a transient transfection experiment evaluating WT and C143A C/EBPβ ability to induce expression of a reporter driven by the C/EBPα promoter was performed, the latter one showed only a 25% decrease in its transactivation potential when compared to WT C/EBPβ, in the presence of glucocorticoids only (figure 30A,B). Thus, we can suggest that C143 was not completely responsible for the C/EBP$\beta_{\Delta 141\text{-}149}$ phenotype.

When C/EBPβ_{C143A} adipogenic potential was tested in NIH 3T3 cells, it showed a similar adipogenic potential as WT C/EBPβ, as evidenced by the adipsin level and the Oil

Figure 30: C/EBPβ$_{C143A}$ has a similar adipogenic potential than C/EBPβ$_{wt}$ during NIH 3T3 differentiation

(A) C/EBPβ activity was measured by the Luciferase reporter assay from the -350/+7 C/EBPα promoter as described previously (N=3 duplicates, + s.e.m.). The protein expression level are also illustrated in **(B)** NIH 3T3 cells that were retrovirally transduced to express the C/EBPβ constructs were harvested at day 0 **(C)** or 4 days post-induction **(D)** without (MI) or with (MID) dex and subjected to a Western analysis to assess the C/EBPβ and adipsin levels. Data represents results observed in two independent experiments. **(E)** The cells were also stained with Oil red O 6 days after induction of differentiation to qualitatively assess lipid accumulation. **(F)** NIH 3T3 cells stably expressing C/EBPβ$_{wt}$ or C/EBPβ$_{C143A}$ were also subjected to a real time RT-PCR reaction 48h after a standard induction of differentiation without (□) or with (■) dex. The C/EBPα **(left panel)** and PPARγ2 **(right panel)** mRNA levels were normalized to actin (N=3, + s.d.).

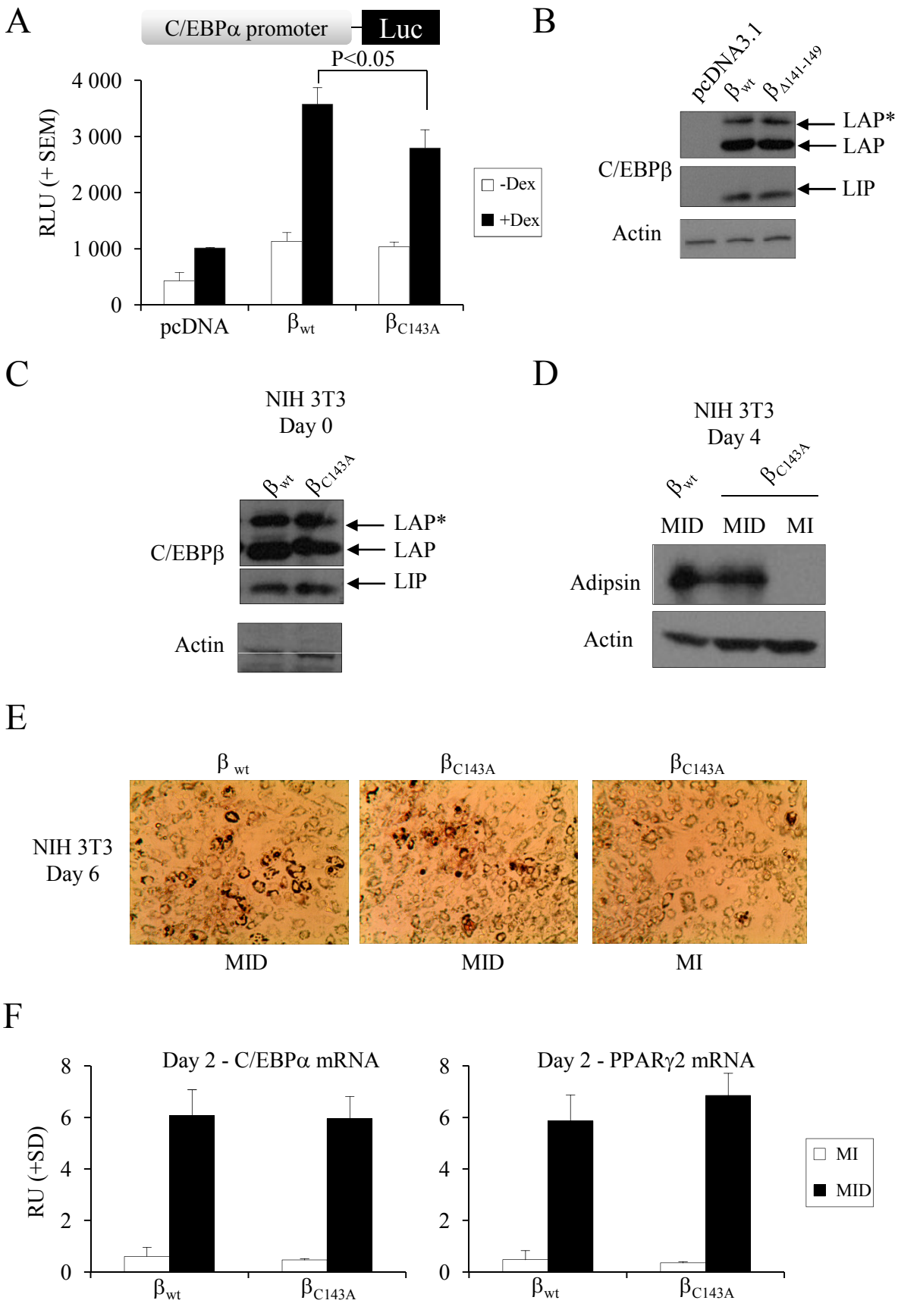
A
C/EBPα promoter
Luc
P<0.05
RLU (+ SEM)
4 000
3 000
2 000
1 000
0
-Dex
+Dex
pcDNA
βwt
βC143A
B
pcDNA3.1
βwt
βΔ141-149
LAP*
LAP
LIP
C/EBPβ
Actin
C
NIH 3T3
Day 0
βwt
βC143A
LAP*
LAP
LIP
C/EBPβ
Actin
D
NIH 3T3
Day 4
βwt
βC143A
MID
MID
MI
Adipsin
Actin
E
NIH 3T3
Day 6
β wt
βC143A
βC143A
MID
MID
MI
F
Day 2 - C/EBPα mRNA
Day 2 - PPARγ2 mRNA
RU (+SD)
8
6
4
2
0
βwt
βC143A
MI
MID

red O staining of lipids (figure 30D,E). Unlike C/EBP$\beta_{\Delta 141\text{-}149}$ whose adipogenic potential was reduced when assessed in NIH 3T3 cells (figure 27C,D), mutation of C143 did not reduce differentiation. Moreover, when endogenous C/EBPα and PPARγ2 mRNA levels were quantified (figure 30F), they showed no significant differences between cells expressing WT or C143A C/EBPβ. These results hence suggest that the residues surrounding C143 are important for C/EBPβ activation.

In summary, I showed in this chapter that amino acids 141-149 in C/EBPβ are required for the transcription factor to reach its maximal activating potential on the C/EBPα promoter, but not on the PPARγ promoter. I also proposed that HDAC1 activity might participate in keeping C/EBP$\beta_{\Delta 141\text{-}149}$ in a repressed state more effectively than it does with WT C/EBPβ. Finally, the presence of a cysteine residue within amino acids 141-149 of C/EBPβ was shown not to be responsible for mediating C/EBPα transcription. Again, these results strongly suggest multiple modes of regulation that could occur through the N-terminus of RD1 and that this region could in fact have a positive effect on LAP*/LAP activation properties, in addition to the repressive effect mediated by LIP translation and mSin3A/HDAC1 association.

CHAPTER 4 - DISCUSSION

Recently, Leutz's group proposed a ''transcription factor code'', in analogy to the histone code, that underline how the post-translational modification profile in a transcription factor will differentially modulate its activity (*276*). In keeping with this code, C/EBPβ transcriptional activity is regulated by numerous post-translational modifications that affect its DNA-binding ability and its interactions with other partners. Although sumoylation and methylation are associated with C/EBPβ repression, acetylation and phosphorylation have been shown to positively affect its activity (*65, 106, 164, 275-276, 279, 281, 283, 297*). In this thesis, I present evidence that helps to explain the mechanism through which C/EBPβ LAP*/LAP/LIP activity are modulated via their interaction with co-regulatory complexes.

4.1 A hydrophobic domain in C/EBPβ is required for mSin3A/HDAC1 binding

When William and co-workers studied C/EBPβ transcriptional activity, they characterized two domains, covering amino acids 136-166 (RD1) and 183-211 (RD2), as being negative regulatory domains. The authors hypothesized that RD1 and RD2 block C/EBPβ activity by interacting and masking the activation and the DNA-binding domain, respectively (*158*). In my work, key determinants for mSin3A/HDAC1 binding to C/EBPβ were mapped within RD1 (figures 6,7). The negative effect of the RD1 observed by William and colleagues can therefore partially be explained by the deletion of amino acids 153-156 that abrogates mSin3A/HDAC1 binding domain (see appendix 6 for a summary of results).

The minimal domain that I identified as being required for a proper interaction with mSin3A/HDAC1 is composed of four amino acids (AAGF) located in the middle of a highly

hydrophobic domain (amino acids 149-160, see appendix 7 for sequences). This observation suggests that a hydrophobic interface could be created when mSin3A and C/EBPβ are in close proximity. Such an occurrence could not only stabilize the interaction between the two proteins, but it could also minimize any misfolding that could occur from exposing the hydrophobic residues to the hydrophilic cellular environment. Although I have not shown that a minimal peptide composed of the 30 amino acids covering RD1 of C/EBPβ is sufficient to bind with mSin3A, the fact that elimination of amino acids 153-156, but not amino acids 141-149 (figure 25), was sufficient to compromise binding strongly suggests that residues 153-156 create one of the interfaces responsible for mediating mSin3A interaction.

A closer look at the protein sequence shows three additional conserved domains composed almost exclusively of hydrophobic amino acids (residues 9-19, 118-131 and 196-210) with, curiously, a cysteine residue in the middle of each of these domains (see appendix 7, residues in bold). Interestingly, three of these four hydrophobic regions have been shown by my results (figure 7-9, 20-21) and others (*158, 294*) to negatively regulate C/EBPβ activity. Additionally, none of these domains are located either in the activation or the bZIP domains. Hence it is most likely that they independently regulate C/EBPβ activity via diverse mechanisms, one of which identified in here as being required for binding to a co-repressor complex (figure 6-7) and another one involving the redox-state of the protein (figure 22). Although RD2 (which includes the hydrophobic domain 196-210) has been stipulated to inhibit C/EBPβ activity by masking its DNA-binding domain, it is also plausible that a misfolded hydrophobic domain compromises the function of its bZIP.

4.2 Titration of HDAC1 from C/EBPβ accounts for a fraction of GR-mediated transactivation of the C/EBPα promoter

Several studies showed that an HDAC1-containing complex inhibits C/EBPβ activity on several promoters (*65-66, 285, 287*). Moreover, to explain how C/EBPβ transcriptional activity is increased upon steroid treatment of the cells in which it is expressed, results from our laboratory suggested that C/EBPβ de-repression involves reduction of its interaction with the mSin3A/HDAC1 co-repressor complex via GR-dependent degradation of HDAC1 through the 26S proteasomal pathway (*66*). We have also shown that GCN5/PCAF-mediated acetylation of C/EBPβ decreases its interaction with mSin3A (*106*), thus suggesting a two step process in the titration of mSin3A/HDAC1 complex from C/EBPβ.

Given that GR has been shown to contribute to C/EBPβ activation by decreasing the mSin3A/HDAC1 complex association, I hypothesized that an initial absence of this co-repressor from C/EBPβ would not require GR-dependent function to reach maximal activity. However, when C/EBP$\beta_{\Delta 153\text{-}156}$ activity was tested on the C/EBPα promoter, the results clearly showed that compromising mSin3A/HDAC1 binding does not fully replace the dex effect. Hence, these observations could be explained by either: 1) the role of GR in activating C/EBPα goes beyond just promoting mSin3A/HDAC1 displacement from the promoter. For instance, studies in our laboratory have identified LMO3, a member of the LIM-only adaptor proteins, as a potential target of GR that might recruit additional regulators to the C/EBPα promoter. LMO3 mRNA expression was shown to be rapidly induced by GR (4h following treatment with dex) and its over-expression in 3T3 L1 preadipocytes was shown to enhance differentiation. 2) Since mSin3A/HDAC1 dissociation from C/EBP$\beta_{\Delta 153\text{-}156}$ was incomplete (70% reduction), this mutant might retain some of its binding ability through association of

mSin3A with the unacetylated lysines 98-102 that require GCN5-mediated acetylation to completely abolish binding with the co-repressor complex. Further binding assays are required to determine the exact mechanism by which GR eliminates mSin3A/HDAC1 binding from C/EBPβ.

Since C/EBPδ has been proposed to have two independent domains mediating mSin3A/HDAC1 binding in its C-terminal region, as shown by *in vitro* and *in vivo* GST pulldown assays, a dual binding domain in C/EBPβ might actually be possible (*289*). The same study also showed that the C/EBPδ bZIP domain was important for mediating the interaction with the mSin3A/HDAC1 complex, thus supporting the hypothesis that C/EBPβ dimerization is required for its association with mSin3A (figure 5). When a C/EBPβ deletion mutant Δ121-198 lacking most of its internal regulatory domains (but still including its bZIP and activation domains) was tested for binding with mSin3A *in vitro*, it showed a highly compromised binding that was similar to C/EBP$\beta_{\Delta 151\text{-}156}$ (80% less binding). Although C/EBP$\beta_{\Delta 121\text{-}198}$ interaction assays were not performed *in vivo*, it is most likely that the outcome will be the same as C/EBP$\beta_{\Delta 153\text{-}156}$ (figure 7) or C/EBP$\beta_{\Delta 141\text{-}168}$ (figure 7), whose interactions with the mSin3A/HDAC1 was highly compromised. From these observations, we can hence suggest that it is highly likely that the role of GR in promoting C/EBPβ activation is less straightforward than just favouring mSin3A/HDAC1 displacement from C/EBPβ-targeted promoters.

It appears that the GR-dependent titration of mSin3A/HDAC1 occurs most likely in several steps, as follow: 1) it will promote HDAC1 proteasomal degradation from the C/EBPβ/mSin3A/HDAC1 complex; 2) thus allowing an active acetylation of C/EBPβ by GCN5; 3) that will further promote mSin3A dissociation (*66, 106*). The GR-dependent

dissociation of mSin3A after HDAC1 degradation is an important step toward C/EBPβ activation even if mSin3A does not have any deacetylase activity. If the activation of C/EBPβ by GR only requires the removal of the deacetylase portion (i.e. HDAC1) from the co-repressor complex, then an inactive HDAC1 in the complex will not need GR-mediated titration of HDAC1 to activate C/EBPβ.

On that account, when a transcription assay on the C/EBPα promoter was performed using a catalytically inactive HDAC1 (D181A mutant), the results showed that co-expression of $HDAC1_{D181A}$ with C/EBPβ did not increase C/EBPβ activity in the absence of dex, by contrast to $C/EBP\beta_{\Delta 153\text{-}156}$ dex-independent activity, which lacks mSin3A/HDAC1 binding (see figure 29A of chapter 3.2). Only GR-mediated activation increased C/EBPβ activity. This observation was also confirmed with a real time RT-PCR reaction performed to quantify endogenous C/EBPα expression during 3T3 L1 preadipocyte differentiation (Kuzmochka *et al.*, unpublished results). These results hence strongly suggest that HDAC1 activity and mSin3A association can independently inhibit C/EBPβ transcriptional activity. Due to its higher molecular weight (approximately 130 KDa), mSin3A could repress C/EBPβ activity by interfering with co-activators recruitment via steric interaction and/or by preventing C/EBPβ to form a suitable conformation for co-activators association.

4.3 Implication of a shared binding domain between co-activators and co-repressors

In an attempt to delineate two independent domains required for GCN5 and mSin3A binding in C/EBPβ, I showed that GCN5 and mSin3A required amino acids 153-156 but not amino acids 141-149 to properly associate with C/EBPβ (figure 25). However, unlike mSin3A, GCN5 binding did not require C/EBPβ bZIP domain (figure 5). It is possible that

the large molecular size of mSin3A requires numerous interfaces on C/EBPβ to mediate an interaction whereas the smaller size of GCN5 (approximately 55KDa) required less determinants to mediate binding (i.e. only amino acids 153-156 are sufficient). From these findings, we can therefore suggest that it is unlikely that both mSin3A and GCN5 could simultaneously bind to C/EBPβ. Interestingly, however, it seems that mSin3A binding to C/EBPβ is stronger than that of GCN5 because when I performed the CoIP experiments in more stringent conditions (150-175mM NaCl and 0.15-2% NP-40), GCN5 association was lost, while mSin3A binding was retained. These results further support the dominant-negative role of the co-repressor complex as HDAC1 recruitment to the C/EBPα promoter decreases histone H4 acetylation, counteracts p300/GCN5 co-activator' effect and prevents the transcriptional pre-initiation complex recruitment (*66*). Thus, the decrease of both HDAC1 and GCN5 interaction with C/EBP$\beta_{\Delta 153\text{-}156}$ showed an increase in adipogenesis since the initial absence of the association of HDAC1 does not require acetylation of C/EBPβ by GCN5 to decrease the co-repressor occupancy from the C/EBPα promoter.

Since two independent CoIP experiments showed that C/EBPβ interacts with both GCN5 and mSin3A/HDAC1 and that GR's activation only reduces the interaction with mSin3A/HDAC1 without affecting that of GCN5 (*66, 106*), an equilibrium model has been proposed to explain the interaction profile between these factors (figure 31A). In conditions where GR is not active, C/EBPβ is hypothesized to exist in complexes that include, among other co-factors, either mSin3A/HDAC1 or GCN5. Upon dex treatment, GR translocates to the nucleus and promotes HDAC1-polyubiquilation via the E3 ligase TIF1β, thus favouring C/EBPβ acetylation by GCN5, which will then promote mSin3A dissociation (*66, 106* and Tomlinson *et al.*, unpublished). This model thus suggests that C/EBPβ is present in at least

Figure 31: Dual regulation of C/EBPβ by mSin3A/HDAC1 and GCN5.

(A) In an equilibrium interaction model between mSin3A/HDAC1 or GCN5 with C/EBPβ, titration of the co-repressor complex from C/EBPβ will favour more GCN5/C/EBPβ complex formation. **(B)** However, since GCN5 or C/EBPβ presence is not increased on the C/EBPα promoter following the dex-induced HDAC1 titration, it is more likely that there is only one population of C/EBPβ complex on the C/EBPα promoter that includes both co-regulatory complexes, where GCN5 is indirectly bound to C/EBPβ through possibly HDAC1. Dex-treatment allows HDAC1 titration, thus promoting GCN5-mediated acetylation of C/EBPβ and consequently mSin3A dissociation. **(C)** It is also possible that p300-mediated acetylation of HDAC1 decreases its binding from GCN5, thus allowing the latter to acetylate C/EBPβ and thus decreases mSin3A (and indirectly HDAC1) binding.

A

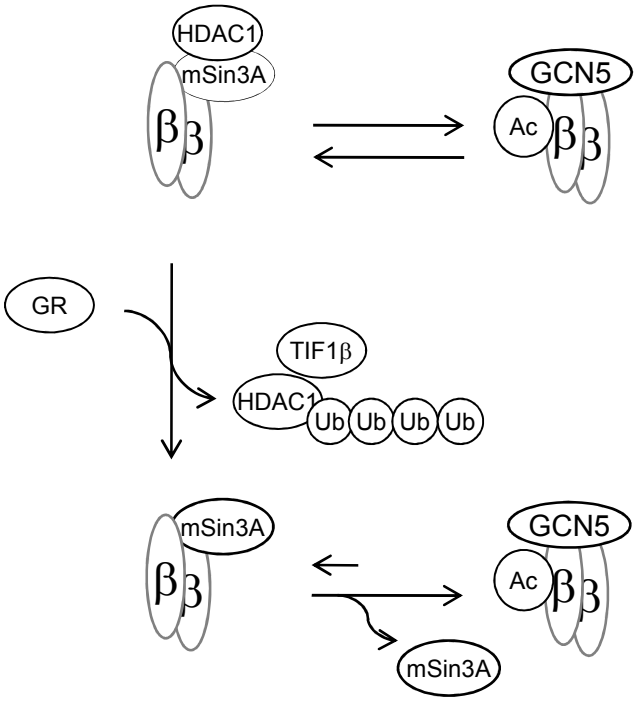

B

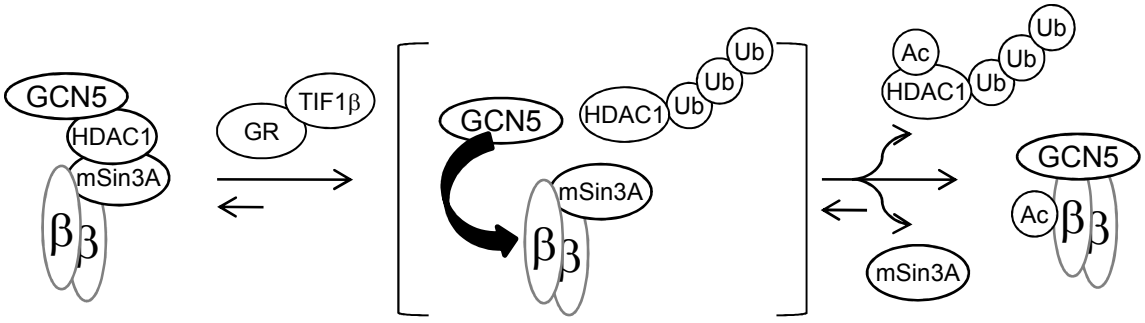

Intermediary state

C

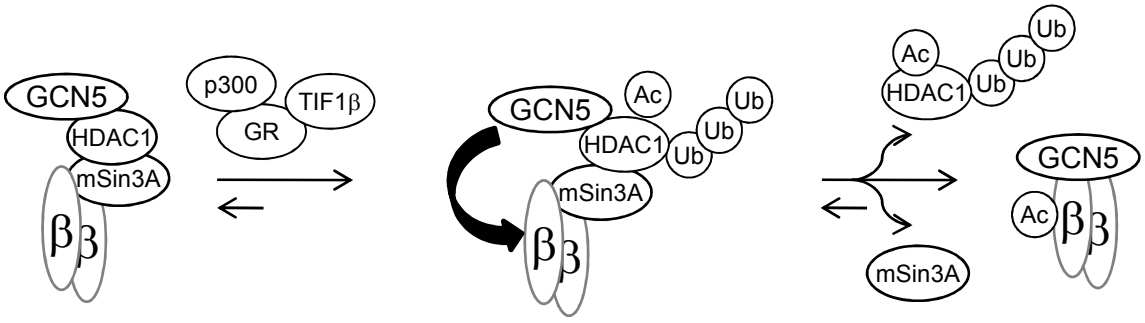

Intermediary state

two sub-populations of complexes (with either mSin3A/HDAC1 or GCN5, among others) that will compete for target promoters.

Taking these findings into consideration, one might expect to see an increase in GCN5 presence on the promoter in the presence of glucocorticoids since the C/EBPβ-competing complex containing mSin3A/HDAC1 will be reduced in number, thus favouring the equilibrium toward more C/EBPβ/GCN5 occupancy of the C/EBPα promoter. When chromatin immunoprecipitation assays were performed on the C/EBPα promoter, it showed that both mSin3A/HDAC1 and GCN5 were located on the promoter, in the absence of steroids (*66, 106*). Upon dex treatment, mSin3A/HDAC1 was reduced from the C/EBPα promoter, whereas no change was observed with respect to GCN5 occupancy (*106*), therefore contradicting our predictions.

To reconcile the ChIP experiments with the equilibrium hypothesis, another model is thus required. It is hence possible that, initially, GCN5 association with C/EBPβ occurs through an indirect association with other co-factors present on the C/EBPβ-Sin3A/HDAC1 complex. For instance, since PCAF, another homologous acetylase, has been shown to directly associate with HDAC1 (*298*), GCN5-HDAC1 association is thus possible. Two possibilities are however likely to occur in such situation. Firstly, the addition of dex will trigger HDAC1 titration from the complex by the TIF1β-mediated ubiquilation (Tomlinson *et al*. unpublished); this event will create an intermediary state in which GCN5 association will be decreased from HDAC1 and thus promote C/EBPβ acetylation. Such acetylation will then decrease mSin3A association, which will favour more C/EBPβ/GCN5 complex formation and increasing target promoter acetylation (figure 31B). Secondly, since HDAC1 activity has been shown to be suppressed by a dex-dependent acetylation mediated by p300

(*250*) and since HDAC1 and p300 co-precipitate with GR as early as 4h following glucocorticoid treatment (*66*), it is thus plausible that reduction of the deacetylase activity from the complex will favour GCN5-mediated acetylation of C/EBPβ and thus a further decrease in mSin3A association (figure 31C). These hypotheses imply that GR-induced HDAC1 post-translational modifications might compromise its association with GCN5, thus allowing the latter to acetylate its target proteins on the promoter region. CoIP experiments in 3T3 L1 cells induced to differentiate in conditions with MI and MID treatment by immunoprecipitating endogenous GCN5 will support such predictions.

4.4 LIP actively represses LAP activity via its association with mSin3A/HDAC1: a newly identified inhibitory mechanism

The absence of activation domains in CEBPβ LIP has led to the hypothesis that its repressive effect is mainly due to its ability to either compete for CCAAT promoter elements with other bZIP factors and/or to heterodimerize with these transcription factors thus reducing their activation potential (*270, 299*). When the potential mSin3A/HDAC1 binding domain in C/EBPβ was located to the first few amino acids of LIP, it suggested that LIP can also bind to the co-repressor complex and thus may in fact be an active repressor of transcription. CoIP experiments confirmed not only the interaction of LIP with HDAC1, but also identified, for the first time, a minimal domain required to mediate such association (figure 13).

Interestingly, the findings presented here suggest a novel inhibitory mechanism by which LIP mediates gene silencing. LIP was shown to inhibit LAP activity on the C/EBPα promoter when it was expressed at a ratio of 2LIP to 1LAP*/LAP (figure 13C,D). However,

a 50% reduction in interaction between LIP_{6C} and HDAC1 was enough to suppress the LIP inhibitory effect when co-expressed at the same ratio. When C/EBPβ activity further increased in the presence of dex in part due to the dissociation of HDAC1, LIP_{6C} was still able to repress LAP activity most likely by a passive repression mechanism which will act to reduce the co-activators loading on LAP/LIP_{6C} dimers since LIP lacks the activation domains. We can thus infer that the HDAC1-dependent active repression of LIP might be the dominant mechanism by which LIP functions (figure 13-14). Hence, the inhibitory function of LIP on C/EBPα activation and adipogenesis is the result of at least two mechanisms: the originally hypothesized passive repression by which LIP heterodimerization with other bZIP members reduces the number of activation domains on the formed dimer (*158, 270*); and the new HDAC1-dependent repressive effect identified here.

When C/EBP$\beta_{\Delta 153\text{-}156}$ (which expresses LIP_{6C} but not WT LIP) activity was assessed with respect to PPARγ activation, it showed no significant increased activity (figure 9B), thus confirming that the HDAC1-repressive effect on C/EBPβ activity is promoter specific (*66*). Also, when the adipsin level was analysed during the induction of differentiation of NIH 3T3 cells in the absence of glucocorticoids (figure 10B, MI condition), its expression was detected without the need for a high PPARγ protein expression, which was still undetectable even at three days post-induction (figure 9C, MI). This observation suggests that C/EBP$\beta_{\Delta 153\text{-}156}$ might, indirectly, render PPARγ activity more efficient, most likely by decreasing the overall mSin3A/HDAC1 co-repressor recruitment to their target promoters. If PPARγ was not expressed at all, then the level of expression of adipsin that was observed could have been due to C/EBP$\beta_{\Delta 153\text{-}156}$ alone. Since HDAC1 recruitment is expected to be decreased on C/EBP$\beta_{\Delta 153\text{-}156}$-targeted promoters, a ChIP assay assessing

histone acetylation profiles on overlapping C/EBPβ and PPARγ target promoters in cells expressing C/EBP$\beta_{\Delta 153\text{-}156}$ needs to be performed to confirm this hypothesis.

By contrast to selectively reducing the HDAC1 presence from promoters without affecting LIP expression, when C/EBPβ_{M152A} activity was measured, it increased expression of all C/EBPβ target genes tested, and more efficiently than C/EBP$\beta_{\Delta 153\text{-}156}$ (compare figures 9-10 to figures 18-19), despite an unaffected affinity of C/EBPβ_{M152A} with HDAC1 (figure 16-17). These results hence show that elimination of LIP is more efficient in promoting LAP activity due to the resulting increase in the recruitment of activation domains to promoters. Since LIP also inhibits C/EBPδ (*154*), the overall increased activity could also be due to an additional contribution from C/EBPδ activity. In other words, the results underline the dominant activating property of having two activation domains (i.e. from LAP/LAP homodimers) over HDAC1-mediated repression.

4.5 Acetylation of lysines 98, 101 and 102 of C/EBPβ is not required for maximum activity to be reached when HDAC1 association is compromised

Previous results from our laboratory have shown that the dex-dependent activation of C/EBPβ not only involves HDAC1 titration from its target promoters, but that dex-treatment also promotes C/EBPβ acetylation, an event that coincides with the displacement of the mSin3A/HDAC1 co-repressor complex (*106*). Although we know that HDAC1 titration from C/EBPβ is caused by a reduction in its level due to the dex-dependent degradation through the proteasomal pathway (*66*), the mechanism by which mSin3A association with C/EBPβ is decreased was not fully defined. Since CoIP and ChIP assays showed that mSin3A association with C/EBPβ was decreased 24h following glucocorticoid treatment, a time point

at which the acetylation levels of histone H4 on the C/EBPα promoter and of C/EBPβ was increased (*66, 106*), we hypothesized that structural changes caused by this post-translational modification could impact C/EBPβ association with mSin3A. This is indeed what was observed since GCN5-mediated acetylation of C/EBPβ decreased its association with mSin3A (figure 4). Moreover, since lysines 98, 101, 102 of C/EBPβ have been identified as being acetylated by GCN5 and PCAF (*106*), when an acetylation mutant ($C/EBP\beta_{K98\text{-}102R}$) interaction with mSin3A was assessed, it showed no decreased interaction with mSin3A upon exposure to either GCN5 or PCAF activity (figure 4), thus supporting the required acetylation event to reduce mSin3A association from C/EBPβ.

Knowing that $C/EBP\beta_{K98\text{-}102R}$ activity and adipogenic potential are compromised, I sought to verify the extent to which acetylation of lysines 98-102 are important for C/EBPβ transcriptional activity in conditions where the transcription factor does not interact with mSin3A/HDAC1. When I deleted the domain required for mSin3A/HDAC1 binding in $C/EBP\beta_{K98\text{-}102R}$ (giving rise to a double mutant $C/EBP\beta_{K98\text{-}102R,\Delta153\text{-}156}$), the new mutant showed an increased adipogenic and transcriptional potential on the C/EBPα promoter in the absence and presence of glucocorticoids when compared to $C/EBP\beta_{K98\text{-}102R}$, whose activity was highly compromised (figure 12). The fact that $C/EBP\beta_{K98\text{-}102R,\Delta153\text{-}156}$ activity on the C/EBPα promoter was still lower than that of $C/EBP\beta_{\Delta153\text{-}156}$ in the presence of glucocorticoids suggested that acetylation at lysines 98-102 in this system has an additional activating role in addition to promoting mSin3A dissociation. For instance, like lysine 39, this cluster of lysines might participate in potentiating the activating properties of the activation domain immediately upstream of K98 (*65*).

Since I showed that C/EBPβ$_{\Delta 153\text{-}156}$ interaction with GCN5 was compromised and that its *in vitro* acetylation level was also reduced by approximately 40% (figure 5), it is possible that another enzyme could be involved in acetylating lysines 98, 101 and/or 102 in C/EBPβ$_{\Delta 153\text{-}156}$, whose interaction could not be affected by the deletion of amino acids 153-156. This hypothesis is plausible as p300 has been shown to bind and acetylate C/EBPβ at lysine 98 (*275, 300-301*). More importantly, p300 has been proposed to bind to the N-terminal domain of C/EBPβ located upstream of amino acids 110 (*300*), hence suggesting that Δ153-156 will most likely not affect p300 binding.

Further, since the dex-dependent increase of C/EBPβ$_{K98\text{-}102R,\Delta 153\text{-}156}$ was similar to that of WT C/EBPβ (figure 12A), it confirms that GR has other roles than potentiating mSin3A/HDAC1 dissociation and acetylation of lysines 98-102. It could be that the increased expression of LMO3 following dex treatment (Tomlinson et *al*., unpublished results) or others unknown co-factors translate some of GR's activating properties. Since LMO3 is a small protein that acts as an adapter that mediates interactions with others proteins (*302*), it might bind and recruit co-activators to the C/EBPα promoter.

By contrast to the transcription assay results, when C/EBPβ$_{K98\text{-}102R,\Delta 153\text{-}156}$ adipogenic potential was assessed, it increased 3T3 L1 adipogenesis to levels statistically similar to C/EBPβ$_{\Delta 153\text{-}156}$, as shown by the quantification of adipsin and C/EBPα protein levels (figure 12E). Curiously, however, early induction of PPARγ was not observed when C/EBPβ$_{K98\text{-}102R,\Delta 153\text{-}156}$ was ectopically expressed, unlike C/EBPβ$_{\Delta 153\text{-}156}$. Because of the established cross regulation of C/EBPα and PPARγ, increased expression of the former is expected to also increase expression of the latter. However, it is also possible that C/EBPβ$_{K98\text{-}102R,\Delta 153\text{-}156}$ could inhibit PPARγ expression. If it is the case, then a competition between C/EBPβ$_{K98\text{-}}$

$_{102R,\Delta153\text{-}156}$ and C/EBPα for binding to the PPARγ promoter will result in less transcription, as opposed to C/EBP$\beta_{\Delta153\text{-}156}$, whose activity with respect to PPARγ transcription is similar to C/EBPβ_{wt}. To confirm this hypothesis, a real time RT-PCR reaction needs to be done in NIH 3T3 cells evaluating the early (24h) induction of PPARγ2 mRNA levels by C/EBP$\beta_{K98\text{-}102R,\Delta153\text{-}156}$, which is expected to be lower than that of WT or Δ153-156 C/EBPβ.

The results presented herein suggest a complex modulation of C/EBPβ transactivation potential by its diverse regulatory domains, mSin3A/HDAC1 and GCN5. However, its acetylation status following disruption of the deacetylase interaction was not evaluated. Although the *in vitro* acetylation assay showed decrease acetate incorporation into C/EBP$\beta_{\Delta153\text{-}156}$ when compared to the WT counterpart, evaluating the acetylation of the specific lysines involved in the interaction with mSin3A would be of great asset to confirm GCN5-dependent acetylation *in vivo*. To do so, antibodies against acetylated lysines 98-102 need to be generated to evaluate the *in vivo* C/EBP$\beta_{\Delta153\text{-}156}$ acetylation status.

4.6 HDAC1-repression of C/EBPβ activity differentially regulates the expression of adipogenic markers

The de-repression mechanism involving HDAC1-exclusion from transcription factors other than C/EBPβ and promoters other than C/EBPα is now relatively common. Just to name a few, such regulation has been shown to happen to HMGA1/RB (*303-304*) and C/EBPδ (*289*). Additionally, the basic helix loop helix transcription factor MyoD involved in skeletal myogenesis is also activated by exclusion of an HDAC1-containing complex (*300, 305*), suggesting that there might be a conserved transcriptional repression/activation mechanism throughout diverse families of transcription factors.

The fact that both LIP and mSin3A/HDAC1 can inhibit C/EBPβ LAP activity by decreasing the number of activation domains and by deacetylating LAP and the promoter environment adds another level of complexity in explaining the activating potential of the different C/EBPβ isoforms. Since at least two mechanisms are involved in inhibiting LAP activity, I sough to determine whether the two inhibitory effects were additive.

When an engineered LAP lacking LIP initiation methionine and compromised for its binding with HDAC1 (C/EBP$\beta_{\Delta 151\text{-}156}$) was used in the differentiation assay, it curiously showed promoter specificity (figure 18-19). Interestingly enough, C/EBP$\beta_{\Delta 151\text{-}156}$ did not highly activate all promoters tested, as it was the case of C/EBPβ_{M152A}. This hence suggests that the collective suppression of LIP and HDAC1 binding in C/EBP$\beta_{\Delta 151\text{-}156}$ gives rise to a highly effective LAP only on some promoters (i.e. GLUT4 and adipsin, but not C/EBPα and PPARγ, when compared to C/EBPβ_{M152A}) and does so in a dex-dependent manner exclusively (figure 18-19). Although the higher GLUT4 mRNA level and the higher adipsin protein level suggest that C/EBP$\beta_{\Delta 151\text{-}156}$ might directly cause the phenotype observed, evaluating mRNA and protein levels does not necessarily prove a higher transcriptional rate. To confirm that C/EBP$\beta_{\Delta 151\text{-}156}$ provides in fact the highest transcriptional rate, reporter assays with the GLUT4 and adipsin promoters, among other factors, need to be performed.

The main difference between the two groups of target genes is the fact that GLUT4 and adipsin require both PPARγ and C/EBPβ (or C/EBPα) activity for them to be transcribed, as opposed to C/EBPα and PPARγ whose transcriptional activation could be activated by C/EBPβ and/or C/EBPδ. Since glucocorticoids mediate C/EBPδ expression (*140, 306*) and since C/EBPδ has been shown to preferentially activate the PPARγ promoter in comparison to C/EBPβ (*172*), it is thus plausible that the dex requirement is to allow

PPARγ protein expression to occur, which will then allow for an enhancement of C/EBP$\beta_{\Delta 151\text{-}156}$ activity on their collective target promoters by increasing co-activator recruitment. Accordingly, C/EBP$\beta_{\Delta 151\text{-}156}$ increased activity on downstream adipocyte target genes (i.e. GLUT4 and adipsin) is not observed in the glucocorticoid-free condition probably because of an absence of PPARγ proteins (figure 18A).

4.7 Proposed C/EBPβ transcriptional regulation model

The mSin3A/HDAC1 complex is proposed to require the domain encompassing amino acids 153-156 of C/EBPβ for proper binding. Since this domain represents the first few amino acids in the LIP isoform, I hypothesized that mSin3A/HDAC1 binding domain could also be located in the LIP isoform. Together, my results suggest that the inhibitory effect of LIP is due not only to its lack of its activation domains, but also to its ability to bind and therefore recruit a co-repressor complex to its target promoters. To explain LIP mechanism of inhibition, a model is proposed in figure 32.

In conditions where LIP is expressed in the absence of glucocorticoids, all the LAP/LAP and LAP/LIP dimers will be bound and actively repressed by mSin3A/HDAC1 (scenario 1 and 2). Since LIP expression decreases LAP/LAP activity, as opposed to LIP_{6C}, whose interaction with mSin3A/HDAC1 is compromised, we could then infer that the inhibitory effect observed in this situation is mainly due to mSin3A/HDAC1 active repressive effect. We cannot however neglect passive repression by LIP homodimers that will compete for the same promoters in conditions where the LIP/LAP ratio is higher than one.

Figure 32: Proposed model highlighting the active repressor role of the C/EPBβ LIP isoform in regulating LAP.

In the absence of glucocorticoids (-DEX), LAP activity is inhibited by its association with the mSin3A/HDAC1 co-repressor complex and thus little transcription is observed. Over expression of LIP favours LAP/LIP dimers formation, thus decreasing the number of activation domains and further decreasing LAP activity (lower panel). In the presence of glucocorticoids (+DEX) however, LAP/LAP activity is increased due to an initial absence of mSin3A/HDAC1. Over expression of LIP in this case causes a LAP/LIP dimer formation and LIP homodimer associated with mSin3A alone since HDAC1 is degraded by the 26S proteasome upon steroids treatment. The different shading of p300/GCN5 symbolizes a stronger (dark) or modest (light) association of p300/GCN5 with LAP isoforms.

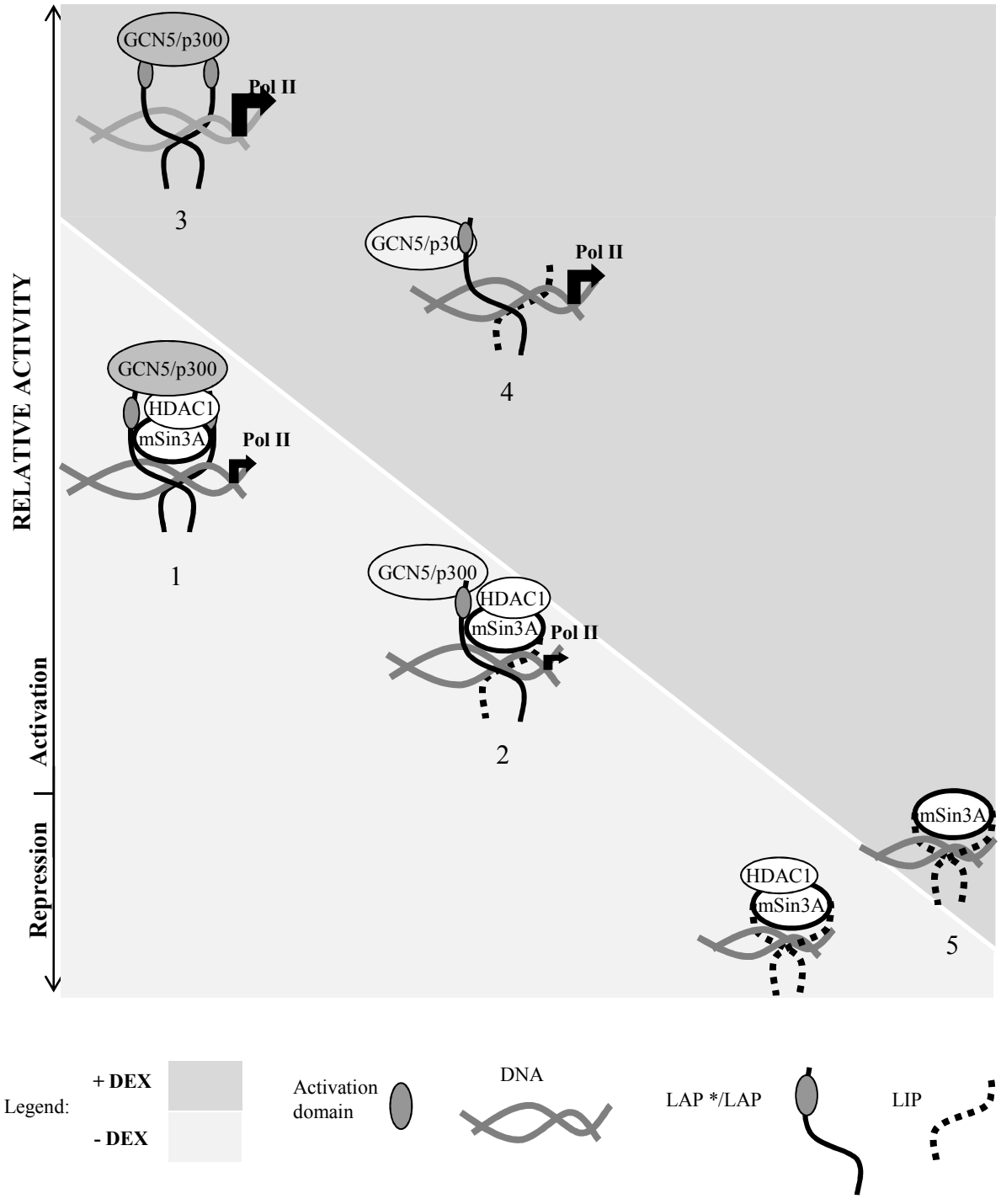
RELATIVE ACTIVITY
Activation
Repression
GCN5/p300
Pol II
3
GCN5/p300
Pol II
4
GCN5/p300
HDAC1
mSin3A
Pol II
1
GCN5/p300
HDAC1
mSin3A
Pol II
2
mSin3A
HDAC1
mSin3A
5
Legend:
+ DEX
- DEX
Activation domain
DNA
LAP */LAP
LIP

Moreover, since LAP/LIP_{6C} dimers show similar activity to LAP homodimers, we can also suggest that the mSin3A/HDAC1 repressive effect of LAP homodimers cancels the activating property of one activation domain since exclusion of mSin3A/HDAC1 and one activation domain results in an unchanged activation potential in LAP/LIP_{6C}. Accordingly, the presence of two activation domains in a LAP homodimer that is unable to associate with mSin3A/HDAC1 nearly doubles its transactivation property (figure 8).

In conditions where glucocorticoids are present, the mechanism of inhibition by LIP occurs through passive repression only (figure 31, +DEX). A LAP homodimer exposed to GR-dependent activation is initially not associated with mSin3A/HDAC1 and shows the highest transcriptional potential (scenario 3). In conditions where LAP and LIP are co-expressed (as in WT C/EBPβ), the formation of LAP/LIP heterodimers would cause a decrease in the number of activation domains when compared to a LAP/LAP homodimers, thus resulting in a reduced transactivation potential (scenario 4). When LIP:LAP ratio is high, the formation of LIP homodimer (in addition to LAP/LIP heterodimer formation) can recruit mSin3A alone to promoters and thus additionally inhibits transcription since HDAC1 is generally titrated upon dex treatment. This model supposes the requirement of lysines 98-102 in decreasing mSin3A binding from LAP; thus the absence of this cluster of lysines from LIP could still favour mSin3A binding and thus inhibits activation (scenario 5).

Although the results suggest that mSin3A associates with LAP*/LAP/LIP and that its interaction with LAP*/LAP is compromised upon acetylation of lysines 98-102, I hypothesize that LIP homodimer will show a sustained association with mSin3A even in the presence of glucocorticoids (figure 32), due to its lack of lysines 98-102. Thus, a CoIP experiment in a C/EBPβ knockout cell line stably expressing FLAG-tagged LIP needs to be

performed. A FLAG resin (Sigma Aldrich) could be used to precipitate LIP from cellular extracts of cells that were exposed to vehicle or dex. Such experiment does not, however, guaranty that LIP will not heterodimerize with other bZIP proteins (i.e. FOS, JUN, CREB) and thus obscure interpretations.

4.8 Cysteine 11 in LAP* interferes with the glucocorticoid-induced potentiation

Since the results presented in figures 20-22 and other studies convincingly demonstrate the inhibitory role of LAP* in regulating diverse promoters (*281-282, 294*), I sought to determine LAP* mechanism of reduced activation on the C/EBPα promoter and during adipogenesis. LAP* has six conserved cysteine residues (C11, C33, C123, C143, C201 and C296) where C11 is absent from LAP. Mutation of C11 to serine on LAP* partially explained its reduced activation since it increased the LPS-induced transcription of the IL-6 gene (*282*). The authors also suggested that the intramolecular disulfide bond formation between C11 and C33 in LAP* might eliminate its ability to bind DNA due to resultant structural change, thus explaining its phenotype.

Although Lee and colleagues convincingly demonstrated how an intramolecular disulfide bond impacts LAP* transcriptional activity (*282*), its activity with respect to LAP or LIP presence was not discussed. When LAP* activity was tested on the C/EBPα promoter, it showed an unpredicted phenotype. Not only that LAP* was refractory to glucocorticoid treatment, but when co-expressed with LIP, the dex-induced potentiation was restored to levels similar to WT C/EBPβ (3 fold increase, figure 21B). On the other hand, LAP does not seem to require LIP expression to respond to glucocorticoids (figure 20B and Douvris *et al*, unpublished results), although its dex-induced potentiation was still lower

than that of WT C/EBPβ (2 fold increase versus 3 fold, respectively). Moreover, while mutation of C11 in LAP* nearly doubled its basal activity, the dex treatment increased its activity to the same extent as LAP (i.e. 2 fold increase) (figure 22A). We can thus conclude that the inhibition caused by cysteine 11 prevents glucocorticoid potentiation of LAP* activity on the C/EBPα promoter.

Whether mSin3A/HDAC1 association is lost from LAP* homodimers upon dex treatment is not established since the immunoprecipitation evaluating such association was done using an antibody that precipitates all three C/EBPβ isoforms (*66, 106*). Data presented here favour the hypothesis that acetylation of lysines 98,101, 102 in either LAP* or LAP compromises their binding with mSin3A. In either case, LAP* reduced activation could be explained as follows (figure 33).

When LIP is co-expressed with LAP* homodimer in the absence of glucocorticoids, the LAP*/LIP dimer activity decreases as it only has 1 activation domain (RU=1). Counter intuitively, the LAP* homodimer does not show an increase in activity upon dex treatment. Even if mSin3A/HDAC1 is excluded, the formation of an intermolecular disulfide (S-S) bond between the two monomers could inhibit its activity by interfering with co-activator recruitment (RU=2). Although C11 has been shown to form an intramolecular disulfide bond with cysteine 33 in a different cellular context that decreased its DNA-binding ability (*282*), this observation does not explain how a LAP* homodimer has a lower activity than a LAP*/LIP heterodimers in the presence of dex since a decrease in activation domain (from LAP* to LIP) should also reduce its transactivation potential (compare RU=2 to RU=3, +dex).

Figure 33: Potential model explaining cysteine 11 inhibitory effect.

The transition between LAP*/LAP* to LAP*/LIP dimer in the absence of dex reduces the former's dimer activity because of a reduced number of activation domains (RU 2 to 1, -dex). By contrast to LAP*/LIP dimer, LAP*/LAP* dimer activity is refractory to glucocorticoids treatment (RU 2, +dex). Mutation of cystein 11 in LAP*/LAP* increases its activity in a dex-independent manner (RU 3, -dex) and LAP*$_{C11A}$ homodimer shows a two fold dex effect (RU 3 –dex to RU 6 + dex). These observations collectively suggest that, like LIP (RU 2 to RU 3, + dex), C11 might be involved in the glucocorticoid-dependent potentiation of LAP* activity; although this residue seems to have an inhibitory effect most likely by forming a disulfide bridge between two adjacent LAP* and therefore preventing proper co-activators recruitment. Note that in this assay, LAP* $_{C11A}$ homodimer and LAP*/LAP heterodimers both have similar activity (RU 6, +dex). However, LAP homodimer still has the highest activation potential, as its dex-dependent potentiation would reach RU 8-10 in this schema (data not shown).

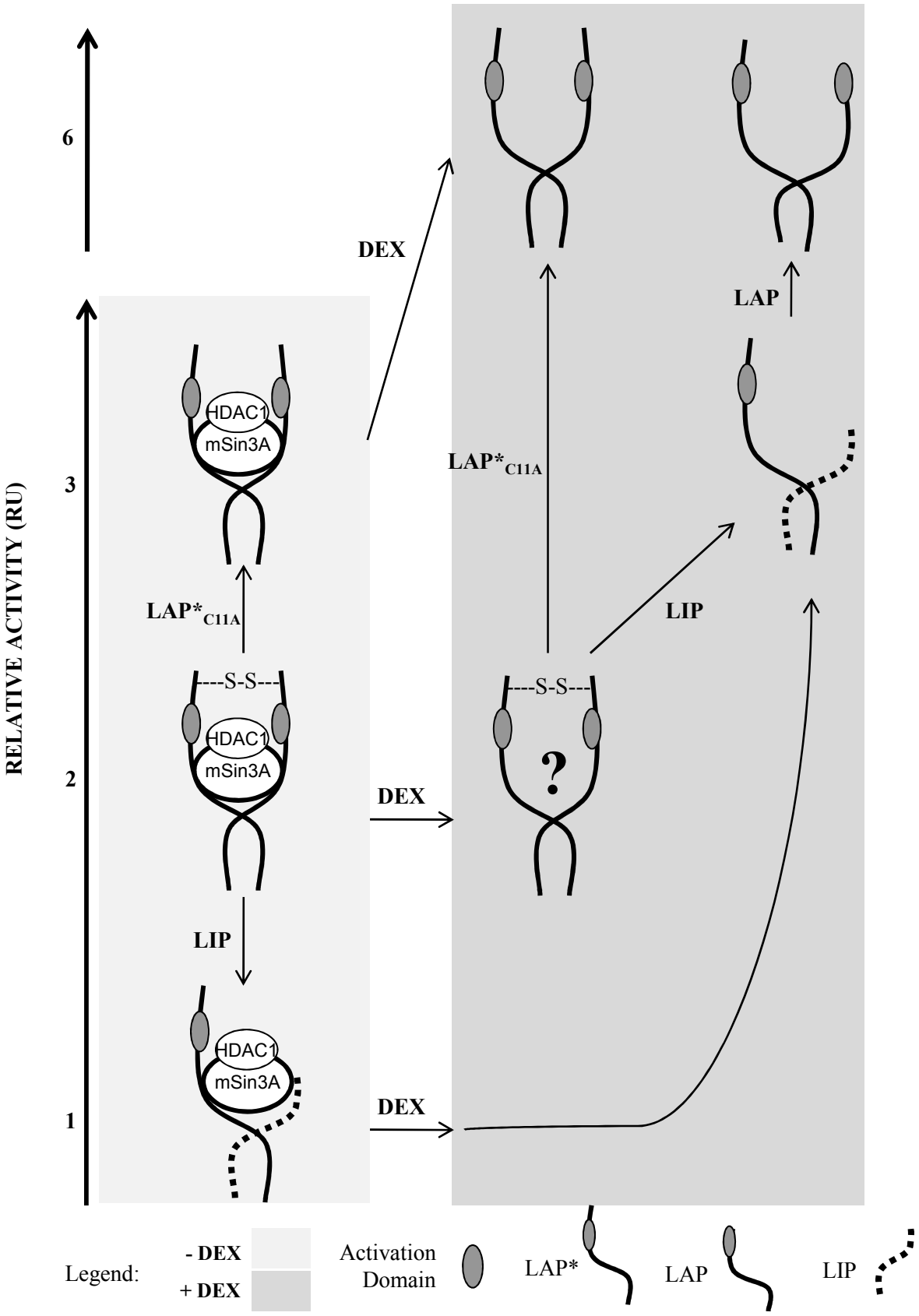
RELATIVE ACTIVITY (RU)
6
3
2
1
DEX
LAP
LAP*C11A
HDAC1
mSin3A
----S-S---
LIP
?
DEX
DEX
Legend:
- DEX
+ DEX
Activation Domain
LAP*
LAP
LIP

A potential explanation is to evoke a co-dependency model where two LAP* will have a reduced activation potential due to an intermolecular S-S bond between their C11, as shown in the model. This hypothesis is plausible since two additional intermolecular S-S bond formation between two C143 and two C296 have been documented (*159*). As opposed to the inhibitory role of C11 however, C143 and C296 oxidation were shown to confer stability to LAP homodimers upon binding to DNA (*159*) . Moreover, regulation of bZIP transcription factors by intermolecular S-S bond formation is evidenced with Fos and Jun since their oxidation has been shown to prevent DNA binding (*307*).

Accordingly, we can speculate that LIP-induced activation of LAP* occurs by reducing S-S bond formation between two LAP* (RU=3, +dex), thus explaining the increased activity observed. Additionally, the presence of LAP with LAP*, instead of LIP, further increases transcription by two fold (RU=6 +dex, extrapolated from C/EBPβ_{M152A} activity in figure 16), demonstrating the additive effect of the activation domains in the absence of a potential intermolecular S-S bond between two LAP*. Interestingly, the dex-induced potentiation of the homodimer LAP*$_{C11A}$ was also translated by a two fold increase (RU=3 to RU=6 +dex), reaching an activity similar to that of C/EBPβ_{M152A} (expressing LAP* and LAP).

These observations strongly support the inhibitory role of C11 in LAP* on the C/EBPα promoter and during adipogenesis. Although preliminary, these results delineate the relative contribution of each C/EBPβ isoform is potentiating transcription in a glucocorticoid-dependent manner. Whether the mSin3A/HDAC1 association with LAP* is affected by C11 needs more investigation. Only immunoprecipitation analysis of tagged LAP* with endogenous mSin3A/HDAC1 in the absence and presence of glucocorticoids, as

well as ChIP analysis on the C/EBPα promoter, will give a definite, yet important, answer to the predictions discussed.

Finally, even if the most reported post-translational modification of cysteine residues in protein is oxidation (and the only modification reported in C/EBPβ), one could not neglect possible prenylation (addition of a hydrophobic chain) that might increase the hydrophobic potential of this domain and thus modulate LAP*' activity. Unfortunately, no data is currently available on possible prenylation of the transcription factors involved in the early stage of the adipogenic cascade.

4.9 LAP*-N-terminal domain reveals potentially diverse inhibitory mechanisms

Given that the MAPK-dependent phosphorylation of LAP* requires the MID cocktail during preadipocyte differentiation (*156*), and since MAPK phosphorylation is also required to decrease the PRMT4/CARM1-dependent arginine 3 dimethylation (*276*), the inhibition of LAP* activity in untreated 3T3 L1 differentiation could be attributed to the constitutive association (and activity) of the methylase. Moreover, the R3 dimethylation in LAP* has been shown to negatively regulate its activity by restraining its interaction with the SWI/SNF complex (*276*), a factor that was previously shown to be essential in activating C/EBPβ target genes (*308*). Further, when LAP adipogenic potential was assessed in the absence of inducers, it showed an approximate 20 fold increase when compared to LAP* (figure 22C,D). This increase is most likely due to an effective SWI/SNF recruitment to promoters because of the absence of R3 methylation in LAP. Additionally, the absence of C11 in LAP is also responsible for a significant fraction of the adipogenic increase since induction of differentiation with LAP*$_{C11A}$ was approximately 5 times higher than LAP* (figure 22C,D).

Even if the chromatin remodelling activity of the SWI/SNF complex might not apply to the Luciferase-based transcription assay since this system does not involve a well organized chromatin-based structure that needs alteration, LAP* association with the PRMT4/CARM1 methylase through its activation domains (*276*) could interfere with co-activator recruitment and thus explain its reduced activity on the C/EBPα promoter (figure 21B). Whether R3 dimethylation is responsible for a fraction of the decreased activity observed with LAP*$_{C11A}$ (when compared to LAP) independently of PRMT4/CARM1 association needs to be determined. Neutralization of the R3 positive charge by methylation increases the N-terminal domain hydrophobicity and may impair LAP* N-terminus folding. Such an event could impact activation domain function. The fact that the first 21 amino acids in LAP* are already composed of 75% hydrophobic residues suggests either a preferential folding to accommodate such an interface or a docking site for a repressor whose interaction could be increased by R3 dimethylation.

Lastly, the CoIP results presented in figure 7 show that LAP* precipitates more effectively with HDAC1 than LAP. It is thus possible that a fraction of LAP* inhibitory effect is also mediated through HDAC1, similarly to LIP. Since amino acids 153-156 of C/EBPβ are present in LAP*/LAP and are required for binding with HDAC1, a conformational change induced by the hydrophobic N-terminal domain of LAP* could favour binding with the co-repressor. Moreover, we can also speculate that R3 dimethylation in LAP* could also modulate HDAC1 binding (*308*) like acetylation of lysines 98, 101, 102 in LAP*/LAP do (figure 4 and *106*).

4.10 A new positive regulatory domain identified in C/EBPβ LAP*/LAP

In this study, the characterization of amino acids 141-149 as being required for mediating LAP*/LAP activity at the C/EBPα promoter during preadipocyte differentiation is a novel finding that explains part of this transcription factor regulatory potential. To start with, I showed that deletion of amino acids 141-149 completely abolished C/EBPβ transcriptional activity on the C/EBPα, but not on the PPARγ, promoter, both on a transiently transfected plasmid and an endogenous chromatinized environment (figure 23, 24, 28). Hence, it appears that this region confers C/EBPβ promoter specificity. In parallel, a study performed by Schwartz and colleagues identified region 105-212 (including both RD1 and RD2) to differentially influence transactivation of MCP-1 and IL-6 transcription in a luciferase-based assay and by semi-quantitative northern analysis of their mRNA levels (*309*).

From my results, I could therefore propose that the region encompassing amino acids 141-149 needs to provide the correct environment for C/EBPβ to be able to regulate different promoters likely due to interaction with promoter-specific co-factors or dimerization partners. Although C/EBP$\beta_{\Delta 141\text{-}149}$ interaction with mSin3A/HDAC1 and GCN5 did not seem to be affected, as shown by CoIP experiments (figure 25), structural changes caused by this deletion might affect other binding partners. Indeed, a direct interaction of C/EBPβ with CRSP130/Sur2, a subunit of a mammalian Mediator Complex that activates C/EBPβ, has been shown to occur partially through the N-terminal domain of RD1 (*310*). Thus, evaluating if a decreased interaction with CRSP130/Sur2 is responsible for the decreased phenotype observed in C/EBP$\beta_{\Delta 141\text{-}149}$, in addition to HDAC1 effect, may explain the activating property of region 141-149.

The presence of highly conserved charged residues within amino acids 141-149 (figure 6C) that are exposed to the solvent (*296*) implies that such region might have an important role in positioning RD1 in a way that allows de-repression from LIP and/or from mSin3A/HDAC1. One possibility is that lysine 144 and/or arginine 145 are subject to post-translational modifications that regulate activity. A possible future study where only these two lysines could be mutated either alone or together would establish their potential involvement in regulating LAP*/LAP activity. For instance, one could mutate lysine 144 to glutamine to mimic acetylation and then evaluate C/EBPβ activity to finally define the different mechanisms by which RD1 acts as a positive regulatory domain. Additionally, since C/EBPβ has been shown to interact with the methyltransferase PRMT4/CARM1, it is thus possible that this enzyme methylates arginine 145 to activate C/EBPβ transactivation potential by favouring co-activators recruitment, as previously shown with arginine 3 dimethylation (*276*).

If region 141-149 of C/EBPβ mediates interaction with specific co-activators, then co-immunoprecipitation (using a tandem affinity purification procedure, or TAP-tag) followed by LC-MS/MS analysis could identify differential partners between of WT C/EBPβ and C/EBP$\beta_{\Delta 141\text{-}149}$. Such an analysis could be performed if the experiments proposed in the previous paragraph were to be unsuccessful.

4.11 Cysteine 143 is not vital for C/EBPβ LAP*/LAP activation potential

Other than the acidic and basic residues discussed previously, RD1 also has a conserved cysteine that has been suggested to form an intramolecular disulfide bond only in LAP* and an intermolecular bond in LAP homodimers *in vitro* (*282-283*). However, cysteine

143's definite role in conferring LAP*/LAP activating properties has not been evaluated. If C143 was in fact required *in vivo* for two LAP* and/or LAP to form a functional dimer (in addition with C202 and C296), then mutation of this residue should completely abolish C/EBPβ activity to levels observed in C/EBP$\beta_{\Delta 141\text{-}149}$. My results, however, show that C/EBPβ_{C143A} displayed transcriptional activity on the C/EBPα promoter that was only slightly compromised in the presence of glucocorticoids and showed no discernable differences in promoting NIH 3T3 adipogenesis, when compared to WT C/EBPβ (figure 30).

There are only two reports that investigated C/EBPβ redox-state and another one showing that exposure of cells to reactive oxygen species (ROS) activates C/EBPβ during preadipocyte differentiation (*159, 282, 311*). Thus, it is not established that disulfide bond formation by C143 is critical in activating the transcription factor. My study provides for the first time evidence suggesting that C143 in C/EBPβ has little role in promoting murine adipogenesis. One way to confirm whether C143 is involved in disulfide bond formation would be to subject immunoprecipitates of WT and C143A C/EBPβ during the initial phase of adipocyte differentiation to reducing and non-reducing gel electrophoresis to assess changes in mobility. Such experiments will also allow us to see whether intramolecular and/or intermolecular disulfide bond occur during adipogenesis based on monomers and dimers electrophoretic mobility.

4.12 HDAC1 and the absence of C143 both suppress C/EBP$\beta_{\Delta 141\text{-}149}$ activity

Functionally, region 141-149 of C/EBPβ seems to be required for this transcription factor to reach its normal transactivation potential on the C/EBPα promoter, whereas it showed no effect on the PPARγ promoter. Whether structural changes are solely responsible

for such phenotype is unlikely since this domain could also mediate interaction with co-activators that might be required for C/EBPβ to activate some promoters. Although I initially hypothesized that the amino acids 141-149 might selectively mediate GCN5 interaction, CoIP experiments showed no requirement for this region for a proper interaction with exogenously expressed GCN5, or HDAC1 for that matter (figure 25). However, co-expression of an inactive HDAC1 with C/EBP$\beta_{\Delta 141\text{-}149}$ was able to significantly increase its activity in the presence of glucocorticoids. This suggests that HDAC1 could be in fact required for keeping C/EBP$\beta_{\Delta 141\text{-}149}$ in an inactive state.

There are at least two potential explanations for why C/EBP$\beta_{\Delta 141\text{-}149}$ displayed a lower activation potential than WT C/EBPβ when co-expressed with inactive HDAC1$_{D181A}$. First, the deletion of C143 contributed to C/EBP$\beta_{\Delta 141\text{-}149}$ reduced activation since C/EBPβ_{C143A} showed a 25% decrease in its activity on the C/EBPα promoter when compared to WT C/EBPβ. Secondly, it is possible that the exclusion of mSin3A/HDAC1 upon glucocorticoid treatment occurs completely with WT than Δ141-149 C/EBPβ. Since GCN5–mediated acetylation of C/EBPβ occurs more effectively after the dex-dependent decrease of HDAC1 occupancy on the C/EBPα promoter (*106*) and concomitantly after the p300-mediated acetylation of HDAC1 that has been reported to decrease its deacetylase activity (*250*), it is hence plausible to propose that alteration of the kinetics of these events by Δ141-149 might be the reason why C/EBP$\beta_{\Delta 141\text{-}149}$ has a much lower activation. To support this hypothesis, I decided to eliminate HDAC1 binding domain in C/EBP$\beta_{\Delta 141\text{-}149}$ and then to test the activating property of the new mutant (which is C/EBP$\beta_{\Delta 141\text{-}156}$). If the repressive effect of HDAC1 is responsible for the suppression of C/EBP$\beta_{\Delta 141\text{-}149}$ transcriptional activity, then decreasing its binding will result in an increase of its transcriptional activity. In fact,

C/EBPβ$_{\Delta 141\text{-}156}$ showed a higher activation potential than C/EBPβ$_{\Delta 141\text{-}149}$ (without and with glucocorticoids, figure 29B). Further, C/EBPβ$_{\Delta 141\text{-}156}$ also showed a higher activity than WT C/EBPβ in the absence of dex, thus mimicking the transcriptional capacity of C/EBPβ$_{\Delta 151\text{-}156}$ (figure 29B). This result suggested that relieving HDAC1 interaction from C/EBPβ$_{\Delta 141\text{-}149}$ by eliminating region 151-156 was sufficient to increase its activity in a manner that was independent of glucocorticoid treatment. Moreover, in the presence of glucocorticoids, C/EBPβ$_{\Delta 141\text{-}156}$ transcriptional activity was further increased and it showed the same activation potential as WT C/EBPβ (in the presence of glucocorticoids).

Interestingly however, C/EBPβ$_{\Delta 141\text{-}156}$ had an activation level that was approximately 30% lower than that of C/EBPβ$_{\Delta 151\text{-}156}$ in the presence of glucocorticoids. Since both mutants do not express LIP and do not properly associate with HDAC1, it means that the absence of region 141-149 in C/EBPβ$_{\Delta 141\text{-}156}$ still caused a diminution in its activity. Since mutation of cysteine 143 within region 141-149 reduced the transcriptional activity of C/EBPβ by approximately 25% (figure 29A), the absence of this residue from C/EBPβ$_{\Delta 141\text{-}156}$ is most likely the reason why it had an activation potential that was 30% lower than C/EBPβ$_{\Delta 151\text{-}156}$.

Other experiments that could be done to further support the hypothesis of a slower HDAC1 release from C/EBPβ$_{\Delta 141\text{-}149}$ in the presence of glucocorticoids include a time-course CoIP analysis of the two factors. Most importantly, a ChIP experiment on the C/EBPα promoter in cells expressing C/EBPβ$_{\Delta 141\text{-}149}$ could be performed to evaluate the glucocorticoid-dependent decrease of HDAC1 and the increase in acetylation of lysines 98, 101 and 102 of C/EBPβ using an antibody specific to these acetylated lysines (which needs to be generated) .

In addition to a delayed HDAC1-release caused by Δ141-149 in C/EBPβ, it is possible that the structural change caused by this deletion affects p300 association with the N-terminal domain of LAP (*300*). Such an impact could consequently decrease p300 recruitment to the C/EBPα promoter, thus decreasing the p300-dependent inhibition of HDAC1. Such a delay in HDAC1 inactivation could also explain the lower C/EBP$\beta_{\Delta 141\text{-}149}$ activation potential. Moreover, since GR-induced acetylation of HDAC1 by p300 occurs within 4h post-treatment (*250*) and since HDAC1 titration requires longer exposure to the glucocorticoid (between 16h-24h) (*66*), it is possible that HDAC1 inhibition by acetylation could be delayed in cells expressing C/EBP$\beta_{\Delta 141\text{-}149}$. Furthermore, when co-expression of an inactive HDAC1 was performed, C/EBP$\beta_{\Delta 141\text{-}149}$ transcriptional activation was increased maybe because the initial lag in p300-dependent inactivation of HDAC1 was not crucial, hence making Δ141-149 a minor set back with respect to C/EBPβ transcriptional activation when HDAC1 is inactive. Finally, the fact that co-expression of inactive HDAC1 with C/EBP$\beta_{\Delta 141\text{-}149}$ still showed an activation potential that was approximately 30% lower than that of WT C/EBPβ (in the presence of inactive $HDAC1_{D181A}$, figure 29A) could be explained by the absence of cysteine 143, as previously discussed. Thus I can suggest that the activating property of the N-terminal region of RD1 occurs in an HDAC1-independent mechanism involving cysteine 143 and in an HDAC1-dependent mechanism that could possibly help relieving HDAC1 from C/EBPβ.

Testing of the predictions could start with a time-course ChIP analysis during the first 48h of NIH 3T3 differentiation evaluating the presence of acetylated and unacetylated HDAC1 on the C/EBPα promoter at 8h intervals. Since Hager and colleagues (*250*) identified the HDAC1 lysines modified by p300, antibodies against these specific residues

could be generated for the purpose of these experiments. Additionally, the level of histone H4 acetylation could also be evaluated, as it will be expected to be detected earlier in WT than Δ141-149 C/EBPβ.

One fundamental observation from these results is that the inactive HDAC1 was not able to increase WT or Δ141-149 C/EBPβ activity in the absence of glucocorticoids, most likely because of the persistent association of mSin3A/HDAC1 with the transcription factor. Such a phenotype emphasizes the importance of dex in decreasing the overall deacetylase activity from the C/EBPβ complex by promoting p300-dependent acetylation of HDAC1 and then titration of HDAC1 from the promoter by mediating its proteasomal degradation through the 26S proteasomal pathway (*66, 250*).

4.13 Insights into the adipogenic transcriptional cascade during NIH 3T3 adipogenesis

The importance of the excess energy that is stored in WAT in the form of triglycerides is of vital necessity for animals when food is scarce. However, the increase in size of the adipose tissue caused by a higher number of adipocytes and lipid content leads to a metabolic dysfunction that alters the body's homeostatis. The current lifestyle in our societies, in which the abundance of hypercaloric diets favours increased storage of lipids forecast an epidemic arising from the metabolic syndromes. Hence, studying the development of adipose tissue is vital in order to determine means by which adipocyte development might be modulated and WAT overdevelopment restrained.

The results presented in this thesis highlight the role of C/EBPβ in modulating preadipocyte differentiation through its many regulatory domains. I identified two

subdomains within RD1 that have interdependent roles in regulating expression of the major adipogenic factors C/EBPα and PPARγ. I also showed significant data that explains some of the specific phenotypes mediated by C/EBPβ LAP*/LAP/LIP isoforms. Finally, the results also emphasize the importance of C/EBPβ redox state in regulating gene transcription of adipocyte markers.

When the initial transcription experiments were performed using C/EBP$\beta_{\Delta 141\text{-}149}$, it was surprising to notice that, albeit inactive on the C/EBPα promoter, C/EBP$\beta_{\Delta 141\text{-}149}$ was able to effectively induce preadipocyte differentiation in a fibroblastic cell line. These results suggested that direct activation of PPARγ by C/EBP$\beta_{\Delta 141\text{-}149}$ accounted for the final phenotype observed. Although the mechanism of C/EBPβ-dependent activation of PPARγ is still unclear, the results presented here and others studies clearly suggest that C/EBPβ is able to directly activate PPARγ transcription, as showed by Luciferase-based transcription assays using the proximal PPARγ promoter, ChIP analysis and quantitative RT-PCR (*65, 140, 174*).

Knowing that C/EBPδ expression is activated by GR, the dex-dependent effect observed in PPARγ activation might be caused not only by increased C/EBPδ expression but also to GR-dependent activation of C/EBPβ. Since C/EBPδ alone cannot efficiently induce endogenous PPARγ expression and thus NIH 3T3 differentiation (*139-140*), we could therefore infer that the cooperative effect of C/EBPδ/C/EBPβ heterodimer and C/EBPβ homodimers are more crucial for PPARγ induction than C/EBPδ homodimers. This hypothesis is further supported by the C/EBPδ/C/EBPβ knockout studies. PPARγ mRNA levels were shown to be highly decreased in C/EBP$\beta^{-/-}$ primary embryonic fibroblast when compared to C/EBP$\delta^{-/-}$ cells and was almost suppressed in double KO

(C/EBPβ$^{-/-}$/C/EBPδ$^{-/-}$) cells (*146*). Nonetheless, C/EBPδ$^{-/-}$ cells still showed less PPARγ expression than WT cells, thus giving C/EBPδ some implication in regulating this important adipogenic factor.

Even if the repression of PPARγ expression by HDAC1 through C/EBPβ was not observed in the Δ153-156 mutant, this does not preclude a possible HDAC1-dependent regulation through other factors. For instance, since inhibition of C/EBPδ activity by the mSin3A/HDAC1 co-repressor complex has already been reported (*289, 312*), this transcription factor could also repress PPARγ expression when glucocorticoids are absent since the HDAC1 protein levels are only reduced upon treatment with dex during adipogenesis (*66*). Hence, the dex-dependent proteasomal degradation of HDAC1 could also relieve C/EBPδ association from the co-repressor complex. Interestingly, HDAC1 was shown to be reduced on the heptaglobin promoter following treatment of intestinal epithelial cells by the pro-inflammatory cytokine IL-1β (*289*), thus relieving C/EBPδ from inhibition, which shows a parallel to the glucocorticoid-dependent activation of C/EBPα expression by C/EBPβ during murine adipogenesis.

Based on these observations, whether C/EBPβ/δ heterodimers will be similarly regulated by the mSin3A/HDAC1 co-repressor complex when compared to C/EBPβ or C/EBPδ homodimers is not known and thus requires further investigations. Since mSin3A/HDAC1 binding interfaces on C/EBPβ or C/EBPδ differ (chapter 3.1 and *289*), heterodimers formation by these two factors might not dispose of an optimal spatial arrangement to either accommodate binding or to allow regulation by displacement of the co-repressor complex upon hormone treatment. That C/EBPβ encodes three different isoforms, all of which are able to associate with mSin3A/HDAC1, adds another level of complexity

when it comes to heterodimers formation with C/EBPδ alone and regulation by the co-repressor complex.

Earlier studies suggested that NIH 3T3 and 3T3 L1 cells differed in their differentiation in that NIH 3T3 cells were insensitive to insulin and failed to induce C/EBPα expression at the onset of differentiation (*139, 143*). The authors confirmed by Northern blot analysis that NIH 3T3 cells ectopically expressing C/EBPβ do not express C/EBPα or GLUT4 mRNA. However, the increased sensitivity of the qRT-PCR experiments performed in this study confirm that both factors could be transcribed from their promoters when C/EBPβ is over-expressed, although to levels probably undetectable by Northern analysis. Moreover, the low level of C/EBPα mRNA is most likely below the threshold required to effectively translate the transcripts, hence explaining why no C/EBPα protein expression was detected by Western blot analysis when investigated in NIH 3T3 differentiation upon expression of ectopic C/EBPβ.

Surprisingly, however, when the NIH 3T3 cells stably expressing C/EBPβ were cultured for a longer period of time before induction of differentiation, the protein expression of both C/EBPα isoforms were detected when assessed by Western analysis (appendix 8A). Over-exposure of the Western blot after the first round of differentiation (i.e. two weeks following the stable expression of C/EBPβ) showed non-specific protein bands, as opposed to the second round of differentiation, performed two weeks later. Only cells expressing C/EBPβ and treated with the full differentiation cocktail, including glucocorticoids, expressed C/EBPα as expected.

These findings suggested that a sustained expression of C/EBPβ in the NIH 3T3 fibroblastic cell line is able to reprogram the cells to probably favour a higher expression of

C/EBPα mRNA that will reach the minimal threshold for it to be effectively translated. A lower level of C/EBPα mRNA could be one of many possibilities explaining why C/EBPα protein expression is initially not effectively detected. For instance, since C/EBPα protein half-life has been shown to be regulated by its ubiquitylation status and hence degraded through the proteasomal pathway (*313-314*), an increased degradation rate might be one of the answers. Moreover, regulation of its mRNA shuttling between the nucleus and cytoplasm could also account for reduction of the translation level during adipogenesis via retention of the messenger by a RNA-binding protein, as previously demonstrated for C/EBPβ whose mRNA were sequestered in the nucleus by HuR, causing reduction of its translation and adipogenesis in MEF cells (*160*). On that account, FMIP (Fms interacting protein) has been suggested to affect C/EBPα mRNA processing and export during adipogenesis of the multipotent C2C12 cells (*315*) whereas CUGBP1 (CUG binding protein 1) and CRT (calreticulin) have been shown to bind C/EBPα mRNA and inhibit its translation (*316*). Together, these findings suggest that the absence of C/EBPα protein expression in NIH 3T3 could be due to post-transcriptional regulation of its transcripts.

Since ectopic expression of PPARγ is not sufficient to induce C/EBPα expression (*139*), we can conclude that during NIH 3T3 differentiation, these cells require a constant expression of C/EBPβ to eventually induce higher levels of C/EBPα mRNA and protein (see figure 34), possibly by regulating the expression or the function of factors involved in C/EBPα mRNA processing or proteasomal degradation.

Figure 34: Fundamental differences between NIH 3T3 and 3T3 L1 differentiation.

(A) Ectopic expression of PPARγ in NIH 3T3 cells is not sufficient to induce C/EBPα protein expression, but is still able to effectively promote adipogenesis. The cells are unresponsive to insulin and do not uptake glucose. **(B)** When C/EBPβ is stably expressed in NIH 3T3 cells, C/EBPα protein expression is detected only after a longer duration of C/EBPβ expression. C/EBPα induction is hence much slower in NIH 3T3 cells even in the presence of glucocorticoids. However, its expression is much more effective in 3T3 L1 over-expressing C/EBPβ, even in the absence of hormone, most likely due to the primed state of the promoter (also refer to figure 3).

A

NIH 3T3 over-expressing PPARγ

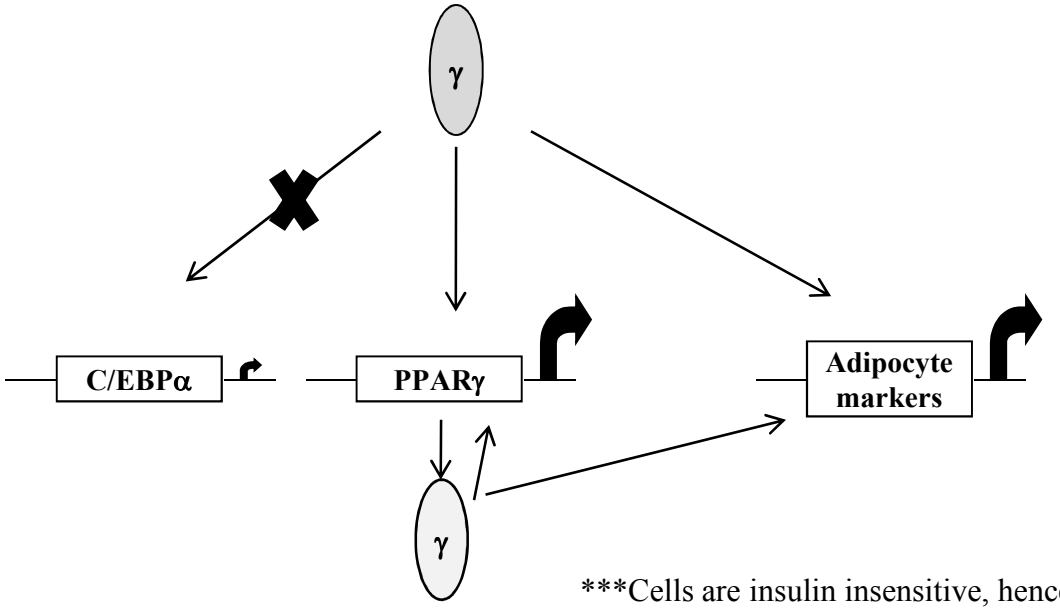

***Cells are insulin insensitive, hence do not uptake glucose

B

NIH 3T3 and 3T3 L1 over-expressing C/EBPβ

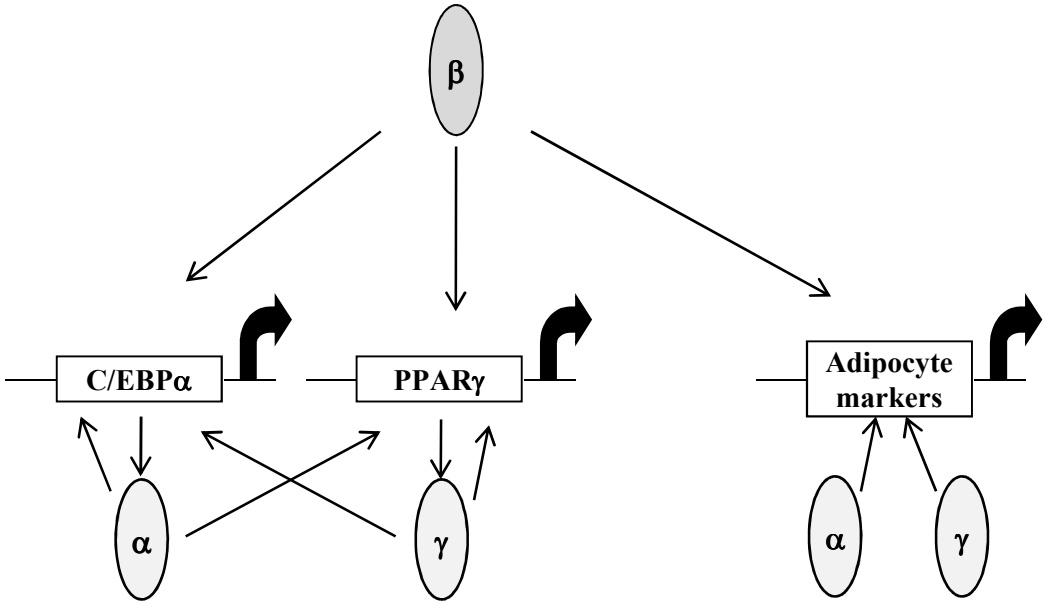

Slower induction in NIH 3T3 cells

4.14 The significance of C/EBPβ-HDAC1 in tissues other than WAT

The fact that C/EBPβ is expressed in most tissues suggests that this factor has an important physiological function in individuals. C/EBPβ is shown to be involved in the development and function of an increasing number of organs like the liver, intestine, lung, adipose tissue, kidney, spleen, testis, ovaries, mammary gland, bones, and brain (*137, 192, 195, 201, 251, 317-319*). Other than its role in regulating energy metabolism (*146-148, 320*), C/EBPβ plays a central role in the acute phase response and immunity (*193, 252-253*), as well as tumour cell proliferation (*254-255*) and progression of diverse cancers (*255-260*). Despite the relatively high number of studies investigating the functions of C/EBPβ in diverse tissues, the detailed mechanism characterizing the interplay between its three isoforms on gene regulation is still unclear.

Since C/EBPβ is involved in various processes (cell proliferation/differentiation, among others), it is evident that this factor's malfunction might promote disease. What is important to consider when studying C/EBPβ activity is the fact that a differential alteration of its activity either via any change of its isoform's ratio or via mutation of any subdomains within its central region (which is located downstream of the AD1-3 and upstream of the bZIP) could give rise to diverse phenotypes only within one cellular context. When mutations that alter C/EBPβ activity occur in a complex organism, the multitude of defect that could arise within each organ could be disastrous. Luckily, the presence of various C/EBP members with some redundant functions could partially rescue C/EBPβ defects, as previously shown in mice (*146-147, 268, 320*).

The broad role of C/EBPβ is further reflected by its inhibition of insulin expression in pancreatic beta-cell via its association with E47, where its expression is associated with a

hyperglycemic state and unbalanced insulin secretion (*321-322*). Knowing that C/EBPβ activity is inhibited by the co-repressor complex mSin3A/HDAC1 (*65-66*) and since C/EBP$\beta_{\Delta 153\text{-}156}$ interaction with the repressor complex is compromised (chapter 3.1), studies using the hyperactive C/EBP$\beta_{\Delta 153\text{-}156}$ may help us understand if the effect of HDAC1 is what causes inhibition of insulin expression and secretion. If it is the case, targeting HDAC1 activity using deacetylase inhibitors (i.e. TSA or VPA) in diabetic mice model would be a good future study on type II diabetes. Since TSA and VPA are not specific for HDAC1, they could give us valuable information as to what extent HDAC1 could affect insulin secretion.

Another implication of C/EBPβ is evidenced by its anti-tumorigenic effect through restoration of TGFβ cytostatic properties in some breast cancers (*255*). The importance of C/EBPβ activity is shown by a high LIP:LAP ratio (hence low transcriptional activity) that favours cell proliferation and breast cancer evolution and metastasis (*255*). Therefore using C/EBP$\beta_{\Delta 153\text{-}156}$ in some cancer studies would be an easy way to assess HDAC1 involvement in the context of C/EBPβ without the use of deacetylase inhibitors. Moreover, the identification of LIP as an HDAC1-associating factor could also explain why an increased LIP:LAP ratio favours cellular proliferation since HDAC1 has been extensively implicated in promoting such process via regulation of the cell cycle checkpoints (*323-326*).

Repression of the tumour suppressor p53 by HDAC1 also helps to explain its pro-proliferative properties (*327*). Since LIP and HDAC1 have been independently implicated in promoting cellular proliferation (*285, 328*), this thesis provides a new molecular clue linking LIP and HDAC1 functions in such process. Interestingly, the fact that upregulation of LIP in some tumour cells correlated with p53 suppression (*329*) and that C/EBPβ has been shown to bind to the p53 promoter (*330*) suggest that the cooperative function of LIP and HDAC1

might be one of the mechanism responsible for downregulation of p53 expression in tumourigenic cells. Furthermore, given that C/EBPβ has been demonstrated to directly associate with p53 through its C-terminus domain (also present in LIP) causing downregulation of p53 activity (*331*) adds another rationalization by which the combined effect of LIP-HDAC1 association and p53 anti-proliferative properties could generally modulate cellular proliferation in cells in which they are all expressed.

Although the role of HDAC1 in promoting MCE has not been investigated in preadipocyte differentiation, the preliminary results presented in the first part of this thesis imply that its association with LAP/LIP could be one of the means by which C/EBPβ promotes this important process during the differentiation of murine adipogenesis. Hence, further analysis of HDAC1 requirement for MCE through LAP and LIP could provide valuable mechanistic information explaining how cellular proliferation is driven by C/EBPβ. The results presented herein were all performed in cultured cell lines. Although they can give great indications as to the role of proteins in defined conditions, it is hard to predict how a complex organism would react to mutations that alter the protein function *in vivo*. Thus, generating knock-in mice with the mutants constructed in the present study could be of great interest to the general readers since C/EBPβ's function is ubiquitous. If one could confirm the phenotypes observed from the analysis obtained from our *in vitro* studies (that C/EBP$\beta_{\Delta 153\text{-}156}$ could increase the size of adipose tissue in mice, while C/EBP$\beta_{\Delta 141\text{-}149}$ could not), it would help us predict if some humans bearing mutation in region equivalent to 153-156 or 141-149 of the C/EBPβ gene are more or less prone for central obesity, respectively, than individuals with the WT gene. Further, if HDAC1 proliferative activity truly occurs

through C/EBPβ, then mice expressing C/EBP$\beta_{\Delta 153\text{-}156}$ might show less tumour formation since the cooperative role of C/EBP$\beta_{\Delta 153\text{-}156}$ and HDAC1 would be partially disrupted.

4.15 New venues to explore

SUMOylation is an important post-translational modification involved in a broad cellular processes and parallel ubiquitylation but does not directly and necessarily target proteins for degradation. This process involves SUMO proteins (small ubiquitin-like modifier) and there are currently four paralogues identified in mammals (SUMO 1-4) (recently reviewed in *332*). These SUMO proteins are conjugated to lysine residues of their target proteins by the Ubc9 (ubiquitin-conjugating 9) enzyme.

Currently, very little is known about the role of SUMO proteins in adipocytes. For instance, desumoylation of C/EBPβ-SUMO-1 at lysine 133 has been shown to be involved in its stability by decreasing its proteasomal degradation, increasing its activity, its binding to C/EBPα and PPARγ promoters and hence increasing 3T3 L1 differentiation (*333*). Moreover, PPARγ sumoylation at lysine 107 decreases NIH 3T3 differentiation when compared to mutant PPARγ_{K107R}, thus suggesting that PPARγ sumoylation inhibits its transcriptional activity (*334-335*). Ubc9 has been shown to be an important regulator of GLUT4 turnover and thus increases insulin-sensitivity in 3T3 L1 cells (*336-337*).

Ubc9' target has not been identified in 3T3 L1 cells but we could infer that Ubc9 could sumoylate a transcription factor upstream of GLUT4 that will allow its de-repression. mSin3A/HDAC1 could be proposed as a target since HDAC1 sumoylation has been shown to decrease its deacetylase activity and repression of a GAL4-based Luciferase assay without affecting its interaction with mSin3A (*338*). Interestingly, a recent study has shown that

sumoylation is associated with gene repression via modulation of transcription factor-associated proteins (recruitment of HDACs and deacetylation of histones) (*339*). Taken together, these studies clearly suggest an involvement of SUMO proteins in regulating adipogenesis. Although more investigation is required to define how SUMO-mediated regulation is involved in the earlier transcriptional cascade.

To further clarify the role of sumoylation during murine adipogenesis, I sought to evaluate whether changes in the sumoylation status of proteins associated with C/EBPβ during the initial phase of adipogenesis took place in a glucocorticoid-dependent manner. To assess the sumoylated profile of proteins during the initial phase of preadipocyte differentiation, a Western blot analysis was performed using 3T3 L1 extracts at specific time-points following induction of differentiation. In this case, no discernable differences were observed between the MI and MID conditions when antibodies against SUMO 1,2,3 were used (data not shown). Such observation, however, does not exclude small differences that could occur within specific protein complexes during the differentiation process. In fact, when endogenous C/EBPβ was immunoprecipitated, a SUMO-reactive 100KDa band was detected in conditions where glucocorticoids were omitted from the differentiation cocktail, 16h following induction of differentiation (appendix 8B). Interestingly, the addition of the hormone prevented its association. Since the band intensity was also decreased at the 24h time-point in the absence of dex, it could be that glucocorticoids accelerate this (these) protein(s) dissociation from C/EBPβ, and that the presence of the hormone it not solely needed for such dissociation.

Given that C/EBPβ starts to bind to DNA approximately 16h following induction of differentiation (*153, 156*), it is plausible to suggest that its interaction with a sumoylated

protein at the promoter would keep it inactive in the absence of dex and that glucocorticoids would in fact displace such factor, as shown with mSin3A/HDAC1 (*66, 106*). To identify such an unknown factor, a TAP-TAG immunoprecipitation assay could be performed in 3T3 L1 cells 16h following differentiation, after which immunoprecipitates could be analysed by LC-MS/MS.

4.16 Concluding remarks

In the present study, I showed that GCN5 and mSin3A require the same determinants for binding to C/EBPβ and that only mSin3A requires the bZIP domain to mediate interaction. Further, I confirmed that not only the mSin3A/HDAC1 co-repressor complex is partially responsible for C/EBPβ LAP*/LAP inhibition, but also that the shorter LIP isoform mediates an active repression mechanism which involves recruitment of the mSin3A/HDAC1 to LAP*/LAP, and thus to their target promoters. This finding elucidates a new active repression mechanism by which LIP acts to suppress transcription. Moreover, the preliminary results investigating C/EBPβ redox-state strongly suggest for a differential role for C11 located in LAP* in modulating LAP*/LAP and LIP activity in heterodimers formation. Surprisingly, C11-mediated repression of LAP* seems to suppress the LAP* homodimer response to glucocorticoids whereas co-expression of LIP with LAP* to form LAP*/LIP heterodimer restores the glucocorticoid effect.

Further, I showed that RD1 in LAP*/LAP is composed of at least two sub-regulatory domains that define their transcriptional potentials. By contrast to the previous hypotheses stating that the full region of RD1 negatively regulates C/EBPβ activity, I showed that its N-terminal region composed of amino acids 141-149 positively mediates LAP*/LAP activation

potential on the C/EBPα, but not the PPARγ promoter by different means, which include a minor involvement of C143. The results also suggest a role for amino acids 141-149 in relieving mSin3A/HDAC1-mediated inhibition of C/EBPβ that could provide the suitable environment for modulation of mSin3A/HDAC1-C/EBPβ interaction.

The results presented in this thesis present only a beginning of the diverse means by which C/EBPβ transcriptional activity is regulated during cellular development. The identification of specific regulatory domains within C/EBPβ, each with independent properties, contributes to a better understanding of the limitless possibilities by which C/EBPβ transcriptional activity is modulated within different cellular context. The prominent role of C/EBPβ in cellular growth and differentiation makes it a pivotal factor that require further investigations to characterize details in its complex functioning. Although increasing reports focus on elucidating its mode of action, having a crystal structure of this factor will help us predict much more effectively how interaction with co-factors might impact regulation of its target promoters.

REFERENCES

1. Luger, K., Mader, A. W., Richmond, R. K., Sargent, D. F. and Richmond, T. J. (1997) Crystal structure of the nucleosome core particle at 2.8 A resolution, *Nature 389*, 251-260.
2. Richmond, T. J., Finch, J. T., Rushton, B. Rhodes, D. and Klug, A. (1984) Structure of the nucleosome core particle at 7 A resolution, *Nature 311*, 532-537.
3. Muthurajan, U. M., Park, Y. J., Edayathumangalam, R. S., Suto, R. K., Chakravarthy, S., Dyer, P. N. and Luger, K. (2003) Structure and dynamics of nucleosomal DNA, *Biopolymers 68*, 547-556.
4. Grewal, S. I., and Jia, S. (2007) Heterochromatin revisited, *Nat Rev Genet 8*, 35-46.
5. Davie, J. R., Saunders, C. A., Walsh, J. M., and Weber, S. C. (1981) Histone modifications in the yeast S. Cerevisiae, *Nucleic Acids Res 9*, 3205-3216.
6. Halleck, M. S., and Gurley, L. R. (1982) Histone variants and histone modifications in chromatin fractions from heterochromatin-rich Peromyscus cells, *Exp Cell Res 138*, 271-285.
7. Wong, M., and Smulson, M. (1984) A relationship between nuclear poly(adenosine diphosphate ribosylation) and acetylation posttranslational modifications. 2. Histone studies, *Biochemistry 23*, 3726-3730.
8. Shiio, Y., and Eisenman, R. N. (2003) Histone sumoylation is associated with transcriptional repression, *Proc Natl Acad Sci U S A 100*, 13225-13230.
9. Nathan, D., Ingvarsdottir, K., Sterner, D. E., Bylebyl, G. R., Dokmanovic, M., Dorsey, J. A., Whelan, K. A., Krsmanovic, M., Lane, W. S., Meluh, P. B., Johnson, E. S., and Berger, S. L. (2006) Histone sumoylation is a negative regulator in Saccharomyces cerevisiae and shows dynamic interplay with positive-acting histone modifications, *Genes Dev 20*, 966-976.
10. Block, J. A., and Atkinson, B. G. (1979) Histones and histone phosphorylation during quail myogenesis in vitro, *Cell Differ 8*, 413-420.
11. Paulson, J. R., and Taylor, S. S. (1982) Phosphorylation of histones 1 and 3 and nonhistone high mobility group 14 by an endogenous kinase in HeLa metaphase chromosomes, *J Biol Chem 257*, 6064-6072.
12. Cooper, E., and Spaulding, S. W. (1985) Hormonal control of the phosphorylation of histones, HMG proteins and other nuclear proteins, *Mol Cell Endocrinol 39*, 1-20.
13. Duerre, J. A., Wallwork, J. C., Quick, D. P., and Ford, K. M. (1977) In vitro studies on the methylation of histones in rat brain nuclei, *J Biol Chem 252*, 6981-6985.
14. Lukasova, E., Koristek, Z., Falk, M., Kozubek, S., Grigoryev, S., Kozubek, M., Ondrej, V., and Kroupova, I. (2005) Methylation of histones in myeloid leukemias as a potential marker of granulocyte abnormalities, *J Leukoc Biol 77*, 100-111.
15. Annunziato, A. T., Eason, M. B., and Perry, C. A. (1995) Relationship between methylation and acetylation of arginine-rich histones in cycling and arrested HeLa cells, *Biochemistry 34*, 2916-2924.
16. Stancheva, I., El-Maarri, O., Walter, J., Niveleau, A., and Meehan, R. R. (2002) DNA methylation at promoter regions regulates the timing of gene activation in Xenopus laevis embryos, *Dev Biol 243*, 155-165.

17. Bauer, U. M., Daujat, S., Nielsen, S. J., Nightingale, K., and Kouzarides, T. (2002) Methylation at arginine 17 of histone H3 is linked to gene activation, *EMBO Rep 3*, 39-44.
18. Strahl, B. D., Ohba, R., Cook, R. G., and Allis, C. D. (1999) Methylation of histone H3 at lysine 4 is highly conserved and correlates with transcriptionally active nuclei in Tetrahymena, *Proc Natl Acad Sci U S A 96*, 14967-14972.
19. Hong, L., Schroth, G. P., Matthews, H. R., Yau, P. and Bradbury, E. M. (1993) Studies of the DNA binding properties of histone H4 amino terminus. Thermal denaturation studies reveal that acetylation markedly reduces the binding constant of the H4 "tail" to DNA, *J Biol Chem 268*, 305-314.
20. Villagra, A., Gutierrez, J., Paredes, R., Sierra, J., Puchi, M., Imschenetzky, M., Wijnen Av, A., Lian, J., Stein, G., Stein, J., and Montecino, M. (2002) Reduced CpG methylation is associated with transcriptional activation of the bone-specific rat osteocalcin gene in osteoblasts, *J Cell Biochem 85*, 112-122.
21. Xiao, T., Kao, C. F., Krogan, N. J., Sun, Z. W., Greenblatt, J. F., Osley, M. A., and Strahl, B. D. (2005) Histone H2B ubiquitylation is associated with elongating RNA polymerase II, *Mol Cell Biol 25*, 637-651.
22. Kao, C. F., Hillyer, C., Tsukuda, T., Henry, K., Berger, S., and Osley, M. A. (2004) Rad6 plays a role in transcriptional activation through ubiquitylation of histone H2B, *Genes Dev 18*, 184-195.
23. Henry, K. W., Wyce, A., Lo, W. S., Duggan, L. J., Emre, N. C., Kao, C. F., Pillus, L., Shilatifard, A., Osley, M. A., and Berger, S. L. (2003) Transcriptional activation via sequential histone H2B ubiquitylation and deubiquitylation, mediated by SAGA-associated Ubp8, *Genes Dev 17*, 2648-2663.
24. Dombradi, V., and Cohen, P. T. (1992) Protein phosphorylation is involved in the regulation of chromatin condensation during interphase, *FEBS Lett 312*, 21-26.
25. Wagner, T. E., Hartford, J. B., Serra, M., Vandegrift, V., and Sung, M. T. (1977) Phosphorylation and dephosphorylation of histone (V (H5): controlled condensation of avian erythrocyte chromatin. Appendix: Phosphorylation and dephosphorylation of histone H5. II. Circular dichroic studies, *Biochemistry 16*, 286-290.
26. Chadee, D. N., Hendzel, M. J., Tylipski, C. P., Allis, C. D., Bazett-Jones, D. P., Wright, J. A., and Davie, J. R. (1999) Increased Ser-10 phosphorylation of histone H3 in mitogen-stimulated and oncogene-transformed mouse fibroblasts, *J Biol Chem 274*, 24914-24920.
27. Thomson, S., Mahadevan, L. C., and Clayton, A. L. (1999) MAP kinase-mediated signalling to nucleosomes and immediate-early gene induction, *Semin Cell Dev Biol 10*, 205-214.
28. Strahl, B. D., and Allis, C. D. (2000) The language of covalent histone modifications, *Nature 403*, 41-45.
29. Araki, Y., Wang, Z., Zang, C., Wood, W. H., 3rd, Schones, D., Cui, K., Roh, T. Y., Lhotsky, B., Wersto, R. P., Peng, W., Becker, K. G., Zhao, K., and Weng, N. P. (2009) Genome-wide analysis of histone methylation reveals chromatin state-based regulation of gene transcription and function of memory CD8+ T cells, *Immunity 30*, 912-925.
30. Tan, J., Lu, J., Huang, W., Dong, Z., Kong, C., Li, L., Gao, L., Guo, J., and Huang, B. (2009) Genome-wide analysis of histone H3 lysine9 modifications in human mesenchymal stem cell osteogenic differentiation, *PLoS One 4*, e6792.

31. Zhang, L., Dai, Y., Peng, W., Lu, J., Zhang, Y., and Wang, L. (2009) Genome-wide analysis of histone H3 lysine 4 trimethylation in peripheral blood mononuclear cells of minimal change nephrotic syndrome patients, *Am J Nephrol 30*, 505-513.
32. Zhang, X., Bernatavichute, Y. V., Cokus, S., Pellegrini, M., and Jacobsen, S. E. (2009) Genome-wide analysis of mono-, di- and trimethylation of histone H3 lysine 4 in Arabidopsis thaliana, *Genome Biol 10*, R62.
33. Mikkelsen, T. S., Ku, M., Jaffe, D. B., Issac, B., Lieberman, E., Giannoukos, G., Alvarez, P., Brockman, W., Kim, T. K., Koche, R. P., Lee, W., Mendenhall, E., O'Donovan, A., Presser, A., Russ, C., Xie, X., Meissner, A., Wernig, M., Jaenisch, R., Nusbaum, C., Lander, E. S., and Bernstein, B. E. (2007) Genome-wide maps of chromatin state in pluripotent and lineage-committed cells, *Nature 448*, 553-560.
34. Bua, D. J., Kuo, A. J., Cheung, P., Liu, C. L., Migliori, V., Espejo, A., Casadio, F., Bassi, C., Amati, B., Bedford, M. T., Guccione, E., and Gozani, O. (2009) Epigenome microarray platform for proteome-wide dissection of chromatin-signaling networks, *PLoS One 4*, e6789.
35. Meersseman, G., Pennings, S. and Bradbury, E. M. (1992) Mobile nucleosomes--a general behavior, *EMBO J 11*, 2951-2959.
36. Flaus, A., Luger, K., Tan, S. and Richmond, T. J. (1996) Mapping nucleosome position at single base-pair resolution by using site-directed hydroxyl radicals, *Proc Natl Acad Sci U S A 93*, 1370-1375.
37. Yang, Z., Zheng, C., and Hayes, J. J. (2007) The core histone tail domains contribute to sequence-dependent nucleosome positioning, *J Biol Chem 282*, 7930-7938.
38. Chung, H. R., and Vingron, M. (2009) Sequence-dependent nucleosome positioning, *J Mol Biol 386*, 1411-1422.
39. Narlikar, G. J., Fan, H. Y., and Kingston, R. E. (2002) Cooperation between complexes that regulate chromatin structure and transcription, *Cell 108*, 475-487.
40. Peterson, C. L., Dingwall, A., and Scott, M. P. (1994) Five SWI/SNF gene products are components of a large multisubunit complex required for transcriptional enhancement, *Proc Natl Acad Sci U S A 91*, 2905-2908.
41. Quinn, J., Fyrberg, A. M., Ganster, R. W., Schmidt, M. C., and Peterson, C. L. (1996) DNA-binding properties of the yeast SWI/SNF complex, *Nature 379*, 844-847.
42. Kruger, W., Peterson, C. L., Sil, A., Coburn, C., Arents, G., Moudrianakis, E. N., and Herskowitz, I. (1995) Amino acid substitutions in the structured domains of histones H3 and H4 partially relieve the requirement of the yeast SWI/SNF complex for transcription, *Genes Dev 9*, 2770-2779.
43. Yudkovsky, N., Logie, C., Hahn, S., and Peterson, C. L. (1999) Recruitment of the SWI/SNF chromatin remodeling complex by transcriptional activators, *Genes Dev 13*, 2369-2374.
44. Armstrong, J. A., Bieker, J. J., and Emerson, B. M. (1998) A SWI/SNF-related chromatin remodeling complex, E-RC1, is required for tissue-specific transcriptional regulation by EKLF in vitro, *Cell 95*, 93-104.
45. Wilson, C. J., Chao, D. M., Imbalzano, A. N., Schnitzler, G. R., Kingston, R. E., and Young, R. A. (1996) RNA polymerase II holoenzyme contains SWI/SNF regulators involved in chromatin remodeling, *Cell 84*, 235-244.
46. Eremenko, T., Granieri, A., and Volpe, P. (1978) Organization, replication and modification of the human genome: differential methylation of two classes of HeLa nuclear DNA separated on Ag+--Cs2SO4 gradients, *Mol Biol Rep 4*, 163-170.

47. Harbers, K., Schnieke, A., Stuhlmann, H., Jahner, D., and Jaenisch, R. (1981) DNA methylation and gene expression: endogenous retroviral genome becomes infectious after molecular cloning, *Proc Natl Acad Sci U S A 78*, 7609-7613.
48. Tan, A. C., Jimeno, A., Lin, S. H., Wheelhouse, J., Chan, F., Solomon, A., Rajeshkumar, N. V., Rubio-Viqueira, B., and Hidalgo, M. (2009) Characterizing DNA methylation patterns in pancreatic cancer genome, *Mol Oncol 3*, 425-438.
49. Cheung, H. H., Lee, T. L., Davis, A. J., Taft, D. H., Rennert, O. M., and Chan, W. Y. (2010) Genome-wide DNA methylation profiling reveals novel epigenetically regulated genes and non-coding RNAs in human testicular cancer, *Br J Cancer 102*, 419-427.
50. Kanai, Y. (2010) Genome-wide DNA methylation profiles in precancerous conditions and cancers, *Cancer Sci 101*, 36-45.
51. Nishiyama, N., Arai, E., Chihara, Y., Fujimoto, H., Hosoda, F., Shibata, T., Kondo, T., Tsukamoto, T., Yokoi, S., Imoto, I., Inazawa, J., Hirohashi, S., and Kanai, Y. (2010) Genome-wide DNA methylation profiles in urothelial carcinomas and urothelia at the precancerous stage, *Cancer Sci 101*, 231-240.
52. Ruike, Y., Imanaka, Y., Sato, F., Shimizu, K., and Tsujimoto, G. (2010) Genome-wide analysis of aberrant methylation in human breast cancer cells using methyl-DNA immunoprecipitation combined with high-throughput sequencing, *BMC Genomics 11*, 137.
53. Kostrewa, D., Zeller, M. E., Armache, K. J., Seizl, M., Leike, K., Thomm, M., and Cramer, P. (2009) RNA polymerase II-TFIIB structure and mechanism of transcription initiation, *Nature 462*, 323-330.
54. Muller, F., Demeny, M. A., and Tora, L. (2007) New problems in RNA polymerase II transcription initiation: matching the diversity of core promoters with a variety of promoter recognition factors, *J Biol Chem 282*, 14685-14689.
55. Juven-Gershon, T., Hsu, J. Y., Theisen, J. W., and Kadonaga, J. T. (2008) The RNA polymerase II core promoter - the gateway to transcription, *Curr Opin Cell Biol 20*, 253-259.
56. Li, J., Wang, J., Nawaz, Z., Liu, J. M., Qin, J., and Wong, J. (2000) Both corepressor proteins SMRT and N-CoR exist in large protein complexes containing HDAC3, *EMBO J 19*, 4342-4350.
57. Xue, Y., Wong, J., Moreno, G. T., Young, M. K., Cote, J., and Wang, W. (1998) NURD, a novel complex with both ATP-dependent chromatin-remodeling and histone deacetylase activities, *Mol Cell 2*, 851-861.
58. Laherty, C. D., Yang, W. M., Sun, J. M., Davie, J. R., Seto, E., and Eisenman, R. N. (1997) Histone deacetylases associated with the mSin3 corepressor mediate mad transcriptional repression, *Cell 89*, 349-356.
59. Zhang, Y., Ng, H. H., Erdjument-Bromage, H., Tempst, P., Bird, A., and Reinberg, D. (1999) Analysis of the NuRD subunits reveals a histone deacetylase core complex and a connection with DNA methylation, *Genes Dev 13*, 1924-1935.
60. Zhang, Y., LeRoy, G., Seelig, H. P., Lane, W. S., and Reinberg, D. (1998) The dermatomyositis-specific autoantigen Mi2 is a component of a complex containing histone deacetylase and nucleosome remodeling activities, *Cell 95*, 279-289.
61. Alland, L., David, G., Shen-Li, H., Potes, J., Muhle, R., Lee, H. C., Hou, H., Jr., Chen, K., and DePinho, R. A. (2002) Identification of mammalian Sds3 as an integral

component of the Sin3/histone deacetylase corepressor complex, *Mol Cell Biol 22*, 2743-2750.
62. McDonel, P., Costello, I., and Hendrich, B. (2009) Keeping things quiet: roles of NuRD and Sin3 co-repressor complexes during mammalian development, *Int J Biochem Cell Biol 41*, 108-116.
63. David, G., Alland, L., Hong, S. H., Wong, C. W., DePinho, R. A., and Dejean, A. (1998) Histone deacetylase associated with mSin3A mediates repression by the acute promyelocytic leukemia-associated PLZF protein, *Oncogene 16*, 2549-2556.
64. Zilfou, J. T., Hoffman, W. H., Sank, M., George, D. L., and Murphy, M. (2001) The corepressor mSin3a interacts with the proline-rich domain of p53 and protects p53 from proteasome-mediated degradation, *Mol Cell Biol 21*, 3974-3985.
65. Ceseña, T., Cui, T., Subramanian, L., Fulton, C., Iñiguez-Lluhí, J., Kwok, R., and Schwartz, J. (2008) Acetylation and deacetylation regulate CCAAT/enhancer binding protein beta at K39 in mediating gene transcription, *Mol Cell Endocrinol. 289*, 94-101.
66. Wiper-Bergeron, N., Wu, D., Pope, L., Schild-Poulter, C., and Hache, R. J. (2003) Stimulation of preadipocyte differentiation by steroid through targeting of an HDAC1 complex, *EMBO J 22*, 2135-2145.
67. Xie, A. Y., and Folk, W. R. (2002) Inhibition of polyomavirus ori-dependent DNA replication by mSin3B, *J Virol 76*, 11809-11818.
68. Rayman, J. B., Takahashi, Y., Indjeian, V. B., Dannenberg, J. H., Catchpole, S., Watson, R. J., te Riele, H., and Dynlacht, B. D. (2002) E2F mediates cell cycle-dependent transcriptional repression in vivo by recruitment of an HDAC1/mSin3B corepressor complex, *Genes Dev 16*, 933-947.
69. Korhonen, P., Tapiola, T., Suuronen, T., and Salminen, A. (1998) Expression of transcriptional repressor protein mSin3A but not mSin3B is induced during neuronal apoptosis, *Biochem Biophys Res Commun 252*, 274-277.
70. Cowley, S. M., Iritani, B. M., Mendrysa, S. M., Xu, T., Cheng, P. F., Yada, J., Liggitt, H. D., and Eisenman, R. N. (2005) The mSin3A chromatin-modifying complex is essential for embryogenesis and T-cell development, *Mol Cell Biol 25*, 6990-7004.
71. Murphy, M., Ahn, J., Walker, K. K., Hoffman, W. H., Evans, R. M., Levine, A. J., and George, D. L. (1999) Transcriptional repression by wild-type p53 utilizes histone deacetylases, mediated by interaction with mSin3a, *Genes Dev 13*, 2490-2501.
72. Tanikawa, J., Nomura, T., Macmillan, E. M., Shinagawa, T., Jin, W., Kokura, K., Baba, D., Shirakawa, M., Gonda, T. J., and Ishii, S. (2004) p53 suppresses c-Myb-induced trans-activation and transformation by recruiting the corepressor mSin3A, *J Biol Chem 279*, 55393-55400.
73. Huang, S., and Brandt, S. J. (2000) mSin3A regulates murine erythroleukemia cell differentiation through association with the TAL1 (or SCL) transcription factor, *Mol Cell Biol 20*, 2248-2259.
74. Somoza, J. R., Skene, R. J., Katz, B. A., Mol, C., Ho, J. D., Jennings, A. J., Luong, C., Arvai, A., Buggy, J. J., Chi, E., Tang, J., Sang, B. C., Verner, E., Wynands, R., Leahy, E. M., Dougan, D. R., Snell, G., Navre, M., Knuth, M. W., Swanson, R. V., McRee, D. E., and Tari, L. W. (2004) Structural snapshots of human HDAC8 provide insights into the class I histone deacetylases, *Structure 12*, 1325-1334.

75. Buggy, J. J., Sideris, M. L., Mak, P., Lorimer, D. D., McIntosh, B., and Clark, J. M. (2000) Cloning and characterization of a novel human histone deacetylase, HDAC8, *Biochem J 350 Pt 1*, 199-205.
76. Mahlknecht, U., Bucala, R., and Verdin, E. (1999) Assignment of the histone deacetylase gene (Hdac3) to mouse chromosome 18B3 by in situ hybridization, *Cytogenet Cell Genet 84*, 192-193.
77. Emiliani, S., Fischle, W., Van Lint, C., Al-Abed, Y., and Verdin, E. (1998) Characterization of a human RPD3 ortholog, HDAC3, *Proc Natl Acad Sci U S A 95*, 2795-2800.
78. Wang, A. H., Bertos, N. R., Vezmar, M., Pelletier, N., Crosato, M., Heng, H. H., Th'ng, J., Han, J., and Yang, X. J. (1999) HDAC4, a human histone deacetylase related to yeast HDA1, is a transcriptional corepressor, *Mol Cell Biol 19*, 7816-7827.
79. Miska, E. A., Karlsson, C., Langley, E., Nielsen, S. J., Pines, J., and Kouzarides, T. (1999) HDAC4 deacetylase associates with and represses the MEF2 transcription factor, *EMBO J 18*, 5099-5107.
80. Lemercier, C., Verdel, A., Galloo, B., Curtet, S., Brocard, M. P., and Khochbin, S. (2000) mHDA1/HDAC5 histone deacetylase interacts with and represses MEF2A transcriptional activity, *J Biol Chem 275*, 15594-15599.
81. Dressel, U., Bailey, P. J., Wang, S. C., Downes, M., Evans, R. M., and Muscat, G. E. (2001) A dynamic role for HDAC7 in MEF2-mediated muscle differentiation, *J Biol Chem 276*, 17007-17013.
82. Haberland, M., Arnold, M. A., McAnally, J., Phan, D., Kim, Y., and Olson, E. N. (2007) Regulation of HDAC9 gene expression by MEF2 establishes a negative-feedback loop in the transcriptional circuitry of muscle differentiation, *Mol Cell Biol 27*, 518-525.
83. Sparling, D. P., Griesel, B. A., Weems, J., and Olson, A. L. (2008) GLUT4 enhancer factor (GEF) interacts with MEF2A and HDAC5 to regulate the GLUT4 promoter in adipocytes, *J Biol Chem 283*, 7429-7437.
84. Haggarty, S. J., Koeller, K. M., Wong, J. C., Grozinger, C. M., and Schreiber, S. L. (2003) Domain-selective small-molecule inhibitor of histone deacetylase 6 (HDAC6)-mediated tubulin deacetylation, *Proc Natl Acad Sci U S A 100*, 4389-4394.
85. Matsuyama, A., Shimazu, T., Sumida, Y., Saito, A., Yoshimatsu, Y., Seigneurin-Berny, D., Osada, H., Komatsu, Y., Nishino, N., Khochbin, S., Horinouchi, S., and Yoshida, M. (2002) In vivo destabilization of dynamic microtubules by HDAC6-mediated deacetylation, *EMBO J 21*, 6820-6831.
86. Hubbert, C., Guardiola, A., Shao, R., Kawaguchi, Y., Ito, A., Nixon, A., Yoshida, M., Wang, X. F., and Yao, T. P. (2002) HDAC6 is a microtubule-associated deacetylase, *Nature 417*, 455-458.
87. Shen, T., Liu, Y., Randall, W. R., and Schneider, M. F. (2006) Parallel mechanisms for resting nucleo-cytoplasmic shuttling and activity dependent translocation provide dual control of transcriptional regulators HDAC and NFAT in skeletal muscle fiber type plasticity, *J Muscle Res Cell Motil 27*, 405-411.
88. Zhou, X., Marks, P. A., Rifkind, R. A., and Richon, V. M. (2001) Cloning and characterization of a histone deacetylase, HDAC9, *Proc Natl Acad Sci U S A 98*, 10572-10577.

89. Gao, L., Cueto, M. A., Asselbergs, F., and Atadja, P. (2002) Cloning and functional characterization of HDAC11, a novel member of the human histone deacetylase family, *J Biol Chem 277*, 25748-25755.
90. Liu, H., Hu, Q., D'Ercole A, J., and Ye, P. (2009) Histone deacetylase 11 regulates oligodendrocyte-specific gene expression and cell development in OL-1 oligodendroglia cells, *Glia 57*, 1-12.
91. Liu, H., Hu, Q., Kaufman, A., D'Ercole, A. J., and Ye, P. (2008) Developmental expression of histone deacetylase 11 in the murine brain, *J Neurosci Res 86*, 537-543.
92. Villagra, A., Cheng, F., Wang, H. W., Suarez, I., Glozak, M., Maurin, M., Nguyen, D., Wright, K. L., Atadja, P. W., Bhalla, K., Pinilla-Ibarz, J., Seto, E., and Sotomayor, E. M. (2009) The histone deacetylase HDAC11 regulates the expression of interleukin 10 and immune tolerance, *Nat Immunol 10*, 92-100.
93. Nagy, Z., and Tora, L. (2007) Distinct GCN5/PCAF-containing complexes function as co-activators and are involved in transcription factor and global histone acetylation, *Oncogene 26*, 5341-5357.
94. Sterner, D. E., and Berger, S. L. (2000) Acetylation of histones and transcription-related factors, *Microbiol Mol Biol Rev 64*, 435-459.
95. Yang, X. J., Ogryzko, V. V., Nishikawa, J., Howard, B. H., and Nakatani, Y. (1996) A p300/CBP-associated factor that competes with the adenoviral oncoprotein E1A, *Nature 382*, 319-324.
96. Li, S., and Shogren-Knaak, M. A. (2009) The Gcn5 bromodomain of the SAGA complex facilitates cooperative and cross-tail acetylation of nucleosomes, *J Biol Chem 284*, 9411-9417.
97. Xu, W., Edmondson, D. G., and Roth, S. Y. (1998) Mammalian GCN5 and P/CAF acetyltransferases have homologous amino-terminal domains important for recognition of nucleosomal substrates, *Mol Cell Biol 18*, 5659-5669.
98. Kuo, M. H., Brownell, J. E., Sobel, R. E., Ranalli, T. A., Cook, R. G., Edmondson, D. G., Roth, S. Y., and Allis, C. D. (1996) Transcription-linked acetylation by Gcn5p of histones H3 and H4 at specific lysines, *Nature 383*, 269-272.
99. Grant, P. A., Eberharter, A., John, S., Cook, R. G., Turner, B. M., and Workman, J. L. (1999) Expanded lysine acetylation specificity of Gcn5 in native complexes, *J Biol Chem 274*, 5895-5900.
100. Martinez, E., Kundu, T. K., Fu, J., and Roeder, R. G. (1998) A human SPT3-TAFII31-GCN5-L acetylase complex distinct from transcription factor IID, *J Biol Chem 273*, 23781-23785.
101. McMahon, S. B., Van Buskirk, H. A., Dugan, K. A., Copeland, T. D., and Cole, M. D. (1998) The novel ATM-related protein TRRAP is an essential cofactor for the c-Myc and E2F oncoproteins, *Cell 94*, 363-374.
102. McMahon, S. B., Wood, M. A., and Cole, M. D. (2000) The essential cofactor TRRAP recruits the histone acetyltransferase hGCN5 to c-Myc, *Mol Cell Biol 20*, 556-562.
103. Liu, L., Scolnick, D. M., Trievel, R. C., Zhang, H. B., Marmorstein, R., Halazonetis, T. D., and Berger, S. L. (1999) p53 sites acetylated in vitro by PCAF and p300 are acetylated in vivo in response to DNA damage, *Mol Cell Biol 19*, 1202-1209.
104. Dilworth, F. J., Seaver, K. J., Fishburn, A. L., Htet, S. L., and Tapscott, S. J. (2004) In vitro transcription system delineates the distinct roles of the coactivators pCAF

and p300 during MyoD/E47-dependent transactivation, *Proc Natl Acad Sci U S A 101*, 11593-11598.
105. Sartorelli, V., Puri, P. L., Hamamori, Y., Ogryzko, V., Chung, G., Nakatani, Y., Wang, J. Y., and Kedes, L. (1999) Acetylation of MyoD directed by PCAF is necessary for the execution of the muscle program, *Mol Cell 4*, 725-734.
106. Wiper-Bergeron, N., Salem, H. A., Tomlinson, J. J., Wu, D., and Hache, R. J. (2007) Glucocorticoid-stimulated preadipocyte differentiation is mediated through acetylation of C/EBPbeta by GCN5, *Proc Natl Acad Sci U S A 104*, 2703-2708.
107. Jacob, A. L., Lund, J., Martinez, P., and Hedin, L. (2001) Acetylation of steroidogenic factor 1 protein regulates its transcriptional activity and recruits the coactivator GCN5, *J Biol Chem 276*, 37659-37664.
108. Kelly, T. J., Lerin, C., Haas, W., Gygi, S. P., and Puigserver, P. (2009) GCN5-mediated transcriptional control of the metabolic coactivator PGC-1beta through lysine acetylation, *J Biol Chem 284*, 19945-19952.
109. Xu, W., Edmondson, D. G., Evrard, Y. A., Wakamiya, M., Behringer, R. R., and Roth, S. Y. (2000) Loss of Gcn5l2 leads to increased apoptosis and mesodermal defects during mouse development, *Nat Genet 26*, 229-232.
110. Maurice, T., Duclot, F., Meunier, J., Naert, G., Givalois, L., Meffre, J., Celerier, A., Jacquet, C., Copois, V., Mechti, N., Ozato, K., and Gongora, C. (2008) Altered memory capacities and response to stress in p300/CBP-associated factor (PCAF) histone acetylase knockout mice, *Neuropsychopharmacology 33*, 1584-1602.
111. Duclot, F., Meffre, J., Jacquet, C., Gongora, C., and Maurice, T. (2010) Mice knock out for the histone acetyltransferase p300/CREB binding protein-associated factor develop a resistance to amyloid toxicity, *Neuroscience*.
112. Samad, F., Yamamoto, K., and Loskutoff, D. J. (1996) Distribution and regulation of plasminogen activator inhibitor-1 in murine adipose tissue in vivo. Induction by tumor necrosis factor-alpha and lipopolysaccharide, *J Clin Invest 97*, 37-46.
113. Hotamisligil, G. S., Shargill, N. S., and Spiegelman, B. M. (1993) Adipose expression of tumor necrosis factor-alpha: direct role in obesity-linked insulin resistance, *Science 259*, 87-91.
114. Zhang, Y., Proenca, R., Maffei, M., Barone, M., Leopold, L., and Friedman, J. M. (1994) Positional cloning of the mouse obese gene and its human homologue, *Nature 372*, 425-432.
115. Pantanetti, P., Garrapa, G. G., Mantero, F., Boscaro, M., Faloia, E., and Venarucci, D. (2004) Adipose tissue as an endocrine organ? A review of recent data related to cardiovascular complications of endocrine dysfunctions, *Clin Exp Hypertens 26*, 387-398.
116. Cinti, S. (2006) The role of brown adipose tissue in human obesity, *Nutr Metab Cardiovasc Dis 16*, 569-574.
117. Green H, a. K. O. (1974) Sublines of mouse 3T3 cells that accumulate lipid, *Cell 1*, 113-116.
118. Green, H., and Kehinde, O. (1979) Formation of normally differentiated subcutaneous fat pads by an established preadipose cell line, *J Cell Physiol 101*, 169-171.
119. Gregoire, F. M., Smas, C. M., and Sul, H. S. (1998) Understanding adipocyte differentiation, *Physiol Rev 78*, 783-809.

120. Tomlinson, J. J., Boudreau, A., Wu, D., Atlas, E., and Hache, R. J. (2006) Modulation of early human preadipocyte differentiation by glucocorticoids, *Endocrinology 147*, 5284-5293.
121. Student, A. K., Hsu, R. Y., and Lane, M. D. (1980) Induction of fatty acid synthetase synthesis in differentiating 3T3-L1 preadipocytes, *J Biol Chem 255*, 4745-4750.
122. Yeh, W. C., Bierer, B. E., and McKnight, S. L. (1995) Rapamycin inhibits clonal expansion and adipogenic differentiation of 3T3-L1 cells, *Proc Natl Acad Sci U S A 92*, 11086-11090.
123. Patel, Y. M., and Lane, M. D. (2000) Mitotic clonal expansion during preadipocyte differentiation: calpain-mediated turnover of p27, *J Biol Chem 275*, 17653-17660.
124. Tang, Q. Q., Otto, T. C., and Lane, M. D. (2003) Mitotic clonal expansion: a synchronous process required for adipogenesis, *Proc Natl Acad Sci U S A 100*, 44-49.
125. Karschner, V. A., and Pekala, P. H. (2009) HuR involvement in mitotic clonal expansion during acquisition of the adipocyte phenotype, *Biochem Biophys Res Commun 383*, 203-205.
126. Habinowski, S. A., and Witters, L. A. (2001) The effects of AICAR on adipocyte differentiation of 3T3-L1 cells, *Biochem Biophys Res Commun 286*, 852-856.
127. Qiu, Z., Wei, Y., Chen, N., Jiang, M., Wu, J., and Liao, K. (2001) DNA synthesis and mitotic clonal expansion is not a required step for 3T3-L1 preadipocyte differentiation into adipocytes, *J Biol Chem 276*, 11988-11995.
128. Girard, J., Perdereau, D., Foufelle, F., Prip-Buus, C., and Ferre, P. (1994) Regulation of lipogenic enzyme gene expression by nutrients and hormones, *FASEB J 8*, 36-42.
129. Foufelle, F., Girard, J., and Ferre, P. (1996) Regulation of lipogenic enzyme expression by glucose in liver and adipose tissue: a review of the potential cellular and molecular mechanisms, *Adv Enzyme Regul 36*, 199-226.
130. Benito, M., Porras, A., Nebreda, A. R., and Santos, E. (1991) Differentiation of 3T3-L1 fibroblasts to adipocytes induced by transfection of ras oncogenes, *Science 253*, 565-568.
131. Porras, A., and Santos, E. (1996) The insulin/Ras pathway of adipocytic differentiation of 3T3 L1 cells: dissociation between Raf-1 kinase and the MAPK/RSK cascade, *Int J Obes Relat Metab Disord 20 Suppl 3*, S43-51.
132. Reusch, J. E., Colton, L. A., and Klemm, D. J. (2000) CREB activation induces adipogenesis in 3T3-L1 cells, *Mol Cell Biol 20*, 1008-1020.
133. Niehof, M., Kubicka, S., Zender, L., Manns, M. P., and Trautwein, C. (2001) Autoregulation enables different pathways to control CCAAT/enhancer binding protein beta (C/EBP beta) transcription, *J Mol Biol 309*, 855-868.
134. Belmonte, N., Phillips, B. W., Massiera, F., Villageois, P., Wdziekonski, B., Saint-Marc, P., Nichols, J., Aubert, J., Saeki, K., Yuo, A., Narumiya, S., Ailhaud, G., and Dani, C. (2001) Activation of extracellular signal-regulated kinases and CREB/ATF-1 mediate the expression of CCAAT/enhancer binding proteins beta and -delta in preadipocytes, *Mol Endocrinol 15*, 2037-2049.
135. Cui, T. X., Kwok, R., and Schwartz, J. (2008) Cooperative regulation of endogenous cAMP-response element binding protein and CCAAT/enhancer-binding protein beta in GH-stimulated c-fos expression, *J Endocrinol 196*, 89-100.
136. Smas, C. M., Chen, L., Zhao, L., Latasa, M. J., and Sul, H. S. (1999) Transcriptional repression of pref-1 by glucocorticoids promotes 3T3-L1 adipocyte differentiation, *J Biol Chem 274*, 12632-12641.

137. Cao, Z., Umek, R. M., and McKnight, S. L. (1991) Regulated expression of three C/EBP isoforms during adipose conversion of 3T3-L1 cells, *Genes Dev 5*, 1538-1552.
138. Boruk, M., Savory, J. G., and Hache, R. J. (1998) AF-2-dependent potentiation of CCAAT enhancer binding protein beta-mediated transcriptional activation by glucocorticoid receptor, *Mol Endocrinol 12*, 1749-1763.
139. Wu, Z., Bucher NLR and Farmer SR. (1995) Conditional ectopic expression of C/EBPb in NIH-3T3 cells induces PPARg and stimulates adipogenesis, *Genes & Development 9*, 2350-2363.
140. Yeh, W., Cao, Z., Classon, M., and McKnight, S. L. (1995) Cascade regulation of terminal adipocyte differentiation by three members of the C/EBP family of leucine zipper proteins, *Genes Dev 9*, 168-181.
141. Freytag, S. O., Paielli, D. L., and Gilbert, J. D. (1994) Ectopic expression of the CCAAT/enhancer-binding protein alpha promotes the adipogenic program in a variety of mouse fibroblastic cells, *Genes Dev 8*, 1654-1663.
142. Okuno, M., Arimoto, E., Nishizuka, M., Nishihara, T., and Imagawa, M. (2002) Isolation of up- or down-regulated genes in PPARgamma-expressing NIH-3T3 cells during differentiation into adipocytes, *FEBS Lett 519*, 108-112.
143. Wu, Z., Xie, Y., Morrison, R. F., Bucher, N. L., and Farmer, S. R. (1998) PPARgamma induces the insulin-dependent glucose transporter GLUT4 in the absence of C/EBPalpha during the conversion of 3T3 fibroblasts into adipocytes, *J Clin Invest 101*, 22-32.
144. Darlington, G. J., Ross, S. E. and MacDougald, O. A. (1998) The role of C/EBP genes in adipocyte differentiation, *J Biol Chem 273*, 30057-30060.
145. Wu, Z., Rosen, E. D., Brun, R., Hauser, S., Adelmant, G., Troy, A. E., McKeon, C., Darlington, G. J., and Spiegelman, B. M. (1999) Cross-regulation of C/EBP alpha and PPAR gamma controls the transcriptional pathway of adipogenesis and insulin sensitivity, *Mol Cell 3*, 151-158.
146. Tanaka, T., Yoshida, N., Kishimoto, T., and Akira, S. (1997) Defective adipocyte differentiation in mice lacking the C/EBPbeta and/or C/EBPdelta gene, *EMBO J 16*, 7432-7443.
147. Millward, C. A., Heaney, J. D., Sinasac, D. S., Chu, E. C., Bederman, I. R., Gilge, D. A., Previs, S. F., and Croniger, C. M. (2007) Mice with a deletion in the gene for CCAAT/enhancer-binding protein beta are protected against diet-induced obesity, *Diabetes 56*, 161-167.
148. Schroeder-Gloeckler, J. M., Rahman, S. M., Janssen, R. C., Qiao, L., Shao, J., Roper, M., Fischer, S. J., Lowe, E., Orlicky, D. J., McManaman, J. L., Palmer, C., Gitomer, W. L., Huang, W., O'Doherty, R. M., Becker, T. C., Klemm, D. J., Jensen, D. R., Pulawa, L. K., Eckel, R. H., and Friedman, J. E. (2007) CCAAT/enhancer-binding protein beta deletion reduces adiposity, hepatic steatosis, and diabetes in Lepr(db/db) mice, *J Biol Chem 282*, 15717-15729.
149. Wang, N. D., Finegold, M. J., Bradley, A., Ou, C. N., Abdelsayed, S. V., Wilde, M. D., Taylor, L. R., Wilson, D. R., and Darlington, G. J. (1995) Impaired energy homeostasis in C/EBP alpha knockout mice, *Science 269*, 1108-1112.
150. Barak, Y., Nelson, M. C., Ong, E. S., Jones, Y. Z., Ruiz-Lozano, P., Chien, K. R., Koder, A., and Evans, R. M. (1999) PPAR gamma is required for placental, cardiac, and adipose tissue development, *Mol Cell 4*, 585-595.

151. Rosen, E. D., Sarraf, P., Troy, A. E., Bradwin, G., Moore, K., Milstone, D. S., Spiegelman, B. M., and Mortensen, R. M. (1999) PPAR gamma is required for the differentiation of adipose tissue in vivo and in vitro, *Mol Cell 4*, 611-617.
152. Tanq, Q., et Lane M.D. (1999) Activation and centromeric localization of CCAAT/enhancer-binding proteins during the mitotic clonal expansion of adipocyte differentiation., *Genes & Development 13*, 2231-2241.
153. Tang, Q., Lane MD. (2000) Role of C/EBP homologous protein (CHOP-10) in the programmed activation of CCAAT/enhancer-binding protein-beta during adipogenesis., *PNAS 97*, 12446-12450.
154. Tanabe, A., Kumahara, C., Osada, S., Nishihara, T., and Imagawa, M. (2000) Gene expression of CCAAT/enhancer-binding protein delta mediated by autoregulation is repressed by related gene family proteins, *Biol Pharm Bull 23*, 1424-1429.
155. Ron, D., and Habener, J. F. (1992) CHOP, a novel developmentally regulated nuclear protein that dimerizes with transcription factors C/EBP and LAP and functions as a dominant-negative inhibitor of gene transcription, *Genes Dev 6*, 439-453.
156. Tang, Q., Grønborg M., Huang H, Kim JW, Otto TC, Pandey A et Lane M.D. (2005) Sequential phosphorylation of CCAAT enhancer-binding protein beta by MAPK and glycogen synthase kinase 3 beta is required for adipogenesis., *PNAS 102*, 9766-9771.
157. Park, B. H., Qiang, L., and Farmer, S. R. (2004) Phosphorylation of C/EBPbeta at a consensus extracellular signal-regulated kinase/glycogen synthase kinase 3 site is required for the induction of adiponectin gene expression during the differentiation of mouse fibroblasts into adipocytes, *Mol Cell Biol 24*, 8671-8680.
158. Williams, S. C., Baer M, Dillner A. J. et Johnson P. F. (1995) CRP2 (C/EBP beta) contains a bipartite regulatory domain that controls transcriptional activation, DNA binding and cell specificity, *EMBO J 14*, 3170-3183.
159. Kim, J., Tang QQ, Li X, Lane MD. (2007) Effect of phosphorylation and S-S bond-induced dimerization on DNA binding and transcriptional activation by C/EBPbeta., *PNAS 104*, 1800-1804.
160. Cherry, J., Jones, H., Karschner, V. A., and Pekala, P. H. (2008) Post-transcriptional control of CCAAT/enhancer-binding protein beta (C/EBPbeta) expression: formation of a nuclear HuR-C/EBPbeta mRNA complex determines the amount of message reaching the cytosol, *J Biol Chem 283*, 30812-30820.
161. Tang, Q. Q., Otto, T. C., and Lane, M. D. (2003) CCAAT/enhancer-binding protein beta is required for mitotic clonal expansion during adipogenesis, *Proc Natl Acad Sci U S A 100*, 850-855.
162. Zhang, J. W., Tang, Q. Q., Vinson, C., and Lane, M. D. (2004) Dominant-negative C/EBP disrupts mitotic clonal expansion and differentiation of 3T3-L1 preadipocytes, *Proc Natl Acad Sci U S A 101*, 43-47.
163. Li, X., Huang, H. Y., Chen, J. G., Jiang, L., Liu, H. L., Liu, D. G., Song, T. J., He, Q., Ma, C. G., Ma, D., Song, H. Y., and Tang, Q. Q. (2006) Lactacystin inhibits 3T3-L1 adipocyte differentiation through induction of CHOP-10 expression, *Biochem Biophys Res Commun 350*, 1-6.
164. Li, X., Kim, J. W., Gronborg, M., Urlaub, H., Lane, M. D., and Tang, Q. Q. (2007) Role of cdk2 in the sequential phosphorylation/activation of C/EBPbeta during adipocyte differentiation, *Proc Natl Acad Sci U S A 104*, 11597-11602.

165. Gao, Y., Zhou, Y., Xu, A., and Wu, D. (2008) Effects of an AMP-activated protein kinase inhibitor, compound C, on adipogenic differentiation of 3T3-L1 cells, *Biol Pharm Bull 31*, 1716-1722.
166. Lee, H., Lee, Y. J., Choi, H., Ko, E. H. and Kim, J. W. (2009) Reactive oxygen species facilitate adipocyte differentiation by accelerating mitotic clonal expansion, *J Biol Chem 284*, 10601-10609.
167. Hishida, T., Nishizuka, M., Osada, S., and Imagawa, M. (2009) The role of C/EBPdelta in the early stages of adipogenesis, *Biochimie 91*, 654-657.
168. Soriano, H. E., Kang, D. C., Finegold, M. J., Hicks, M. J., Wang, N. D., Harrison, W., and Darlington, G. J. (1998) Lack of C/EBP alpha gene expression results in increased DNA synthesis and an increased frequency of immortalization of freshly isolated mice [correction of rat] hepatocytes, *Hepatology 27*, 392-401.
169. Sugahara, K., Iyama, K. I., Kimura, T., Sano, K., Darlington, G. J., Akiba, T., and Takiguchi, M. (2001) Mice lacking CCAAt/enhancer-binding protein-alpha show hyperproliferation of alveolar type II cells and increased surfactant protein mRNAs, *Cell Tissue Res 306*, 57-63.
170. Umek, R. M., Friedman, A. D., and McKnight, S. L. (1991) CCAAT-enhancer binding protein: a component of a differentiation switch, *Science 251*, 288-292.
171. Clarke, S. L., Robinson, C. E., and Gimble, J. M. (1997) CAAT/enhancer binding proteins directly modulate transcription from the peroxisome proliferator-activated receptor gamma 2 promoter, *Biochem Biophys Res Commun 240*, 99-103.
172. Elberg, G., Gimble JM and Tsai SY. (2000) Modulation of the murine peroxisome proliferator-activated receptor y2 promoter by CCAAT/Enhancer-binding proteins, *The Journal of Biological Chemistry 275*, 27815-27822.
173. Hamm, J., Park BH and Farmer SR. (2001) A role for C/EBPbeta in regulating peroxisome proliferator-activated receptor gamma activity during adipogenesis in 3T3-L1 preadipocytes., *J Biol Chem. 276*, 18464-18471.
174. Tang, Q., Zhang JW and Lane MD. (2004) Sequential gene promoter interaction by C/EBPb, C/EBPa and PPARg during adipogenesis, *Biochemical and Biophysical Research Communication 318*, 213-218.
175. Wu, Z., Bucher NLR and Farmer SR. (1996) Induction of peroxisome proliferator-activated receptor g during the conversion of 3T3 fibroblasts into adipocytes is mediated by C/EBPb, C/EBPd and glucocorticoids, *Molecular and Cellular Biology 16*, 4128-4136.
176. Oishi, Y., Manabe, I., Tobe, K., Tsushima, K., Shindo, T., Fujiu, K., Nishimura, G., Maemura, K., Yamauchi, T., Kubota, N., Suzuki, R., Kitamura, T., Akira, S., Kadowaki, T., and Nagai, R. (2005) Kruppel-like transcription factor KLF5 is a key regulator of adipocyte differentiation, *Cell Metab 1*, 27-39.
177. Hunt, C. R., Ro, J. H., Dobson, D. E., Min, H. Y., and Spiegelman, B. M. (1986) Adipocyte P2 gene: developmental expression and homology of 5'-flanking sequences among fat cell-specific genes, *Proc Natl Acad Sci U S A 83*, 3786-3790.
178. Christy, R. J., Yang, V. W., Ntambi, J. M., Geiman, D. E., Landschulz, W. H., Friedman, A. D., Nakabeppu, Y., Kelly, T. J., and Lane, M. D. (1989) Differentiation-induced gene expression in 3T3-L1 preadipocytes: CCAAT/enhancer binding protein interacts with and activates the promoters of two adipocyte-specific genes, *Genes Dev 3*, 1323-1335.

179. Mason, M. M., He, Y., Chen, H., Quon, M. J., and Reitman, M. (1998) Regulation of leptin promoter function by Sp1, C/EBP, and a novel factor, *Endocrinology 139*, 1013-1022.
180. Gustafson, B., Jack, M. M., Cushman, S. W., and Smith, U. (2003) Adiponectin gene activation by thiazolidinediones requires PPAR gamma 2, but not C/EBP alpha-evidence for differential regulation of the aP2 and adiponectin genes, *Biochem Biophys Res Commun 308*, 933-939.
181. Koshiishi, C., Park, H. M., Uchiyama, H., and Tanaka, Y. (2008) Regulation of expression of the mouse adiponectin gene by the C/EBP family via a novel enhancer region, *Gene 424*, 141-146.
182. Kockar, F. T., Foka, P., Hughes, T. R., Kousteni, S., and Ramji, D. P. (2001) Analysis of the Xenopus laevis CCAAT-enhancer binding protein alpha gene promoter demonstrates species-specific differences in the mechanisms for both auto-activation and regulation by Sp1, *Nucleic Acids Res 29*, 362-372.
183. Lin, F. T., and Lane, M. D. (1994) CCAAT/enhancer binding protein alpha is sufficient to initiate the 3T3-L1 adipocyte differentiation program, *Proc Natl Acad Sci U S A 91*, 8757-8761.
184. Brun, R. P., Tontonoz, P., Forman, B. M., Ellis, R., Chen, J., Evans, R. M., and Spiegelman, B. M. (1996) Differential activation of adipogenesis by multiple PPAR isoforms, *Genes Dev 10*, 974-984.
185. El-Jack, A. K., Hamm, J. K., Pilch, P. F., and Farmer, S. R. (1999) Reconstitution of insulin-sensitive glucose transport in fibroblasts requires expression of both PPARgamma and C/EBPalpha, *J Biol Chem 274*, 7946-7951.
186. Lefterova, M. I., Zhang, Y., Steger, D. J., Schupp, M., Schug, J., Cristancho, A., Feng, D., Zhuo, D., Stoeckert, C. J., Jr., Liu, X. S., and Lazar, M. A. (2008) PPARgamma and C/EBP factors orchestrate adipocyte biology via adjacent binding on a genome-wide scale, *Genes Dev 22*, 2941-2952.
187. Landschulz, W. H., Johnson, P. F., Adashi, E. Y., Graves, B. J., and McKnight, S. L. (1988) Isolation of a recombinant copy of the gene encoding C/EBP, *Genes Dev 2*, 786-800.
188. Landschulz, W. H., Johnson, P. F., and McKnight, S. L. (1989) The DNA binding domain of the rat liver nuclear protein C/EBP is bipartite, *Science 243*, 1681-1688.
189. Shuman, J. D., Vinson, C. R., and McKnight, S. L. (1990) Evidence of changes in protease sensitivity and subunit exchange rate on DNA binding by C/EBP, *Science 249*, 771-774.
190. Vinson, C. R., Sigler, P. B., and McKnight, S. L. (1989) Scissors-grip model for DNA recognition by a family of leucine zipper proteins, *Science 246*, 911-916.
191. Herrera, R., Ro, H. S., Robinson, G. S., Xanthopoulos, K. G., and Spiegelman, B. M. (1989) A direct role for C/EBP and the AP-I-binding site in gene expression linked to adipocyte differentiation, *Mol Cell Biol 9*, 5331-5339.
192. Akira, S., Isshiki, H., Sugita, T., Tanabe, O., Kinoshita, S., Nishio, Y., Nakajima, T., Hirano, T., and Kishimoto, T. (1990) A nuclear factor for IL-6 expression (NF-IL6) is a member of a C/EBP family, *EMBO J 9*, 1897-1906.
193. Isshiki, H., Akira, S., Sugita, T., Nishio, Y., Hashimoto, S., Pawlowski, T., Suematsu, S., and Kishimoto, T. (1991) Reciprocal expression of NF-IL6 and C/EBP in hepatocytes: possible involvement of NF-IL6 in acute phase protein gene expression, *New Biol 3*, 63-70.

194. Chang, C. J., Chen, T. T., Lei, H. Y., Chen, D. S., and Lee, S. C. (1990) Molecular cloning of a transcription factor, AGP/EBP, that belongs to members of the C/EBP family, *Mol Cell Biol 10*, 6642-6653.
195. Descombes, P., Chojkier, M., Lichtsteiner, S., Falvey, E., and Schibler, U. (1990) LAP, a novel member of the C/EBP gene family, encodes a liver-enriched transcriptional activator protein, *Genes Dev 4*, 1541-1551.
196. Roman, C., Platero, J. S., Shuman, J., and Calame, K. (1990) Ig/EBP-1: a ubiquitously expressed immunoglobulin enhancer binding protein that is similar to C/EBP and heterodimerizes with C/EBP, *Genes Dev 4*, 1404-1415.
197. Williams, S. C., Cantwell, C. A., and Johnson, P. F. (1991) A family of C/EBP-related proteins capable of forming covalently linked leucine zipper dimers in vitro, *Genes Dev 5*, 1553-1567.
198. Luethy, J. D., Fargnoli, J., Park, J. S., Fornace, A. J., Jr., and Holbrook, N. J. (1990) Isolation and characterization of the hamster gadd153 gene. Activation of promoter activity by agents that damage DNA, *J Biol Chem 265*, 16521-16526.
199. Vinson, C., Acharya, A., and Taparowsky, E. J. (2006) Deciphering B-ZIP transcription factor interactions in vitro and in vivo, *Biochim Biophys Acta 1759*, 4-12.
200. Hsu, W., Kerppola, T. K., Chen, P. L., Curran, T., and Chen-Kiang, S. (1994) Fos and Jun repress transcription activation by NF-IL6 through association at the basic zipper region, *Mol Cell Biol 14*, 268-276.
201. Tominaga, H., Maeda, S., Hayashi, M., Takeda, S., Akira, S., Komiya, S., Nakamura, T., Akiyama, H., and Imamura, T. (2008) CCAAT/enhancer-binding protein beta promotes osteoblast differentiation by enhancing Runx2 activity with ATF4, *Mol Biol Cell 19*, 5373-5386.
202. Umesono, K., Murakami, K. K., Thompson, C. C., and Evans, R. M. (1991) Direct repeats as selective response elements for the thyroid hormone, retinoic acid, and vitamin D3 receptors, *Cell 65*, 1255-1266.
203. Leid, M., Kastner, P., Lyons, R., Nakshatri, H., Saunders, M., Zacharewski, T., Chen, J. Y., Staub, A., Garnier, J. M., Mader, S., and et al. (1992) Purification, cloning, and RXR identity of the HeLa cell factor with which RAR or TR heterodimerizes to bind target sequences efficiently, *Cell 68*, 377-395.
204. Tontonoz, P., Graves, R. A., Budavari, A. I., Erdjument-Bromage, H., Lui, M., Hu, E., Tempst, P., and Spiegelman, B. M. (1994) Adipocyte-specific transcription factor ARF6 is a heterodimeric complex of two nuclear hormone receptors, PPAR gamma and RXR alpha, *Nucleic Acids Res 22*, 5628-5634.
205. Tontonoz, P., Hu, E., Graves, R. A., Budavari, A. I., and Spiegelman, B. M. (1994) mPPAR gamma 2: tissue-specific regulator of an adipocyte enhancer, *Genes Dev 8*, 1224-1234.
206. Desvergne, B., and Wahli, W. (1999) Peroxisome proliferator-activated receptors: nuclear control of metabolism, *Endocr Rev 20*, 649-688.
207. Fajas, L., Auboeuf, D., Raspe, E., Schoonjans, K., Lefebvre, A. M., Saladin, R., Najib, J., Laville, M., Fruchart, J. C., Deeb, S., Vidal-Puig, A., Flier, J., Briggs, M. R., Staels, B., Vidal, H., and Auwerx, J. (1997) The organization, promoter analysis, and expression of the human PPARgamma gene, *J Biol Chem 272*, 18779-18789.
208. Zhu, Y., Qi, C., Korenberg, J. R., Chen, X. N., Noya, D., Rao, M. S., and Reddy, J. K. (1995) Structural organization of mouse peroxisome proliferator-activated

receptor gamma (mPPAR gamma) gene: alternative promoter use and different splicing yield two mPPAR gamma isoforms, *Proc Natl Acad Sci U S A 92*, 7921-7925.
209. Auboeuf, D., Rieusset, J., Fajas, L., Vallier, P., Frering, V., Riou, J. P., Staels, B., Auwerx, J., Laville, M., and Vidal, H. (1997) Tissue distribution and quantification of the expression of mRNAs of peroxisome proliferator-activated receptors and liver X receptor-alpha in humans: no alteration in adipose tissue of obese and NIDDM patients, *Diabetes 46*, 1319-1327.
210. Tontonoz, P., Hu, E., and Spiegelman, B. M. (1994) Stimulation of adipogenesis in fibroblasts by PPAR gamma 2, a lipid-activated transcription factor, *Cell 79*, 1147-1156.
211. Chrousos, G. P., and Kino, T. (2005) Intracellular glucocorticoid signaling: a formerly simple system turns stochastic, *Sci STKE 2005*, pe48.
212. Nakamura, A., Kohsaka, T., Jin, D., and Kobayashi, N. (1992) Influence of glucocorticoid, aspirin, and gamma globulin on interleukin-6 production in the hepatoma cell line, *Immunopharmacology 24*, 31-36.
213. Kimberly, R. P. (1992) Glucocorticoid therapy for rheumatic diseases, *Curr Opin Rheumatol 4*, 325-331.
214. Wu, W., Chaudhuri, S., Brickley, D. R., Pang, D., Karrison, T., and Conzen, S. D. (2004) Microarray analysis reveals glucocorticoid-regulated survival genes that are associated with inhibition of apoptosis in breast epithelial cells, *Cancer Res 64*, 1757-1764.
215. Adcock, I. M., Nasuhara, Y., Stevens, D. A., and Barnes, P. J. (1999) Ligand-induced differentiation of glucocorticoid receptor (GR) trans-repression and transactivation: preferential targetting of NF-kappaB and lack of I-kappaB involvement, *Br J Pharmacol 127*, 1003-1011.
216. Kim, J. B., Ju, J. Y., Kim, J. H., Kim, T. Y., Yang, B. H., Lee, Y. S., and Son, H. (2004) Dexamethasone inhibits proliferation of adult hippocampal neurogenesis in vivo and in vitro, *Brain Res 1027*, 1-10.
217. Derfoul, A., Perkins, G. L., Hall, D. J., and Tuan, R. S. (2006) Glucocorticoids promote chondrogenic differentiation of adult human mesenchymal stem cells by enhancing expression of cartilage extracellular matrix genes, *Stem Cells 24*, 1487-1495.
218. Sundberg, M., Savola, S., Hienola, A., Korhonen, L., and Lindholm, D. (2006) Glucocorticoid hormones decrease proliferation of embryonic neural stem cells through ubiquitin-mediated degradation of cyclin D1, *J Neurosci 26*, 5402-5410.
219. Schmid, W., Cole, T. J., Blendy, J. A., and Schutz, G. (1995) Molecular genetic analysis of glucocorticoid signalling in development, *J Steroid Biochem Mol Biol 53*, 33-35.
220. Neri, G., Malendowicz, L. K., Andreis, P., and Nussdorfer, G. G. (1993) Thyrotropin-releasing hormone inhibits glucocorticoid secretion of rat adrenal cortex: in vivo and in vitro studies, *Endocrinology 133*, 511-514.
221. Becker, P. B., Gloss, B., Schmid, W., Strahle, U., and Schutz, G. (1986) In vivo protein-DNA interactions in a glucocorticoid response element require the presence of the hormone, *Nature 324*, 686-688.

222. Langer, S. J., and Ostrowski, M. C. (1988) Negative regulation of transcription in vitro by a glucocorticoid response element is mediated by a trans-acting factor, *Mol Cell Biol 8*, 3872-3881.
223. Sakai, D. D., Helms, S., Carlstedt-Duke, J., Gustafsson, J. A., Rottman, F. M., and Yamamoto, K. R. (1988) Hormone-mediated repression: a negative glucocorticoid response element from the bovine prolactin gene, *Genes Dev 2*, 1144-1154.
224. Weinberger, C., Hollenberg, S. M., Rosenfeld, M. G., and Evans, R. M. (1985) Domain structure of human glucocorticoid receptor and its relationship to the v-erb-A oncogene product, *Nature 318*, 670-672.
225. Carlstedt-Duke, J., Stromstedt, P. E., Wrange, O., Bergman, T., Gustafsson, J. A., and Jornvall, H. (1987) Domain structure of the glucocorticoid receptor protein, *Proc Natl Acad Sci U S A 84*, 4437-4440.
226. Danielian, P. S., White, R., Lees, J. A., and Parker, M. G. (1992) Identification of a conserved region required for hormone dependent transcriptional activation by steroid hormone receptors, *EMBO J 11*, 1025-1033.
227. Hollenberg, S. M., Weinberger, C., Ong, E. S., Cerelli, G., Oro, A., Lebo, R., Thompson, E. B., Rosenfeld, M. G., and Evans, R. M. (1985) Primary structure and expression of a functional human glucocorticoid receptor cDNA, *Nature 318*, 635-641.
228. Drouin, J., Sun, Y. L., Tremblay, S., Lavender, P., Schmidt, T. J., de Lean, A., and Nemer, M. (1992) Homodimer formation is rate-limiting for high affinity DNA binding by glucocorticoid receptor, *Mol Endocrinol 6*, 1299-1309.
229. Wallberg, A. E., Flinn, E. M., Gustafsson, J. A., and Wright, A. P. (2000) Recruitment of chromatin remodelling factors during gene activation via the glucocorticoid receptor N-terminal domain, *Biochem Soc Trans 28*, 410-414.
230. Wallberg, A. E., Neely, K. E., Hassan, A. H., Gustafsson, J. A., Workman, J. L., and Wright, A. P. (2000) Recruitment of the SWI-SNF chromatin remodeling complex as a mechanism of gene activation by the glucocorticoid receptor tau1 activation domain, *Mol Cell Biol 20*, 2004-2013.
231. Grenier, J., Trousson, A., Chauchereau, A., Cartaud, J., Schumacher, M., and Massaad, C. (2006) Differential recruitment of p160 coactivators by glucocorticoid receptor between Schwann cells and astrocytes, *Mol Endocrinol 20*, 254-267.
232. Grenier, J., Trousson, A., Chauchereau, A., Amazit, L., Lamirand, A., Leclerc, P., Guiochon-Mantel, A., Schumacher, M., and Massaad, C. (2004) Selective recruitment of p160 coactivators on glucocorticoid-regulated promoters in Schwann cells, *Mol Endocrinol 18*, 2866-2879.
233. Chang, C. J., Chen, Y. L., and Lee, S. C. (1998) Coactivator TIF1beta interacts with transcription factor C/EBPbeta and glucocorticoid receptor to induce alpha1-acid glycoprotein gene expression, *Mol Cell Biol 18*, 5880-5887.
234. Meyer, T., Gustafsson, J. A., and Carlstedt-Duke, J. (1997) Glucocorticoid-dependent transcriptional repression of the osteocalcin gene by competitive binding at the TATA box, *DNA Cell Biol 16*, 919-927.
235. Scott, D. K., Stromstedt, P. E., Wang, J. C., and Granner, D. K. (1998) Further characterization of the glucocorticoid response unit in the phosphoenolpyruvate carboxykinase gene. The role of the glucocorticoid receptor-binding sites, *Mol Endocrinol 12*, 482-491.

236. Falkner, K. C., and Prough, R. A. (2007) Regulation of the rat glutathione S-transferase A2 gene by glucocorticoids: crosstalk through C/EBPs, *Drug Metab Rev 39*, 401-418.
237. Schule, R., Rangarajan, P., Kliewer, S., Ransone, L. J., Bolado, J., Yang, N., Verma, I. M., and Evans, R. M. (1990) Functional antagonism between oncoprotein c-Jun and the glucocorticoid receptor, *Cell 62*, 1217-1226.
238. Iwasaki, Y., Oiso, Y., Saito, H., and Majzoub, J. A. (1997) Positive and negative regulation of the rat vasopressin gene promoter, *Endocrinology 138*, 5266-5274.
239. Reichardt, H. M., Kaestner, K. H., Tuckermann, J., Kretz, O., Wessely, O., Bock, R., Gass, P., Schmid, W., Herrlich, P., Angel, P., and Schutz, G. (1998) DNA binding of the glucocorticoid receptor is not essential for survival, *Cell 93*, 531-541.
240. Reichardt, H. M., Tuckermann, J. P., Bauer, A., and Schutz, G. (2000) Molecular genetic dissection of glucocorticoid receptor function in vivo, *Z Rheumatol 59 Suppl 2*, II/1-5.
241. Linhart, H. G., Ishimura-Oka, K., DeMayo, F., Kibe, T., Repka, D., Poindexter, B., Bick, R. J., and Darlington, G. J. (2001) C/EBPalpha is required for differentiation of white, but not brown, adipose tissue, *Proc Natl Acad Sci U S A 98*, 12532-12537.
242. Tang, Q. Q., Jiang, M. S., and Lane, M. D. (1999) Repressive effect of Sp1 on the C/EBPalpha gene promoter: role in adipocyte differentiation, *Mol Cell Biol 19*, 4855-4865.
243. Tang, Q. Q., Jiang, M. S., and Lane, M. D. (1997) Repression of transcription mediated by dual elements in the CCAAT/enhancer binding protein alpha gene, *Proc Natl Acad Sci U S A 94*, 13571-13575.
244. Wang, X., Pan, L., Feng, Y., Wang, Y., Han, Q., Han, L., Han, S., Guo, J., Huang, B., and Lu, J. (2008) P300 plays a role in p16(INK4a) expression and cell cycle arrest, *Oncogene 27*, 1894-1904.
245. Crish, J. F., and Eckert, R. L. (2008) Synergistic activation of human involucrin gene expression by Fra-1 and p300--evidence for the presence of a multiprotein complex, *J Invest Dermatol 128*, 530-541.
246. Chen, Y. J., Wang, Y. N., and Chang, W. C. (2007) ERK2-mediated C-terminal serine phosphorylation of p300 is vital to the regulation of epidermal growth factor-induced keratin 16 gene expression, *J Biol Chem 282*, 27215-27228.
247. Guo, I. C., Shih, M. C., Lan, H. C., Hsu, N. C., Hu, M. C., and Chung, B. C. (2007) Transcriptional regulation of human CYP11A1 in gonads and adrenals, *J Biomed Sci 14*, 509-515.
248. Han, I., and Kudlow, J. E. (1997) Reduced O glycosylation of Sp1 is associated with increased proteasome susceptibility, *Mol Cell Biol 17*, 2550-2558.
249. Domenzain-Reyna, C., Hernandez, D., Miquel-Serra, L., Docampo, M. J., Badenas, C., Fabra, A., and Bassols, A. (2009) Structure and regulation of the versican promoter: the versican promoter is regulated by AP-1 and TCF transcription factors in invasive human melanoma cells, *J Biol Chem 284*, 12306-12317.
250. Qiu, Y., Zhao, Y., Becker, M., John, S., Parekh, B. S., Huang, S., Hendarwanto, A., Martinez, E. D., Chen, Y., Lu, H., Adkins, N. L., Stavreva, D. A., Wiench, M., Georgel, P. T., Schiltz, R. L., and Hager, G. L. (2006) HDAC1 acetylation is linked to progressive modulation of steroid receptor-induced gene transcription, *Mol Cell 22*, 669-679.

251. Poli, V., Mancini, F. P., and Cortese, R. (1990) IL-6DBP, a nuclear protein involved in interleukin-6 signal transduction, defines a new family of leucine zipper proteins related to C/EBP, *Cell 63*, 643-653.
252. Calonge, E., Alonso-Lobo, J. M., Escandon, C., Gonzalez, N., Bermejo, M., Santiago, B., Mestre, L., Pablos, J. L., Caruz, A., and Alcami, J. (2010) c/EBPbeta is a major regulatory element driving transcriptional activation of the CXCL12 promoter, *J Mol Biol 396*, 463-472.
253. Pham, T. H., Langmann, S., Schwarzfischer, L., El Chartouni, C., Lichtinger, M., Klug, M., Krause, S. W., and Rehli, M. (2007) CCAAT enhancer-binding protein beta regulates constitutive gene expression during late stages of monocyte to macrophage differentiation, *J Biol Chem 282*, 21924-21933.
254. Ng, P. K., Tsui, S. K., Lau, C. P., Wong, C. H., Wong, W. H., Huang, L., and Kumta, S. M. (2010) CCAAT/enhancer binding protein beta is up-regulated in giant cell tumor of bone and regulates RANKL expression, *J Cell Biochem*.
255. Gomis, R. R., Alarcon, C., Nadal, C., Van Poznak, C., and Massague, J. (2006) C/EBPbeta at the core of the TGFbeta cytostatic response and its evasion in metastatic breast cancer cells, *Cancer Cell 10*, 203-214.
256. Zahnow, C. A., Younes, P., Laucirica, R., and Rosen, J. M. (1997) Overexpression of C/EBPbeta-LIP, a naturally occurring, dominant-negative transcription factor, in human breast cancer, *J Natl Cancer Inst 89*, 1887-1891.
257. Milde-Langosch, K., Loning, T., and Bamberger, A. M. (2003) Expression of the CCAAT/enhancer-binding proteins C/EBPalpha, C/EBPbeta and C/EBPdelta in breast cancer: correlations with clinicopathologic parameters and cell-cycle regulatory proteins, *Breast Cancer Res Treat 79*, 175-185.
258. Koslowski, M., Tureci, O., Biesterfeld, S., Seitz, G., Huber, C., and Sahin, U. (2009) Selective activation of trophoblast-specific PLAC1 in breast cancer by CCAAT/enhancer-binding protein beta (C/EBPbeta) isoform 2, *J Biol Chem 284*, 28607-28615.
259. Hour, T. C., Chen, J., Huang, C. Y., Guan, J. Y., Lu, S. H., and Pu, Y. S. (2002) Curcumin enhances cytotoxicity of chemotherapeutic agents in prostate cancer cells by inducing p21(WAF1/CIP1) and C/EBPbeta expressions and suppressing NF-kappaB activation, *Prostate 51*, 211-218.
260. Xiao, W., Hodge, D. R., Wang, L., Yang, X., Zhang, X., and Farrar, W. L. (2004) Co-operative functions between nuclear factors NFkappaB and CCAT/enhancer-binding protein-beta (C/EBP-beta) regulate the IL-6 promoter in autocrine human prostate cancer cells, *Prostate 61*, 354-370.
261. Ramathal, C., Bagchi, I. C., and Bagchi, M. K. (2010) Lack of CCAAT Enhancer Binding Protein Beta (C/EBP{beta}) in Uterine Epithelial Cells Impairs Estrogen-Induced DNA Replication, Induces DNA Damage Response Pathways, and Promotes Apoptosis, *Mol Cell Biol 30*, 1607-1619.
262. Buck, M., and Chojkier, M. (2007) C/EBPbeta associates with caspase 8 complex proteins and modulates apoptosis in hepatic stellate cells, *J Clin Gastroenterol 41 Suppl 3*, S295-299.
263. Buck, M., and Chojkier, M. (2007) C/EBPbeta phosphorylation rescues macrophage dysfunction and apoptosis induced by anthrax lethal toxin, *Am J Physiol Cell Physiol 293*, C1788-1796.

264. Mukherjee, D., Kaestner, K. H., Kovalovich, K. K., and Greenbaum, L. E. (2001) Fas-induced apoptosis in mouse hepatocytes is dependent on C/EBPbeta, *Hepatology 33*, 1166-1172.
265. Ferrini, J. B., Rodrigues, E., Dulic, V., Pichard-Garcia, L., Fabr, J. M., Blanc, P., and Maurel, P. (2001) Expression and DNA-binding activity of C/EBPalpha and C/EBPbeta in human liver and differentiated primary hepatocytes, *J Hepatol 35*, 170-177.
266. Mihailovic, M., Petrovic, M., and Bogojevic, D. (2000) Correlation between acute phase-related expression of C/EBPbeta and transcriptional regulation of the haptoglobin gene during rat liver development, *Gen Physiol Biophys 19*, 317-321.
267. Dinic, S., Ivanovic-Matic, S., Bogojevic, D., Mihailovic, M., and Poznanovic, G. (2000) C/EBPalpha and C/EBPbeta are persistently associated with the rat liver nuclear matrix throughout development and the acute phase response, *Cell Biol Int 24*, 691-698.
268. Chen, S. S., Chen, J. F., Johnson, P. F., Muppala, V., and Lee, Y. H. (2000) C/EBPbeta, when expressed from the C/ebpalpha gene locus, can functionally replace C/EBPalpha in liver but not in adipose tissue, *Mol Cell Biol 20*, 7292-7299.
269. Cappelletti, M., Alonzi, T., Fattori, E., Libert, C., and Poli, V. (1996) C/EBPbeta is required for the late phases of acute phase genes induction in the liver and for tumour necrosis factor-alpha, but not Interleukin-6, regulation, *Cell Death Differ 3*, 29-35.
270. Ossipow, V., Descombes P and Schibler U. (1993) CCAAT/enhancer-binding protein mRNA is translated into multiple proteins with different transcription activation potentials, *PNAS 90*, 8219-8223.
271. Xiong, W., Hsieh CC, Kurtz AJ, Rabek JP and Papaconstantinou J. (2001) Regulation of CCAAT/enhancer-binding protein-beta isoform synthesis by alternative translational initiation at multiple AUG start sites., *Nucleic Acids Res 29*, 3087-3098.
272. Pei, D. Q., and Shih, C. H. (1991) An "attenuator domain" is sandwiched by two distinct transactivation domains in the transcription factor C/EBP, *Mol Cell Biol 11*, 1480-1487.
273. Kowenz-Leutz, E., Twamley G, Ansieau S, et Leutz A. (2004) Novel mechanism of C/EBPb (NF-M) transcriptional control: activation through derepression, *Genes & Development 8*, 2781-2791.
274. Piwien-Pilipuk G, M. O., Schwartz J. (2002) Dual regulation of phosphorylation and dephosphorylation of C/EBPbeta modulate its transcriptional activation and DNA binding in response to growth hormone., *J Biol Chem. 277*, 44557-44565.
275. Ceseña, T., Cardinaux, J., Kwok, R., and Schwartz, J. (2007) CCAAT/enhancer-binding protein (C/EBP) beta is acetylated at multiple lysines: acetylation of C/EBPbeta at lysine 39 modulates its ability to activate transcription., *J Biol Chem. 282*, 956-967.
276. Kowenz-Leutz, E., Pless, O., Dittmar, G., Knoblich, M., and Leutz, A. (2010) Crosstalk between C/EBPbeta phosphorylation, arginine methylation, and SWI/SNF/Mediator implies an indexing transcription factor code, *EMBO J*.
277. Venter, J. C. e. a. (2001) The sequence of the human genome, *Science 291*, 1304-1351.

278. Wang, W. L., Lee, Y. C., Yang, W. M., Chang, W. C., and Wang, J. M. (2008) Sumoylation of LAP1 is involved in the HDAC4-mediated repression of COX-2 transcription, *Nucleic Acids Res 36*, 6066-6079.
279. Berberich-Siebelt, F., Berberich, I., Andrulis, M., Santner-Nanan, B., Jha, M. K., Klein-Hessling, S., Schimpl, A., and Serfling, E. (2006) SUMOylation interferes with CCAAT/enhancer-binding protein beta-mediated c-myc repression, but not IL-4 activation in T cells, *J Immunol 176*, 4843-4851.
280. Kim, J., Cantwell, C. A., Johnson, P. F., Pfarr, C. M., and Williams, S. C. (2002) Transcriptional activity of CCAAT/enhancer-binding proteins is controlled by a conserved inhibitory domain that is a target for sumoylation, *J Biol Chem 277*, 38037-38044.
281. Eaton, E. M., and Sealy, L. (2003) Modification of CCAAT/enhancer-binding protein-beta by the small ubiquitin-like modifier (SUMO) family members, SUMO-2 and SUMO-3, *J Biol Chem 278*, 33416-33421.
282. Su, W. C., Chou, H. Y., Chang, C. J., Lee, Y. M., Chen, W. H., Huang, K. H., Lee, M. Y., and Lee, S. C. (2003) Differential activation of a C/EBP beta isoform by a novel redox switch may confer the lipopolysaccharide-inducible expression of interleukin-6 gene, *J Biol Chem 278*, 51150-51158.
283. Kim, J. W., Tang, Q. Q., Li, X., and Lane, M. D. (2007) Effect of phosphorylation and S-S bond-induced dimerization on DNA binding and transcriptional activation by C/EBPbeta, *Proc Natl Acad Sci U S A 104*, 1800-1804.
284. Wang, H., Larris, B., Peiris, T. H., Zhang, L., Le Lay, J., Gao, Y., and Greenbaum, L. E. (2007) C/EBPbeta activates E2F-regulated genes in vivo via recruitment of the coactivator CREB-binding protein/P300, *J Biol Chem 282*, 24679-24688.
285. Wang, G. L., Salisbury, E., Shi, X., Timchenko, L., Medrano, E. E., and Timchenko, N. A. (2008) HDAC1 promotes liver proliferation in young mice via interactions with C/EBPbeta, *J Biol Chem 283*, 26179-26187.
286. Xu, M., Nie, L., Kim, S. H., and Sun, X. H. (2003) STAT5-induced Id-1 transcription involves recruitment of HDAC1 and deacetylation of C/EBPbeta, *EMBO J 22*, 893-904.
287. Zuo, Y., Qiang, L., and Farmer, S. R. (2006) Activation of CCAAT/enhancer-binding protein (C/EBP) alpha expression by C/EBP beta during adipogenesis requires a peroxisome proliferator-activated receptor-gamma-associated repression of HDAC1 at the C/ebp alpha gene promoter, *J Biol Chem 281*, 7960-7967.
288. Wethkamp, N., and Klempnauer, K. H. (2009) Daxx is a transcriptional repressor of CCAAT/enhancer-binding protein beta, *J Biol Chem 284*, 28783-28794.
289. Turgeon, N., Valiquette C, Blais M, Routhier S, Seidman EG et Asselin C. (2008) Regulation of C/EBPdelta-dependent transactivation by histone deacetylases in intestinal epithelial cells., *J Cell Biochem 103*, 1573-1583.
290. Li, X., Kim JW, Grønborg M, Urlaub H, Lane MD, Tang QQ. (2007) Role of cdk2 in the sequential phosphorylation/activation of C/EBPbeta during adipocyte differentiation., *PNAS 104*, 11597-11602.
291. Tang, Q., Otto TC, Lane MD. (2003) CCAAT/enhancer-binding protein beta is required for mitotic clonal expansion during adipogenesis., *PNAS 100*, 850-855.
292. Orellana, D., Liu, X., Wang, G. L., Jin, J., Iakova, P., and Timchenko, N. A. (2010) Calmodulin controls liver proliferation via interactions with C/EBPbeta-LAP and C/EBPbeta-LIP, *J Biol Chem*.

293. Baldwin, B. R., Timchenko, N. A., and Zahnow, C. A. (2004) Epidermal growth factor receptor stimulation activates the RNA binding protein CUG-BP1 and increases expression of C/EBPbeta-LIP in mammary epithelial cells, *Mol Cell Biol 24*, 3682-3691.
294. Uematsu, S., Kaisho, T., Tanaka, T., Matsumoto, M., Yamakami, M., Omori, H., Yamamoto, M., Yoshimori, T., and Akira, S. (2007) The C/EBP beta isoform 34-kDa LAP is responsible for NF-IL-6-mediated gene induction in activated macrophages, but is not essential for intracellular bacteria killing, *J Immunol 179*, 5378-5386.
295. Finnin, M. S., Donigian, J. R., Cohen, A., Richon, V. M., Rifkind, R. A., Marks, P. A., Breslow, R., and Pavletich, N. P. (1999) Structures of a histone deacetylase homologue bound to the TSA and SAHA inhibitors, *Nature 401*, 188-193.
296. Lee, S., Miller, M., Shuman, J. D., and Johnson, P. F. (2010) CCAAT/Enhancer-binding protein beta DNA binding is auto-inhibited by multiple elements that also mediate association with p300/CREB-binding protein (CBP), *J Biol Chem 285*, 21399-21410.
297. Pless, O., Kowenz-Leutz, E., Knoblich, M., Lausen, J., Beyermann, M., Walsh, M. J., and Leutz, A. (2008) G9a-mediated lysine methylation alters the function of CCAAT/enhancer-binding protein-beta, *J Biol Chem 283*, 26357-26363.
298. Yamagoe, S., Kanno, T., Kanno, Y., Sasaki, S., Siegel, R. M., Lenardo, M. J., Humphrey, G., Wang, Y., Nakatani, Y., Howard, B. H., and Ozato, K. (2003) Interaction of histone acetylases and deacetylases in vivo, *Mol Cell Biol 23*, 1025-1033.
299. Descombes, P., and Schibler, U. (1991) A liver-enriched transcriptional activator protein, LAP, and a transcriptional inhibitory protein, LIP, are translated from the same mRNA, *Cell 67*, 569-579.
300. Mink, S., Haenig, B., and Klempnauer, K. H. (1997) Interaction and functional collaboration of p300 and C/EBPbeta, *Mol Cell Biol 17*, 6609-6617.
301. Schwartz, C., Beck, K., Mink, S., Schmolke, M., Budde, B., Wenning, D., and Klempnauer, K. H. (2003) Recruitment of p300 by C/EBPbeta triggers phosphorylation of p300 and modulates coactivator activity, *EMBO J 22*, 882-892.
302. Hinks, G. L., Shah, B., French, S. J., Campos, L. S., Staley, K., Hughes, J., and Sofroniew, M. V. (1997) Expression of LIM protein genes Lmo1, Lmo2, and Lmo3 in adult mouse hippocampus and other forebrain regions: differential regulation by seizure activity, *J Neurosci 17*, 5549-5559.
303. Esposito, F., Pierantoni, G. M., Battista, S., Melillo, R. M., Scala, S., Chieffi, P., Fedele, M., and Fusco, A. (2009) Interaction between HMGA1 and retinoblastoma protein is required for adipocyte differentiation, *J Biol Chem 284*, 25993-26004.
304. Jin, J., Wang, G. L., Shi, X., Darlington, G. J., and Timchenko, N. A. (2009) The age-associated decline of glycogen synthase kinase 3beta plays a critical role in the inhibition of liver regeneration, *Mol Cell Biol 29*, 3867-3880.
305. Mal, A., Sturniolo M, Schiltz RL, Ghosh MK et Harter ML. (2001) A role for histone deacetylase HDAC1 in modulating the transcriptional activity of MyoD: inhibition of the myogenic program., *EMBO J 20*, 1739-1753.
306. MacDougald, O. A., Cornelius, P., Lin, F. T., Chen, S. S., and Lane, M. D. (1994) Glucocorticoids reciprocally regulate expression of the CCAAT/enhancer-binding protein alpha and delta genes in 3T3-L1 adipocytes and white adipose tissue, *J Biol Chem 269*, 19041-19047.

307. Bannister, A. J., Cook, A., and Kouzarides, T. (1991) In vitro DNA binding activity of Fos/Jun and BZLF1 but not C/EBP is affected by redox changes, *Oncogene 6*, 1243-1250.
308. Kowenz-Leutz, E., and Leutz, A. (1999) A C/EBP beta isoform recruits the SWI/SNF complex to activate myeloid genes, *Mol Cell 4*, 735-743.
309. Spooner, C. J., Guo, X., Johnson, P. F., and Schwartz, R. C. (2007) Differential roles of C/EBP beta regulatory domains in specifying MCP-1 and IL-6 transcription, *Mol Immunol 44*, 1384-1392.
310. Mo, X., Kowenz-Leutz, E., Xu, H., and Leutz, A. (2004) Ras induces mediator complex exchange on C/EBP beta, *Mol Cell 13*, 241-250.
311. Lee, H., Lee, Y. J., Choi, H., Ko, E. H., and Kim, J. W. (2009) Reactive oxygen species facilitate adipocyte differentiation by accelerating mitotic clonal expansion, *J Biol Chem 284*, 10601-10609.
312. Lai, P. H., Wang, W. L., Ko, C. Y., Lee, Y. C., Yang, W. M., Shen, T. W., Chang, W. C., and Wang, J. M. (2008) HDAC1/HDAC3 modulates PPARG2 transcription through the sumoylated CEBPD in hepatic lipogenesis, *Biochim Biophys Acta 1783*, 1803-1814.
313. Trivedi, A. K., Bararia, D., Christopeit, M., Peerzada, A. A., Singh, S. M., Kieser, A., Hiddemann, W., Behre, H. M., and Behre, G. (2007) Proteomic identification of C/EBP-DBD multiprotein complex: JNK1 activates stem cell regulator C/EBPalpha by inhibiting its ubiquitination, *Oncogene 26*, 1789-1801.
314. Shim, M., and Smart, R. C. (2003) Lithium stabilizes the CCAAT/enhancer-binding protein alpha (C/EBPalpha) through a glycogen synthase kinase 3 (GSK3)-independent pathway involving direct inhibition of proteasomal activity, *J Biol Chem 278*, 19674-19681.
315. Mancini, A., El Bounkari, O., Norrenbrock, A. F., Scherr, M., Schaefer, D., Eder, M., Banham, A. H., Pulford, K., Lyne, L., Whetton, A. D., and Tamura, T. (2007) FMIP controls the adipocyte lineage commitment of C2C12 cells by downmodulation of C/EBP alpha, *Oncogene 26*, 1020-1027.
316. Timchenko, L. T., Iakova, P., Welm, A. L., Cai, Z. J., and Timchenko, N. A. (2002) Calreticulin interacts with C/EBPalpha and C/EBPbeta mRNAs and represses translation of C/EBP proteins, *Mol Cell Biol 22*, 7242-7257.
317. Sterneck, E., Tessarollo, L., and Johnson, P. F. (1997) An essential role for C/EBPbeta in female reproduction, *Genes Dev 11*, 2153-2162.
318. Seagroves, T. N., Lydon, J. P., Hovey, R. C., Vonderhaar, B. K., and Rosen, J. M. (2000) C/EBPbeta (CCAAT/enhancer binding protein) controls cell fate determination during mammary gland development, *Mol Endocrinol 14*, 359-368.
319. Nadeau, S., Hein, P., Fernandes, K. J., Peterson, A. C., and Miller, F. D. (2005) A transcriptional role for C/EBP beta in the neuronal response to axonal injury, *Mol Cell Neurosci 29*, 525-535.
320. Rahman, S. M., Schroeder-Gloeckler, J. M., Janssen, R. C., Jiang, H., Qadri, I., Maclean, K. N., and Friedman, J. E. (2007) CCAAT/enhancing binding protein beta deletion in mice attenuates inflammation, endoplasmic reticulum stress, and lipid accumulation in diet-induced nonalcoholic steatohepatitis, *Hepatology 45*, 1108-1117.
321. Lu, M., Seufert, J. and Habener, J.F. (1997) Pancreatic beta-cell-specific repression of insulin gene transcription by CCAAT/enhancer-binding protein beta. Inhibitory

interactions with basic helix-loop-helix transcription factor E47, *J Biol Chem. 272*, 28349-28359.
322. Wang, L., Shao, J., Muhlenkamp, P., Liu, S., Klepcyk, P., Ren, J., and Friedman, J. E. (2000) Increased insulin receptor substrate-1 and enhanced skeletal muscle insulin sensitivity in mice lacking CCAAT/enhancer-binding protein beta, *J Biol Chem 275*, 14173-14181.
323. Stadler, J. A., Shkumatava, A., Norton, W. H., Rau, M. J., Geisler, R., Fischer, S., and Neumann, C. J. (2005) Histone deacetylase 1 is required for cell cycle exit and differentiation in the zebrafish retina, *Dev Dyn 233*, 883-889.
324. Park, J. H., Jung, Y., Kim, T. Y., Kim, S. G., Jong, H. S., Lee, J. W., Kim, D. K., Lee, J. S., Kim, N. K., and Bang, Y. J. (2004) Class I histone deacetylase-selective novel synthetic inhibitors potently inhibit human tumor proliferation, *Clin Cancer Res 10*, 5271-5281.
325. Kawai, H., Li, H., Avraham, S., Jiang, S., and Avraham, H. K. (2003) Overexpression of histone deacetylase HDAC1 modulates breast cancer progression by negative regulation of estrogen receptor alpha, *Int J Cancer 107*, 353-358.
326. Zhou, Q., Melkoumian, Z. K., Lucktong, A., Moniwa, M., Davie, J. R., and Strobl, J. S. (2000) Rapid induction of histone hyperacetylation and cellular differentiation in human breast tumor cell lines following degradation of histone deacetylase-1, *J Biol Chem 275*, 35256-35263.
327. Juan, L. J., Shia, W. J., Chen, M. H., Yang, W. M., Seto, E., Lin, Y. S., and Wu, C. W. (2000) Histone deacetylases specifically down-regulate p53-dependent gene activation, *J Biol Chem 275*, 20436-20443.
328. Luedde, T., Duderstadt, M., Streetz, K. L., Tacke, F., Kubicka, S., Manns, M. P., and Trautwein, C. (2004) C/EBP beta isoforms LIP and LAP modulate progression of the cell cycle in the regenerating mouse liver, *Hepatology 40*, 356-365.
329. Rask, K., Thorn, M., Ponten, F., Kraaz, W., Sundfeldt, K., Hedin, L., and Enerback, S. (2000) Increased expression of the transcription factors CCAAT-enhancer binding protein-beta (C/EBBeta) and C/EBzeta (CHOP) correlate with invasiveness of human colorectal cancer, *Int J Cancer 86*, 337-343.
330. Boggs, K., and Reisman, D. (2007) C/EBPbeta participates in regulating transcription of the p53 gene in response to mitogen stimulation, *J Biol Chem 282*, 7982-7990.
331. Schneider-Merck, T., Pohnke, Y., Kempf, R., Christian, M., Brosens, J. J., and Gellersen, B. (2006) Physical interaction and mutual transrepression between CCAAT/enhancer-binding protein beta and the p53 tumor suppressor, *J Biol Chem 281*, 269-278.
332. Wilkinson, K. A., and Henley, J. M. (2010) Mechanisms, regulation and consequences of protein SUMOylation, *Biochem J 428*, 133-145.
333. Chung, S. S., Ahn, B. Y., Kim, M., Choi, H. H., Park, H. S., Kang, S. A., Park, S. G., Kim, Y. B., Cho, Y. M., Lee, H. K., Chung, C. H., and Park, K. S. (2010) Control of Adipogenesis by the SUMO-Specific Protease SENP2, *Mol Cell Biol*.
334. Yamashita, D., Yamaguchi, T., Shimizu, M., Nakata, N., Hirose, F., and Osumi, T. (2004) The transactivating function of peroxisome proliferator-activated receptor gamma is negatively regulated by SUMO conjugation in the amino-terminal domain, *Genes Cells 9*, 1017-1029.
335. Lim, S., Ahn, B. Y., Chung, S. S., Park, H. S., Cho, B. J., Kim, M., Choi, S. H., Lee, I. K., Lee, S. W., Choi, S. J., Chung, C. H., Cho, Y. M., Lee, H. K., and Park, K. S.

(2009) Effect of a peroxisome proliferator-activated receptor gamma sumoylation mutant on neointimal formation after balloon injury in rats, *Atherosclerosis 206*, 411-417.
336. Liu, L. B., Omata, W., Kojima, I., and Shibata, H. (2007) The SUMO conjugating enzyme Ubc9 is a regulator of GLUT4 turnover and targeting to the insulin-responsive storage compartment in 3T3-L1 adipocytes, *Diabetes 56*, 1977-1985.
337. Shibata, H. (2005) [Regulation of insulin sensitivity by subcellular GLUT4 targeting], *Rinsho Byori 53*, 942-949.
338. David, G., Neptune, M. A., and DePinho, R. A. (2002) SUMO-1 modification of histone deacetylase 1 (HDAC1) modulates its biological activities, *J Biol Chem 277*, 23658-23663.
339. Nayak, A., Glockner-Pagel, J., Vaeth, M., Schumann, J. E., Buttmann, M., Bopp, T., Schmitt, E., Serfling, E., and Berberich-Siebelt, F. (2009) Sumoylation of the transcription factor NFATc1 leads to its subnuclear relocalization and interleukin-2 repression by histone deacetylase, *J Biol Chem 284*, 10935-10946.

APPENDICES

Appendix 1 Primers used for cloning

Table 1: GST fusion constructs for bacterial protein expression used in the *in vitro* binding assays.

Plasmid name	Primers used for cloning
pGEX2T-C/EBPβ	Construct generated by Louise Pope (full length LAP*)
pGEX2T-C/EBPβ$_{K98\text{-}102R}$	Construct generated by Dr Nadine Wiper-Bergeron (*106*)
pGEX2T-C/EBPβ$_{108C}$	Forward: **ACTCGGATCC**TACGTGAGCCTCGGCCGCGC Reverse: **ACGCGAATTC**CTAGCAGTGGCCCGCCGAGGC
pGEX2T-C/EBPβ$_{N107}$	Forward: **ACTCGGATCC**ATGCACCGCCTGCTGGCCTG Reverse: **ACGCGAATTC**ACCGTAGTCGGCCGGCTTCTTG
pGEX2T-C/EBPβ$_{N140}$	Forward: **ACTCGGATCC**ATGCACCGCCTGCTGGCCTG Reverse: **ACGCGAATTC**GGGTTCGAAGCCCGGCTCCGC
pGEX2T-C/EBPβ$_{N168}$	Forward: **ACTCGGATCC**ATGCACCGCCTGCTGGCCTG Reverse: **ACGCGAATTC**CGCCTGGTAGCCCAGGTAGGC
pGEX2T-C/EBPβ$_{N184}$	Forward: **ACTCGGATCC**ATGCACCGCCTGCTGGCCTG Reverse: **ACGCGAATTC**GCTGGACGACGACGACGTGGAC
pGEX2T-C/EBPβ$_{N217}$	Forward: **ACTCGGATCC**ATGCACCGCCTGCTGGCCTG Reverse: **ACGCGAATTC**CGTCTTCTTGGCCTTGGCCTTG
pGEX2T-C/EBPβ$_{\Delta151\text{-}156}$	Upper: GGGCGCGTCGTCCGCGCGCTTG Lower: CCGTTCGCCCTGCGCGCCTACC
pGEX2T-C/EBPβ$_{\Delta141\text{-}149}$	Upper: GGGTTCGAAGCCCGGCTCCGC Lower: CCCGCCATGGCGGCCGGTTTC
pGEX2T-C/EBPβ$_{\Delta141\text{-}168}$	Upper: GGGTTCGAAGCCCGGCTCCGC Lower: ACGCCGAGCGGCAGCAGCGGC
pGEX2T-C/EBPβ$_{\Delta129\text{-}168}$	Upper: GGGAGGCGGCGGCGGGAAGC Lower: ACGCCGAGCGGCAGCAGCGGC
pGEX2T-C/EBPβ$_{\Delta141\text{-}184}$	Upper: GGGTTCGAAGCCCGGCTCCGC Lower: CCGCCCGGCACGCCGAGCCCC
pGEX2T-C/EBPβ$_{\Delta129\text{-}184}$	Upper: GGGAGGCGGGCGGGAAGC Lower: CCGCCCGGCACGCCGAGCCCC

Table 2: Mammalian expression constructs for transient transfection experiments in NIH 3T3, 3T3 L1 and Cos7 cells. All cDNA were cloned between the EcoRI and BamHI sites of the pcDNA3.1(-) vector.

Plasmid name	Primers used for cloning
pcDNA3.1(-)	Plasmid obtained from Invitrogen and used for subsequent cloning
pcDNA-C/EBPβ	Forward: **ACTCGAATTC**ATGCACCGCCTGCTGGCCTG Reverse: **ACGCGGATCC**CTAGCAGTGGCCCGCCGAGGC
pcDNA-C/EBPβ$_{\Delta 153\text{-}156}$	Upper: CATGGCGGGCGCGTCGTCCGCGCGCTTGCAGTC Lower: CCGTTCGCCCTGCGCGCCTACC
pcDNA-C/EBPβ$_{\Delta 151\text{-}156}$	Forward: **ACTCGAATTC**ATGCACCGCCTGCTGGCCTG Reverse: **ACGCGGATCC**CTAGCAGTGGCCCGCCGAGGC (pGEX2T-C/EBPβ$_{\Delta 151\text{-}156}$ used as template)
pcDNA-C/EBPβ$_{\Delta 141\text{-}149}$	Forward: **ACTCGAATTC**ATGCACCGCCTGCTGGCCTG Reverse: **ACGCGGATCC**CTAGCAGTGGCCCGCCGAGGC (pGEX2T-C/EBPβ$_{\Delta 141\text{-}149}$ used as template)
pcDNA-C/EBPβ$_{\Delta 141\text{-}168}$	Forward: **ACTCGAATTC**ATGCACCGCCTGCTGGCCTG Reverse: **ACGCGGATCC**CTAGCAGTGGCCCGCCGAGGC (pGEX2T-C/EBPβ$_{\Delta 141\text{-}168}$ used as template)
pcDNA-C/EBPβ$_{LIP}$	Forward: **ACTCGAATTC**ATGGCGGCCGGTTTCCCGTTC Reverse: **ACGCGGATCC**CTAGCAGTGGCCCGCCGAGGC
pcDNA-C/EBPβ$_{LIP\ 6C}$	Forward: **ACTCGAATTC**ATGCCGTTCGCCCTGCGCGCC Reverse: **ACGCGGATCC**CTAGCAGTGGCCCGCCGAGGC
pcDNA-C/EBPβ$_{M152A}$	Upper: GAA ACC GGC CGC **C**G**C** GGC GGG CGC GTC GTC Lower: GAC GAC GCG CCC GCC **GC**G GCG GCC GGT TTC
pcDNA-C/EBPβ$_{M22,152A}$	Constructed by Adrianna Douvris, a former honour student
pcDNA-C/EBPβ$_{22C,M152A}$	Constructed by Adrianna Douvris, a former honour student
pcDNA-C/EBPβ$_{C11A,M22,152A}$	Forward: **ACTCGAATTC**ATGCACCGCCTGCTGGCCTG GGACGCAGCAGCCCTCCCG Reverse: **ACGCGGATCC**CTAGCAGTGGCCCGCCGAGG CCAGCAGCGGCTCGGGC
pcDNA-C/EBPβ$_{C143A}$	Upper: CGCGCGCTTGGCGTCCGCGGGTTCG Lower: CGAACCCGCGGACGCCAAGCGCGCG-3
pcDNA-HA-C/EBPβ	Forward: **ACTCGAATTC**ATGTACCCATATGATGTTCCTG ACTATGCT**ATG**CACCGCCTGCTGGCCTG Reverse: **ACGCGGATCC**CTAGCAGTGGCCCGCCGAGGC
pcDNA-HA-C/EBPβ$_{22C}$	Forward: **ACTCGAATTC**ATGTACCCATATGATGTTCCTG ACTATGCTATGGAAGTGGCCAACTTCTAC Reverse: **ACGCGGATCC**CTAGCAGTGGCCCGCCGAGGC
pcDNA-C/EBPβ$_{22C}$	Forward: **ACTCGAATTC**ATGGAAGTGGCCAACTTCTAC Reverse: **ACGCGGATCC**CTAGCAGTGGCCCGCCGAGGC

Table 3: Mammalian expression constructs for transient transfection experiments in NIH 3T3 and Cos7 cells.

Plasmid name	Primers used for cloning
pMSV-C/EBPβ	Plasmid obtained from Dr McKnight for expression of full length murine C/EBPβ and used as template for further deletion mutants
pMSV-C/EBPβ$_{\Delta 151\text{-}156}$	Upper: GGGCGCGTCGTCCGCGCGCTTG Lower: CCGTTCGCCCTGCGCGCCTACC
pMSV -C/EBPβ$_{\Delta 141\text{-}149}$	Upper: GGGTTCGAAGCCCGGCTCCGC Lower: CCCGCCATGGCGGCCGGTTTC
pMSV-C/EBPβ$_{\Delta 141\text{-}156}$	Upper: GGGTTCGAAGCCCGGCTCCGC Lower: CCGTTCGCCCTGCGCGCCTACC
pMSV-C/EBPβ$_{\Delta 141\text{-}152}$	Upper: GGGTTCGAAGCCCGGCTCCGC Lower: ATGGCGGCCGGTTTCCCGTTCG

Appendix 2 Retroviral vectors constructed and plasmids obtained from other laboratories

Table 4: Retroviral vectors constructed for stable expression of C/EBPβ proteins in murine NIH 3T3 and 3T3 L1 cells

Plasmid name	Cloning method
pLXSN from Clonetech	For mammalian cell infection experiments
pLXSN-C/EBPβ	Cloned between the EcoRI and BamHI restriction site. Insert was cut from the pcDNA-C/EBPβ construct and ligated into pLXSN.
pLXSN -C/EBP$\beta_{\Delta 153\text{-}156}$	Insert was cut using EcoRI and BamHI enzymes from the pcDNA- C/EBP$\beta_{\Delta 153\text{-}156}$ construct and ligated into pLXSN.
pLXSN -C/EBP$\beta_{\Delta 151\text{-}156}$	Insert was cut using EcoRI and BamHI enzymes from the pcDNA- C/EBP$\beta_{\Delta 151\text{-}156}$ construct and ligated into pLXSN.
pLXSN -C/EBP$\beta_{\Delta 141\text{-}149}$	Insert was cut using EcoRI and BamHI enzymes from the pcDNA- C/EBP$\beta_{\Delta 141\text{-}149}$ construct and ligated into pLXSN.
pLXSN -C/EBP$\beta_{\Delta 141\text{-}168}$	Insert was cut using EcoRI and BamHI enzymes from the pcDNA- C/EBP$\beta_{\Delta 141\text{-}168}$ construct and ligated into pLXSN.
pLXSN -C/EBPβ_{LIP}	Insert was cut using EcoRI and BamHI enzymes from the pcDNA- C/EBPβ_{LIP} construct and ligated into pLXSN.
pLXSN -C/EBP$\beta_{LIP\ 6C}$	Insert was cut using EcoRI and BamHI enzymes from the pcDNA- C/EBP$\beta_{LIP\ 6C}$ construct and ligated into pLXSN.
pLXSN -C/EBPβ_{M152A}	Insert was cut using EcoRI and BamHI enzymes from the pcDNA- C/EBPβ_{M152A} construct and ligated into pLXSN.
pLXSN -C/EBP$\beta_{M22,\ 152A}$	Constructed by Adrianna Douvris using the same procedure.
pLXSN -C/EBP$\beta_{C11A,\ M22,152A}$	Insert was cut using EcoRI and BamHI enzymes from the pcDNA- C/EBP$\beta_{\ C11A,\ M22,152A}$ construct and ligated into pLXSN.
pLXSN -C/EBP$\beta_{22C,M152A}$	Insert was cut using EcoRI and BamHI enzymes from the pcDNA- C/EBP$\beta_{22C,M152A}$ construct and ligated into pLXSN.
pLXSN -C/EBPβ_{C143A}	Insert was cut using EcoRI and BamHI enzymes from the pcDNA- C/EBPβ_{C143A} construct and ligated into pLXSN.

Table 5: Additional constructs used for some of the experiments that were already in Dr Robert Haché's laboratory

Plasmid	Type	Description	Original source
pTL-GR	Mammalian expression vector	For expression of full length rat GR	Joanne Savory
pMSV-C/EBPα	Mammalian expression vector	For expression of full length murine C/EBPα	Dr. S.K. McKnight
pMSV-C/EBPβ	Mammalian expression vector	For expression of full length murine C/EBPβ	Dr S.K. McKnight
pMSV-C/EBPδ	Mammalian expression vector	For expression of full length murine C/EBPδ	Dr S.K. McKnight
pRL-CMV	Reporter vector	Plasmid containing the CMV promoter upstream of the Renilla Luciferase cDNA	Promega
pCX14/12	Reporter vector	Plasmid containing the murine C/EBPα promoter (-350 to +7) upstream of the Luciferase cDNA	Dr P. Antonsen
pC478	Reporter vector	Plasmid containing the murine PPARγ promoter (-609 to +52) upstream of the Luciferase cDNA	Dr J. Gimble
pcDNA3.1(-)-mSin3A	Mammalian expression vector and *in vitro* translation	For expression of human mSin3A	Dr X.J. Yang
pcDNA3.1(-)-HDAC1	Mammalian expression vector and *in vitro* translation	For expression of human HDAC1 with a C-terminal HA and FLAG tag	Dr X.J. Yang
pFLAG-hGCN5	Mammalian expression vector	For expression of human FLAG-GCN5	Dr S. Kochbin
pHIS-hGCN5	Bacterial expression	For expression of human GCN5 in bacteria and purification using the 6XHis tag	Dr S. Kochbin
pmmGCN5	Mammalian expression vector and *in vitro* translation	For expression of murine GCN5	Dr S. Roth

Appendix 3 Antibodies used

Table 6: Antibodies used for western blot analysis, immunofluorescence and/or immunoprecipitation

1^{o} antibody	Supplier (Dilution for western blotting)	Application
C/EBPα (14-AA)	Santa Cruz Biotechnology (1:400)	Wertern blot
C/EBPβ (C-19)	Santa Cruz Biotechnology (1:400)	Wertern blot and immunoprecipitation
PPARγ (H-100)	Santa Cruz Biotechnology (1:400)	Wertern blot
Adipsin (P1-6)	Santa Cruz Biotechnology (1:400)	Wertern blot
Actin (H-300)	Santa Cruz Biotechnology (1:400)	Wertern blot
HDAC1 (C-19)	Santa Cruz Biotechnology (1:400)	Wertern blot and immunoprecipitation
GCN5 (H-75)	Santa Cruz Biotechnology	Immunoprecipitation
Gal4 (DBD)	Santa Cruz Biotechnology	Immunoprecipitation
Cyclin A (C-19)	Santa Cruz Biotechnology (1:400)	Wertern blot
Cyclin B1 (H-433)	Santa Cruz Biotechnology (1:400)	Wertern blot
SUMO1 (FL-101)	Santa Cruz Biotechnology (1:400)	Wertern blot
SUMO2/3 (FL-103)	Santa Cruz Biotechnology (1:400)	Wertern blot
FLAG M2 monoclonal	Sigma Aldrich (1:1000)	Wertern blot
P27/Kip1	BD (1:500)	Wertern blot

Appendix 4 Primers for qPCR and ChIP

Table 7: Primers used for real time PCR reactions and ChIP assays (murine sequences)

Name	Primer	Application
PPARγ2	Forward: GAA ACT CTG GGA GAT TCT CC Reverse: GCT GGA GAA ATC AAC TGT GG	Real time RT-PCR
C/EBPα	Forward: TGG ACA AGA ACA GCA ACG AG Reverse: CCA TGG CCT TGA CCA AGG AG	Real time RT-PCR
β actin	Forward: GAC TTC GAG CAA GAG ATG GC Reverse: CCA GAC AGC ACT GTG TTG GC	Real time RT-PCR
C/EBPα Promoter	Forward: TAGTGTTGGCTGGAAGTGGGTGACTTAGAGGC Reverse: TTCTCCTGTGACTTTCCAAGGCGGTGAGTG	Chromatin immunoprecipitation

Appendix 5 Schema of all deletion mutants used

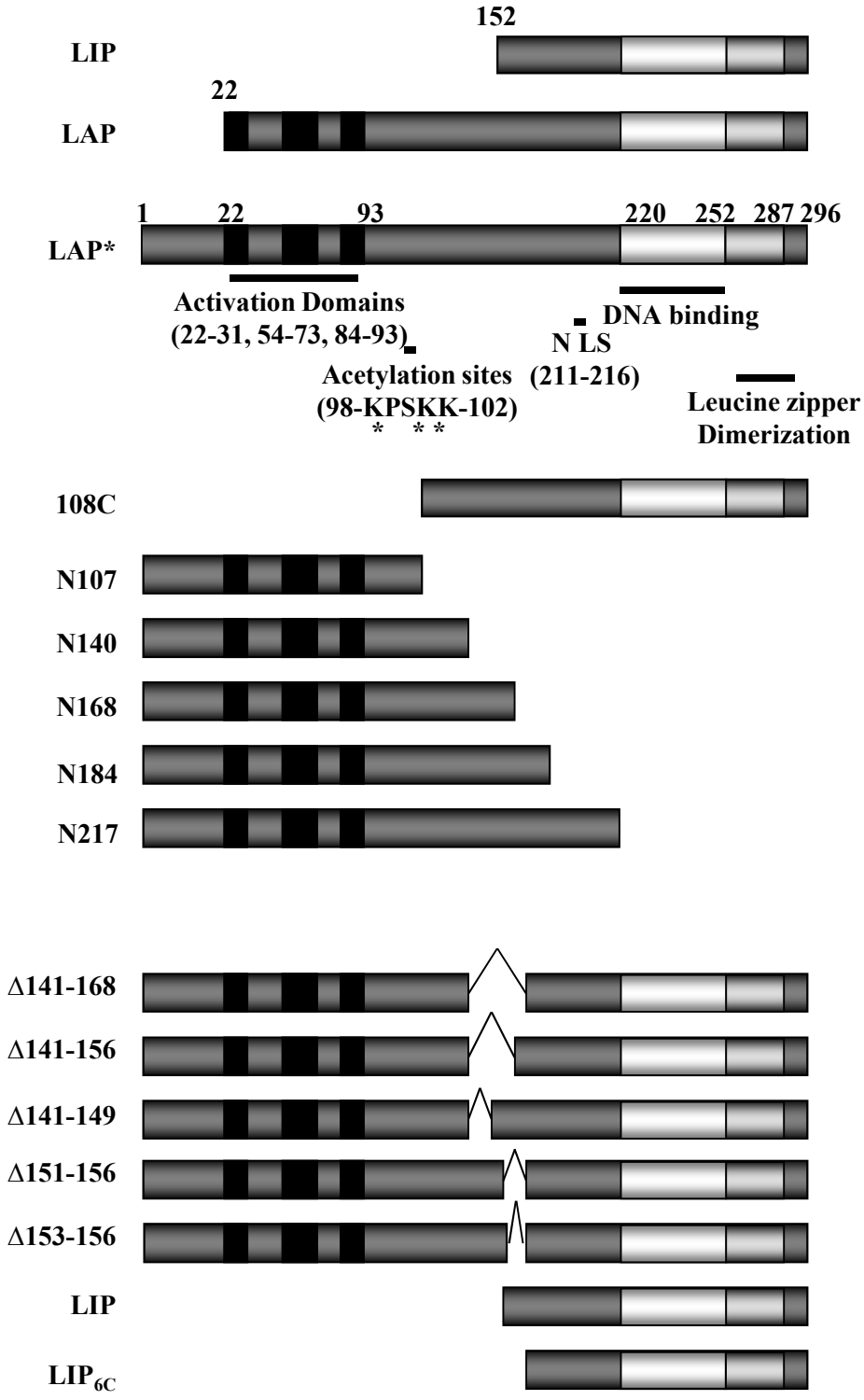

Appendix 6 Summary of the properties of C/EBPβ deletion mutants

Table 8: Summary of the properties of C/EBPβ deletion mutants from various assays (approximate values in % compared to WT)

		C/EBPβ				
		WT	**Δ151-156**	**Δ141-149**	**ΔM152A**	**Δ153-156**
LIP expression		YES	NO	YES	NO	YES
***In vitro* Acetylation with PCAF**		**100**	50	100		50
Interaction with HDAC1		**100**	20	100	90	30
Interaction with GCN5		**100**	20	100		**20**
Recruitment of HDAC1 to the C/EBPα promoter		**100**	20	**100**	**100**	20
C/EBPα - promoter transcription assay	**- Dex**	20	60	5	60	60
	+ Dex	**100**	150	10	150	150
C/EBPα mRNA	**Day 1 MI**	25	80	25	80	**50**
	Day 1 MID	**100**	200	50	200	100
PPAR mRNA	**Day 1 MI**	20	40	20	40	20
	Day 1 MID	**100**	200	100	200	100
Differentiation (Adipsin level)	**MI**	10	50	10	50	**30**
	MID	**100**	200	100	200	100

Appendix 7 Protein sequence of murine C/EBPβ highlighting its different domains

The different hydrophobic domains represent the residues in bold, the activation domains are underligned, the basic and the leucine residues in the bZIP domain (219-296) are underligned and in bold, respectively.

1	MHRLLAWD**AACLPPPPAAF**RP	21
22	MEVANFYYEPDCLAYGAKAARAAPRAPA	49
50	AEPAIGEHERAIDFSPYLEPLAPAADFAAP	79
80	APAHHDFLSDLFADDYGAKPSKKPADYGY	108
109	VSLGRAGAK**AAPPACFPPPPPAA**LKAEPGFE	139
140	PADCKRADD**APAMAAGFPFAL**RAYLGYQA	168
169	TPSGSSGSLS**T**SSSSS**S**PPG**T**PSPAD	193
194	AK**AAPAACFAGPPAAPA**KAKAKKTV	218
219	DKLSDEYKMRRERNNIAVRKSRDKAKMRN**L**ETQ	251
252	HKV**L**E**L**TAENER**L**QKKVEQ**L**SRE**L**ST**L**RN**L**FKQ**L**PEP**LL**ASAGHC	296

Appendix 7 **Additional experimental figures**

(A) **Ectopic expression of C/EBPβ in NIH 3T3 cells induces C/EBPa protein expression only when its expression is maintained for a longer period.**

NIH 3T3 cells stably expressing C/EBPb were induced to differentiate with the inducer cocktails and harvested 4 days later to assess C/EBPa protein expression. The first round of differentiation refers to induction of differentiation approximately two weeks after infection of the cells with the retroviruses to stably express the transcription factor, whereas the second round is when induction of differentiation was performed four weeks following infection.

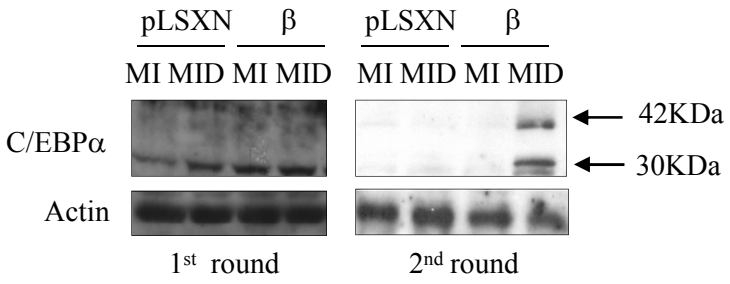

(B) Sumoylation profile of C/EBPβ-associated proteins during the early phase of 3T3 L1 differentiation.

3T3 L1 cells were differentiated with the inducer cocktail prior to immunoprecipitation of endogenous C/EBPβ. Each experiment was performed twice at the indicated time-point, where 0h represents the time at which the cells were treated with either MI (-) or MID (+), at 2 days post-confluency. Western blot of the Sumo 2/3 (A) and Sumo 1 (B) - associated proteins are shown.

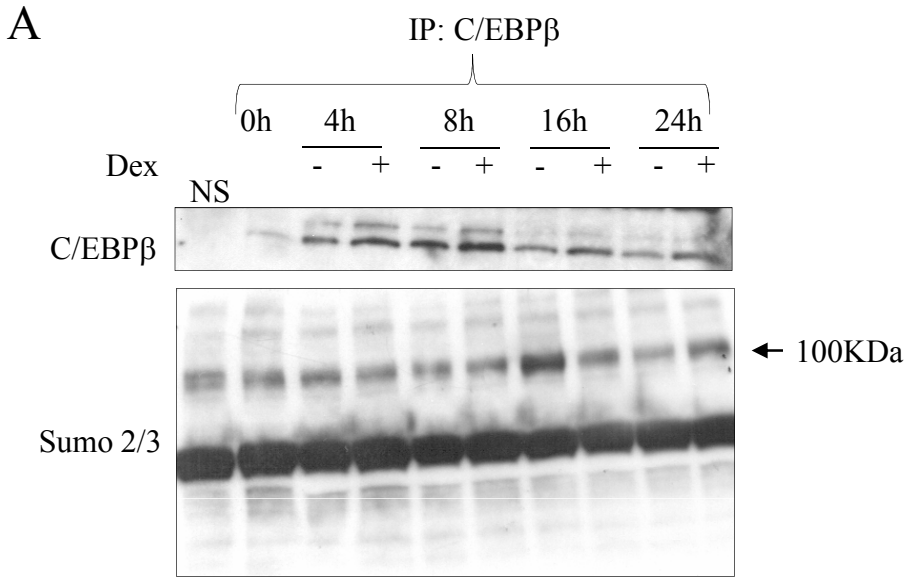

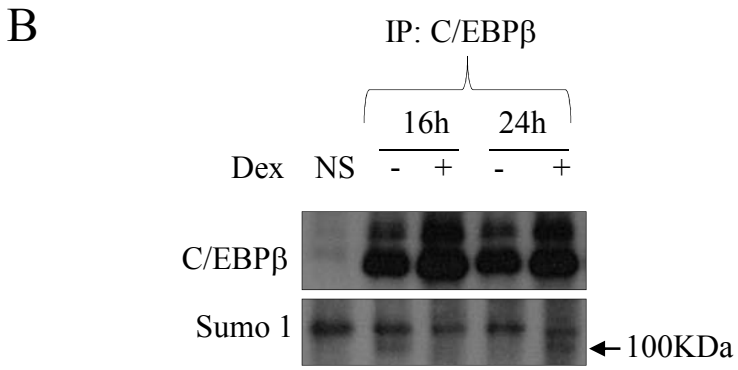

Appendix 9 Contribution of collaborators

An honours undergraduate student, Adrianna Douvris, generated the pcDNA-C/EBP$\beta_{M22,152A}$ and the pcDNA-C/EBP$\beta_{22C,152A}$ constructs and performed some of the replicate experiments in figure 21B.